Design and Synthesis of Chemical Tools for Ageing Research

Hayley Louise Rand

Supervisor: Prof. Mark C. Bagley

Submitted to the University of Sussex in part fulfilment of the requirements of the degree of Doctor of Philosophy, September 2017

Declaration

I hereby declare that the work presented in this thesis was carried out at the University of Sussex under the supervision of Prof. M. C. Bagley between the dates of September 2013 and March 2017. The work presented in this thesis is my own, unless otherwise stated, and has not been submitted in whole or in part form for award of another degree.

Hayley L. Rand

Acknowledgements

First and foremost, I would like to thank my supervisor, Prof. Mark Bagley, for giving me the most colourful and interesting of projects. His enthusiasm for chemistry is inspiring and I am most grateful for his support and constant encouragement.
I would like to thank the School of Life Sciences at the University of Sussex for funding my studies.

I would like to thank the staff at the University of Sussex chemistry department. My co-supervisor Prof. Simon Ward, for his helpful advice and support when it was needed, Dr Alaa Abdul-Sada for performing mass spectrometry measurements and Dr Iain Day for his help with tuition and advice on understanding NMR spectroscopy experiments. Also, special thanks to Alex, Paul and Barry for all their help.

I would like to thank my colleagues, past and present, Dr. Jessica Dwyer, Dr. David Neill-Hall and Tyler Nichols.

I would like to thank my friends, who have become like a second family; Tom Moore, Katie Duffell, Rhiannon Jones, Jessica Dwyer, Irene Maluenda, Adam Close, Daniel Guest, Mark Whelan, Oran O'Doherty, Chris Gallop and Ash Deadman. You have all helped me get through this experience, keeping me sane during the more challenging times and just having the most fun at the best of times! I really don't think I could have got through it all without you. Extra special thanks go to Jessica Dwyer for all the proof reading and helpful hints and tips, and to Tom Moore for being a wonderfully supportive partner.

Last, but certainly not least, I would like to thank my family who have always supported and encouraged me. My parents, Mark and Helen, and my siblings Cerys and Callum, have been so wonderful and I hope they know how much I love and appreciate them.

Abstract

The work described in this thesis involves developing synthetic methods to produce a range of drug-like small molecules that can be used as chemical tools to understand and modulate disease pathophysiology. There are two types of such tools investigated in this thesis: diagnostic tools for imaging experiments, and inhibitory tools for modulating biochemical pathways.

The imaging tools are designed to target apoptosis, accumulating in cells undergoing early-stage apoptotic events, and contain a fluorescent tag, thus providing a real-time technique for observing and monitoring these events and even to modulate them from inside the cell. The imaging agent would then be used to guide the design of a radiolabelled small molecule that can be used alongside traditional cancer therapies, to preferentially enter cells going through apoptosis, ensuring that these cells commit to cell death and do not recover.

The inhibitory tools are designed to study the molecular mechanisms of MK2, a protein that has been implicated in disease progression and cellular ageing events. This worked used the premature ageing syndrome, Werner's Syndrome as a model for normal human ageing.

In Chapter 2, several fluorescent markers are considered for the development of a real-time imaging tool to target apoptosis. The structures of the fluorescent agents are based on two structures known to preferentially enter cells going through the early stages of apoptosis; didansyl cystine and ML10. The conclusion of this investigation led to ML10 being used as the basis for further development of fluorescent agents. The formation of several novel BODIPY compounds is described, with one compound tested in a cell line for its ability to preferentially enter cells going through the early stages of apoptosis. The results of this test led to an investigation into the lipophilicity of BODIPY compounds versus ML10. This investigation involved the use of software to generate cLogP values as a guide for potential designs of further BODIPY structures. The development of a drug-like

structure that can mimic the action of the BODIPY compound is also explored, with the inclusion of a step to insert iodine-131 at a later stage in the development.

In Chapter 3, microwave-assisted organic synthesis was used to develop novel routes toward benzothiophene derivatives, which formed part of a new route towards the Pfizer developed MK2 inhibitor PF-3644022. This work was published in Organic and Biomolecular Chemistry. The full route was proposed in the doctoral thesis of Dr. Jessica Dwyer, and the latter part of this thesis set out to improve the yield of the final step. A collaboration with the Kostakis group led to an investigation into the use of the catalyst $Zn_2Y_2(C_{21}H_{25}NO_3)_4$ for its applicability to the Doebner-type multi-component reaction that would lead to the formation of PF-3644022. Although no conclusive results were obtained from the reactions trialled, the work opened up new channels of collaboration for the Bagley group and potential for further exploration of the use of isoskeletal coordination cluster catalysts in organic multi-component reactions.

Overall, the aim of this work was to deliver rapid routes to these chemical tools so that, through *in vivo* and *in vitro* biological studies, we can better understand the role of kinase targets during disease progression and therapy in healthy and diseased cells. In this context, this work establishes novel routes to new chemical tools, validates their identity and action, and explores their application in providing new insights into biochemical processes and new opportunities for chemical intervention in pathophysiological events.

Abbreviations

Aβ	β-amyloid peptides
ACT	Adoptive cell transfer
AD	Alzheimer's disease
$AgNO_3$	Silver nitrate
AIDS	Acquired immunodeficiency syndrome
ALPS	Autoimmune lymphoproliferative syndrome
ATP	Adenosine tri-phosphate
BAK	BCL2 homologous antagonist/killer
BAX	BCL2-associated X protein
BCL2	B-cell lymphoma 2
BH3	BCL2 homology 3 domain
BIM	BCL2-like protein 11
(±)-BINAP	(±)-2,2′-Bis(diphenylphosphino)-1,1′-binaphthalene
Boc	*tert*-Butyloxycarbonyl
BODIPY	4,4-difluoro-4-bora-3a,4a-diaza-s-indacene
CAR	Chimeric antigen receptor
CC	Coordination cluster
CD8	Cluster of differenciation
CDKI	Cylin-dependent kinase inhibitor protein
CLK	Cdc2-like kinase
CNS	Central nervous system
DBU	1,8-diazabicyclo[5.4.0]undec-7-ene
DCM	Dichloromethane
DCR2	Decoy death receptor-2
DDC	*N,N'*-didansyl –L-cystine
DDR	DNA damage response
DEC1	Differentiated embryo -chonrocyte expressed-1
DFG	Aspartic acid (D), phenylalanine (F), glycine (G)
DMF	Dimethylformamide
DMSO	Dimethyl sulfoxide

DNA	Deoxyribonucleic acid
DR	Death receptor
DS	Down's syndrome
DSCR 1	Downs syndrome critical region 1
ER	Endoplasmic reticulum
ERK2	Extracellular signal-regulated protein kinase 2
FADD	FAS-associated death domain
FC	Flash chromatography
FDA	Food and Drug Administration
FRET	Förster (or fluorescence) resonance energy transfer
h	Hour
HCl	Hydrochloric acid
HDAi	Histone deacetylase inhibition
HF	Hydrofluoric acid
HeLa	Henrietta Lacks
HSA	Human serum albumin
IAPs	Inhibitors of apoptosis
IBX	*o*-Iodoxybenzoic acid
IL-1β	Interleukin-1β
IUPAC	International Union of Pure and Applied Chemistry
JNK	c-Jun N-terminal kinases
km	Kilometer
LIMK	LIM-kinase (LIM – Lin11, Isl-1, Mec-3)
MAPK	Mitogen-activated protein kinase
MCR	Multicomponent reaction
MK2	Mitogen activated protein kinase-activated protein kinase 2
MPTP	Mitochondrial permeability transition pore
mRNA	Messenger ribonucleic acid
mTOR	Mechanistic target of rapamycin
NBS	*N*-bromosuccinimide
NCCD	Nomenclature Committee on Cell Death
NClS	*N*-chlorosuccinimide
NEt_3	Triethylamine

NFAT	Nuclear factor of activated T cells
NFATc	Nuclear factor of activated T cells
NFTs	Neurofibrillary tangles
NIS	*N*-iodosuccinimide
NIR	Near infra-red
PARP	Poly ADP ribose polymerase
PEG	Polyethylene glycol
PeT	Photo-induced electron transfer
PET	Positron emission tomography
PIM	Proto-oncogen serine/threonine-protein kinase
pK_a	Acid dissociation constant
$POCl_3$	Phosphorus oxychloride
pRB	Retinoblastoma protein
R1-mAb	Monoclonal anti-FGFR1 antibodies
RAS	Proto-oncogene protein
RT	Room temperature
SAHFs	Senescence associated heterochromatic foci
SAR	Structure-activity relationship
SDFs	Senescence associated DNA-damage foci
STS	Staurosporine
TEY	Threonine (T), glutamic acid (E), tyrosine (Y)
TFA	Trifluoroacetic acid
THF	Tetrahydrofluran
TLC	Thin layer chromatography
TNF	Tumour necrosis factor
TNF-α	Tumour necrosis factor-α
TP53	Tumour protein 53
TRAIL	TNF-related apoptosis-inducing ligand
WS	Werner's Syndrome
XIAP	X-linked inhibitor of apoptosis

Table of Contents

Declaration ..... **i**

Acknowledgements ..... **ii**

Abstract ..... **iii**

Abbreviations ..... **v**

Table of Contents ..... **viii**

Chapter 1 – Introduction **1**

1.1. CELL DEATH 1

1.1.1. Apoptosis 2

1.1.2. Autophagy 11

1.1.3. Cornification 12

1.1.4. Necrosis 13

1.1.5. Senescence 14

1.2. CANCER 16

1.2.1. Cancer Therapy 17

1.3. IMAGING CELLS 29

1.3.1. Fluorescence 29

1.3.2. Aposense – Small Molecule Detectors of Apoptosis 31

1.4. AGEING 34

1.4.1. Werner's Syndrome 34

1.5. P38 AND MK2 37

1.5.1. The p38 MAPK cascade 38

1.5.2. P38 inhibitors 39

1.5.3. MK2 inhibitors 41

1.6. PROJECT AIMS 46

1.6.1. Microwave-assisted organic synthesis 47

Chapter 2: Diagnostic tools **49**

2.1. BACKGROUND AND AIMS 49

2.2. INTRODUCTION 49

2.2.1. Investigation into small-molecule fluorescent probes 51

2.3. RESULTS 67

2.3.1. Didansyl cystine based fluorophores 67

2.3.2. Development of BODIPY library 70

2.3.3. Towards a drug-like structure 101
2.4. FUTURE PERSPECTIVES 105
2.5. CONCLUSION 107

Chapter 3: Inhibitory tools 108
3.1. BACKGROUND AND AIMS 108
3.1.1. Background of PF-3644022 (33) 108
3.2. SYNTHETIC ROUTES 112
3.2.1. Formation of 5-nitrobenzo[b]thiophene-2-carboxylic acid (106) 112
3.2.2. Formation of 3-bromo-5-nitrobenzo[b]thiophene-2-carboxylate (110) 116
3.2.3. Formation of (R)-methyl 3((2-((tert-butoxycarbonyl)amino)propyl-amino-5-nitrobenzo[b]thiophene-2-carboxylate (112) 116
3.2.4. Formation of (3R)-3-methyl-9-nitro-1,2,3,4-tetrahydro-5H-[1]benzothieno[3,2-e][1,4]diazepin-5-one (115) 121
3.2.5. Formation of (3R)-9-amino-3-methyl-1,2,3,4-tetrahydro-5H-[1]benzothieno[3,2-e][1,4]diazepin-5-one (116) 122
3.2.6. Formation of (R)-10-methyl-3-(6-methylpyridin-3-yl)-9-10-11-12-tetrahydro-8H-[1,4]diazepino[5',6':4,5]thieno[3,2-f]quinoline-8-one. PF-3644022 (33) 123
3.3. FUTURE PERSPECTIVES 135
3.4. CONCLUSION 137

Chapter 4 – Conclusions 138

Chapter 5 – Experimental 142
CHAPTER 2 143
3,3'-disulfanediylbis(2-(5-(dimethylamino)naphthalene-1-sulfonamido)propanoic acid) (26) 143
General Procedure for BODIPY Synthesis 144
10-(5-bromopentyl)-2,8-diethyl-5,5-difluoro-1,3,7,9-tetramethyl-5H-dipyrrolo[1,2-c:2',1'-f][1,3,2]diazaborinin-4-ium-5-uide (69) 144
10-(3-bromopropyl)-2,8-diethyl-5,5-difluoro-1,3,7,9-tetramethyl-5H-dipyrrolo[1,2-c:2',1'-f][1,3,2]diazaborinin-4-ium-5-uide (76) 145
10-(5-bromopentyl)-5,5-difluoro-5H-dipyrrolo[1,2-c:2',1'-f][1,3,2]diazaborinin-4-ium-5-uide (58) 145
10-(3-bromopropyl)-5,5-difluoro-5H-dipyrrolo[1,2-c:2',1'-f][1,3,2]diazaborinin-4-ium-5-uide (60) 146
10-(bromomethyl)-5,5-difluoro-5H-dipyrrolo[1,2-c:2',1'-f][1,3,2]diazaborinin-4-ium-5-uide (62) 147

10-(bromomethyl)-5,5-difluoro-3-(1H-pyrrol-2-yl)-5H-dipyrrolo[1,2-c:2',1'-f][1,3,2]diazaborinin-4-ium-5-uide (63) 147
10-(Bromomethyl)-5,5-difluoro-3,7-dimethyl-5H-dipyrrolo[1,2-c:2',1'-f][1,3,2]diazaborinin-4-ium-5-uide (83) 148
General Procedure for Attachment of Methylated Meldrum's Acid to BODIPY 148
2,8-diethyl-5,5-difluoro-1,3,7,9-tetramethyl-10-(5-(2,2,5-trimethyl-4,6-dioxo-1,3-dioxan-5-yl)pentyl)-5H-dipyrrolo[1,2-c:2',1'-f][1,3,2]diazaborinin-4-ium-5-uide (75) 149
5,5-difluoro-3,7-dimethyl-10-((2,2,5-trimethyl-4,6-dioxo-1,3-dioxan-5-yl)methyl)-5H-dipyrrolo[1,2-c:2',1'-f][1,3,2]diazaborinin-4-ium-5-uide (84) 149
General Procedure for Ring Opening Meldrum's Acid 150
10-(6,6-dicarboxyheptyl)-2,8-diethyl-5,5-difluoro-1,3,7,9-tetramethyl-5H-dipyrrolo[1,2-c:2',1'-f][1,3,2]diazaborinin-4-ium-5-uide (73) 150
Dimethyl 2-((6-chloropyridin-3-yl)methyl)-2-methylmalonate (88) 151
2-((6-Chloropyridin-3-yl)methyl)-2-methylmalonic acid (89) 151
CHAPTER 3 153
Methyl 3-Aminobenzo[b]thiophene-2-carboxylate (107) 153
Methyl 3-Aminothieno[2,3-b]pyridine-2-carboxylate (108) 154
Methyl 5-nitrobenzo[b]thiophene-2-carboxylate (105) 155
5-Nitrobenzo[b]thiophene-2-carboxylic acid (106) 156
3-Bromo-5-nitrobenzo[b]thiophene-2-carboxylic acid (109) 157
Methyl 3-bromo-5-nitrobenzo[b]thiophene-2-carboxylate (110) 157
(R)-Methyl 3-((2-((tert-butoxycarbonyl)amino)propyl)amino)-5-nitrobenzo[b]thiophene-2-carboxylate (112) 158
(3R)-3-Methyl-9-nitro-1,2,3,4-tetrahydro-5H-[1]benzothieno[3,2-e][1,4]diazepin-5-one (115) 159
(3R)-9-Amino-3-methyl-1,2,3,4-tetrahydro-5H-[1]benzothieno[3,2-e][1,4]diaepin-5-one (116) 160
tert-Butyl ([2R]-1-aminopropan-2-yl)carbamate (111) 160
6-Methylpyridine-3-carboxaldehyde (120) 161

Chapter 6 – Bibliography 163

Chapter 1 – Introduction

This chapter will discuss the background and premise for the projects described in this thesis. First there will be a discussion on the different forms of cell death and cellular ageing and the implication in human health. The scope for therapeutic intervention will also be explored. The second half of this chapter will include a discussion on the scope for development of kinase inhibitors, specifically p38 and MK2, in order to investigate their roles in human ageing and age-related diseases. The rare autosomal disorder, Werner's Syndrome, will also be discussed as a model for normal ageing.

1.1. Cell death

Death is an inevitable part of life for all living organisms including cells. Without cell death, an average 80 year old human would be in possession of a 16 km intestine and carry around approximately two tons of bone marrow and lymph nodes.[1] As such, "programmed cell death" is a normal part of a cell's lifecycle, usually at the end of its replicative lifespan, but can be triggered by external factors (described later in **Chapter 1**). It is worth noting at this point that programmed cell death is not a term that can be used synonymously with apoptosis, which is a common misconception.

In 2009, the Nomenclature Committee on Cell Death (NCCD) published a set of guidelines to classify and define different types of cell death and the associated morphological changes.[2] The NCCD described four distinct modes of cell death; apoptosis, autophagy, cornification and necrosis, with apoptosis and necrosis being the most widely used classifications of mammalian cell death.[2] Each mode of cell death will now be described in **sections 1.1.1-1.1.5.** In **section 1.1.5,** cellular senescence will be discussed, though not as a form of cell death but in respect to cellular ageing. This is an important process to consider when discussing human ageing and Werner's Syndrome (WS) in **section 1.3.**

As a genetically controlled process, programmed cell death has been linked to several diseases such as cancers, viral infections, autoimmune diseases, neurodegenerative disorders, and AIDS (acquired immunodeficiency syndrome).[3]

Therefore it can be postulated that by altering the course of programmed cell death, there is a potential to create new therapies for a range of diseases. These will be discussed in **section 1.2**.

1.1.1. Apoptosis

Apoptosis is a form of programmed cell death and is a natural part of a cell's lifecycle. It is a very important process which controls the regulation and maintenance of cell populations in tissues, as part of homeostasis. It is also a defence mechanism that is employed by cells that are damaged or diseased in order to stop replication of mutations in new cells, therefore protecting the organism from further damage.[4] According to a review by Ulukaya, Acilan and Yilmaz in 2011, abnormal rates of apoptosis have been linked to several disorders.[5] Increased rates of apoptosis are linked to disorders such as AIDS, neurodegenerative disorders, insulin-dependent diabetes, hepatitis C infection, myocardial infarction and atherosclerosis and decreased rates of apoptosis are linked to autoimmune diseases and cancer.

The term "apoptosis" was proposed in 1972 by Kerr, Wyllie and Currie and was derived from a Greek word, meaning "dropping off".[6] Prior to their publication, cell death was assumed to take place but no study had considered the mechanisms behind it, and therefore no classification of the different types of cell death had been proposed. Using electron microscopy to visualize cells, the authors described two distinct stages taking place during the newly described apoptosis; the first was the formation of apoptotic bodies and the second was phagocytosis. Since then many studies have been carried out to try and understand the mechanisms underlying apoptosis and we now know that there is in fact several stages.

Apoptosis is characterised by distinct, observable morphological changes; an apoptotic cell appears to shrink, chromatin aggregates and condenses around the nuclear membrane and the cellular membrane remains intact whilst undergoing a process called blebbing (the membrane starts to pinch in and detach from the main cell as an apoptotic body). Apoptotic bodies containing condensed cell organelles are then cleared away by phagocytes; this process is controlled and highly regulated and as such does not trigger an inflammatory response (**Figure 1**).

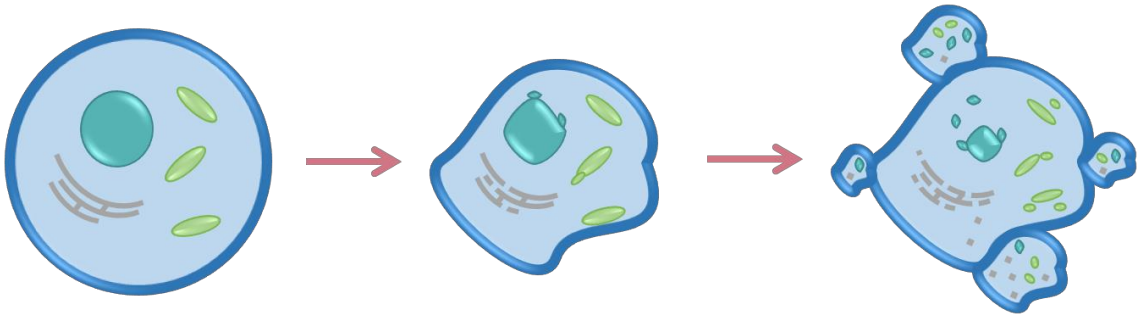

Figure 1: Diagram depicting a cell undergoing apoptosis. Cell and organelles undergo shrinkage and blebbing, followed by the formation of apoptotic bodies.

For apoptosis to occur, cysteine proteases of the caspase family need to be activated sequentially. This can be done via one of three pathways; the death receptor mediated pathway (extrinsic pathway), the mitochondrial mediated pathway (intrinsic pathway) or the endoplasmic reticulum (ER) stress pathway. The death receptor and mitochondrial mediated pathways both rely on caspase-3 to initiate apoptosis (Figure 2). The death receptor pathway requires a member of the tumour necrosis factor (TNF) kinase family to bind to the death receptors on the surface of the cell. This recruits the protein Fas-associated death domain (FADD) which in turn recruits caspase-8, leading to the activation of caspase-3. The mitochondrial mediated pathway employs proapoptotic and antiapoptotic members of the BCL2 protein family and is initiated by oxygen radicals, γ radiation or DNA injury.[7] These stimuli activate proapoptotic BH3 (BCL2 homology 3 domain) proteins which inhibit the antiapoptotic BCL2 proteins, thereby allowing proapoptotic BAX and BAK proteins to increase the permeability of the mitochondria, releasing cytochrome *c* which activates caspase-9 which in turn activates caspase-3.[7–9]

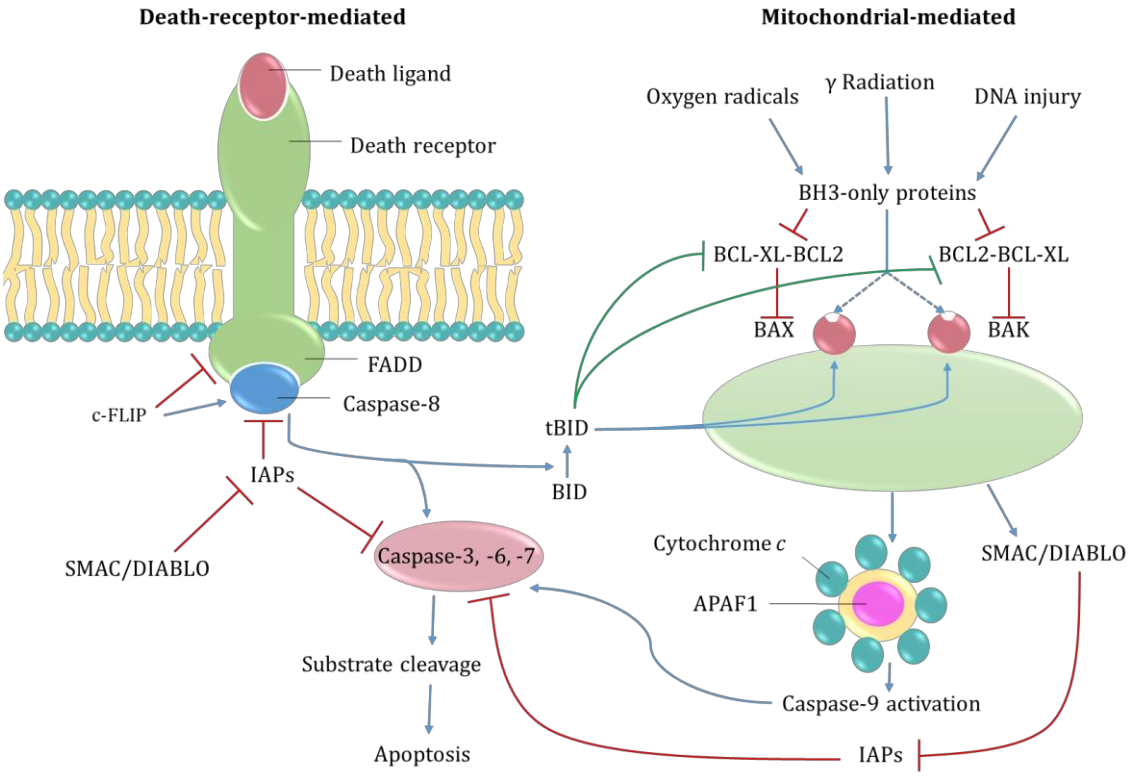

Figure 2: Pathways leading to the activation of caspase-3, known as an executioner caspase, triggering apoptosis. Left: Death receptor mediated pathway. Right: Mitochondrial mediated pathway. Adapted from Swanson et al. 2009.[9]

The ER stress pathway occurs when the main functions of the ER are disturbed; the main functions of the ER are folding, modification and the sorting of newly synthesized proteins, Ca^{2+} storage and signalling.[10] Overloading or depleting the Ca^{2+} stocks leads to changes in protein folding and subsequently ER stress. If the stress is prolonged this leads to accumulation of procaspase-12 in the ER membrane, which is then activated and cleaved by m-calpain. This can also be brought on by mobilization of intracellular Ca^{2+} stores. Activated procaspase-12 goes on to activate caspases that lead to apoptosis.[11]

1.1.1.1. Disorders associated with apoptosis

As mentioned previously, apoptosis has been found to play a role in many disorders. Disorders such as AIDS, neurodegenerative disorders, insulin-dependent diabetes, hepatitis C infection, myocardial infarction and atherosclerosis have been linked to increased rates of apoptosis whilst decreased rates of apoptosis are linked to

autoimmune diseases and cancer.[5] As such many therapeutics have been developed with the aim to either induce or prevent apoptosis.

Cancer

If the process leading to the initiation of apoptosis is defective, then this can lead to potentially cancerous growths known as neoplasms, increased expression of prosurvival BCL2 family proteins and mutations of the tumour suppressor gene TP53. TP53 is also the encoder of the protein p53 which suppresses tumour growth by initiating apoptosis in response to DNA damage. Therefore, by mutating TP53, apoptosis is not induced when DNA damage occurs, leading to the formation of abnormal growths.[7,9,12,13] The development of cancers and therapeutic interventions will be discussed in more detail in **section 1.2**.

Immune system

The proapoptotic BH3-only protein BIM is relied upon for the deletion of clones of B and T cells that express autoreactive antigen receptors. Both BIM and the death receptor FAS mediate the killing of mature, antigen activated B and T cells during the shut-down of immune responses. Defects in the FAS ligand or receptor appear in patients suffering with autoimmune lymphoproliferative syndrome (ALPS), a rare genetic disorder which causes lymphocytes to accumulate in the lymph nodes, liver and spleen causing them to enlarge.[11] It is also thought that the FAS death receptor is involved in type 1 diabetes by CD8 T cells expressing the FAS ligand interacting with FAS receptors on insulin secreting cells, thereby inducing cell death and leading to the loss of beta cells from pancreatic islets.[9]

Neurological disorders

There is evidence to suggest that, whilst neurons are in the development stage, they are particularly susceptible to apoptosis being triggered by noxious stimuli which leads to the development of neonatal brain disorders.[14] For example, foetal alcohol syndrome, a disorder brought on by the consumption of alcohol during pregnancy that can lead to both physical and mental impairments in the child, is caused by ethanol induced blockage of the *N*-methyl-D-aspartate (NMDA) receptor and activation of γ-aminobutyric acid (GABA) receptor leading to neurodegeneration via

apoptosis.[15] These same receptors are also modulated by general anaesthetics and animal models have shown that use of general anaesthetics during pregnancy could also cause defects in brain development.[16]

Cardiovascular diseases

Apoptosis can be triggered prematurely by lack of oxygen due to decreased blood flow, otherwise known as hypoxia, during events such as a myocardial infarction.[9] This can lead to an increase in the size of an infarction. Therefore, it could be hypothesized that if apoptosis could be inhibited then this would prevent cell loss. For example, the use of cyclosporine (**1, Figure 3**) as an apoptosis inhibitor has been trialled in patients suffering with an acute myocardial infarction before undergoing a percutaneous coronary intervention and the results showed a significant reduction in the size of the infarcted tissue when imaged by MRI (magnetic resonance imaging) in comparison to a control group of patients.[17] **1** works as an apoptosis inhibitor by blocking mitochondrial permeability-transition pores, which as discussed in **section 1.1.1.**, leads to release of cytochrome *c* and induction of apoptosis.

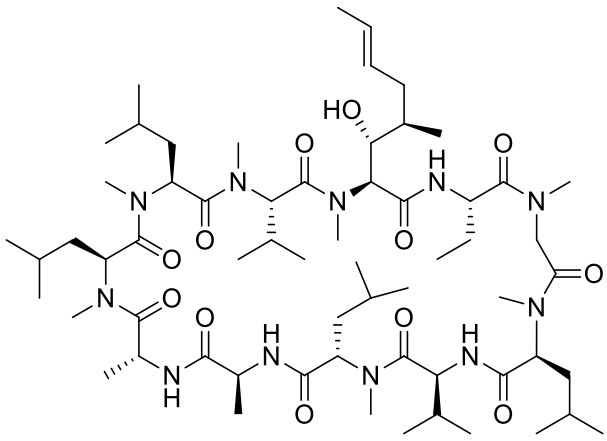

1

Figure 3: Cyclosporine.

Sepsis

Sepsis is a serious condition with a high mortality rate that is brought on by the immune system overreacting to a severe infection, causing inflammation

throughout the body which ends in immunosuppression.[18–20] The immunosuppression means that the body loses its ability to fight the primary infection as well becoming susceptible to new infections.[9] Animal studies have shown that there is an increase in apoptosis of lymphoid organs and parenchymal tissues, leading to the conclusion that apoptosis plays a role in organ failure in severe cases.[18,20] The increase of lymphocyte apoptosis has been shown to be a cause of sepsis lethality in experiments where apoptosis of lymphocytes was inhibited which resulted in improved survival.[21] There is also evidence to suggest that the septic response may be accelerated by a combination of overactivation of neutrophils and macrophages as well as poorly regulated cell death; delayed apoptosis of neutrophils and necrosis in tissues.[20] Therefore targeting cell death for therapeutic intervention in the treatment of sepsis is an attractive prospect.

1.1.1.2. Reversal of apoptosis

For a long time, apoptosis was considered as an irreversible process; once it had been induced the cell would die. However, there is now evidence to suggest that this is not the case. Though the "point of no return" is still debated, it is generally accepted that apoptosis is irreversible after caspase activation and once DNA damage had occurred.

In 1996, Look *et al.* demonstrated that the E2A-HLF fusion gene, the chimeric oncogene responsible for the transformation of B-cells into leukaemic cells, was able to extend cell survival as well as reverse IL-3 (interleukin-3) dependent and p53-mediated apoptosis.[22] During the study cells were treated with $ZnSO_4$ and the growth factor, IL-3, was removed. Cells that did not express E2A-HLF went through the process of apoptosis, whereas cells that did express E2A-HLF survived and went on to resume their normal cell cycle upon the return of IL-3.[22] The study also provided evidence that cells that overexpressed E2A-HLF were protected from p53 mediated apoptosis when exposed to ionized radiation, thus leading the authors to conclude that E2A-HLF positive leukaemic cells were protected against both radiation and drug-induced apoptosis. Though this study did not provide evidence that the process of apoptosis could be reversed once initiated, it did provide significant evidence to prove that cancerous cells were able employ mechanisms to

evade apoptosis-inducing agents, surviving in their presence and carrying on with normal cellular functions once the agent had been removed.

A report by Fung *et. al.* in 2009 showed that cancer cells that had an apoptosis-inducing agent applied to them were able to recover once the agent was removed and could even go on to continue to proliferate.[23] The group first tested HeLa cells by exposing them to the apoptosis-inducer jasplakinolide (**2**, **Figure 4**) and observed the morphological changes using real-time living cell microscopy after 3 hours of exposure.

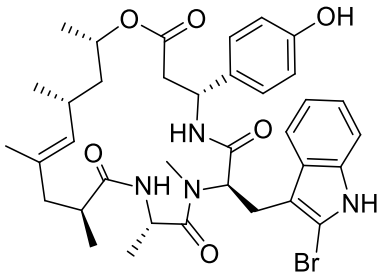

2

Figure 4: Jasplakinolide.

Aside from visual confirmation of apoptosis, further confirmation was acquired using colorimetric caspase assays to monitor the activation of apoptotic protease caspases and cleavage of pro-caspase-3 and an MTT assay to confirm the dysfunction of mitochondria. Cell counting revealed that 96% of the cells displayed characteristic hallmarks of apoptosis. The cells were then washed and cultured in fresh medium. After 14.5 hours, it was observed using living cell microscopy that the cells regained their normal morphology, with a cell count confirming 92% of the cells had regained their normal morphology after 24 hours (**Figure 5**).

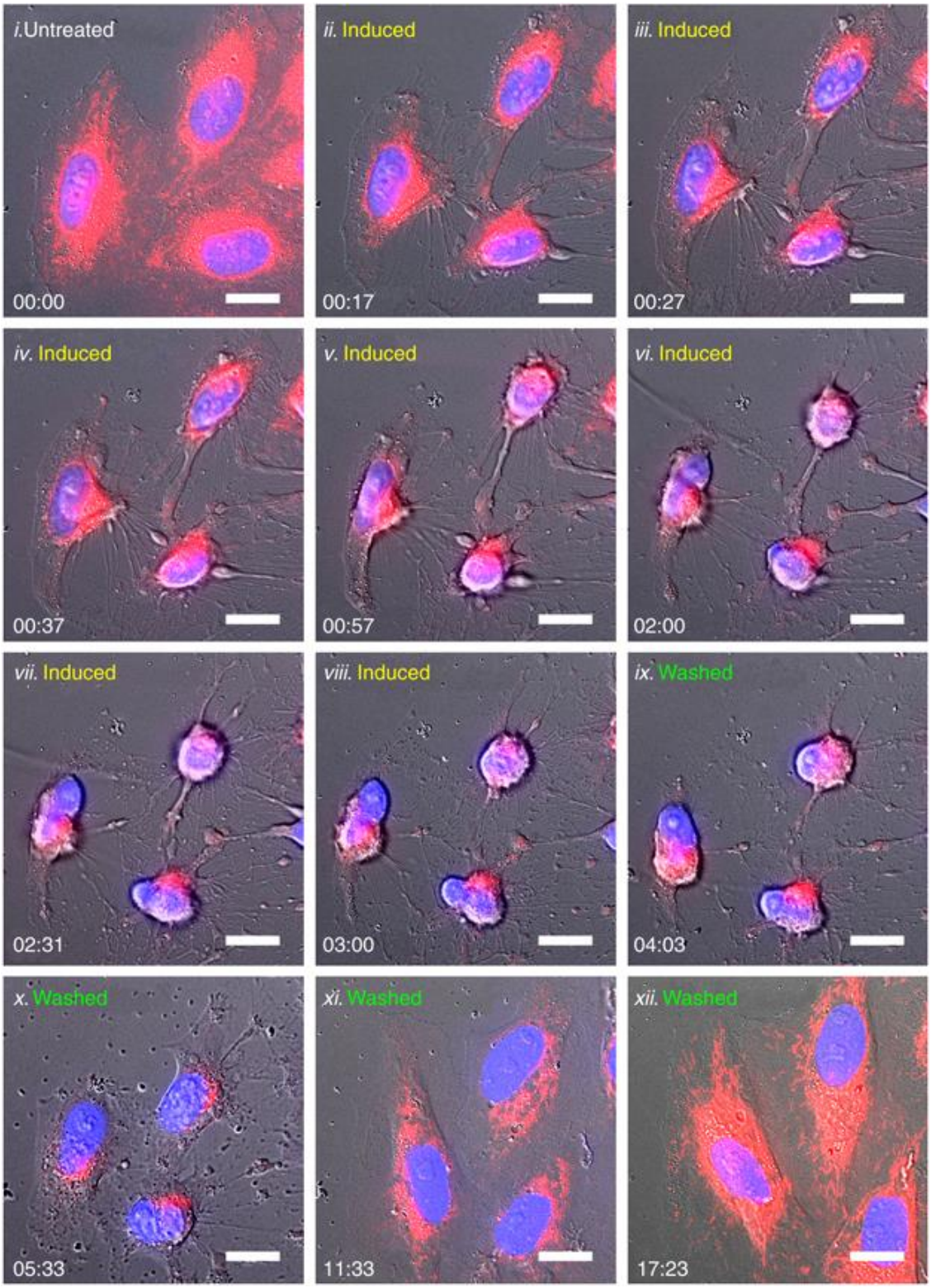

Figure 5: Images taken to show the application of apoptosis-inducing agents causing cells to go through the early stages of apoptosis (images ii – viii) followed by removal of the apoptosis-inducing agent by washing, leading to the cells regaining their normal morphology (images ix – xii). Image used with permission from Nature Publishing Group.[23]

Survival was further proven by the cells going on to proliferate with no significant difference in percentage proliferation compared to the control cells. The study included testing HeLa cells with different apoptosis-inducing agents such as ethanol and staurosporine (**3**, **Figure 6**). Other cancer cell lines were also tested; human skin cancer A375, liver cancer HepG2, breast cancer MCF7 and prostate cancer PC3. The authors were able to demonstrate the ability of cancer cells to potentially escape the culling process during treatments such as chemotherapy. Therefore, recurrence of cancer in patients undergoing chemotherapy was proposed to be due to the proliferation of surviving cancer cells in the intervals between treatments, as well as the deficiency of apoptotic pathways in cancer cells, anticancer drug resistance of the tumorigenic stem cells and the inefficiency of drug penetration into solid tumours.

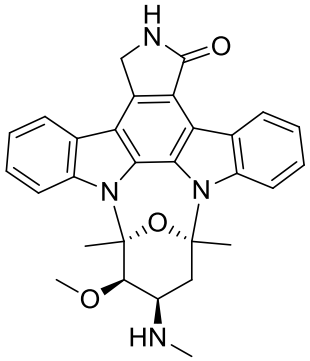

3

Figure 6: Staurosporine.

The study also suggested that the "point of no return" was in proportion with the amount of nuclear fragmentation that had taken place: the more nuclear fragmentation that had occurred, the less likely it was that the cell would survive.[23]

In 2012, the same group published another report, this time proposing the term "anastasis" (derived from a Greek word meaning "rise to life") to refer to the phenomenon of cells recovering from apoptosis.[24] This study presented evidence that cells can recover even once the "executioner caspase", caspase-3, has been activated. This was found to be true in several different cell lines. Liver and heart cells, embryonic fibroblast NIH 3T3 cells and HeLa cells were all exposed to an

apoptosis-inducing agent (ethanol, DMSO or jasplakinolide (**2**, **Figure 4**), morphological and biochemical hallmarks of apoptosis were observed (cell shrinkage, blebbing, etc.) and then the apoptosis-inducing agent was washed away, after which point a reversal of apoptosis and subsequent proliferation was observed. Gel electrophoresis assays carried out once the apoptotic-inducing agent had been applied, then again after the agent had been removed, detected that DNA damage had occurred during apoptosis, but that the damage had been repaired after removal of the agent. Despite this apparent repair, micronuclei (fragments of unrepaired DNA) were found to be present and even formed in daughter cells during the first cell division after reversal of apoptosis. Due to the genetic alteration of these cells, the authors suggested that the reversal of apoptosis could be carcinogenic. This mechanism for survival could be the reason why repeated injury leads to increased susceptibility for developing cancer; for example, alcoholics are at an increased risk of developing liver cancer. This mechanism for survival after a crisis leads to genomic rearrangements that could explain cancer cells' ability to survive treatments such as chemo- and radiotherapy and then go on to become resistant. Mutations that occur in cells that were healthy before chemo- or radiotherapy may also explain the development of new tumours.

This apparent escape mechanism from apoptosis has been the driving force behind one of the research topics discussed in this thesis. The hypothesis is that by developing chemical tools that can preferentially enter cells going through apoptosis, those tools could then be used to deliver a molecular cargo into the cells. This molecular cargo could then be used to ensure that the cell does indeed die, therefore substantially reducing the risk of cancers returning post-treatment and developing resistance to chemo- and radiotherapeutics.

1.1.2. Autophagy

This term is derived from the Greek words "auto" meaning self and "phagy" meaning to eat. This is a process by which a cell will "eat" organelles that are deemed non-essential in an effort to survive when exposed to certain stress conditions, either environmentally or developmentally.[9,25] For instance, these stress conditions can include deprivation of nutrients, misfolding of proteins or damage to the

mitochondria. Autophagy has been linked to many diseases and has led to the development of many drug candidates, many of which specifically target various forms of cancer.[26,27]

1.1.3. Cornification

Cornification is a type of programmed cell death that is responsible for the formation of skin, hair and nails.[2,28] The process involves removal of organelles from the cell followed by the accumulation of keratin in the cytoplasm to provide strength. Cross-linking of transglutaminase proteins and the covalent attachment of lipids, excreted into the extracellular space, to the cornified envelope proteins leads to the formation of a waterproof barrier (**Figure 7**).[28]

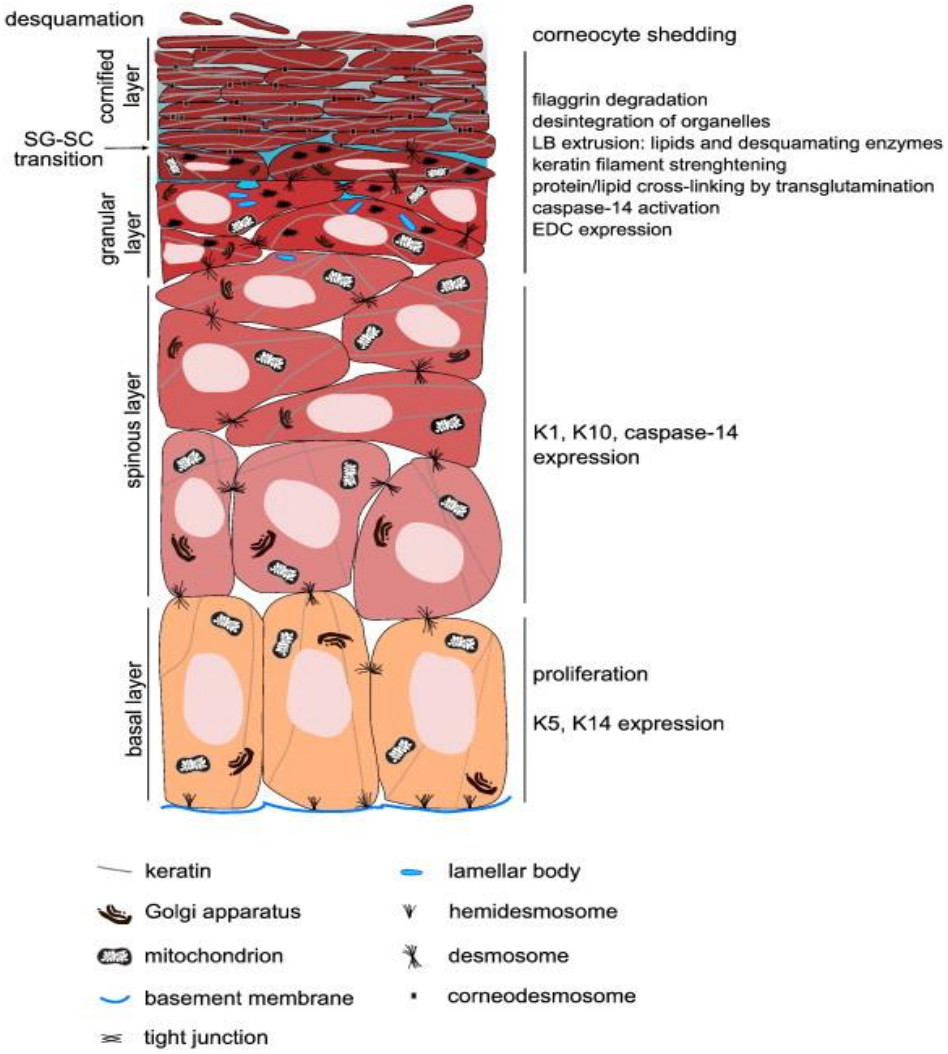

Figure 7: Process of cornification. Image used with permission from Elsevier.[28]

1.1.4. Necrosis

Derived from the Greek word "nekros" meaning corpse, necrosis is characterized by the swelling of a cell and its organelles, eventually leading to the rupture of the cell membrane and the spilling of the cell contents outside of the cell (**Figure 8**). This traumatic type of cell death triggers an immune response in the form of inflammation. As such, the process is not considered as programmed cell death, but an accidental cell death that is in response to some kind of trauma. However, there is evidence to suggest that in certain instances necrosis can be triggered, therefore making it a controlled form of cell death known as "necroptosis".[29,30]

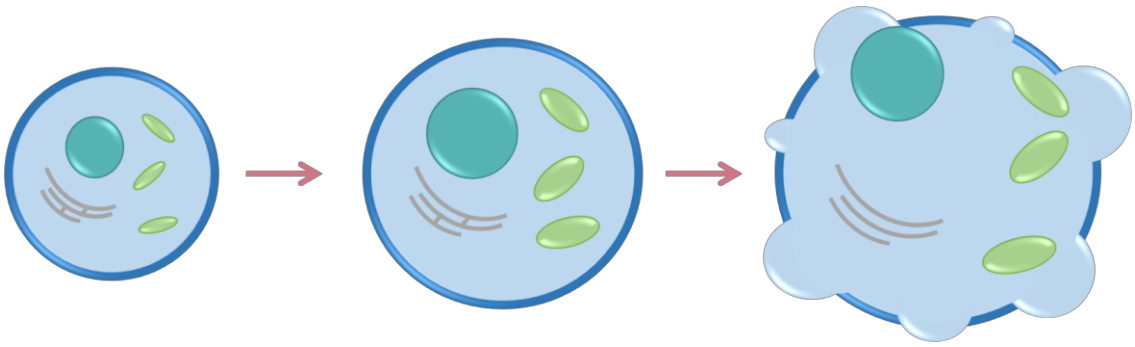

Figure 8: Diagram depicting a cell undergoing necrosis. The cell and organelles swell until the cell membrane ruptures, spilling the contents outside of the cell, which then triggers an inflammatory response.

1.1.4.1. Necroptosis

Necroptosis, otherwise known as regulated necrosis, is initiated by the binding of TNF to the receptor TNFR1 and subsequent activation of RIP1 and RIP3 kinases.[2,28–30] Like necrosis, it is characterised by cellular and organelle swelling culminating in a ruptured cell membrane and leakage of the cell's contents. The controlled nature of this form of necrosis was discovered when a small molecule known as necrostatin-1 (**4**, **Figure 9**) was shown to suppress necrosis by inhibiting RIPK1 thereby blocking the effect of TNF.[29] This showed that, since necrosis could be regulated, there was scope to investigate its therapeutic potential. Necroptosis has been linked to inflammatory disorders such as Crohn's disease and multiple sclerosis but it is not known whether necroptosis is a causative factor of these conditions or whether it is a consequence of them.[29]

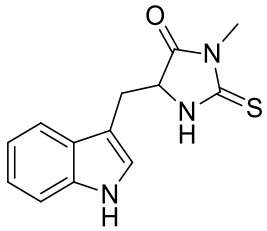

4

Figure 9: Necrostatin-1.

1.1.5. Senescence

The term senescence is derived from the Latin word "senex" which means old age and as such the term senescence is often used interchangeably with the terms "cellular ageing" or "replicative senescence". Cellular senescence was an idea first put forward by Hayflick in 1965 in a report that proved that cells did indeed have a limited replicative lifespan and can therefore be thought of as going through an ageing or senescence process; this was the opposite view to that held within the scientific community at the time.[31] Characteristic hallmarks of senescence are growth arrest, resistance to apoptosis and altered gene expression, though these characteristics are not unique to senescent cells. Instead, the tumour suppressor gene p16 is used as a marker to indicate apoptosis, though this can also be somewhat unreliable as not all senescent cells express p16 and tumour cells that have pRB function also express p16.[32] Other markers that can identify senescent cells include DEC1 (differentiated embryo-chondrocyte expressed-1), p15 (a CDKI), DCR2 (decoy death receptor-2), SAHFs (senescence associated heterochromatic foci) and SDFs (senescence associated DNA-damage foci).

There are a few factors that can cause cells to senesce. Telomere-dependent senescence occurs when telomeres become critically short, rendering proliferation impossible. This is due to a phenomenon known as the end-replication problem where, during DNA replication, DNA polymerase is unable to completely replicate DNA ends, proteins which cap the ends of telomeres as protection from degradation.[33] Each time the cell replicates, the telomeres are slightly shortened until eventually they become critically short. If DNA becomes damaged this can induce DNA-damage-initiated senescence, leading to the expression of p16. Chromatin perturbance, specifically euchromatin formation promoted by chemical

histone deacetylase inhibition (HDAi), appears to induce senescence, though the mechanism for this process is poorly understood. Oncogene-induced senescence has been observed when an oncogenic form of RAS was expressed in normal human fibroblasts.[32] Senescence can be induced by chronic stimulation of interferon-β which increases the concentration of intracellular oxygen radicals leading to a p53-dependent DDR (DNA damage response) and senescence. Stress has also been suggested to induce senescence by inducing p16-dependent, telomere-independent senescence, often referred to as cell-culture stress or culture shock.[32]

Cellular senescence has been linked to both cancer and ageing. For cancer progression, senescence can act as a barrier, suppressing tumorigenesis due to the requirement of cell proliferation. The link between ageing and senescence is not clear cut, as though it appears that the number of senescent cells increases with age, it is not clear whether they actually play a contributory part in the ageing process. Recently there has been progress made in this field that suggests that by inducing senescent cells to go through apoptosis they can be cleared from the body and reverse the signs of ageing.[34,35] The FOXO (foxhead box O) family of proteins was identified as being a potential therapeutic target for this process due to their involvement in cell cycle arrest, survival and stem cell signalling. FOXOs interact with p53 to induce cell cycle arrest and senescence. FOXO4 was identified as the factor responsible for interacting with p53 to prevent apoptosis. A cell-permeable-peptide was synthesized that interfered with the FOXO4-p53 interaction which induced apoptosis. In mouse models, fitness, fur density and renal function were restored.[35]

1.1.5.1. p53

p53 is a tumour suppression protein that responds to cellular stresses to stop the proliferation of cells that have developed mutations. The role of p53 is to bind to DNA where it recognizes damage. It can then initiate growth arrest, DNA repair or apoptosis. During growth arrest, the cdk inhibitor p21 is activated and the cell is stopped from proliferating until its DNA is repaired.[36] If repair is not possible, cell death by apoptosis is initiated via the activation of proapoptotic factors, such as BAX.[36] Mutation of p53 can therefore lead to the formation of neoplasms.

1.2. Cancer

In order for cells to form tumours that go on to become malignant, they require a succession of the six hallmarks of cancer, the proposition of which was introduced by Hanahan and Weinberg in 2000, an update of which was published in 2011 to include the potential of two hallmarks and two "enabling characteristics".[37,38] The originally reported six hallmarks are sustaining proliferative signalling, evading growth suppressors, resisting cell death, enabling replicative immortality, inducing angiogenesis and activating invasion and metastasis. Each of these hallmarks relies upon genome instability to generate genetic diversity that advances acquisition and inflammation and fosters multiple hallmark functions, the details of which will now be described.

Sustaining proliferative signalling

Homeostasis, i.e. the careful balance between cell proliferation and cell death, is thrown into upset by cancer cells which can continue proliferating. They are able to do this in a number of ways. While normal cells rely on other cells to produce mitotic growth signals to become proliferative, cancer cells have developed the ability to be proliferatively autonomous by producing and responding to their own growth factors in a positive feedback loop, also known as autocrine stimulation. They do this either by producing growth factor ligands or the cancer cells may send signals to recruited healthy cells within the tumour to provide them with various growth factors.[39,40]

Evading growth suppressors

As well as being able to sustain proliferation, cancer cells must also evade growth suppressors. Two key proteins involved in tumour growth suppression are RB (retinoblastoma-associated) and TP53 proteins. Cancer cells that are deficient in these pathways lack the ability to process intra- and extracellular signals that would signal that a cell should not go through the growth and division cycle.[41–43]

Resisting cell death

The process of apoptosis has been described in **section 1.1.1.** It is thought that cancer cells can employ various strategies to avoid triggering apoptosis. Most

commonly the tumour suppressor TP53 is missing from cancer cells, meaning that the upregulation of BH3-only proteins cannot occur. Apoptosis can also be avoided by the increased expression of anti-apoptotic regulators and survival signals, such as BCL-2 and Igf1/2, respectively, via the downregulation of pro-apoptotic factors such as BAX and BIM.[7,8,12,27]

Enabling replicative immortality

During the proliferation of healthy cells, telomeres become shortened until eventually they are no longer able to perform the duty of protecting the ends of chromosomal DNA from end-to-end fusion. Once telomeres are too short, apoptosis is induced. Cancer cells express telomerase, a DNA polymerase that adds segments to telomeres, circumventing any shortening of the telomeres during proliferative cycles. This essentially leads to cancerous cells becoming immortal.[44,45]

Inducing angiogenesis

For tumours to grow they must meet the same set of requirements as normal tissues, including access to nutrients and oxygen and the removal of carbon dioxide and waste. Angiogenesis is the process by which new blood vessels are produced and is normally only active in adults during wound healing or the female reproductive cycle. However, during tumour growth, angiogenesis is activated and causes existing vessels to grow new vessels to supply neoplastic growths.[46–48]

Activating invasion and metastasis

Cancer cells are able to escape the tumour mass and colonize other tissues. This can be achieved in two ways. The first is through the loss or downregulation of cell-to-cell and cell-to-matrix adhesion molecules, a family of proteins known as cadherins. The second is through the upregulation of adhesion molecules that are normally expressed during embryogenesis and organogenesis, such as N-cadherin.[49–51]

1.2.1. Traditional cancer therapy

There are many options for treating cancer and it is common to use several different treatment options at once to maximise the chances of treatment working. Once cancer is detected it will be treated as aggressively as possible (limitations of the

treatment will depend on the type/stage of cancer and the tolerance of the patient). Due to the toxicity of therapeutics, treatment needs to be delivered in cycles, killing cancer cells and shrinking the tumour size a little bit at a time, allowing the patient to recover in between cycles. Obviously, this can only be true if treatment is given with a curative intent. Sadly, that is not always possible and all that can be offered is treatment for palliative care, i.e. treatment would be provided either to extend the patient's life expectancy or to ease pain and suffering. In this case, treatments need to be carefully monitored to ensure that the side effects are not worse than the effects of the disease itself.

Chemotherapy and radiotherapy will be discussed here as these therapies focus on damaging cancer cells to induce cell death. However, these are not the only two forms of cancer treatment. There is also hormone therapy and targeted therapies such as use of protein kinase inhibitors, differentiating agents and immunotherapy.

1.2.1.1. Chemotherapy

Chemotherapy as a cancer treatment has a rather interesting history. During World War II, an attack on a cargo of mustard gas (**6**, **Figure 10**) led to a town being engulfed by the mustard gas (**6**), killing or severely burning more than 1000 of the town's inhabitants.[52] Autopsies of the victims led to the discovery that **6** had destroyed most of their white blood cells, suggesting a preferential attack of the chemicals on the bone marrow. Subsequently, a hypothesis was put forward that **6** could target cancer cells due to their similar nature of fast proliferation. Eventually this led to the development of mechlorethamine (**7**), a derivative of **6** which is still in use as a chemotherapeutic agent today against Hodgkin's disease, leukaemia and brain tumors.[52] Since then, a plethora of drugs have been developed that are derived from **6**, all working by targeting DNA and preventing it from replicating and dividing.

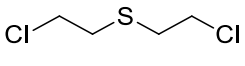

6

Figure 10: Mustard gas.

These chemotherapeutic drugs target proliferative cells indiscriminately, meaning that healthy cells that proliferate quickly are targeted as well as cancer cells, such as the digestive tract, skin and hair follicles and bone marrow.[53] This leads to many unpleasant side effects, including vomiting, diarrhoea, depression, hair loss and susceptibility to infections. As such, other drugs have been developed in order to combat these debilitating side effects, some examples of which will now be discussed.

Alkylating agents

This class of drugs work by reacting with DNA, forming covalent bonds that cause DNA breaks.[54–56] Examples of alkylating agents are derivatives of mustard gas (**6**) some of which are shown in **Figure 11**, though these are not the only class of alkylating agents used as chemotherapeutics.[57]

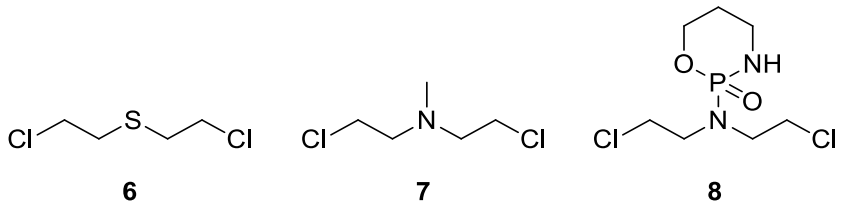

Figure 11: Examples of alkylating agents. **Left**: Mustard gas (**6**). **Middle**: Mechlorethamine (**7**). **Right**: Cyclophosphamide (**8**).

Platinum containing compounds are another form of alkylating agent. The three main platinum compounds currently used as chemotherapeutic agents are Cisplatin (**9**), Carboplatin (**10**) and Oxaliplatin (**11**) (**Figure 12**). All three work intracellularly, forming covalent bonds with nucleotides.[57–59]

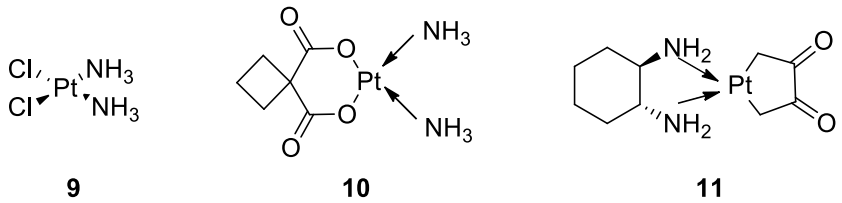

Figure 12: Examples of platinum containing alkylating agents: cisplatin (**9**), carboplatin (**10**) and oxiplatin (**11**).

Antimetabolites

Antimetabolites can work in two ways, either they inhibit the proteins needed for DNA synthesis or they become incorporated into DNA and RNA causing damage to or termination of the chain.[54,55,57,59] These modes of action are a consequence of the antimetabolites closely resembling the naturally occurring purines and pyrimidines (**Figure 13**).

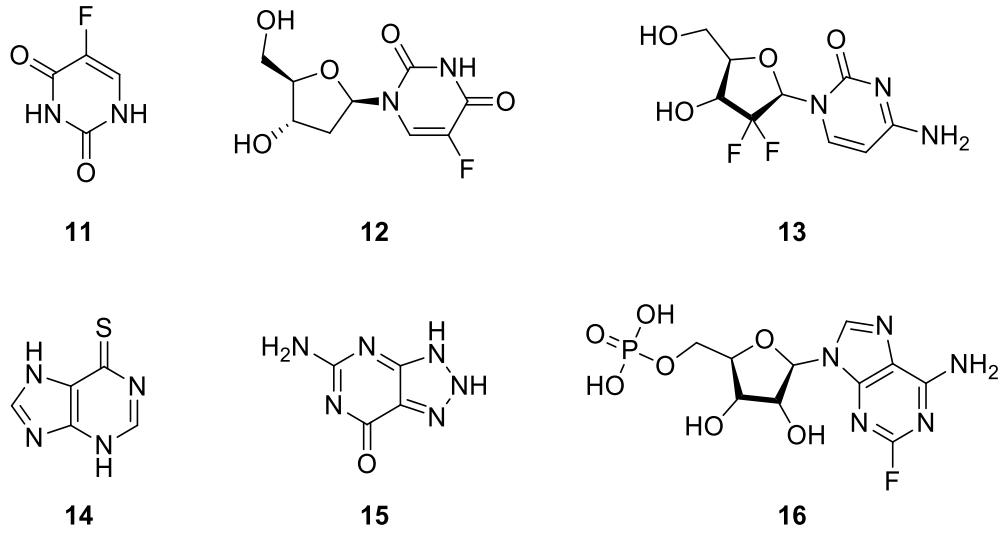

Figure 13: Examples of antimetabolites. Top row pyrimidine analogues: 5-fluorouracil (**11**), floxuridine (**12**) and gemcitabine (**13**). Bottom row purine analogues: mercaptopurine (**14**), azaguanine (**15**) and fludarabine (**16**).

Topoisomerase inhibitors

Topoisomerase is a class of proteins that help DNA strands separate for replication. By inhibiting this process, DNA damage is induced followed by cell death.[57,59] Examples of topoisomerase inhibitors are seen in **Figure 14**.

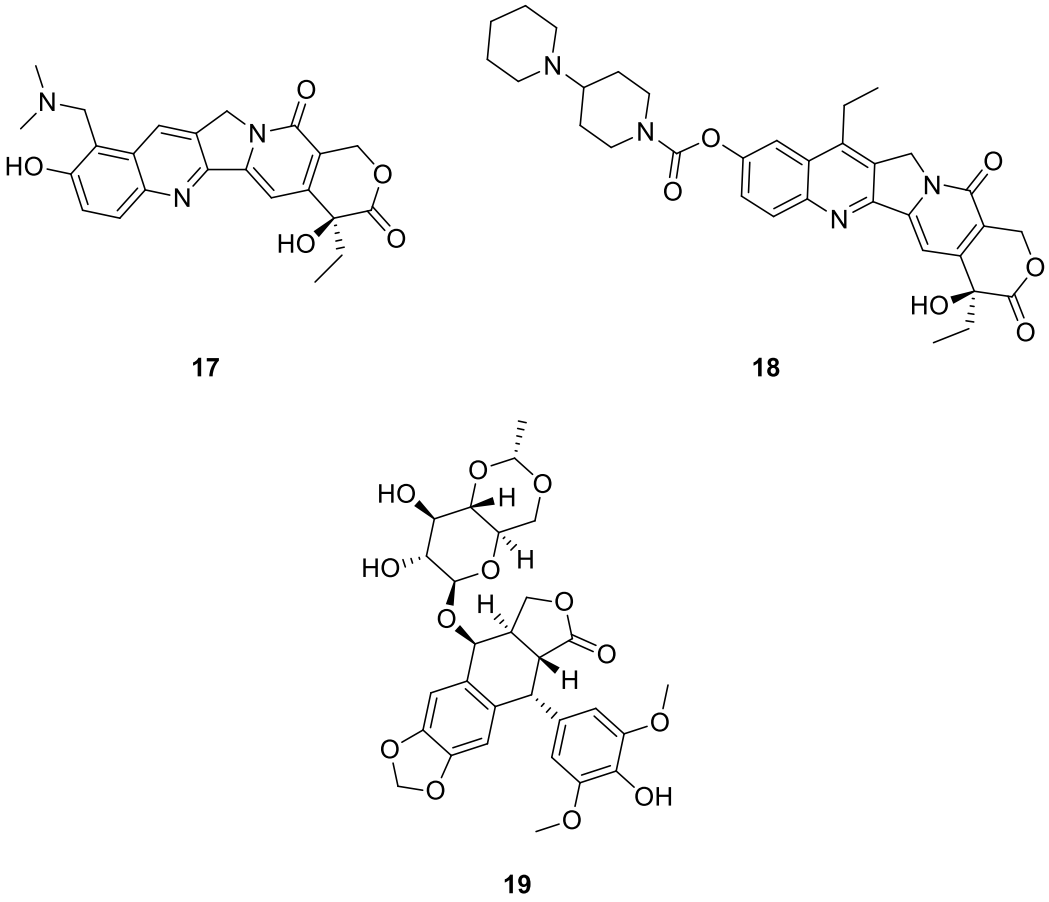

Figure 14: Examples of topoisomerase inhibitors. **Top**: topotecan (**17**), irinotecan (**18**). **Bottom**: etopside (**19**).

Antitumor antibiotics/anthracyclines

Originally produced by microorganisms as a class of antibiotics, these chemotherapeutics work in several different ways. They can cause DNA damage, generate free radicals to cause oxidative stress and also act as topoisomerase inhibitors.[57,59] Some examples of antitumor antibiotics/anthracyclines can be seen in **Figure 15**.

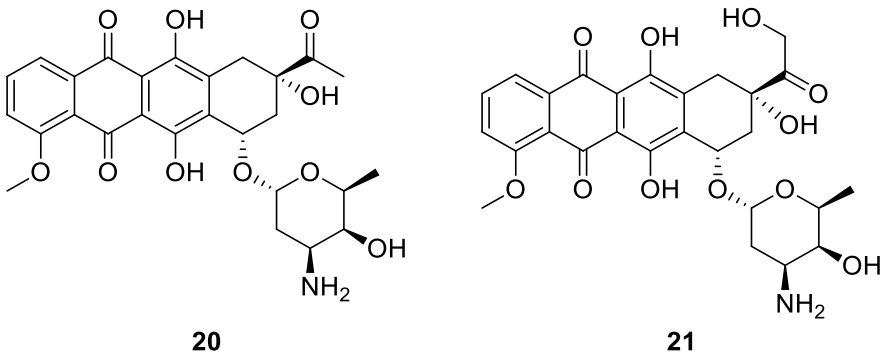

20 **21**

Figure 15: Examples of anti-tumour antibiotics: daunorubicin (**20**), doxorubicin (**21**).

Corticosteroids

These can be natural or synthetic hormones and work by inducing apoptosis through binding to receptors inside the cells.[59] Examples of cortico steroids can be seen in **Figure 16**.

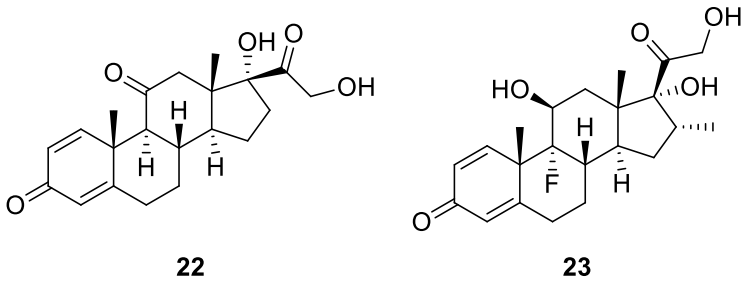

22 **23**

Figure 16: Examples of corticosteroids: prednisone (**22**), dexamethasone (**23**).

1.2.1.2. Radiotherapy

Radiation therapy uses ionizing radiation to kill and control the growth of cancer cells that are localized to one area. It works by damaging DNA which induces cell death. Radiation beams must pass through other organs to reach the tumour, and so to spare the surrounding healthy tissues from damage, the beams are delivered from several different angles and intersect the tumour to provide the highest dose of radiation at the tumour site.[59] How the surrounding tissues respond to the radiation beams limits the dosage that can be used. The aim of treatment is to deliver the highest dose possible to the tumour whilst maintaining the health and functionality of the surrounding tissues. Due to the retention of functionality in the surrounding

tissues, radiation therapy is ideal for targeting cancers that have grown around critical structures such as the spinal cord or large vessels.[56,60,61]

1.2.2. Apoptotic pathway targeted cancer therapies

As discussed above in **section 1.2.**, one of the hallmarks of cancer is evasion of apoptosis by cancer cells.[37,38] This means that malignant cells are not cleared from the body, and can go on to replicate, forming neoplasms. Therefore, the apoptosis pathways present an interesting target for therapeutic intervention. Development of therapeutic agents include those that target both the extrinsic and intrinsic pathways, described in greater detail in **sections 1.2.2.1** and **1.2.2.2.** respectively.

1.2.2.1. Extrinsic pathway intervention

The extrinsic pathway requires extracellular signals to induce apoptosis, which are referred to as death ligands. Death ligands bind to death receptors (DR) which leads to the recruitment Fas-associated death domain (FADD) which in turn recruits caspase-8, leading to the activation of caspase-3, -6, and -7. This triggers the cleavage of proteins and the cytoskeleton leading to cell death (**Figure 17**).[9,62] DR's are therefore a target for therapeutic intervention, with TNF and Fas showing extensive *in vitro* anti-tumour activity.[63] However, *in vivo* tests using animal models have shown that TNF and Fas activate non-specific TNF receptors, which resulted in damage to several tissues leading to septic shock and hepatic failure.[64,65] Therefore, there is a need for agents which are able to induce the extrinsic pathway without associated toxicity or serious adverse events. Development of other DR extrinsic pathway inducers with improved tolerability are detailed below.

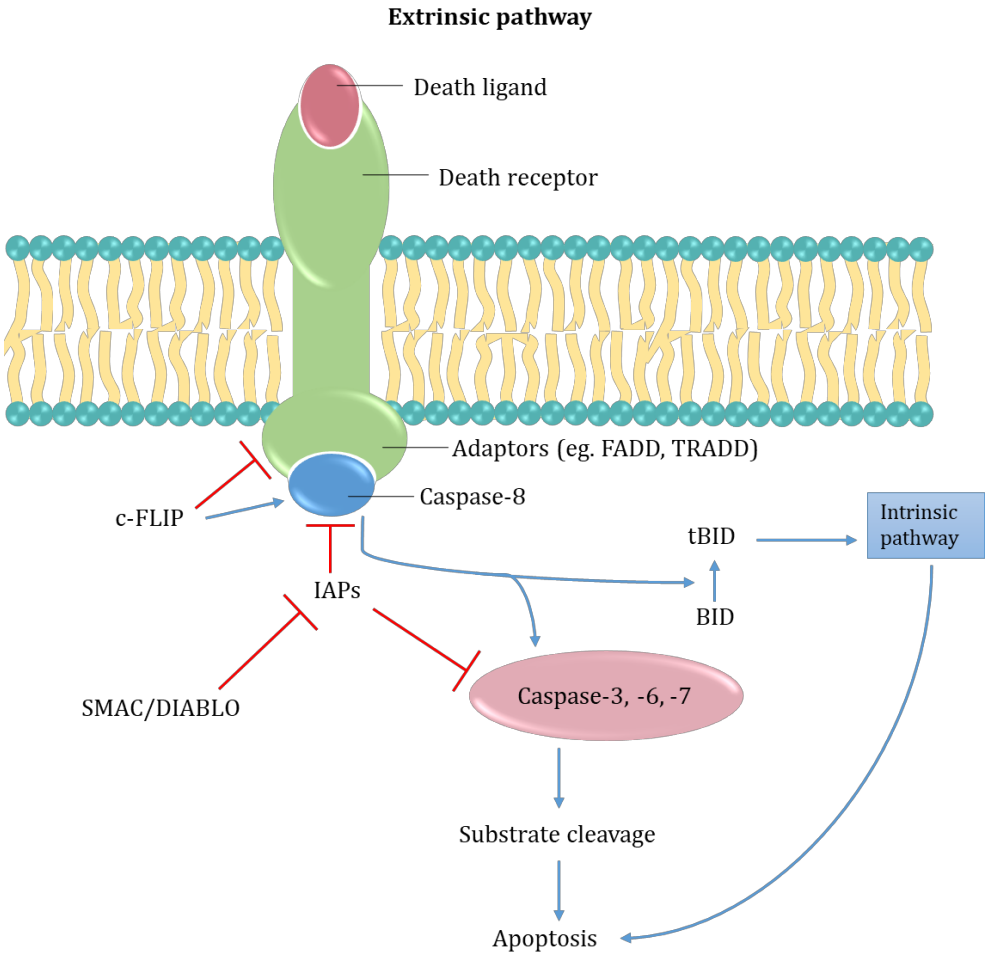

Figure 17: Extrinsic apoptosis pathway. Adapted from Swanson *et al*. 2009 and Pfeffer and Singh 2018.[9,62]

TRAIL/APO2L

Tumour necrosis factor (TNF)-related apoptosis-inducing ligand (TRAIL), also known as Apo-2 ligand (Apo2L), is a member of the TNF superfamily and has been found to be an effective extrinsic pathway inducer that is not associated with the toxicities of Fas and TNF.[63,66] TRAIL/APO2L induces apoptosis in many tumour cell types by binding the TRAIL trimer to the TRAIL-Receptor (TRAIL-R) 1 or TRAIL-R2 (also known as death receptors DR4 and DR5), resulting in TRAIL trimerisation. This leads to the recruitment of FADD, eventually leading to cell death.[67–69] Promisingly, in preclinical testing, when TRAIL was used in combination with chemotherapy or radiotherapy, a significant reduction in tumour growth was observed.[70–72]

The two main therapeutic strategies that have been tested clinically are a recombinant form of human TRAIL (Apo2L.0 or AMG-951/Dulanermin) and antibodies that specifically target TRAIL-R1 or TRAIL-R2.[67] Although these two strategies have been shown to be safe and well tolerated in patients, the clinical studies showed that the tumour cells will either become resistant during the course of treatment, or were already resistant at initiation of treatment.[68,73–79] To try to overcome this apparent TRAIL resistance, recent studies have been focussed on the development of second generation TRAIL-based therapies that have a greater cytotoxic effect on cancer cells.[67]

Current methods to stabilise TRAIL and increase its elimination half-life involves the single-chain TRAIL (sc-TRAIL) approach, and linking TRAIL with molecules that exhibit better pharmacokinetic properties such as human serum albumin (HAS) or polyethylene glycol (PEG).[80–82] For the sc-TRAIL approach, the molecule is expressed as a trimer, in which the three molecules are interlinked head-to-tail, preventing errors being introduced during expression whilst also preventing off-target interactions.[80] The TRAIL-linking approach, with HSA or PEG, has been shown to increase the elimination half-life, stability and solubility in *in vivo* studies.[81]

Monoclonal antibodies

Monoclonal antibodies have demonstrated the ability to induce apoptosis and be effective in tumour regression by activating TRAIL-R1 and TRAIL-R2.[63,82] in preclinical trials, TRAIL-R1 and TRAIL-R2 antibodies such as mapatumamab and conatumumab have been shown to be quite efficacious whilst also demonstrating a favourable safety and stability profile.[82–84] Both of these antibodies, as well as many others, have been studied as both a monotherapy and in combination with traditional cancer therapies. Whilst both mapatumumab and conatumumab proved effective as monotherapy, only conatumumab demonstrated efficacy as a combination therapy.[82] Monoclonal antibodies have a much longer half-life than TRAIL/APO2 which provides the potential advantage of a less frequent dosing regimen.[63]

Adoptive cell transfer (ACT)

In order to try to overcome the issue of resistance development observed when using certain extrinsic pathway inducers, treatment could be tailored to each patient, whereby specific biomarkers of resistance are identified in order to characterise cells with high expression levels of death receptors which would be sensitive to antibodies.[82,85] One exciting new development that takes this approach is a type of immunotherapy called adoptive cell transfer (ACT), in which a patient's own immune cells are modified in order to improve their ability to target tumour cells.[86]

One such ACT therapy that has gained a lot of attention recently is CAR-T, which uses genetically modified T cells. This therapy has been dubbed "the living drug" since it works by drawing the patients' blood, separating out the T cells then employing a disarmed virus to genetically engineer the T cells to produce receptors on their surface called chimeric antigen receptors (CAR). The patient would then go through a round of chemotherapy to deplete their lymphocytes, before receiving an infusion of their CAR-T cells.[86]

These modified CAR-T cells have demonstrated an ability to induce apoptosis specifically in tumour cells by triggering the TRAIL receptor DR4, as well as trigger the mechanisms of T cell cytotoxicity.[87,88] So far, two CAR-T therapies have been approved by the Food and Drug Administration (FDA), one, Kymriah (tisagenlecleucel), indicated for the treatment of children with acute lymphoblastic leukemia (ALL) and the other, Yescarta (axicabtagene ciloleucel), indicated for adults with advanced lymphomas. Research is still currently ongoing into the use of CART-T and ACT-type therapies for use against other types of cancer and solid tumours.[86]

1.2.2.2. Intrinsic pathway intervention

The intrinsic apoptosis pathway is stimulated by proapoptotic and antiapoptotic members of the BCL2 protein family and is initiated by oxygen radicals, γ radiation or DNA injury.[7] These stimuli result in the upregulation of pro-apoptotic BH3-only (BCL2 homology 3 domain) proteins which inhibit the antiapoptotic BCL2

proteins, leading to the activation of proapoptotic BAX and BAK proteins. BAX is regulated by the tumour suppressor gene p53, and once activated BAX and BAK oligomerise which increases the permeability of the mitochondria.[89] This leads to the release of cytochrome *c* which activates caspase-9 and in turn activates the executioner caspase-3, -6, and -7. The executioner caspases then go on to break down proteins, which leads to cell death. (**Figure 18**).[7–9,62,68]

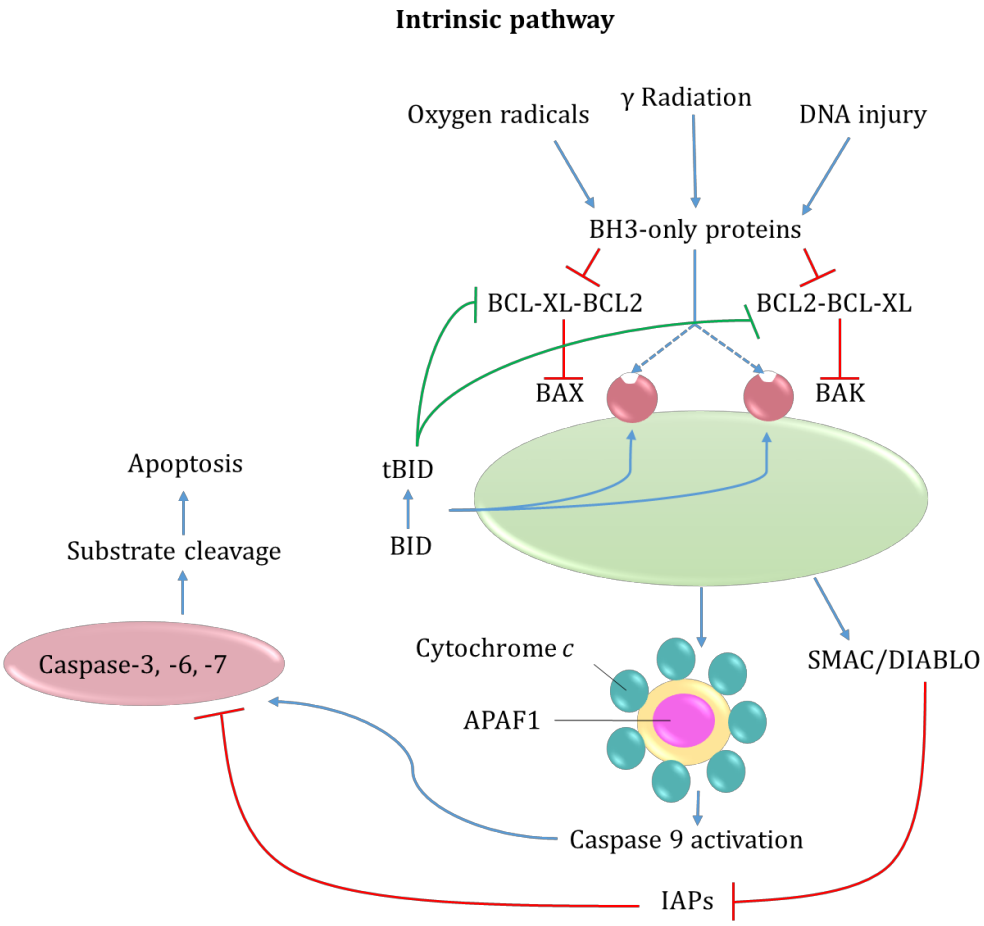

Figure 18: Intrinsic apoptosis pathway. Adapted from Swanson *et al.* 2009 and Pfeffer and Singh 2018.[9,62]

Since BH3-only proteins play a key role in regulating and promoting apoptosis they are an appealing target for therapeutic intervention.[90–93] It has been found that over expression of prosurvival BCL-2 proteins is present in various tumours and as such, many lines of enquiry have been explored attempting to inhibit BCL-2, a few of which are discussed briefly below.[68,94,95]

Antisense oligonucleotides

Antisense oligonucleotides are short, single-stranded pieces of DNA that have been synthetically sequenced to target mRNA, enhancing the effects of cytotoxic drugs. Though not a complex procedure, use of oligonucletides has been constricted by their susceptibility to intracellular degradation.[96–99] However, a new generation of antisense oligonucleotides are currently being tested in clinical settings which are proving to have a greater stability than their predecessors, and have a favourable safety profile.[100–102] One of the most promising candidates is oblimersen (also known as G3139 and Genasense) which has been tested in clinical trials as a monotherapy as well as in combination with many anticancer agents against several cancer types.[95,103–106] Oblimersen is of special interest as it is the first oligonucleotide that has been proven to downregulate BCL-2 in human tumours within 3-5 days of starting treatment.[68,102]

BH3 mimetics

BH3-only proteins can initiate apoptosis by either neutralising antiapoptotic BCL-2 proteins, or by activating BAK and BAX.[93,107–109] The former mode of action works by the BH3-only proteins binding to the hydrophobic pocket via four hydrophobic residues.[110,111] This mode of action is very well understood and as such has been exploited by drug developers leading to the development of many small-molecule BH3-mimetics.[112–116]

Targeting inhibitors of apoptosis proteins (IAPs)

Inhibitors of apoptosis proteins (IAPs) are a family of proteins that inhibit apoptosis by blocking caspase function, which prevents signalling the extrinsic apoptotic pathway, thereby inhibiting cell death.[117,118] It has been found that overexpression of IAPs in tumour cells is linked to an overall poor survival rate and is associated with the development of resistance to chemotherapeutics.[119–121] Therefore, targeting IAPs for the development of anticancer therapies has proven a popular strategy. Small-molecule inhibitors of IAPs have been developed which act by either binding to the IAPs itself, or by interfering with IAP mRNA and protein expression.[117,122]

1.3. Imaging cells

In this project, before molecules could be developed that could potentially carry a molecular cargo into a cell going through apoptosis and ensuring that the cell dies, it was important to ensure that we were indeed only targeting apoptotic cells. Therefore, a model to test where the cargo was being delivered had to be developed. By attaching a fluorescent marker to the drug-delivering molecule, visualisation of the targeted cells would be possible. Different fluorophores were investigated (**Chapter 2**) and eventually a series of BODIPY (4,4-difluoro-4-bora-3a,4a-diaza-*s*-indacene) derivatives were developed.

1.3.1. Fluorescence

Fluorescence, was first described in 1565 by the Spanish physician and botanist Nicolás Monardes, who noted that when wood from the Lignum nephriticum tree was soaked in water the water took on a blue colour.[123] The Aztecs had been using the water for its medicinal properties as a diuretic. According to Rodriguez *et al.* the chemical responsible for the blue colour was matlaline (**25**, named after the Aztec word for blue, "matlali") which is not actually present in the plant but is produced when one of the tree's flavonoids, coatline B (**24**), undergoes spontaneous oxidation upon exposure to slightly alkaline water (**Scheme 1**).[124]

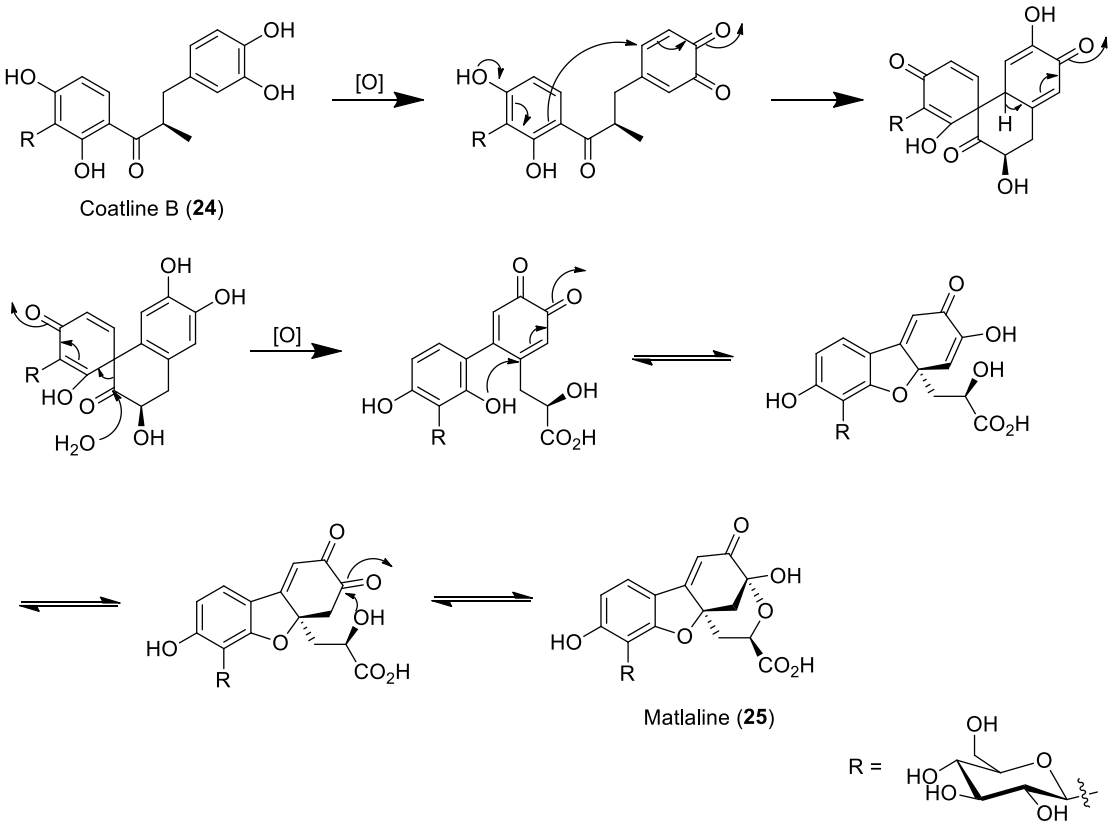

Scheme 1: Mechanism proposed by Rodriguez *et al.* for the formation of matlaline via the spontaneous oxidation of coatline B.[124]

Edward D. Clarke and Rene-Just Hauy separately reported in 1819 and 1822 respectively about the dichroic nature of calcium fluoride; it appeared blue under reflected light and green under transmitted light.[123] In 1833 Sir David Brewster reported that sunlight passing through a solution containing chlorophyll fluoresced red and in 1845 Sir John Herschel reported that an acidic solution of quinine sulfate appeared blue in certain lights.[123] However it was not until 1852 that the phenomenon was fully investigated by Sir George Stokes, who observed that the wavelengths of the emitted light were longer than the wavelength of the dispersed light; this later became known as Stokes Law. Though Stokes referred to the phenomenon as "dispersive reflection", in a footnote he proposed that the term fluorescence should be used instead.[123]

Fluorescence occurs when light of a certain wavelength (specific to the fluorophore being observed) promotes a π-electron to a singlet excited state, meaning that the spin of the electron is opposite to its pair in the ground state. As such the transition

from the excited state back to the ground state is spin-allowed and occurs quickly, emitting a photon in the process (**Figure 19**).[125] This process is different to phosphorescence which occurs when electrons are promoted to the triplet state and are no longer spin-paired to the electron in the ground state. In this situation the process of the electron returning to the ground state takes a lot longer and the emission of light continues long after the incident light source is removed.[125]

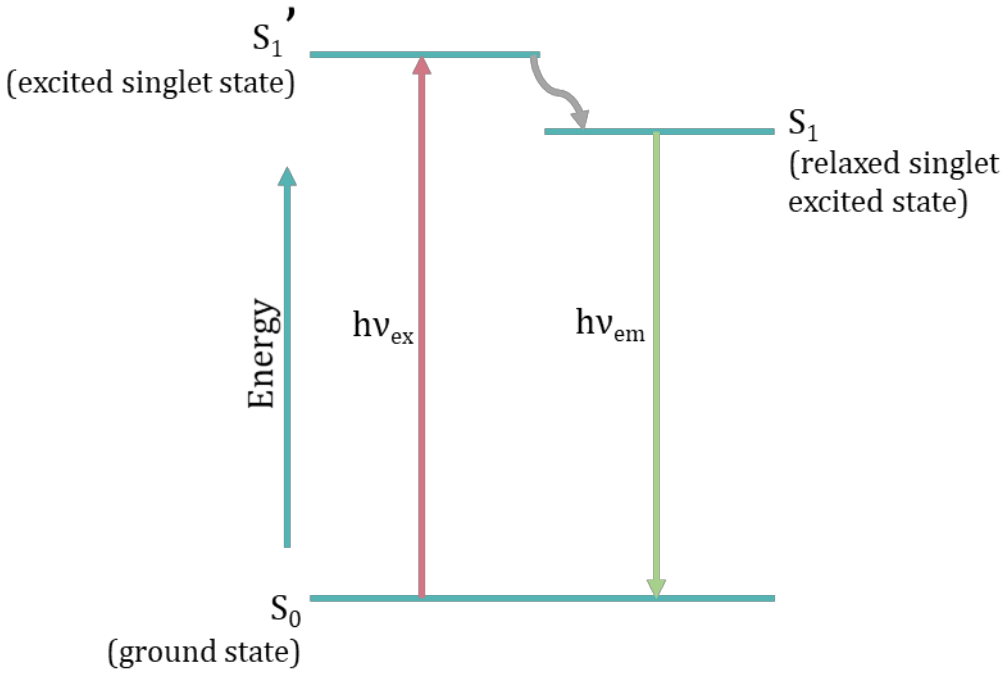

Figure 19: Jablonski diagram depicting a π-electron being promoted to a singlet excited state followed by its return to ground state, emitting a photon in the process.

1.3.2. Aposense – Small molecule detectors of apoptosis

An aposense is an umbrella term for a family of small, non-peptidic molecules that can preferentially enter apoptotic or necrotic cells during the early stages of cell death and accumulate in them for identification via fluorescence imaging. This method was originally reported by Shirvan *et al.* as a non-invasive method for imaging renal tubular cell injury in renal ischemia.[126] In their report the authors described the binding method of *N,N'*-didansyl-L-cystine (DDC, **26**, **Figure 20**) to apoptotic cells and used its fluorescent characteristics and its radiolabelled (^{3}H) derivative for identification and quantification purposes.

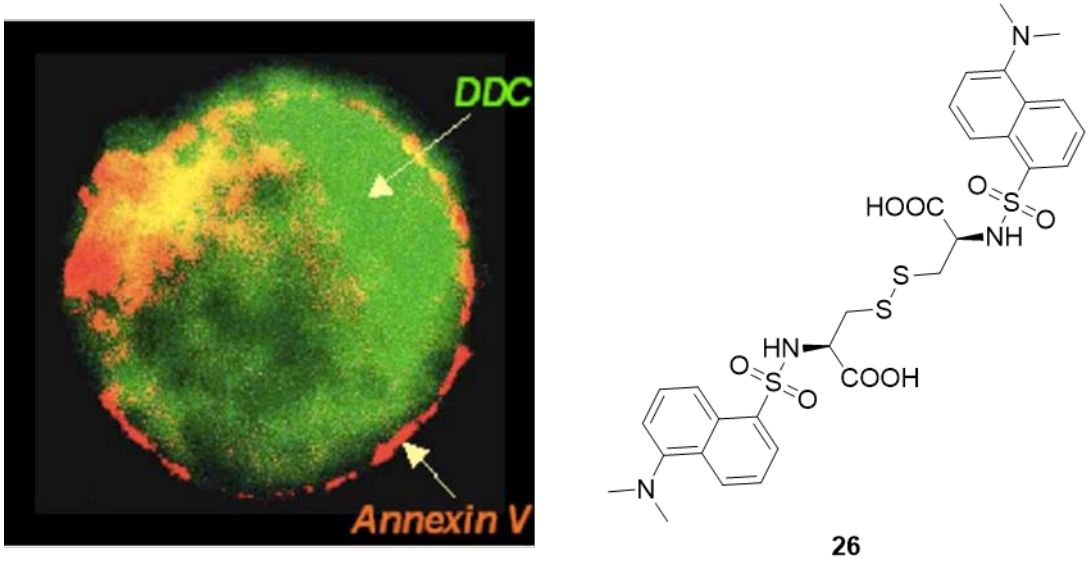

Figure 20: Left: Image of an apoptotic cell with DDC (**26**) accumulated in the cytoplasm and annexin V bound to the membrane.[126] **Right**: 3,3'-disulfanediylbis(2-(5-(dimethylamino)naphthalene-1-sulfonamido)propanoic acid) aka *N,N'*-didansyl-L-cystine (DDC, **26**).

The studies were carried out using adult T-cell leukemia Jurkat cells and cervical carcinoma HeLa cells, in which apoptosis was induced and then imaged by staining with DDC and annexin V and viewed using fluorescence microscopy and flow cytometry. Visualization showed that the DDC accumulated in the cytoplasm and annexin V attached to the cell membrane, as shown in **Figure 20**. This method was then transferred to animal models where renal ischemia was induced in rats in one kidney, using the other as a control to try and image the induced cell death. It was subsequently found that annexin V, a well-known apoptosis marker that had already been investigated in animal models and clinical trials, had a high affinity for the intact renal cortex and so proved unusable for this study.[127] The authors clearly demonstrated the successful application of fluorescent chemical tools as a non-invasive, real-time technique for the diagnosis and monitoring of conditions like renal ischemia.

We were particularly interested in this behaviour as apoptotic cells share many characteristic hallmarks with senescent cells, the build-up of which is the mechanistic basis for triggering accelerated ageing in Werner's syndrome (**section 1.4.1.**). Senescence has been linked to both cancer and ageing. Cancerous cells need mutations, which occur in the p53 and p16-pRB pathways, to avoid telomere-

dependent and oncogene-induced senescence. Studies have also shown that markers for senescence are more abundant in aged organisms than younger ones. Furthermore, currently there are no small or large molecule detectors of senescence.[32]

1.4. Ageing

Ageing is often accompanied by a number of age-related diseases such as Alzheimer's and Parkinson's disease, arthritis and various forms of cancer.[128] The build-up of senescent cells has been linked to both ageing and cancer (**section 1.1.5.**). By using the premature ageing syndrome Werner's Syndrome (WS) as a model for normal ageing phenotypes, this project aimed to increase our understanding of the underlying causes of ageing and the role senescence plays in the ageing process; ultimately to use that knowledge in order to improve the quality of life for a population that is living longer than ever before.

1.4.1. Werner's Syndrome

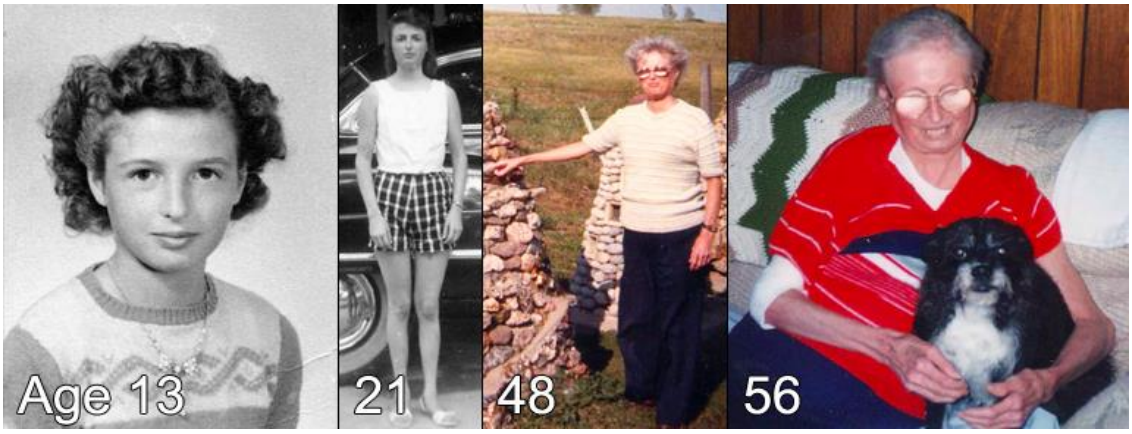

Figure 21: Different stages of the life of a patient with Werner's Syndrome, illustrating how the disease presents itself as premature ageing.[129]

The rare autosomal recessive disorder known as Werner's Syndrome (WS) is caused by a mutation of the WRN gene, which encodes for RecQ helicase. RecQ helicase is involved in DNA replication, recombination and repair. Sufferers of WS exhibit premature ageing, as shown in **Figure 21**,[129] and as a result have a reduced median life expectancy of around 47 years. Due to these factors WS is often used to study the mechanisms of normal human ageing. The premature ageing is thought to be caused by a stress–induced growth arrest mediated by p38 MAPK. The mitogen activated protein kinases (MAPKs) are a family of enzymes essential for inflammatory cell signalling and so have long been investigated as targets in drug development for diseases such as rheumatoid arthritis and Crohn's disease and are thought to be involved in accelerated cellular ageing in WS.

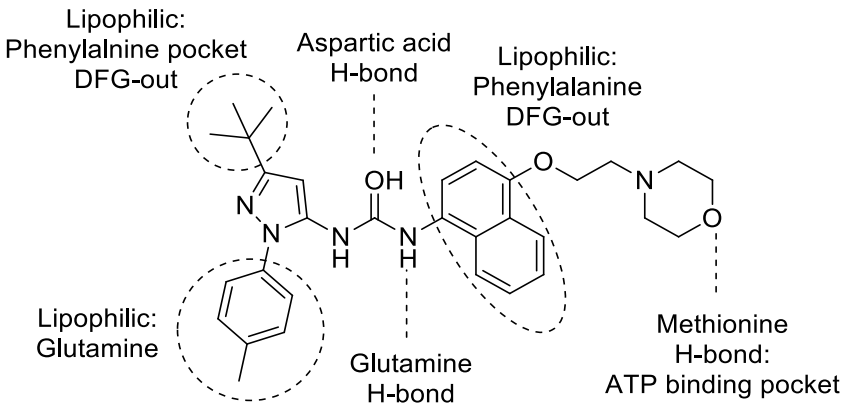

27

Figure 22: BIRB 796 interactions with p38 as summarised by Regan *et al.*[130]

The most promising advancement in developing a drug for people living with WS has been BIRB 796 (**27**, **Figure 22**) which was developed by the German pharmaceutical company, Boehringer Ingelheim. It is a *N*-pyrazolyl-*N'*-naphthyl urea that inhibits p38 MAPK[130] and JNK. BIRB 796 and other compounds of the same class are of special interest due to their different binding mode to p38 MAPK when compared to other ATP site kinase inhibitors. Torcellini *et al.* reported the mode of binding of *N*-pyrazolyl and *N*-aryl urea based inhibitors of p38 MAPK, including BIRB 796.[131] It was found that when p38 was exposed to the ureas investigated during the study, they occupied a binding domain not previously seen in other Ser/Thr kinases, the DFG-motif (Asp168-Phe169-Gly170 motif) which exhibits a DFG-out conformation, which the ureas can occupy. This unique binding mode is facilitated by movement of a phenylalanine side chain found in the DFG-motif of the activation loop. P38 is one component of the MAPK intracellular enzyme cascade that is responsible for regulating key signalling pathways, which lead to the production of some pro-inflammatory cytokines such as TNF-α and IL-1β.

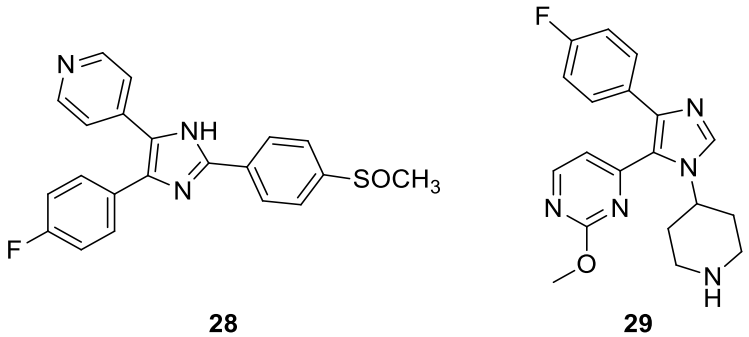

28 **29**

Figure 23: SB 203580 (**28**) and SB 242235 (**29**).

Torcellini *et al.* described the process by which BIRB 796 was selected for clinical trials.[131] The study began with the pyrinidinyl imidazole SB 203580 (**28**, **Figure 23**), which had been identified as an orally active, potent and selective inhibitor of p38 MAPK during animal testing. SB 242235 (**29**, **Figure 23**), an analogue of SB 203580, was also tested in human clinical trials after it was shown to inhibit endotoxin-induced *ex vivo* production of TNF-α and IL-1β. Unfortunately, during clinical trials of BIRB 796 involving patients with Crohn's disease, Schreiber *et al.* found elevated levels of alanine transaminase (ALT), a biomarker for hepatic toxicity in clinical pathology.[132] This led Miyamoto *et al.* to propose a possible mechanism for the hepatotoxicity of BIRB 796.[133] This effectively ended the trial.

1.5. P38 and MK2

The p38 MAPKs are a family of proteins that consists of four isoforms; α, β, γ and δ with each isoform triggering a different response. P38α and β are found throughout the body, whereas p38γ is found exclusively in skeletal muscle and p38δ is predominantly found in the testes, pancreas and small intestine.[134,135] Only p38α and β activate MK2.[135] The role of p38 is to activate downstream kinase targets or to directly activate other targets inside the nucleus to trigger an immunological response, such as inflammation. However, if p38α is over-activated this can lead to a feedback loop that leads to production of pro-inflammatory cytokines such as TNF-α and ILs which exacerbates diseases such as rheumatoid arthritis and inflammatory bowel disease.[134–136] Due to the role of p38 in numerous disease pathophysiologies it is an obvious target for therapeutic intervention and, as such, inhibitors have been studied extensively for their use as anti-inflammatory agents.[130,137–139]

MK2 belongs to a family of mitogen activated protein kinases and is a phosphorylation target for p38. MAPKs are important for cellular functions such as proliferation, apoptosis, gene regulation, differentiation and motility and also co-transport p38 MAPKs to the cytoplasm.[140,141] MK2 is a Ser/Thr protein kinase of the calcium/calmodulin-dependent protein kinase family that is a direct downstream substrate of p38 kinases that regulates lipo-polysaccharide stimulated TNF-α.[142] Since p38 knockout mice have been found to be lethal,[143] MK2 is a potential alternative target for inhibition as MK2 knockout mice are viable, display a reduced expression of TNF-α when stimulated with lipopolysaccharides and are resistant to developing arthritis in disease models.[144,145]

Previously, p38α MAPK, the upstream activator of MK2, has been targeted for inhibition by the small molecule inhibitor SB 203580 (**28**) which blocked the synthesis of pro-inflammatory cytokines at the post-transcriptional level, but showed relatively poor kinase selectivity.[141,146] However, it was observed that the inhibitor worked by preventing activation of MK2. This was evidence that corroborated observations made in MK2-deficient animal models, which also showed that p38 MAPK activity was unaffected by a deficiency in MK2.

Figure 24: The p38 signalling pathway, adapted from Bagley *et al.* 2010. [147]

1.5.1. The p38 MAPK cascade

The p38 MAPK cascade is activated when extracellular factors such as UV light, stress or pro-inflammatory cytokines such as TNF-α and IL-β[135,148] activate cell surface receptors and induce the three step pathway to p38 activation; MAPKKK (mitogen activated protein kinase kinase kinase) activates MKK3/4/6 (mitogen activated protein kinase kinase) which activates p38 (**Figure 24**).[136] From this point, p38 can either directly activate transcription factors or activate MK2 or MSK1/2 (**Figure 25**).[136,149] Activation of MK2 leads to the production of pro-inflammatory cytokines whereas activation of MSK1/2 leads to the production of anti-inflammatory cytokines.[136]

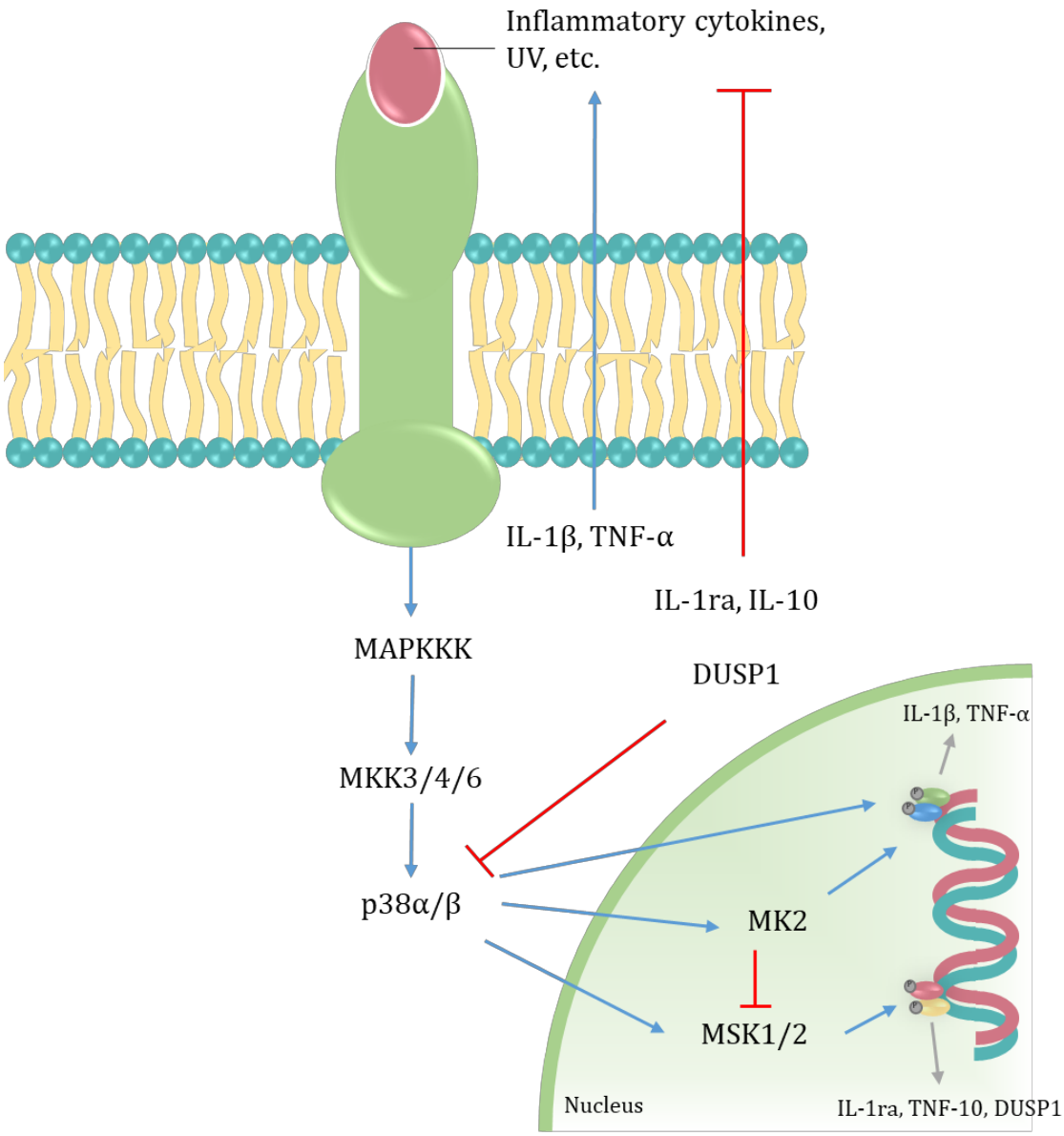

Figure 25: Overview of the p38 cascade. Extracellular factors activate a cell surface receptor which activates MAPKKK which then activates MKK3/4/6 which activates p38α. P38α can then directly activate transcription factors or the protein kinase targets MK2 or MSK1/2.

1.5.2. P38 inhibitors

Due to the role of p38 in the overproduction of pro-inflammatory cytokines involved in the pathogenesis of many inflammatory diseases, it is quite an attractive target for inhibition. BIRB 796 has already been discussed in **section 1.4.1.** but some other examples of p38 inhibitors will be briefly discussed here to demonstrate the work that has gone into trying to develop a novel inhibitor of p38 that can be used as a therapeutic agent for the treatment of inflammatory diseases.

Vertex Pharmaceuticals proceeded to phase II clinical trials with their pyrimido-pyridazinone-based candidate, VX-745 (**30**, **Figure 26**), and found the inhibitor was well tolerated by RA sufferers. It selectively inhibited p38α with an IC_{50} of 5 nM. However, the clinical trials were suspended due to adverse neurological effects in dogs.[150,151] The company followed-up with a new inhibitor, VX-702 (**31**, **Figure 26**), which was not able to cross the blood-brain barrier.[152] This new inhibitor progressed to phase II clinical trials; however, the therapeutic effect was not much greater than in the placebo group, and so the trials ended.[150]

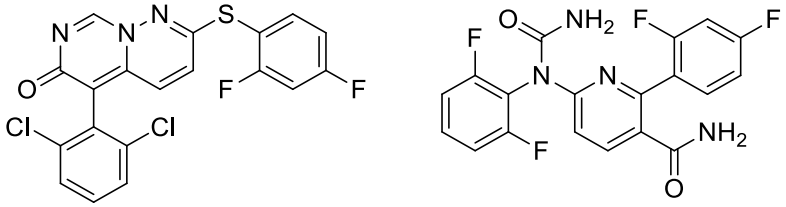

30 **31**

Figure 26: Examples of p38 inhibitors: VX-745 (**30,** phase II), VX-702 (**31**, phase II).

Roche developed RO-4402257 (**32**, **Figure 27**) as a selective inhibitor of the p38α isoform which had an IC_{50} of 14 nM.[153] This inhibitor progressed to phase II clinical trials involving RA sufferers, where it failed to show efficacy and was responsible for several undesirable side effects, such as infections, skin disorders and dizziness in patients.[148,154]

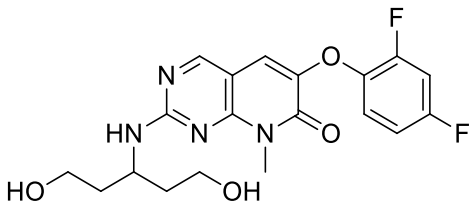

32

Figure 27: P38 inhibitor RO-4402257.

From the examples presented here it is obvious that while selectively targeting p38 is not too much of an issue, developing an efficacious therapeutic without off-target effects is and this has led to the failure of many p38 inhibitors that have progressed to clinical trials.[155] These effects could be due to the fact that p38 controls feedback

loops that block upstream kinases that can activate other pro-inflammatory pathways, thus inhibition of p38 could lead to over activation of these other kinases.[155,156] Therefore, it has been suggested that p38 should no longer be targeted for therapeutic intervention, and therapies should instead be targeted upstream or downstream of p38.[148,157,158]

1.5.3. MK2 inhibitors

As mentioned previously, the p38 inhibitor SB 203580 worked by preventing activation of the downstream kinase MK2, making MK2 an interesting potential target for inhibition.[141,146] As further evidence of MK2's suitability for inhibition, it was found that p38 knockout mice were lethal whereas MK2 knockout mice were not only viable but had reduced levels of TNF-α.[157,159,160] MK2 also mediates the phosphorylation of HSP27, a protein that is involved with cell migration and actin remodelling. The MK2/HSP27 pathway has been implicated in F-actin stress fibre formation in WS cells. The build-up of these fibres is thought to be involved in the premature ageing of WS cells, and also the cell migration of cancer cells. Hence therapeutic intervention may be beneficial for a range of disorders including cancers.[155,161] Using high throughput screening (HTS), many ATP-competitive small molecules targeting MK2 have been identified as potential candidates for further derivatization and development into potential therapeutics.

Pfizer investigated derivatives of benzopyranopyridines, pyrrolopyridinones, carbolines and benzothiophenes (**Figure 28**).[160,162–164] Derivatives of carbolines were also investigated by Boehringer-Ingelheim (**Figure 29**).[165]

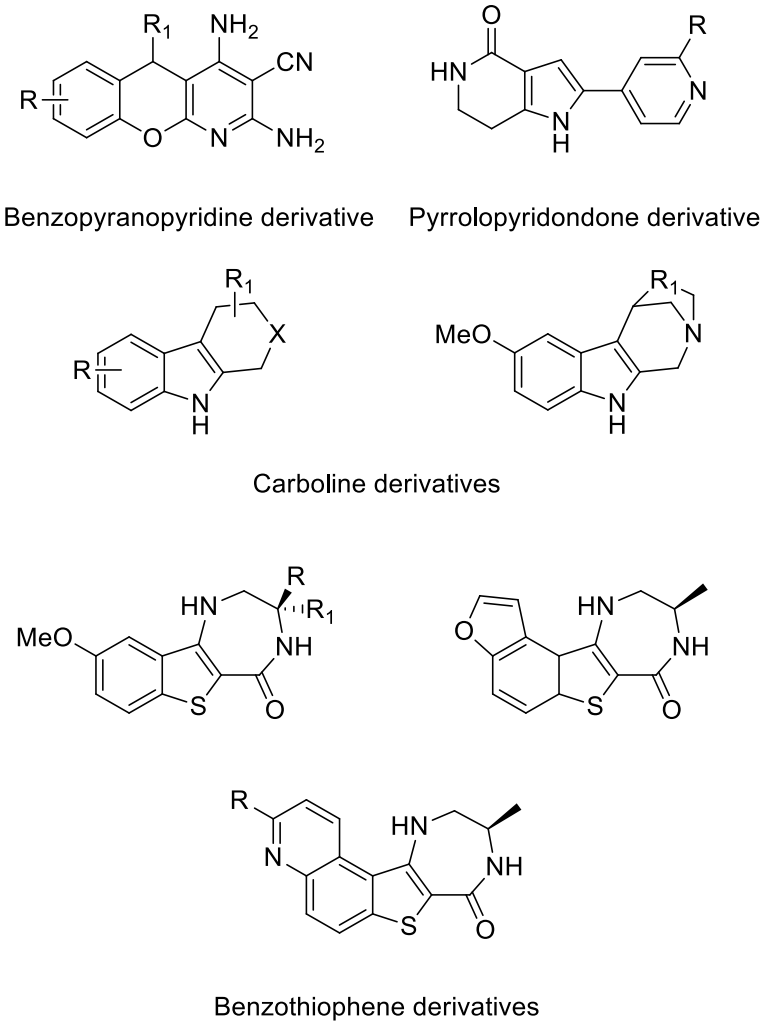

Figure 28: Pfizer developed a range of pharmacophores into MK2 inhibitors. R, R_1 and X = points of derivatization.

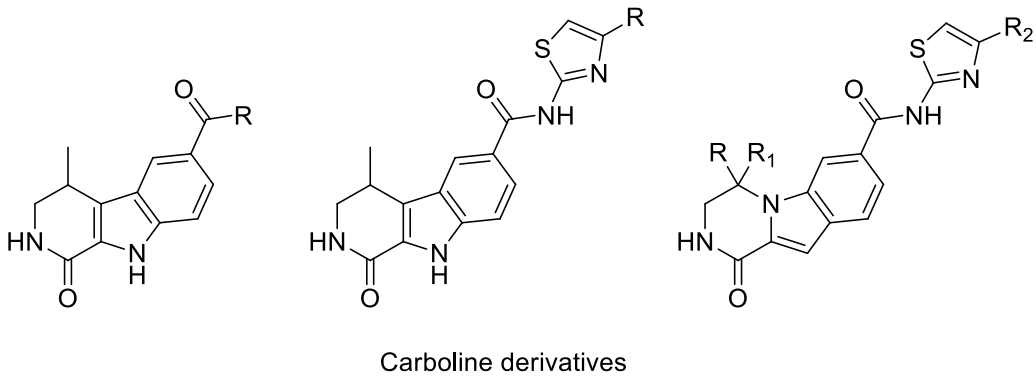

Figure 29: Boehringer-Ingleheim developed a series of carbolines as MK2 inhibitors. R, R_1 and R_2 = points of derivatization.

Anderson *et al.* at Pfizer determined from the SAR analysis of pyrrolopyridinone compounds that conformationally constrained moieties were able to occupy the hinge region of MK2 and could gain good selectivity.[160] This observation eventually led to the development of a fused heterocyclic benzo[*b*]thiophene derivative, PF-3644022 (**33**, **Figure 30**), which is a highly potent inhibitor of MK2.[142] Unfortunately, through animal testing it was found that PF-3644022 caused acute hepatoxicity.[166]

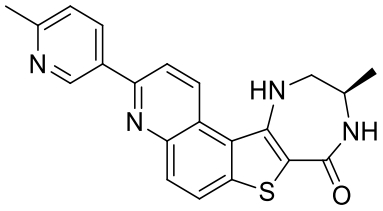

33

Figure 30: PF-3644022.

However, it has been used as a tool to investigate the role of MK2 in WS, and the link between MK2/p38 and the Sonic Hedgehog (Shh) pathways in breast cancer development. A recent study presented evidence that Shh, a protein that plays a pivotal role in cancer progression, could activate p38 and MK2 which would go on to activate PFKFB3, a protein responsible for promoting glycolysis and proliferation in breast cancer cells. The direct involvement of MK2 was proven by treatment of the cells with **33** and a decrease in the levels of PFKFB3 was observed.[167] Thus, the development of MK2 inhibitors presents an intriguing possibility for the development of anti-cancer therapies. Efforts to develop new synthetic routes towards **33** will be discussed in **Chapter 3**.

A wealth of pharmacophores have been investigated by many different companies and it has been determined that ATP-competitive inhibitors suffer from poor solubility, poor cell permeation and poor selectivity since the MK2 binding site is structurally very similar to other kinases.[155] As such, future work in this area is being focused on non-ATP-competitive inhibitors.

Through a combination of HTS and ALIS (automated ligand identification system, an integrated system of sequential rapid size-exclusion chromatography, reverse-phase chromatography, and electrospray ionization mass spectrometry, used for identification of non-covalent small molecule ligands from combinatorial libraries) techniques Merck identified that derivatives of furan-2-carboxamides as potential non-ATP competitive MK2 inhibitors (**Figure 31**).[168,169] Further derivatization created more rigid structures in the form of dihydrooxadiazole, imidazole, and tricyclic azepinone derivatives.[170–173]

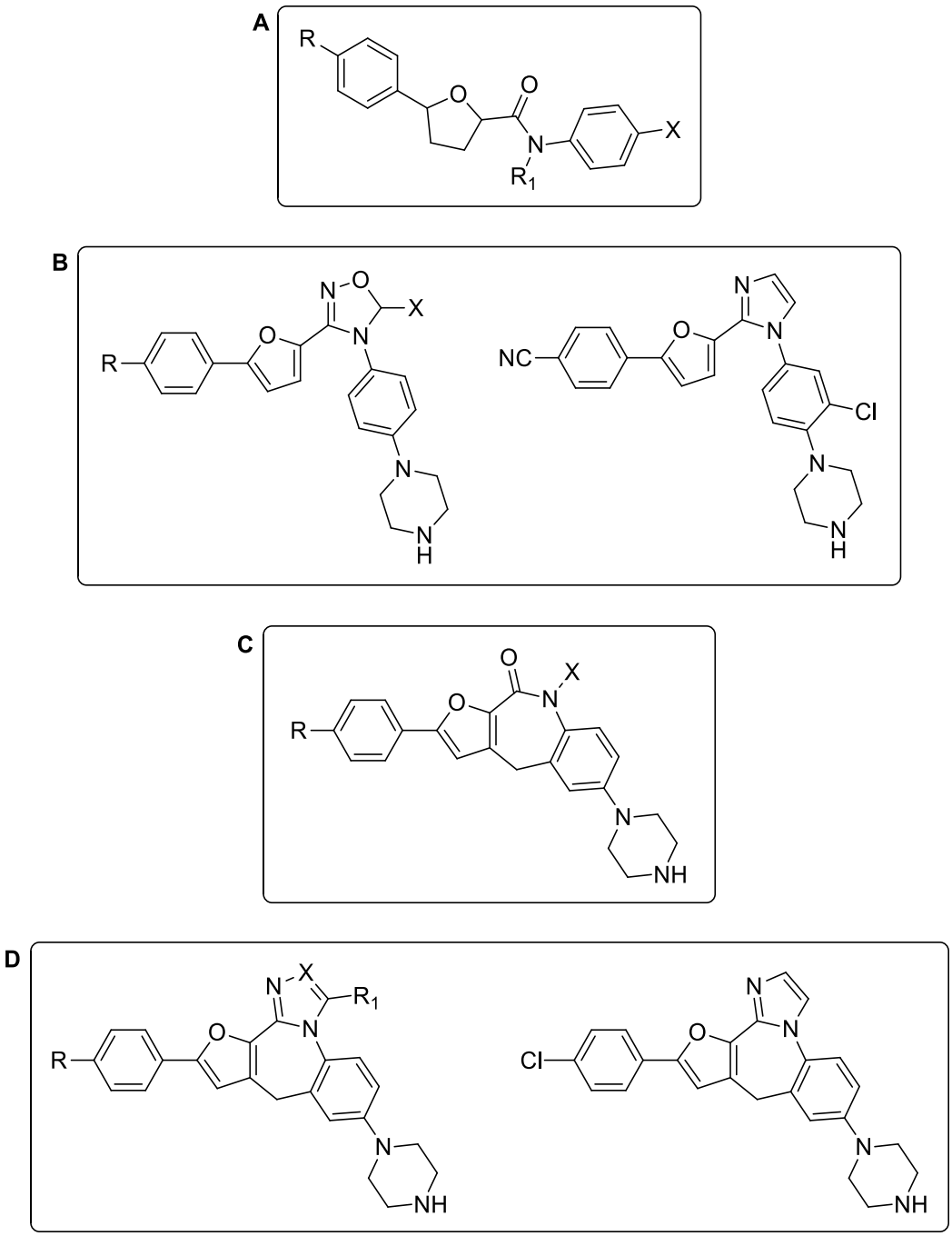

Figure 31: Merck developed non-ATP competitive MK2 inhibitors: furan-2-carboxamide derivative (**A**) which was further derivatized to create more rigid structures in the form of dihydrooxadiazole and imidazole derivatives (**B**) and tricyclic azepinone derivatives (**C**). Addition of a fourth condensed ring (**D**) further restricted conformational flexibility.

Finally, a fourth condensed ring was added to further restrict conformational flexibility.[173] These analogues showed promising results; they did not suffer from solubility issues and presented good affinity and activity. This study demonstrates the great promise for the future development of non-ATP competitive inhibitors.

1.6. Project Aims

The aim of this project was to develop two types of chemical tools; diagnostic tools and inhibitory tools.

To develop diagnostic tools for imaging, we have expanded on work originally reported by Shirvan *et al.* on the use of the aposense molecule *N,N'*-didansyl-L-cystine (DDC, **26**), who investigated it as part of a non-invasive method for imaging renal tubular cell injury in renal ischemia.[126] In order for us to create novel aposense molecules, a series of BODIPY (4,4-difluoro-4-bora-3a,4a-diaza-s-indacene) based molecules have been designed and synthesized. BODIPYs were chosen due to their favourable fluorescence emission and excitation wavelength and the relatively simple and cost-effective methods by which they could be synthesized. Fluorophores are typically difficult to make and expensive to buy, hence not ideal in a medicinal chemistry setting. By tagging small molecules with fluorophores we hoped to be able to visualise cellular events, in order that we could better design molecules that could target cells undergoing morphological changes and deliver molecular cargos to the cell interior. The hope was that this would lead to new opportunities for developing therapeutic regimes for accelerated ageing disorders and in cancer treatments (both chemo- and radiotherapy).

Inhibitors being developed as part of this thesis have a common motif in the form of benzothiophenes. The synthetic goal for the first stage of this project was to develop a rapid route to this core motif. This was established in collaboration with Dr. Jessica Dwyer, whose goal it was to introduce functionality suitable for subsequent elaboration to target inhibitors. Using microwave irradiation and our established conditions and reagents, excellent results were achieved. The methods developed appeared to be superior to other routes which relied upon halogenation. Leading on from this, a new synthetic route towards the MK2 inhibitor, PF-3644022 (**33**), has been developed in collaboration with Dr. Dwyer. To conclude, a rapid, microwave-assisted method for the preparation of benzothiophenes for further derivatization to synthesize chemical tools has been developed for the formation of LIMK, PIM and MK2 inhibitor scaffolds. This work has been published in Organic & Biomolecular Chemistry.[174]

1.6.1. Microwave-assisted organic synthesis

Microwave-assisted organic synthesis was first implemented in the mid-1980s but development of microwave-assisted methods was rather slow due to a lack of controllability and issues with safety, though mostly due to a lack of understanding of microwave dielectric heating.[175] The mid-1990s saw the introduction of microwave equipment developed specifically for organic chemistry reactions, thus the technique became incredibly popular due to increased safety precautions, the potential for solvent-free reactions to be carried out and the possibility of drastically reducing reaction times whilst achieving high yields. Microwave reaction times are usually reduced compared with conventional heating, for example via an oil bath or aluminium heating block, because conventional heating heats the sample slowly allowing a temperature gradient to develop and create local hotspots, which can lead to the production of side products or even reagent decomposition. During microwave dielectric heating, the microwave radiation can pass straight through the walls of the vessel, quickly and uniformly heating the reactants and solvent, which reduces the formation of unwanted side products and decomposition. By using sealed vessels to create pressurized systems, solvents can be heated above their atmospheric boiling point thus creating energy profiles which normally cannot be achieved safely by conventional heating.

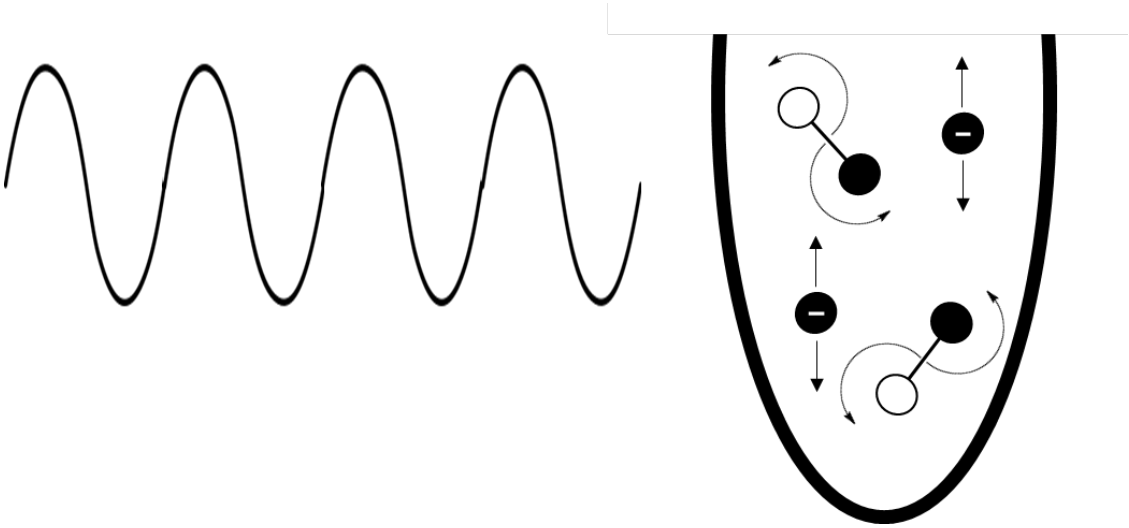

Figure 32: Diagram depicting the oscillating field and its effects on molecules in solution. Polar molecules rotate to align themselves with the alternating electric field whilst ions rapidly move along with the applied field.

As a form of electromagnetic radiation, microwave radiation can be split into two components, the magnetic field component and the electric field component, the latter of which is responsible for the dielectric heating and causes the dipolar polarization mechanism and the conduction mechanism. It is through a combination of these two mechanisms that rapid temperature gradients can be achieved (**Figure 32**).

The dipolar polarization mechanism is the process by which the microwave radiation causes a polar molecule to rotate to align itself with the alternating electric field. The frequency of irradiation chosen in a microwave reactor is sufficiently low to stop the molecule from precisely following the oscillating field, so that a phase difference between the dipole and the orientation of the field causes energy to be lost as heat during friction and collisions with other molecules.

The conduction mechanism occurs through addition of ions to the solution and is a much stronger method of generating heat than the dipolar polarisation mechanism. Ions align with the oscillating electric field and follow the applied field rapidly, colliding with other molecules resulting in the conversion of kinetic energy to heat energy. Therefore, adding ions to a non-polar solution will permit the solution to be heated via microwave irradiation.

The use of microwave technology has been become widely recognised as a reliable and highly efficient technique. The scope of microwave-assisted organic synthesis is incredibly wide with few limitations to the types of reactions that can be carried out. As such, it is now extensively employed in research and development[176,177] as well as being relied upon throughout this project to specifically conduct heterocyclic synthesis and metal-mediated reactions efficiently.

Chapter 2: Diagnostic tools

2.1. Background and aims

The aim of this project was to create a fluorescent chemical tool that would selectively accumulate in cells going through the early stages of apoptosis. This molecule would then be used as a proof-of-concept to design further chemical tools through substitution at the position of the fluorophore with a molecular cargo, while still maintaining selectivity towards accumulation in apoptotic cells. There are several examples of apoptosis imaging agents and several molecular imaging techniques, however this project was only concerned with fluorescent probes to be used in *in vitro* testing. **Figure 33** depicts a flow diagram outlining each planned stage of this project in sequence.

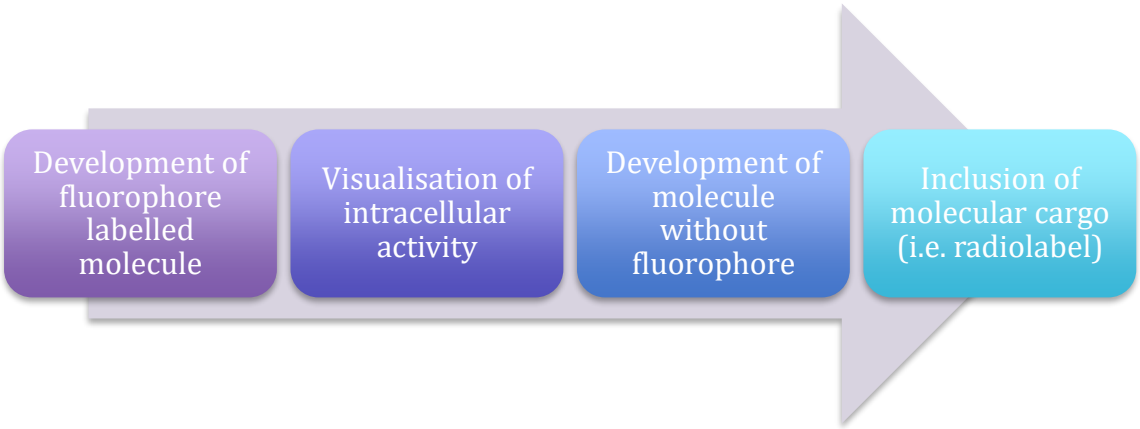

Figure 33: Stages of development of chemical tools that are selective towards cells going through the early stages of apoptosis.

2.2. Introduction

Using fluorophores to observe biological events in cells and organisms has been of interest to the scientific community since the first report of an organic fluorescent molecule, quinine sulfate, written in 1845 by Sir John Herschel (**34**, **Figure 34**).[178,179] The term fluorescence did not find use until 1852 when George Stokes made the suggestion in a report on the discovery of fluorescent molecules.[180]

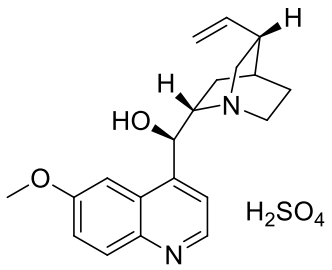

34

Figure 34: Quinine sulfate, discovered by Sir John Herschel in 1845.[179]

Since then, a huge array of fluorescent probes and indicators have been developed that are able to target biological events such as pH changes, the presence of metal ions, protein activities and signalling events, allowing these behaviours to be observed by an investigator. Fluorescence imaging techniques are not only useful for biological research but can be used as a non-invasive technique for the diagnosis and treatment of diseases through being able to detect biological events in cells or tissue. The first report of fluorescent probes that could bind to cells in order for them to be observed was in 1914 by von Prowazek[181], previous studies into imaging biological samples involved plants, bacteria and animal tissues that could spontaneously fluoresce.[178]

Some of the more popular small-molecule fluorophores, and ones that feature in this report, are fluorescein, rhodamine and BODIPY dyes (**Figure 35**). Fluorescein and rhodamine dyes have been in use since the late nineteenth century.[178,182,183] Since then, many derivatives of these probes have been developed, with investigations into structural modifications still being continued.

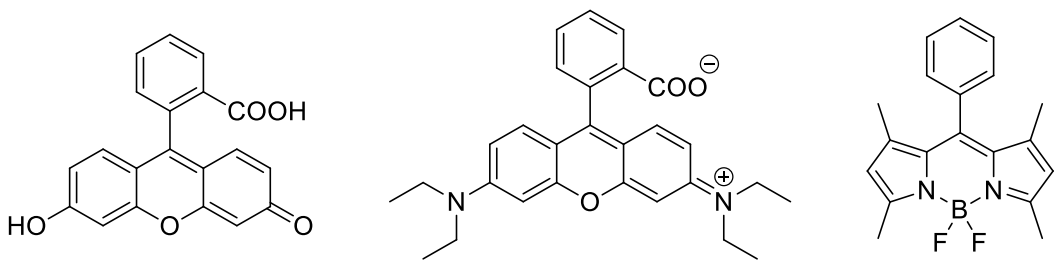

35 **36** **37**

Figure 35: General structures of fluorescein (**35**), rhodamine (**36**) and BODIPY (**37**).

One of the most useful developments in fluorescence imaging has been structural modification to include an "on/off" functionality. This is the altering of the optical properties of a molecule in response to its environment that allows an investigator to "see" these changes. This can be achieved through photoinduced electron transfer (PeT) or Föster (or fluorescence) resonance energy transfer (FRET). PeT-based probes work by transferring an electron to or from the fluorophore in the excited state, from or to an electron donor or acceptor that is introduced to the vicinity, resulting in a change in the intensity of fluorescence observed (**Figure 36**).

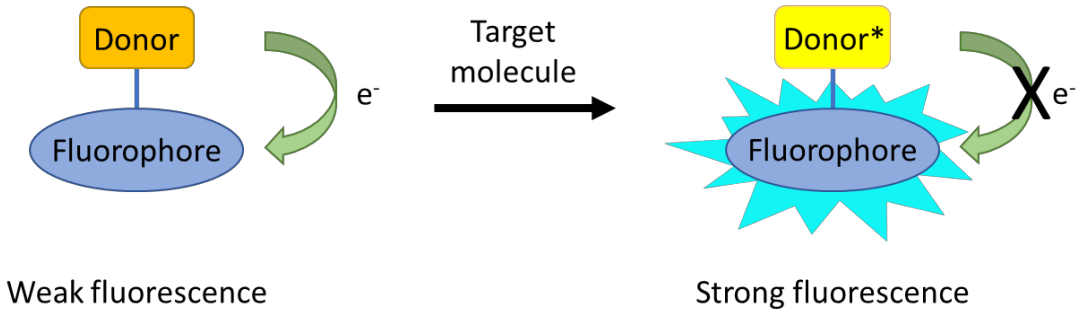

Figure 36: Schematic representation of PeT-based fluorescent probes, modified from Terai and Nagano 2012.[178]

FRET-based probes work via a non-radiative transfer of energy between two linked fluorophores, one acting as a donor and one as an acceptor. As a result of this exchange, fluorescence observed from this system is very weak, but when the linker that attaches the two fluorophores is broken, FRET is cancelled and a strong fluorescence is observed from the donor molecule (**Figure 37**).

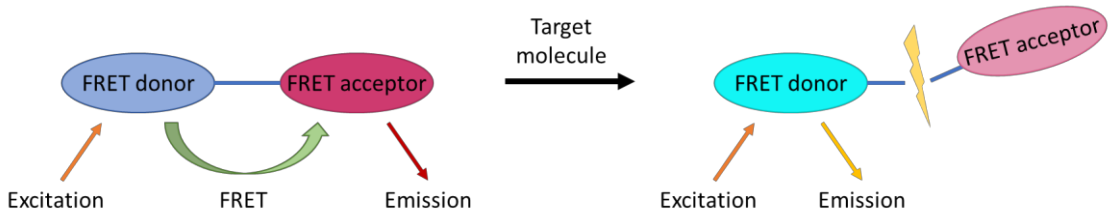

Figure 37: Schematic representation of FRET-based fluorescent probes, modified from Terai and Nagano 2012.[178]

2.2.1. Investigation into small-molecule fluorescent probes

The fluorophores developed during this project were designed as a model to guide the development of a drug-like structure that would carry a molecular cargo into apoptotic cells. Since the molecular cargo in question would be a radiopharmaceutical, which would require specialist training and equipment to handle, as well as specialist storage, the fluorophore model was deemed easier, safer and a more efficient approach to guide the process of drug development.

Two reports on existing apoptosis detectors were taken into consideration at the start of this project. The first was a report by Shirvan *et al.* on the development of a fluorescent probe, didansyl cystine (**26**, **Figure 38**) that could preferentially enter and accumulate inside apoptotic cells (**section 2.2.1.1**).[126] The second was a report by Ziv *et al*. on the development of a PET (positron emission tomography) imaging agent known as ML10 (**38**, **Figure 38**), that could preferentially detect and enter apoptotic cells (**section 2.2.1.2**).[184]

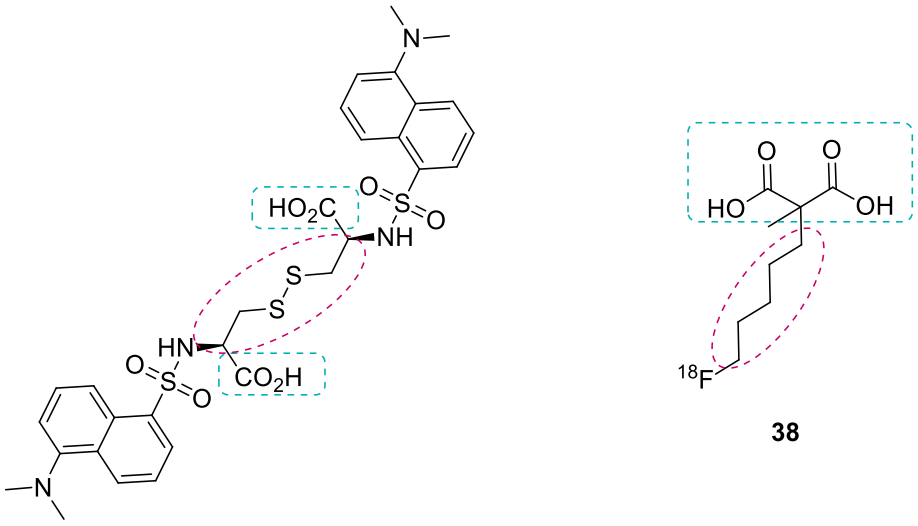

Figure 38: Didansyl cystine (**26**) and ML10 (**38**) both contain a di-carboxylic acid, a linker unit of 5/6 atoms.

Interestingly, both structures featured a dicarboxylic acid, a linker and small fluorescent unit (although ML10 features a radiolabel, the authors had briefly investigated an analogue containing a fluorophore). This project oversaw the modification of these structures to achieve the goal of developing new properties.

2.2.1.1. Didansyl Cystine based fluorophores

The first probe to be investigated as part of this project was didansyl cystine ((2*R*,2'*R*)-3,3'-disulfanediylbis(2-(5-(dimethylamino)naphthalene-1-sulfonamido) propanoic acid, DDC, **26**). As has already been discussed in **Chapter 1.3.2** this probe was originally reported by Shirvan *et al.* as a non-invasive method for imaging renal tubular cell injury in renal ischemia.[126]

DDC (**26**) was particularly attractive as it was reported to be able to pass through the cell membrane and accumulate intracellularly with a high specificity for cells undergoing apoptosis. The cell lines used by Shirvan *et al*. were human adult T-cell leukemia Jurkat cells and cervical carcinoma HeLa cells. Apoptosis was induced in the Jurkat cells either by treatment with IgM anti-Fas (CD95) antibody or with the caspase inhibitor Z-VAD-FMK in DMSO before the cells were incubated with the IgM anti-Fas antibody, whereas the HeLa cells were treated with staurosporine. Since our tests would involve different cell lines it was decided to synthesise DDC and observe its capabilities *in vitro* before considering what modifications should be carried out in order for the molecule to deliver a molecular cargo intracellularly.

As will be discussed in **section 2.3.1.** there was a need to find other fluorophores to incorporate onto the cystine unit linker. After an investigation into appropriate fluorescent units using the Thermo Fisher Scientific's Fluorescence SpectraViewer, available via the Thermo Fisher Scientific website, fluoroscein isothiocyanate (FITC) and rhodamine B isothiocyanate were chosen as candidates for further investigation.

Fluorescein and its derivatives are some of the most widely used set of fluorophores for biological research due to their exceptional fluorescence quantum yield, their high absorptivity and good solubility in water. FITC (**39**, **Figure 39**) is a small molecule with wide-ranging applications in biology. Its most common use is to label and track cells in fluorescence microscopy.

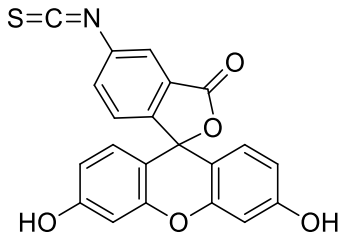

39

Figure 39: Fluoroscein isothiocyanate (FITC) (**39**). λ_{ex} 492 nm, λ_{em} 518 nm.

Rhodamine B isothiocyanate (**40**, **Figure 40**) is also a small molecule that has found widespread use in biology, mainly as a protein labelling probe.

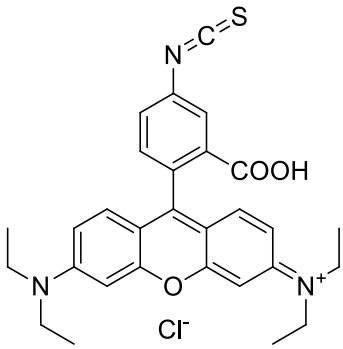

40

Figure 40: Rhodamine B isothicyanate (**40**). λ_{ex} 543 nm, λ_{em} 580 nm.

2.2.1.2. ML10 based fluorophores

ML10 (2-(5-fluoropentyl)-2-methylmalonic acid, **38**, see **Figure 41**) was developed as a PET (positron emission tomography) imaging agent of apoptosis by Ziv *et al.*[184] Since there is considerable evidence to support the hypothesis that apoptosis plays a significant role in the pathophysiology of many diseases (**Chapter 1.1.1.**), Ziv *et al*. set out to develop a PET tracer that could be made available for clinical diagnosis.

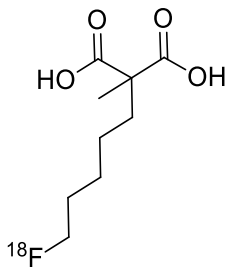

38

Figure 41: ML10 (**38**).

The group took inspiration from a class of proteins that bind to the membrane of cells undergoing apoptosis, which undergoes a loss of membrane potential and becomes permanently acidified due to the externalization of phosphatidylserine (PS). Though it was known that the γ-carboxyglutamic-acid (Gla, **41**, **Figure 42**) domain proteins, the anticoagulant proteins C and S, and the anti-apoptotic protein gas6 could bind to apoptotic cells, they had not been investigated for their potential use as apoptosis probes. All of these proteins had in common domains rich in the uncommon amino acid Gla, which is formed in the liver by the γ-carboxylation of glutamate.

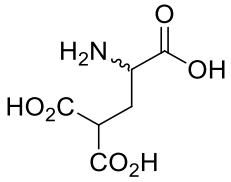

41

Figure 42: The uncommon amino acid DL-γ-carboxyglutamic acid (Gla).

Gla contains an alkyl malonate group which seems to be responsible for enabling the binding of the proteins to the acidic membranes. It was therefore hypothesised that the small molecule apoptosis probe should contain an alkyl malonate building block. The proposed mechanism of the uptake of ML10 into apoptotic cells is shown in **Figure 43**.

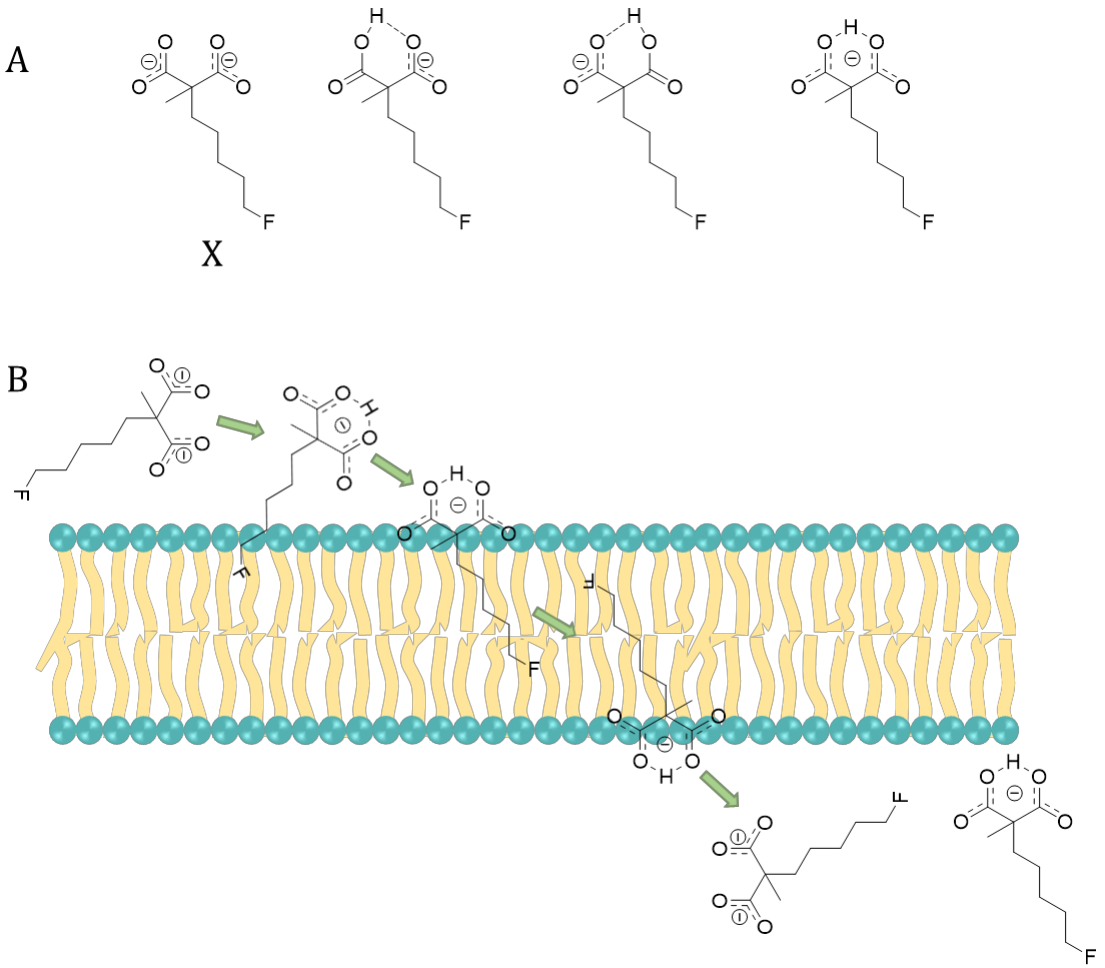

Figure 43: Proposed mechanism for ML10 uptake in apoptotic cells, modified from Ziv *et al.*[184] **A**: Protonation states of the malonate moiety of ML10, where **X** is favoured in aqueous conditions. **B:** Proposed mechanism for the transit of ML10 through a cell membrane of a cell going through the early stages of apoptosis, as such the membrane would be intact, externalization of PS leads to acidified external membrane which allows ML10 to capture a proton. This results in increased hydrophobicity and charge dispersion of ML10 which allows ML10 to enter the membrane. Passage through the membrane and delivery into the cytosol facilitated by depolarisation of ML10 and reacidification upon entrance to an acidic cytosol, characteristic of an apoptotic cell.

However, there is a slight flaw with this theory of passive diffusion of ML10 across the cell membrane. Permeability is usually governed by polarity and size, and as such, passive diffusion is usually limited to very small, moderately polar molecules or nonpolar gases. In fact, the cell membrane is almost impossible to cross for larger, uncharged polar molecules as well as all charged molecules. Therefore, these types of molecules require active transport to carry them across the membrane and into the cell.[185] Amino acids fall into the category of larger molecules that require active transport, and they make use of secondary active transporters that harness the

stored energy from the electrochemical gradient of another solute.[185,186] Since the structure of ML10 was based on the uncommon amino acid DL-γ-carboxyglutamic acid (Gla), and it would also carry a charge in aqueous conditions, it is therefore possible that it would also require the use of an active transporter to cross the cell membrane.

Modifications were made to the malonate unit: adding an alkyl chain to make the molecule amphipathic for better interaction with the cell membrane, optimised to include five carbon atoms, and addition of a methyl group at the α-position to prevent *in vivo* metabolism.

To test the viability of the newly designed probe, a number of easily observable derivatives were examined: a tritium labelled derivative (^{3}H-ML10) and a fluorescent derivative where the fluorine had been swapped with a dansyl group (ML10-dansyl). Apoptosis was induced in Jurkat cells by treatment with anti-Fas antibody. ^{3}H-ML10 and ML10-dansyl were tested alongside propidium iodide (PI, a marker of membrane disruption i.e. late stage apoptosis) and Annexin-V (an early stage apoptosis probe that adheres to the cell membrane upon the externalisation of PS (phosphatidylserine)). The results showed that both ^{3}H-ML10 and ML10-dansyl accumulated inside cells shortly after the apoptosis was induced, indicated by the fact that there was no PI uptake in the cells. ^{3}H-ML10 uptake appeared to coincide with the uptake of Annexin-V.

The method Ziv *et al*. used to prepare ML10-dansyl is described in **Scheme 2**. This involved first the preparation of 3-(5-bromo-pentyloxy)tetrahydropyran (**44**) by the protection of 5-bromopentanol (**42**) with dihydropyran (**43**), catalysed by pyridinium p-toluene sulfonate (PPTS). (**44**) was coupled with α-methyl di-*tert*-butyl-malonate (**45**) in the presence of potassium bis(trimethylsilyl)amide (KHMDS), forming the α-methyl, THP pentyl substituted malonate (**46**). The protecting groups were then removed with PPTS in ethanol to provide 2-(5-hydroxypentyl)-2-methyl-malonic-acid di-*tert*-butyl ester (**47**). The Boc-protected dansyl group (**49**) was prepared by reacting 5-dimethylamino-1-naphthalenesulfonamide (**48**), di-*tert*-butyl-dicarbonate and small amounts of 4-

dimethylaminopyridine in the presence of triethylamine. A Mitsonubo reaction was carried out to couple the Boc-dansyl amide (**49**) to 2-(5-hydroxy-pentyl)-2-methyl-malonic-acid di-*tert*-butyl (**47**), which involved reacting with triphenylphosphine and diisopropyl azodicarboxylate (DIAD). Removal of the *tert*-butyl protecting groups by hydrolysis using TFA at low temperature resulted in the final product, ML10-dansyl (**51**).

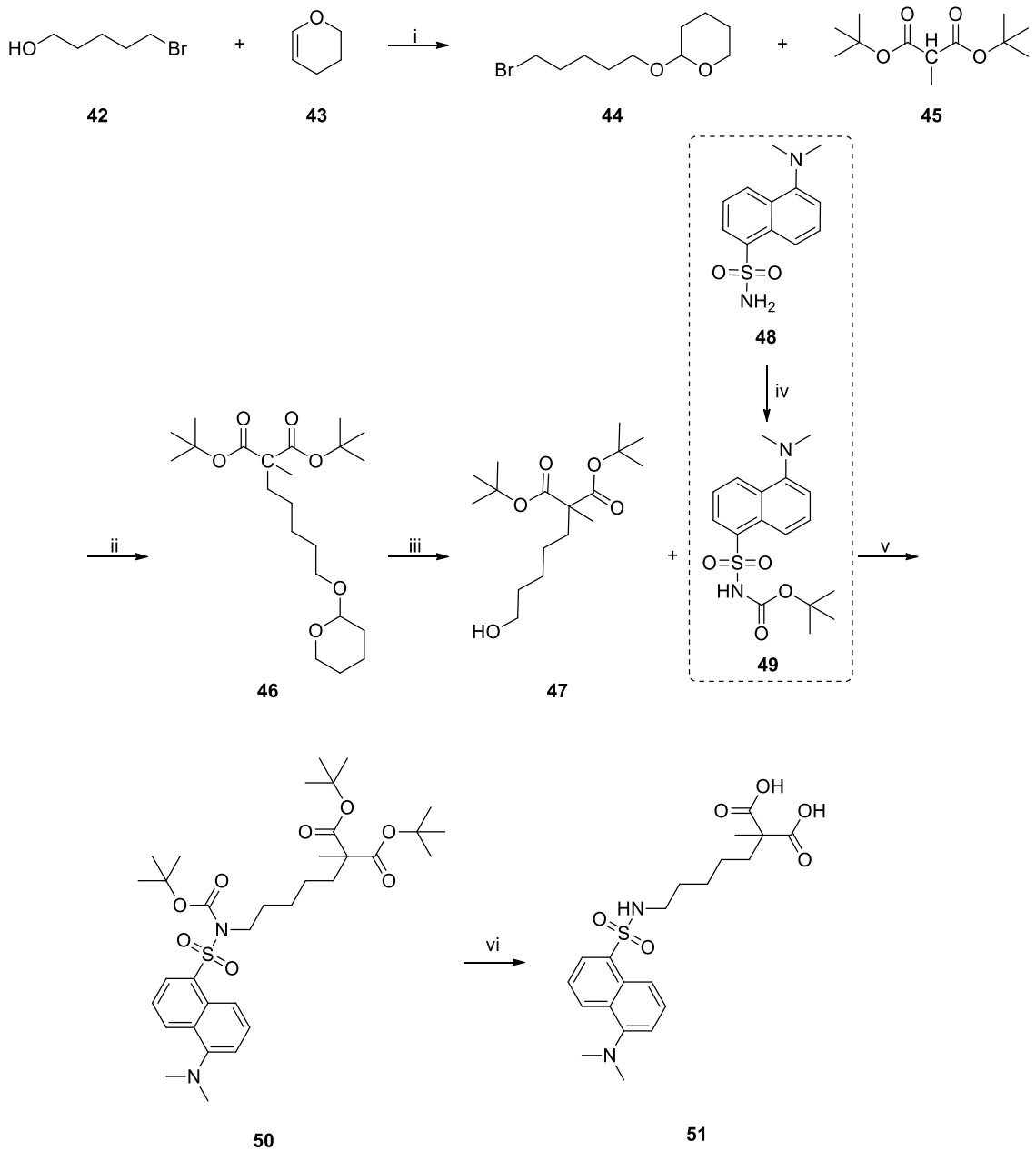

Scheme 2: Preparation of ML10-dansyl as reported by Ziv *et al.*[184] Reagents and conditions: i) Pyridinium *p*-toluenesulfonate (PPTS); ii) Potassium bis(trimethylsilyl)amide (KHMDS); iii) EtOH, PPTS; iv) di-*t*-butyl-dicarbonate, NEt_3, 4-dimethylaminopyridine; v) Mitsunobo conditions, PPh_3, DIAD; vi) TFA, low temp.

This study confirmed that an alkyl malonate derivative could successfully target apoptotic cells, and more importantly could do so with a fluorophore attached to the alkyl chain. We already knew that the dansyl group used in this case would not be suitable to observe with our equipment and so a new fluorophore was sought.

Mitsunobo reaction

The Mitsunobo reaction was first described in 1967 by Mitsunobo and Yamada for the preparation of esters from carboxylic acids using quaternary phosphonium salts.[187] Since its inception, the process has been developed and is now much more widely applied as a dehydrative coupling of alcohols (usually primary and secondary alcohols, though tertiary alcohols have been used on occasion) to a pronucleophile, mediated by a reaction between a trialkyl- or triarylphosphine and a dialkyl azodicarboxylate (**Scheme 3**). When reactions are carried out using secondary alcohols, a complete inversion of stereochemistry is observed.

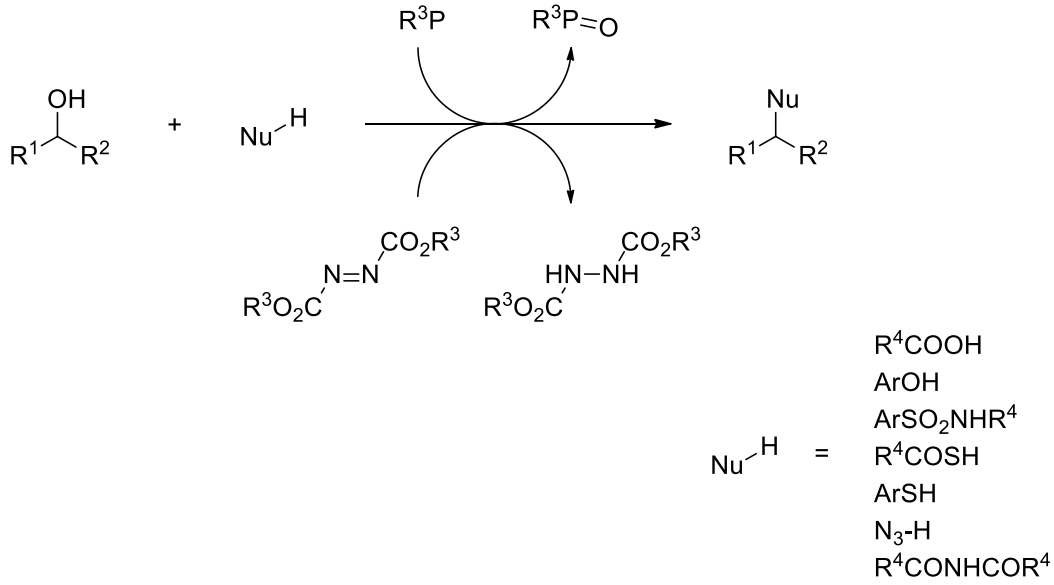

Scheme 3: General scheme of the Mitsunobo reaction.

Generally, in order for the Mitsunobu reaction to proceed it is widely accepted that the pK_a of the pronucleophile must be at least 11 or lower to be compatible with the dialkyl azodicarboxylate. This is because the acidic proton of the betaine, formed as a result of the reaction between triphenylphosphine and DEAD, needs to be removed to prevent alkylation of DEAD. Standard reaction conditions are usually

fairly mild, typically carried out between room temperature and 0 °C and tolerated solvents include THF, diethyl ether, dichloromethane, toluene, and in some instances more polar solvents such as ethyl acetate, acetonitrile and DMF can be used.[188]

The Mitsunobo reaction can form both C-C bonds and C-heteroatom bonds depending on the type of pronucleophile employed. (Thio)carboxylic acids, (thio)phenols, imides and sulfonamides form C-O, C-S and C-N bonds. Using the example presented above in **Scheme 2** a C-N bond is formed. The first stage involves the triphenyl phosphine reacting with the DIAD or DEAD via a nucleophilic attack which forms the betaine intermediate. The betaine intermediate then deprotonates the alcohol, forming an ion pair. The phosphonium ion binds to the oxygen, activating it as a leaving group and allowing nucleophilic substitution by the amine of the dansyl group (**Scheme 4**).

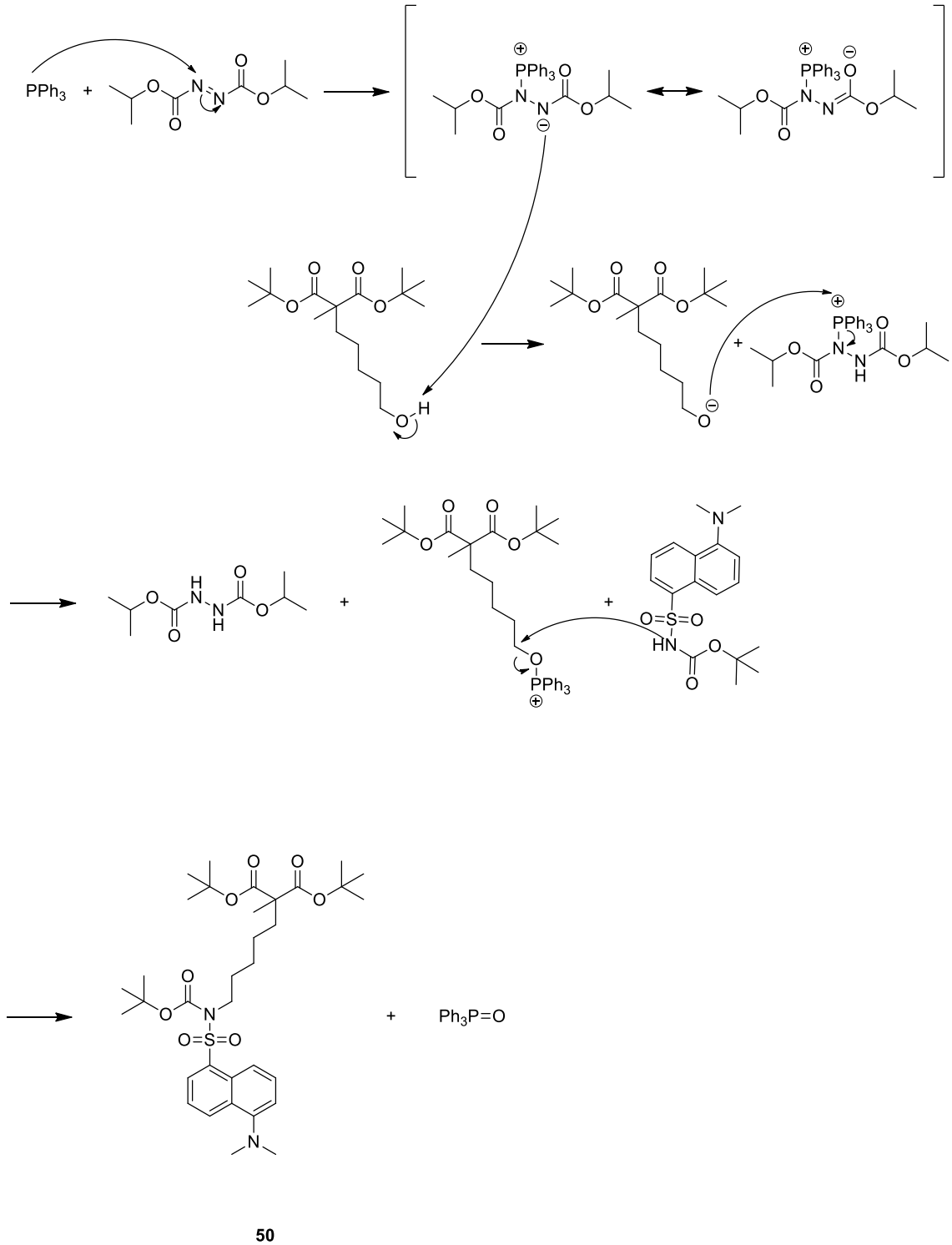

50

Scheme 4: Proposed mechanism for the formation of ML10-dansyl via Mitsunobo conditions, as described by Ziv *et al*.[184]

Currently there are limited instances of the Mitsunobo reaction being used for C-C bond forming reactions due to the relatively high pK_a of carbon acids. The first C-C bond forming example was reported in 1985 by Falck and Manna and involved using

lithium cyanide to displace an activated alcohol to produce the corresponding organic nitrile.[189] Meldrum's acid has also been used successfully as a pronucleophile due to having a pK_a of 4.97, though the presence of two acidic protons makes control during the alkylation step difficult resulting in double C-alkylation. Shing *et al*. overcame the controllability problem by simply using a mono-substituted Meldrum's acid for coupling with primary alcohols; coupling with secondary alcohols was problematic and required catalytic amounts of Pd(0) to promote C- alkylation over O-alylation.[190]

2.2.1.2.1. BODIPYs

The class of dyes known as BODIPY (4,4-difluoro-4-bora-3a,4a-diaza-s-indacene) dyes was chosen as the most suitable (**52**, **Figure 44**).

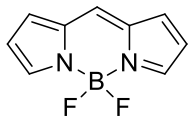

52

Figure 44: BODIPY core structure.

The BODIPY scaffold has been incredibly useful as a functional fluorescent probe due to its relatively high photostability, overall neutral charge, high fluorescence quantum yield and sharp excitation and emission spectra.[191–194] BODIPY-based probes can be applied to both cell and *in vivo* imaging, with the latter possible due to the tunability of the BODIPY dye's fluorescence via chemical modifications[194–196] to the near infra-red (NIR) region of the spectrum. NIR fluorescence is very useful as NIR light can penetrate deep into tissues without causing significant damage or light scattering, allowing observations of targets *in vivo*.[197]

Though the BODIPY scaffold is highly hydrophobic, which would usually be problematic for the visualization of biological samples, the BODIPY scaffold can be modified easily to incorporate hydrophilic groups. Without the hydrophilic groups, the dyes tend to accumulate within subcellular membranes but with the incorporation of solubilizing groups such as tetraethylene glycol, and alkoxy and carboxylate groups, BODIPYs can instead accumulate in the cytosol. However,

membrane permeability depends on the entire structure, thus when designing BODIPY based probes it is necessary to consider the pK_a, logP and logD.

BODIPYs also have the advantage of possessing an "on/off" functionality whereby the fluorescent property can be controlled by Förster resonance energy transfer (FRET)[198] or photo-induced electron transfer (PeT)[199–201] in response to target molecules using the FRET or the PeT process as a quenching mechanism. By considering changes of the molecular structure and the effects on the frontier orbital energy level, the molecules can be designed to signal in response to changes in pH, protein activity, interactions between biomolecules and cells, and the presence of cations. There are several examples of this type of BODIPY structure that are commercially available.

BODIPYs are considered as a neutral molecule since the charge is spread throughout the conjugated ring system. It is therefore usually depicted in an uncharged form.

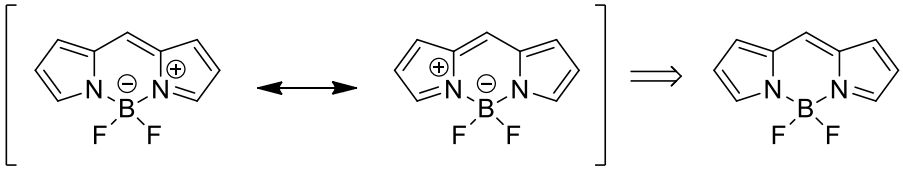

Scheme 5: Resonance forms of the BODIPY core structure resulting in depiction as an uncharged molecule.

The first BODIPY was reported in 1968 by Treibs and Kreuzer.[202] Whilst trying to form acylated pyrroles by using 2,4-dimethylpyrrole (**53**), acetic acid and boron trifluoride as a Lewis acid catalyst, a highly fluorescent compound was formed instead. This was due to the acid catalysed condensation of the pyrrole to form a dipyrrin which was complexed with the boron trifluoride diethyl etherate (**Scheme 6**).

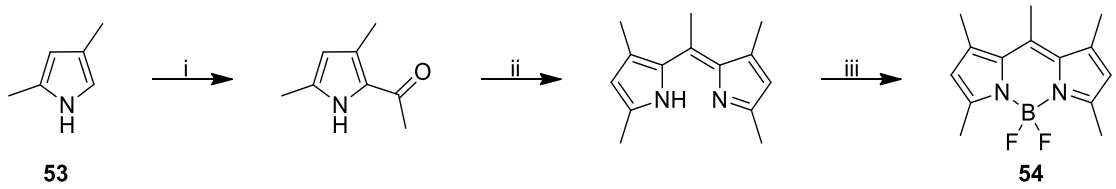

Scheme 6: Fist example of BODIPY synthesis carried out by Treibs and Kreuzer in 1968.[202] Reagents and conditions: i) Ac_2O, $BF_3.Et_2O$; ii) H^+; iii) Ac_2O, $BF_3.Et_2O$.

BODIPYs can be easily and cheaply synthesized from readily available materials and can also be easily modified making them a very attractive group of fluorophores to use for this study. The reaction proceeds via a Vilsmeier type reaction. BODIPYs are easily prepared by reacting a pyrrole with at least one free α-position, with an acid chloride and boron trifluoride diethyl etherate in the presence of a tertiary amine (**Scheme 7**).

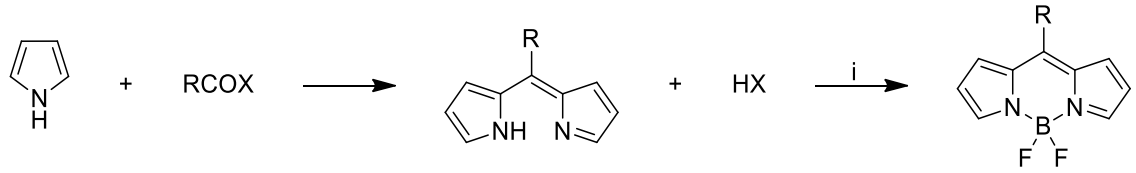

Scheme 7: General reaction scheme for the formation of the core BODIPY structure. i) Tertiary amine, $BF_3.Et_2O$.

It is worth mentioning that the IUPAC numbering of dipyrrins and dipyrromethene is different to BODIPY numbering (**Figure 45**), however the central carbon is always referred to as the *meso* position in line with porphyrin nomenclature.[203]

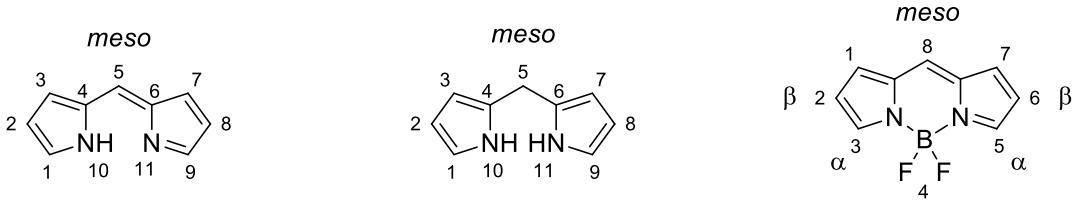

Figure 45: IUPAC numbering of dipyrrin, dipyrromethene and BODIPY.[203]

Though the BODIPY core structure requires a relatively straightforward synthetic procedure, extra care must be taken when working with pyrroles due to their highly reactive nature.

Pyrrole polymerisation

Pyrroles are exceptionally good at electrophilic substitution reactions. The delocalization from the N lone pair is spread evenly around the ring and since it is a five-membered ring, the delocalization can be drawn easily anywhere around the ring (**Scheme 8**). A consequence of the delocalisation of the N lone pair is the ring becomes electron rich, raising the energy level of the HOMO and therefore making the ring more nucleophilic and more readily attacked by electrophiles.

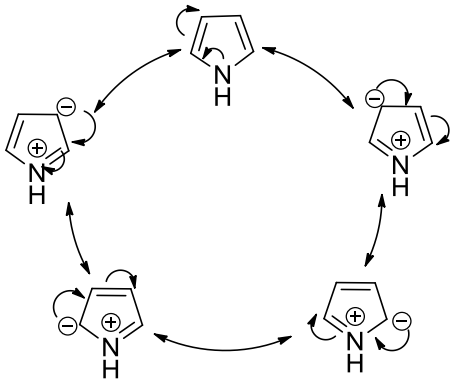

Scheme 8: Resonance forms of pyrrole.

The stabilization of regioisomeric transition states during electrophilic aromatic substitution through pyrrole resonance means that pyrrole can be easily attacked at any carbon. This can pose a problem for reactions where only mono-substitution is required, such as the reaction required for BODIPY synthesis. Protonation can also occur at any of the carbons around the ring which leads to polymerisation of pyrroles (**Scheme 9**) especially under strongly acidic conditions i.e. acids with a pK_a <-4, such as HCl which is generated during the formation of the BODIPY core.

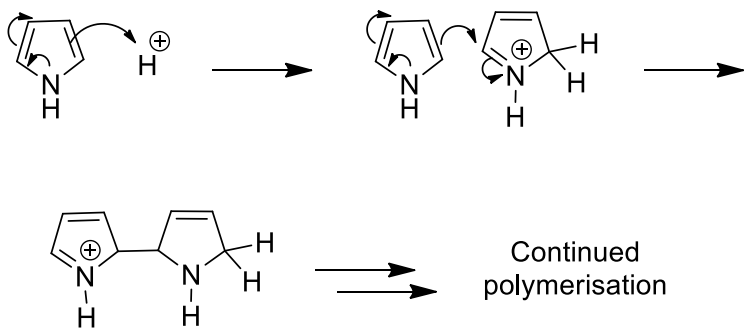

Scheme 9: Polymerisation of pyrroles.

In the absence of strong acids, it is possible to control the substitution of pyrroles and achieve only mono-substituted products using either the Vilsmeier reaction or the Mannich reaction. This is because most reagents will attack first at the 2- or 5-positions and will only attack the 3- or 4-positions if 2- and 5- are unavailable. Although it was mentioned earlier that delocalization is evenly spread around the pyrrole, intermediate products of reactions at the 2- and 5-positions are slightly more stable due to having a linear conjugated system i.e. both double bonds are conjugated with N^+, as opposed to the cross-conjugated intermediate products from reactions at the 3- and 4-positions (**Scheme 10**).

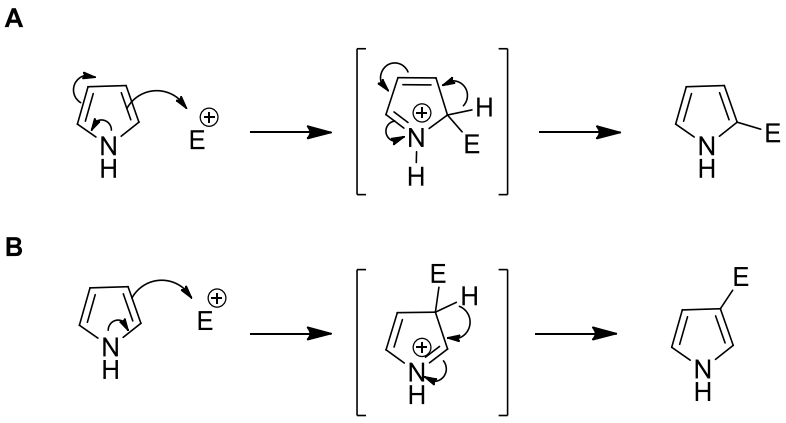

Scheme 10: Comparison of stability of intermediates of reactions with pyrroles. **A**: Reaction with electrophile at 2-position. **B**: Reaction with electrophile at 3-position.

Vilsmeier reaction

The Vilsmeier reaction is an acylation type reaction which involves reacting phosphorus oxychloride ($POCl_3$) with *N,N*-dimethylamide to create a carbon electrophile in the absence of a strong or Lewis acid. The amide reacts with $POCl_3$ forming an iminium cation which reacts with the pyrrole via a nucleophilic substitution reaction which provides the much more stable iminium salt. The salt is then hydrolysed with sodium carbonate and water which removes any acid formed and attaches the formyl group (**Scheme 11**).

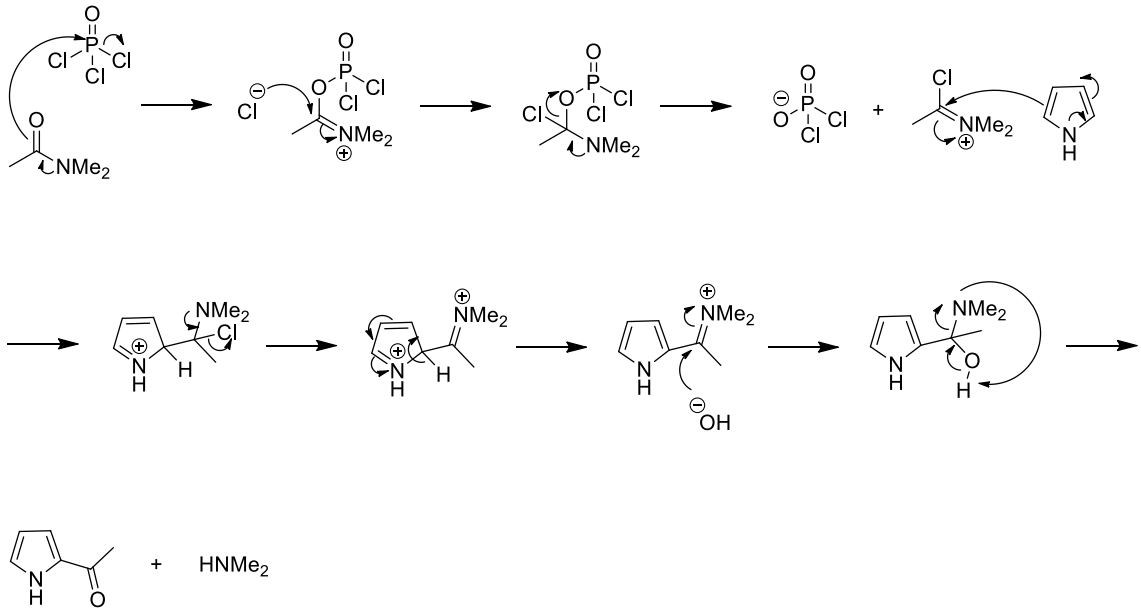

Scheme 11: Vilsmeier reaction mechanism.

Mannich reaction

The reaction is initiated with the protonation of formaldehyde which goes on to react with an amine, forming an iminium cation. The iminium cation reacts with the pyrrole via an electrophilic substitution reaction (**Scheme 12**).

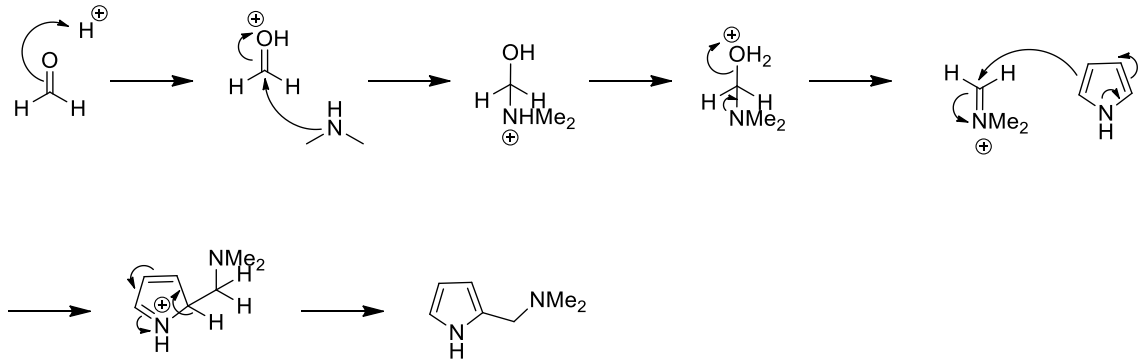

Scheme 12: Mannich reaction meachanism.

2.3. Results

2.3.1. Didansyl cystine based fluorophores

The synthetic route towards DDC (**26**) was quite straightforward. A mixture of cystine (**55**, 1 equiv.) and potassium carbonate was dissolved in equal quantities of acetone and water. Dansyl chloride (**48**, 2 equiv.) was then added and the mixture was allowed to stir at room temperature for 1.5 h. After this time, the acetone was

removed and the solution acidified with citric acid (2 M), causing the product to precipitate out of solution as a yellow solid, to be collected by vacuum filtration in near quantitative yield (**Scheme 13**).

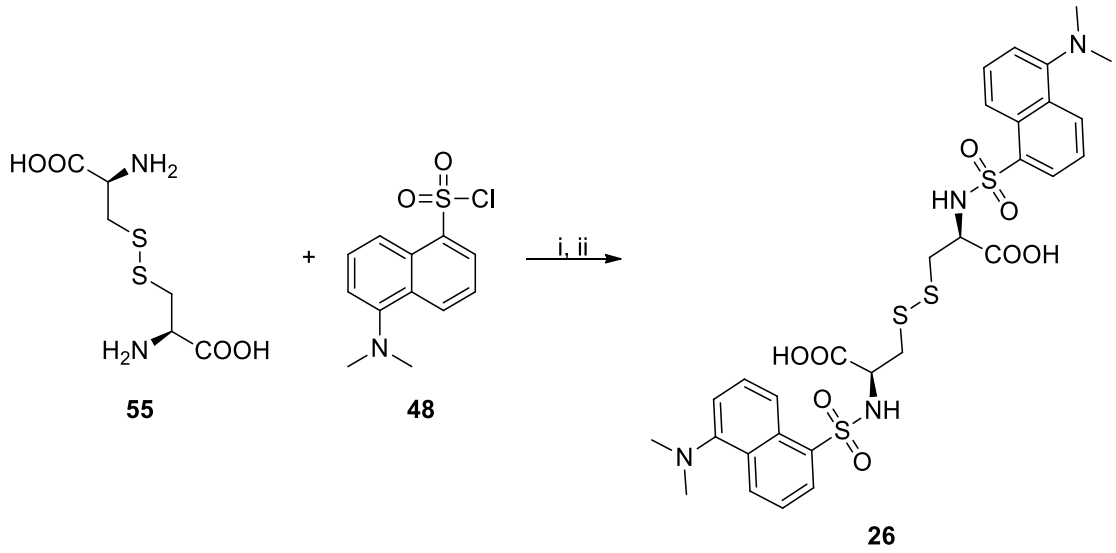

Scheme 13: Formation of DDC (**26**). Reagents and conditions: i) K_2CO_3, water/acetone (1:1), 1.5 h, RT; (ii) acidify with citric acid (2 M), 99%.[126]

The biological properties of DDC (**26**) were imaged *in vitro* by Dr. Karen Marshall. It was found that the wavelength for excitation of DDC (**26**) lay outside of the range of the fluorescence microscopes (λ_{ex} 365 nm, λ_{em} 420 nm). Therefore, it was decided to incorporate alternative fluorophores that could be imaged on site. The new fluorophores had to meet certain criteria to be considered; 1) commercially available and inexpensive, 2) relatively small molecule preferably non-charged in order to pass through a cell membrane, 3) wavelength of excitation no lower than λ_{ex} 405 nm, 4) accessible using an isothiocyanate group for easy addition onto a cystine unit. This task was carried out using the Thermo Fisher Scientific's Fluorescence SpectraViewer, available via the Thermo Fisher Scientific website. Using this method, two fluorophores were identified as being ideal candidates; fluoroscein isothiocyanate (**39**, FITC) and rhodamine B isothiocyanate (**40**).

The same reaction conditions employed for the formation of DDC (**26**) were used since the thiourea bond is usually one that forms easily under mild, aqueous conditions in the presence of base. However, upon addition of citric acid (2 M), no

precipitate was seen to form. An extraction was attempted but no product was ever isolated.

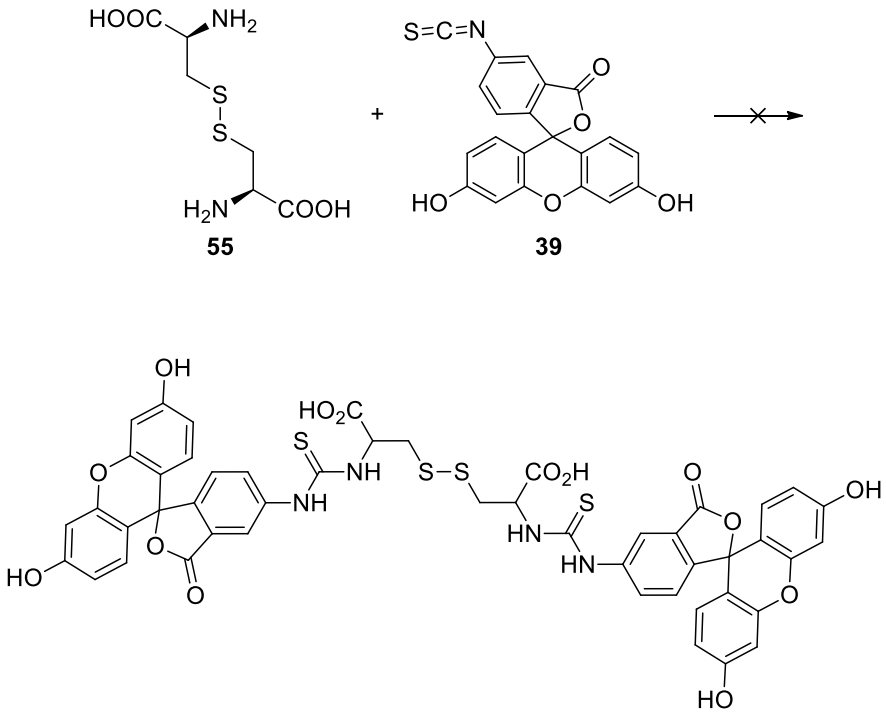

Scheme 14: Proposed reaction scheme for the formation of a cystine-fluorescein derivative.

Again, the same reactions conditions used for the formation of DDC (**26**) were employed to prepare the rhodamine derivative but without success (**Scheme 15**).

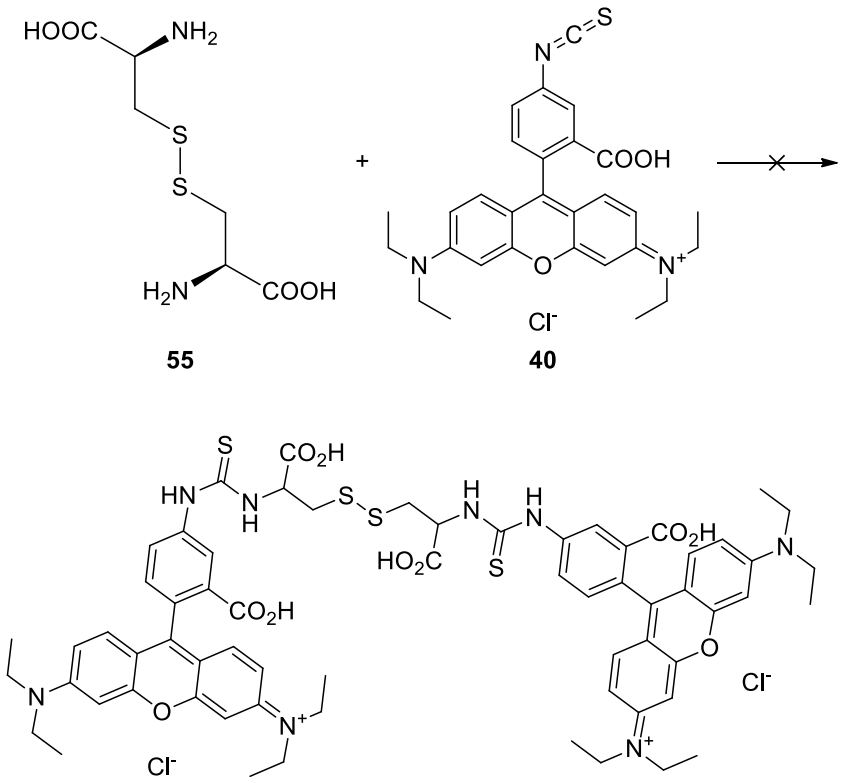

Scheme 15: Proposed reaction scheme for the formation of the cystine-rhodamine derivative.

Since it was now apparent that the using a cystine unit as a tether to the fluorophores was not going to be achieved easily it was decided to abandon this approach and take inspiration instead from another small molecule that had been proven to preferentially enter apoptotic cells.

2.3.2. Development of BODIPY library

Since it was already known that an alkyl malonate with a five-carbon tether was necessary, it was decided to aim to synthesize a compound with the general structure as seen in **Figure 46**.

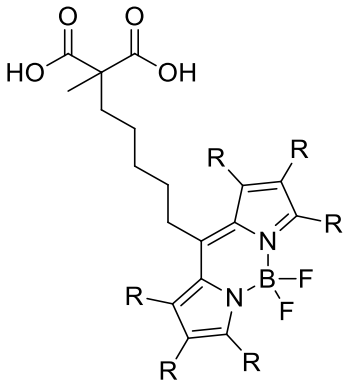

Figure 46: General structure of ML10-BODIPY derivative.

2.3.2.1. Unsubstituted Pyrrole

The first BODIPY attempted was the simplest using an unsubstituted pyrrole (**56**) and a method developed by Jiao *et al*.[204] (**Scheme 16**). The pyrrole (**56**) needed to be freshly distilled for use in this reaction and the reaction carried out under an inert atmosphere. The first step required mixing the pyrrole with 6-bromohexanoyl chloride (**57**), allowing the mixture to stir at room temperature for 12 h. To counteract the effects of pyrrole polymerization, a large amount of dry solvent was required as well as a 10:1 ratio of pyrrole (**56**) to 6-bromohexanoyl chloride (**57**). Argon was allowed to flow through the vessel slowly to purge the flask of HCl gas generated during the reaction. A colour change was observed to take place over this time from a pale yellow to a dark red. After this time, triethylamine was added followed by the slow dropwise addition of boron trifluoride diethyletherate. During this stage HF gas released as a by-product so again the argon was fed through the vessel. The temperature was then increased to 50 °C and the mixture allowed to stir overnight.

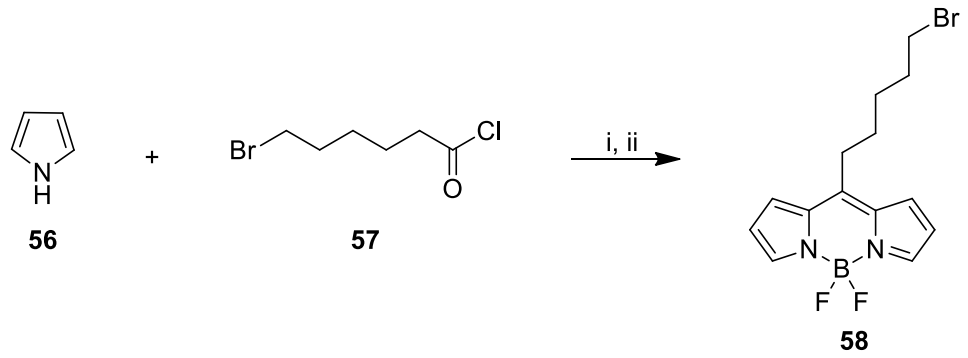

56 57 58

Scheme 16: Formation of **58**. Reagents and conditions: i) Inert atmosphere, 1,2-dichloroethane, RT, 12 h; ii) NEt_3, $BF_3.Et_2O$, 50 °C, overnight, 43%.

Purification was carried out using flash chromatography using a gradient elution solvent system of 100% hexane to 10% ethyl acetate in hexane. During this stage, it was noted that a black substance, assumed to be a product of pyrrole polymerization, was unable to pass through the frit of the column. This substance was found to block the column following a scale up attempt. A silica plug was employed in an attempt to remove the substance before carrying out flash chromatography, however it was found that a lot of the substance still eluted, making scale up of the process problematic.

Whilst a reasonable yield was achieved (43%), it was observed by TLC analysis that other fluorescent side products had formed during the reaction that were not removed by column chromatographic purification. An attempt was made to purify the product further by recrystallization but with little success. ^{1}H NMR spectroscopic analysis also showed prominent peaks not belonging to the product. Upon further analysis, the peaks were attributed to **58**, **58** without BF_2 coordination, and acyl chloride starting material (**57**) in a 1:1:3 ratio (**Figure 47**). This meant that the actual yield of **58** was 9%.

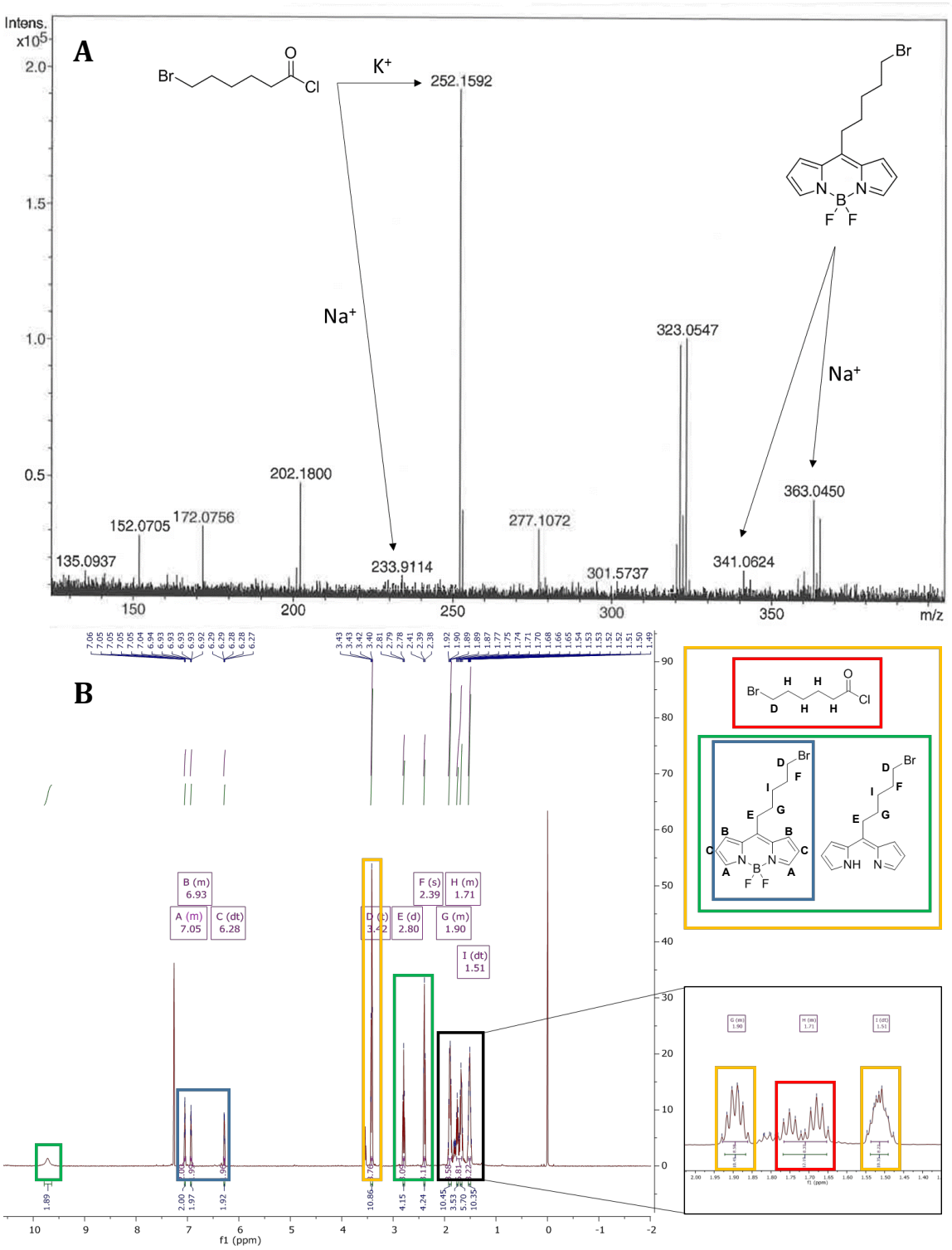

Figure 47: Analysis of **58**. **A**: Mass spectrum showing *m/z* of **58** and starting material. **B**: ^{1}H NMR spectrum showing the presence of product **58**, **58** with uncoordinated BF_2, and starting material **57** in a 1:1:3 ratio respectively.

The synthesis of two additional unsubstituted pyrrole-based BODIPY analogues was attempted bearing a shorter alkyl linking chain (**Scheme 17**) using the same conditions laid out above.

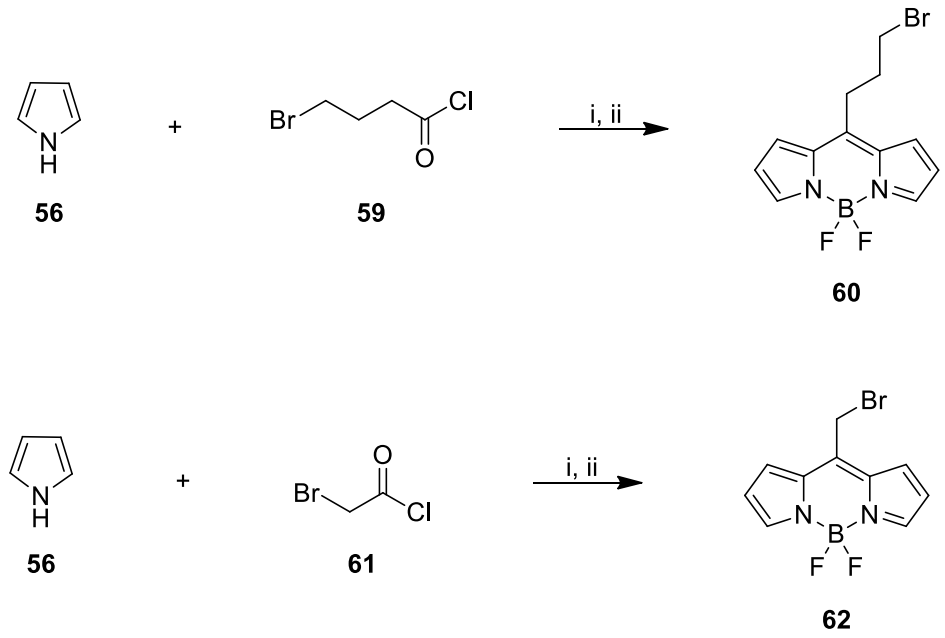

Scheme 17: BODIPY analogues with shorter alkyl chains. Reagents and conditions: i) Inert atmosphere, 1,2-dichloroethane, RT, 12 h; ii) NEt_3, $BF_3.Et_2O$, 50 °C, overnight, 18% (**60**), 15% (**62**).

Step 1 was successfully carried out for both examples, however yields achieved for **60** and **62** were very low, 18% and 15% respectively. Interestingly there appeared to be no other products present in either of these samples. The ^1H NMR spectrum for **60** suggested that **60** might be present without coordinated BF_2, however the peak did not integrate to anything substantial, the other peaks integrated correctly for **60** and the mass spectrum only showed the presence of **60** (**Figure 48**). In contrast, the ^1H NMR spectrum for **62** only showed peaks consistent with 62 (**Figure 49**).

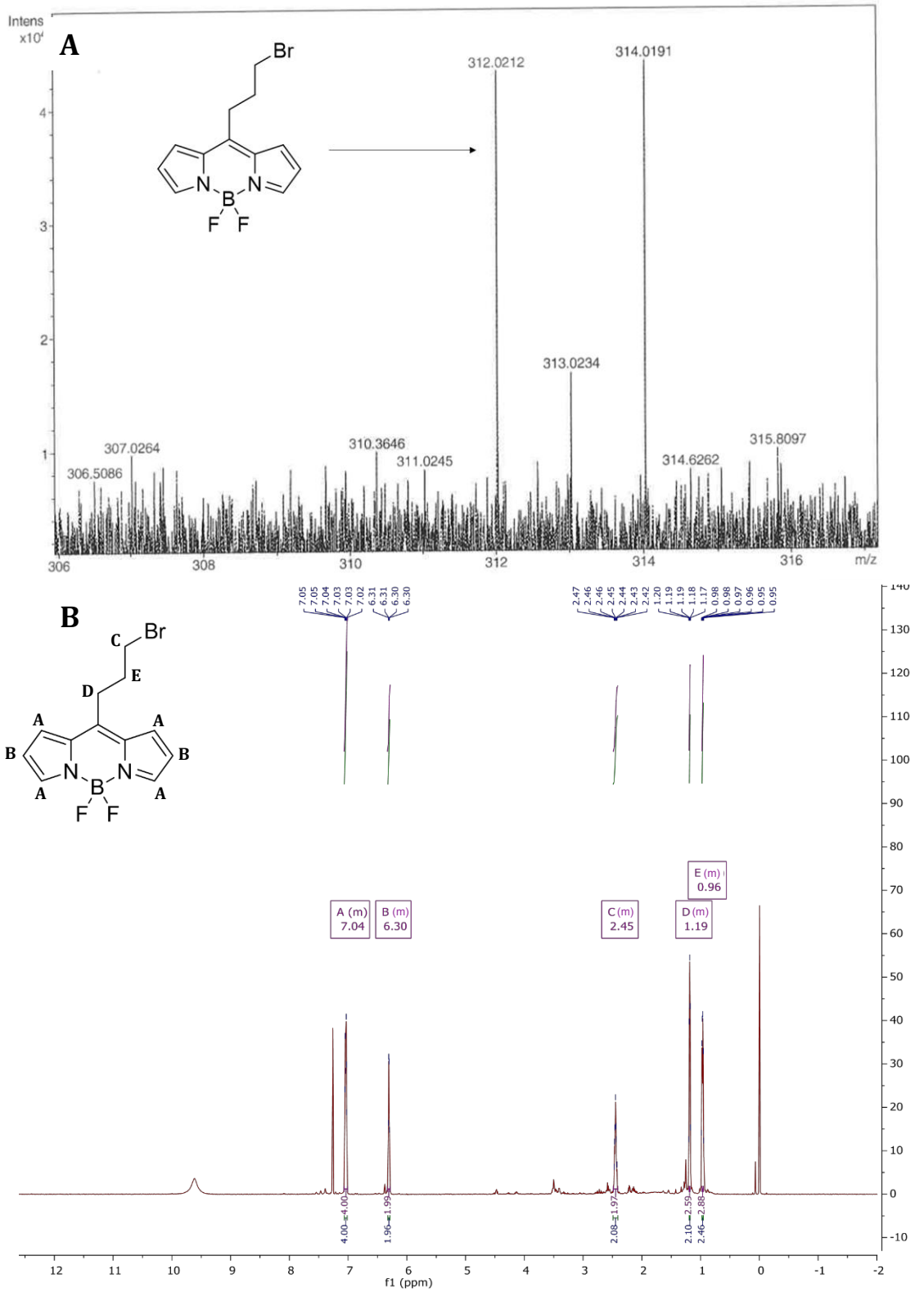

Figure 48: Analysis of **60**. **A**: Mass spectrum showing *m/z* of **60**. **B**: NMR spectroscopic analysis showing peaks consistent with the presence of product **60**.

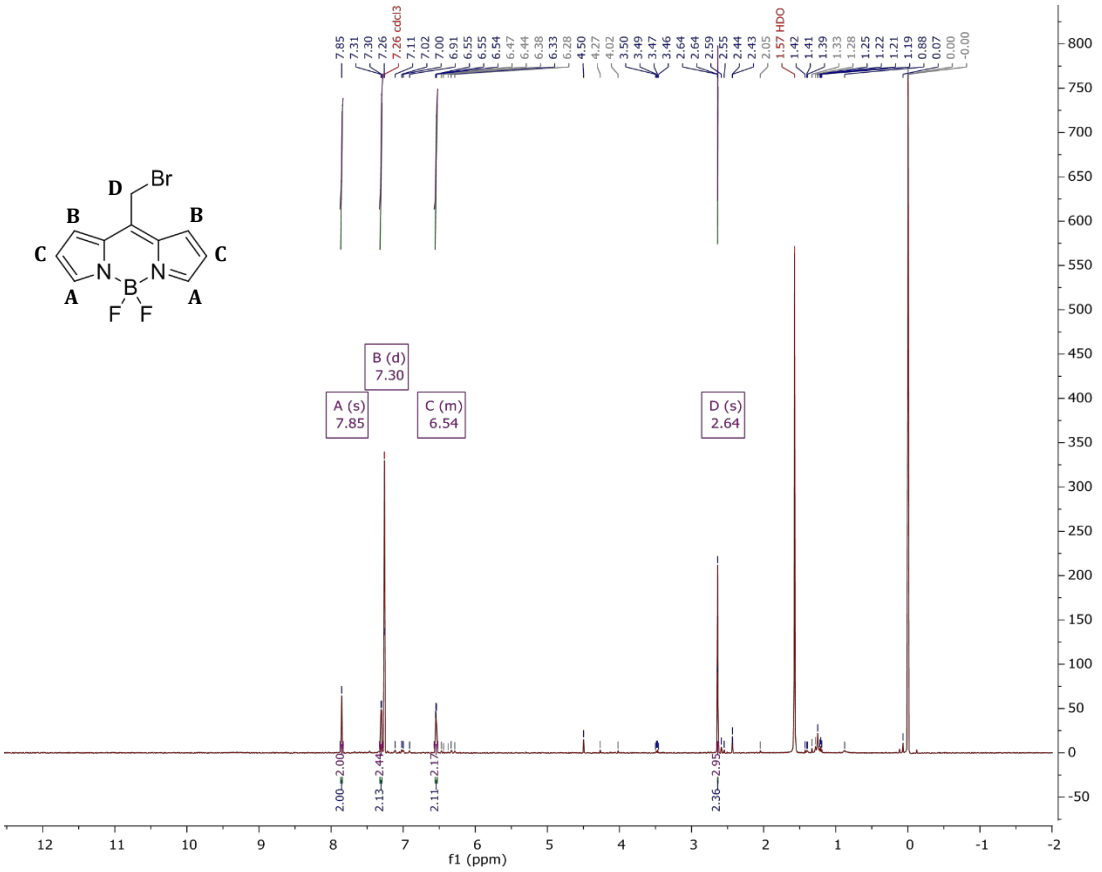

Figure 49: Analysis of **62**. ^{1}H NMR spectroscopic analysis showing peaks consistent with the presence of product **62**.

In the case of **62**, it was found that a side product, **63**, had formed that could be isolated in almost the same yield as the main product (**Scheme 18**).

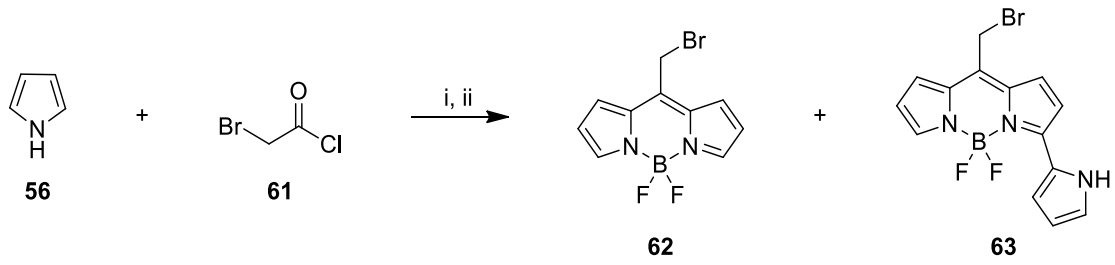

Scheme 18: Formation of **62** and side product **63**. Reagents and conditions: i) Inert atmosphere, 1,2-dichloroethane, RT, 12 h; ii) NEt_3, $BF_3.Et_2O$, 50 °C, overnight, 15% (**62**), 11% (**63**).

Product **63** was isolated in an 11% yield and quite interestingly had completely different visual characteristics to product **62**. Whilst product **62** was isolated as an orange solid which fluoresced yellow/green in solution, product **63** was isolated as a dark purple solid and bright pink in solution. Product **63** melted over a range of

124.6 – 130.9°C, indicating that the sample was impure. This was confirmed by ^{1}H NMR spectroscopic analysis which showed peaks in the allylic region that did not belong to the product (**Figure 50**).

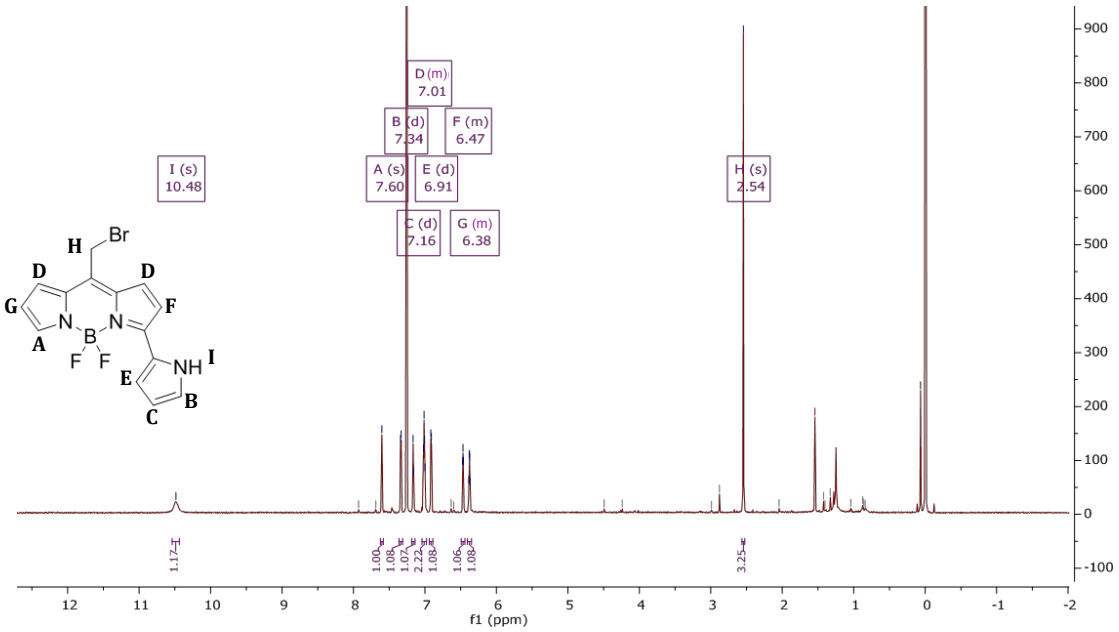

Figure 50: Analysis of **63**. ^{1}H NMR spectrum showing peaks consistent with the presence of product **63**.

A proposed mechanism for the generation of products **62** and **63** is shown in **Scheme 19**. It is thought that the extra pyrrole addition occurred during the first stage of the reaction whilst the acyl chloride was reacting with half of the pyrrole present, generating HCl in the process (step **A**), which would help the remaining pyrrole start polymerising (step **B**). Both forms of pyrrole will then go on to form the backbone of the BODIPY core (step **C**). During the work-up stage, the mixture would be exposed to air causing the oxidation and rearomatisation of the substituted pyrrole (step **D**).

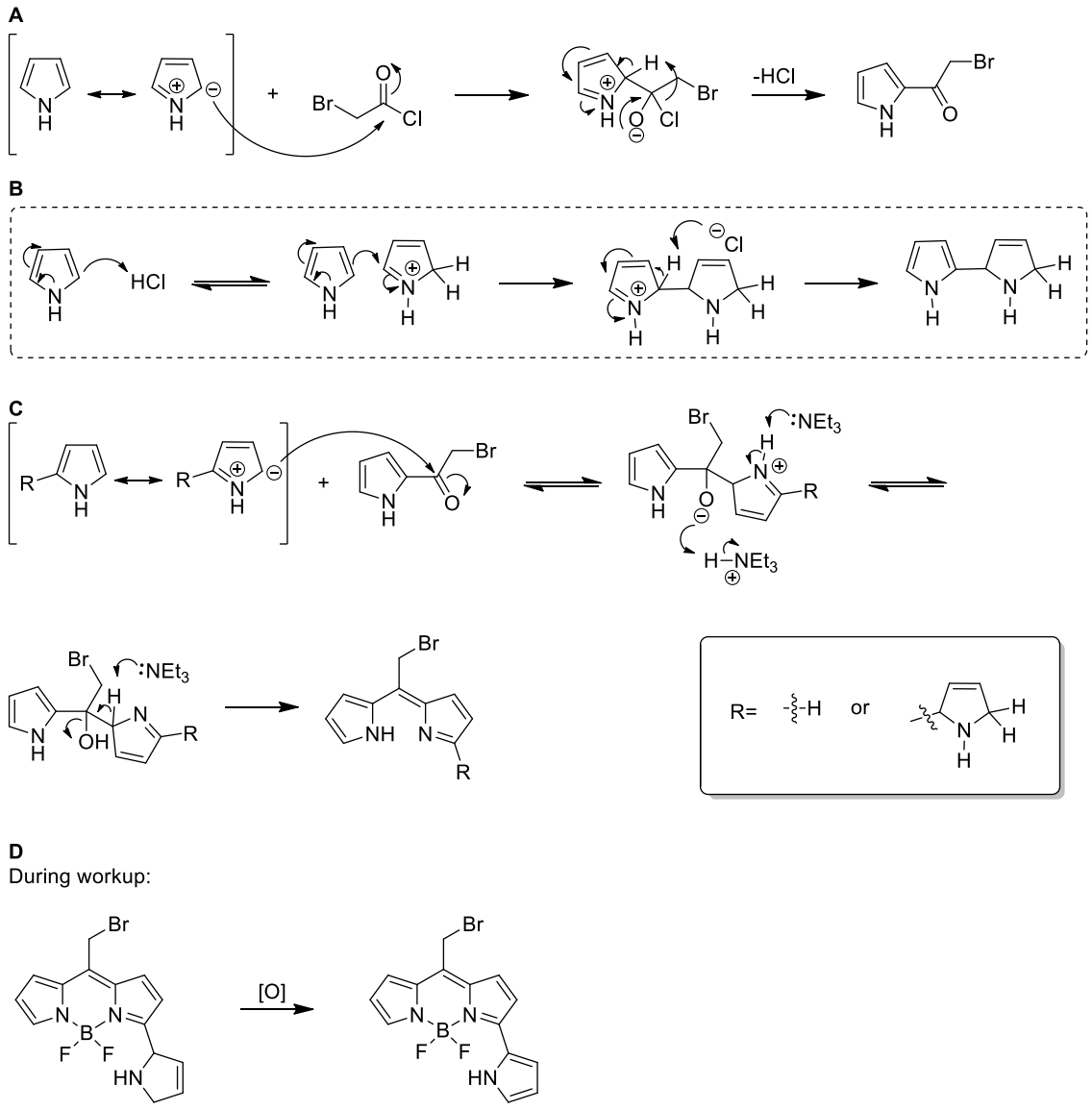

Scheme 19: Proposed mechanism for the formation of **62** and **63**. **A:** Acyl chloride reacts with pyrrole generating HCl in the process. **B:** HCl catalyses pyrrole polymerization. **C:** Both unsubstituted and newly substituted pyrrole go on to form the backbone of the BODIPY core. **D:** Oxidation causes rearomatisation of pyrrole.

Attempts were made to carry out step 2 (**Scheme 20**) but the desired products could not be isolated.

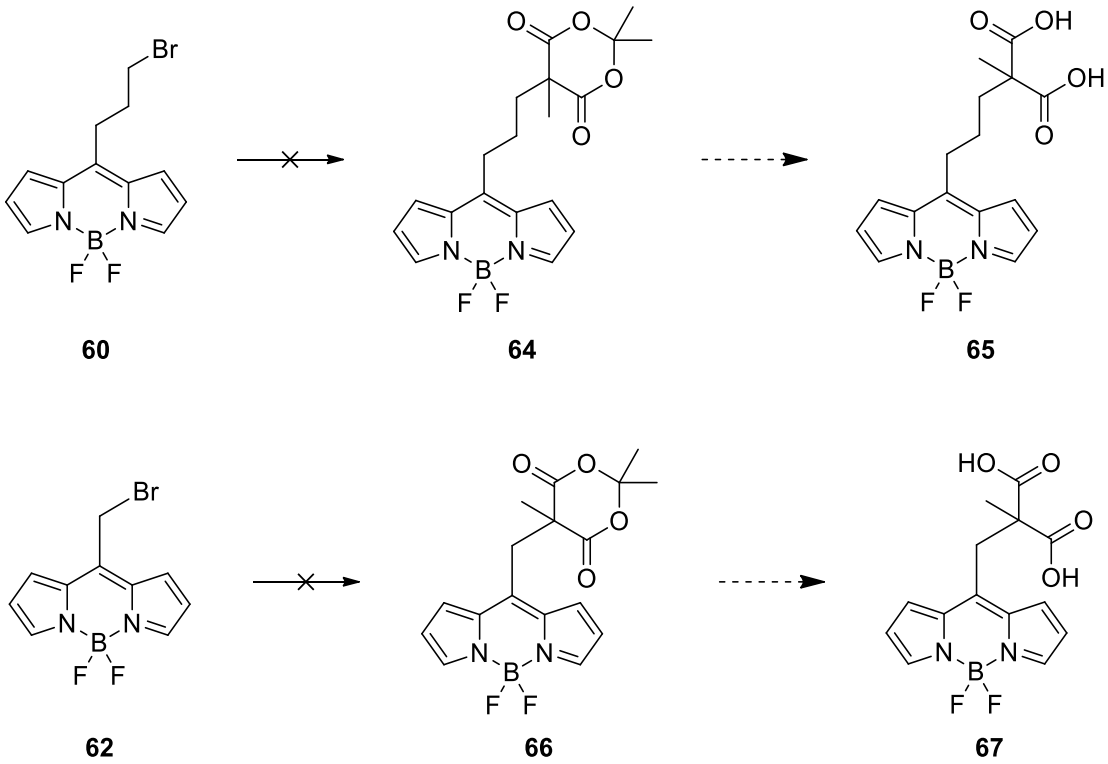

Scheme 20: Proposed routes to unsubstituted pyrrole based BODIPY dyes with shorter carbon chain lengths.

Due to the difficulties encountered with polymerization using an unsubstituted pyrrole, the low yielding reactions and difficulty in obtaining pure products, it was decided to attempt to access a BODIPY derivative starting from a trisubstituted pyrrole.

2.3.2.2. Trisubstituted Pyrrole

It was decided that for a trisubstitued pyrrole to be considered for investigation for this project, it should to be commercially available, inexpensive and contain small "R" groups, such as methyl or ethyl groups. The pyrrole that fell into this category was 3-ethyl-2,4-dimethyl-1*H*-pyrrole (**68**, **Figure 51**).

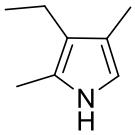

68

Figure 51: 3-ethyl-2,4-dimethyl-1*H*-pyrrole (**68**).

Again the reactions conditions developed by Jiao *et al*.[204] were employed and **69** was achieved in a 54% yield (**Scheme 21**). The product was obtained as red, iridescent crystals.

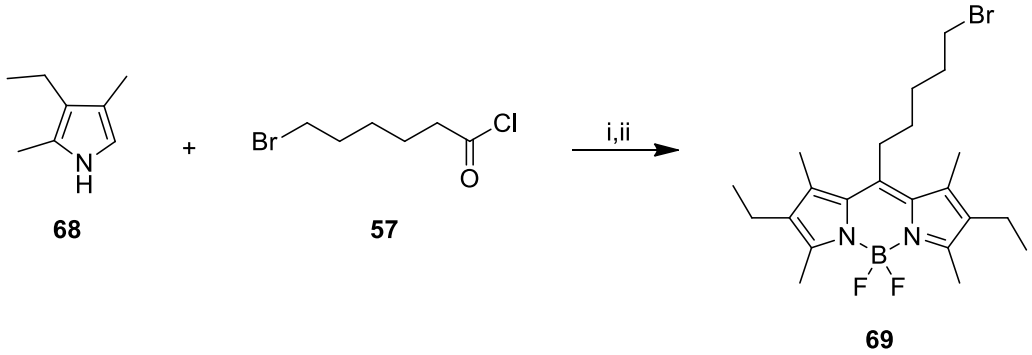

68 **57** **69**

Scheme 21: Formation of **69**. Reagents and conditions: i) Inert atmosphere, 1,2-dichloroethane, 12 h, RT; ii) NEt_3, $BF_3.Et_2O$, 50 °C, overnight, 54%.

Purification was carried out with flash chromatography using a solvent gradient 100% hexane to 40% ethyl acetate in hexane. A black substance, assumed to be the same as described in **section 2.3.2.1.**, was formed during this reaction and was unable to pass through the frit, therefore a one-pot scale up was not attempted. It was also notable that an NH peak was not present in the ^1H NMR spectrum leading to the conclusion that the only product present was **69** and not **69** without coordinated BF_2. A mass spectrometric analysis confirmed that the only product consistent with the analytical data was **69** (with Na^+). A melting point of 150.5-151.3 °C indicated a high level of purity (**Figure 52**).

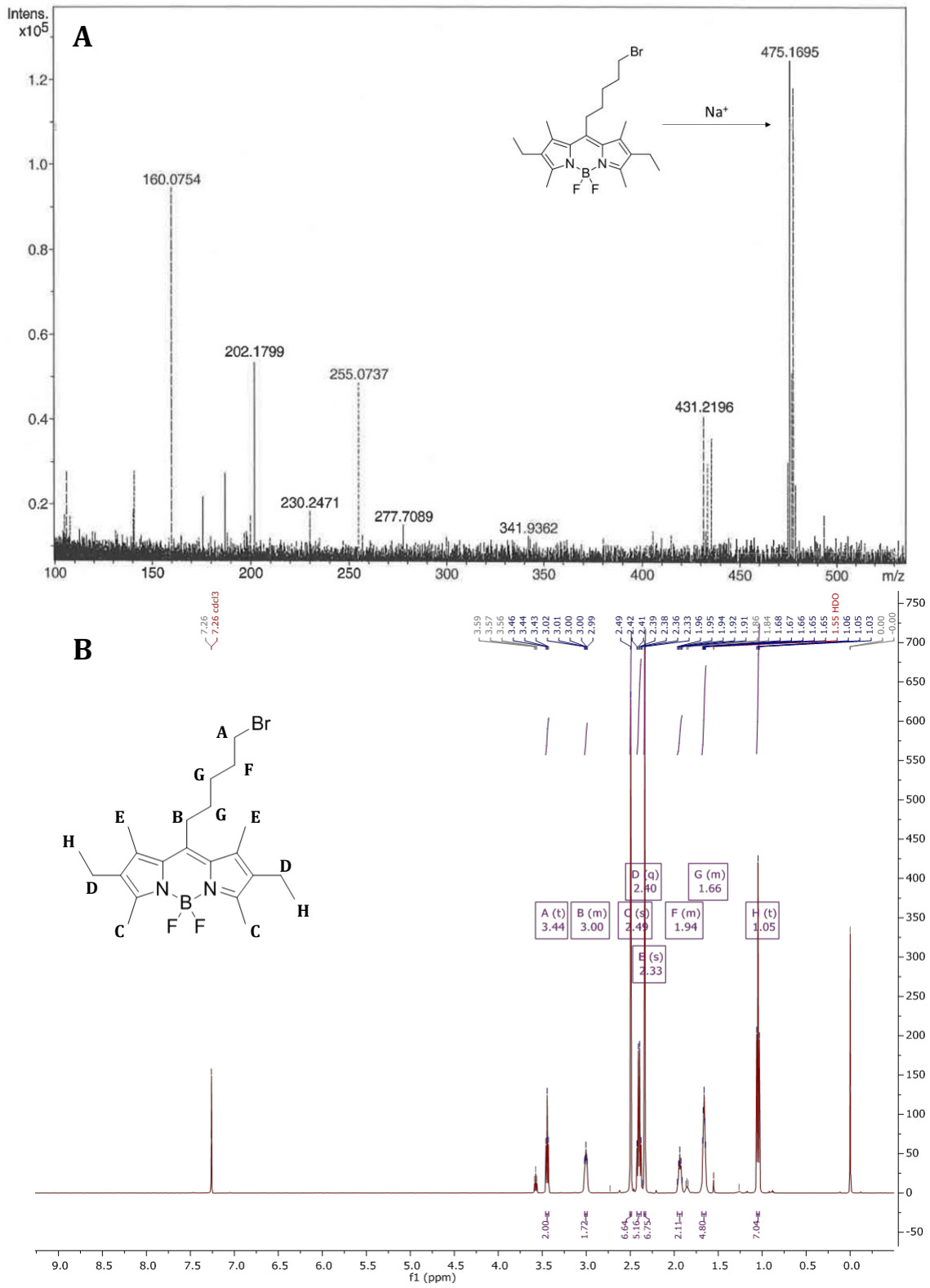

Figure 52: Analysis of **69**. **A**: Mass spectrum showing *m/z* of **69**. **B**: ^{1}H NMR spectrum showing peaks consistent with the presence of product **69**.

In order to scale up the synthesis of **69**, for the sake of efficiency it was decided to attempt several reactions in parallel using a carousel. For this to be feasible, the amount of solvent had to be significantly reduced. Since the pyrrole being used only had one α-position free, it was postulated that polymerization would be less of a risk, therefore the requirement for a large amount of solvent might not be as necessary as for the reaction involving the unsubstituted pyrrole. A test reaction was set up in a round bottomed flask using a much smaller quantity of solvent and a yield of 40% was achieved. The same reaction conditions and scale were then used for a reaction in a carousel tube. However, after a few minutes of stirring the reaction mixture appeared to undergo a rapid and violent reaction, resulting in the formation of a black solid. It was postulated that this was due to the formation of HCl, which in the tall carousel tube could condense before being expelled by the flow of argon, thus returning to the reaction mixture, setting off a very quick chain reaction of pyrrole polymerization. It was therefore decided that a scale up using this method would be too unsafe and unreliable and scale up attempts were abandoned.

For the next stage, it was necessary to replace the bromine with the malonate group. There were two ways that this could be achieved. The first method that was considered involved synthesizing the malonate then attaching it to the alkyl chain via a substitution process. This would involve methylation of the commercially available di-*tert*-butyl malonate (**70**) by treating it with sodium hydride to deprotonate the central carbon, followed by reaction with methyl iodide to access **71**. C-C bond formation using **71** and **69** could then be achieved using potassium iodide to swap the bromine for iodine, followed by the addition of **71** and potassium carbonate. A simple deprotection of the *tert*-butyl groups using TFA would give access to **73** (**Scheme 22**).

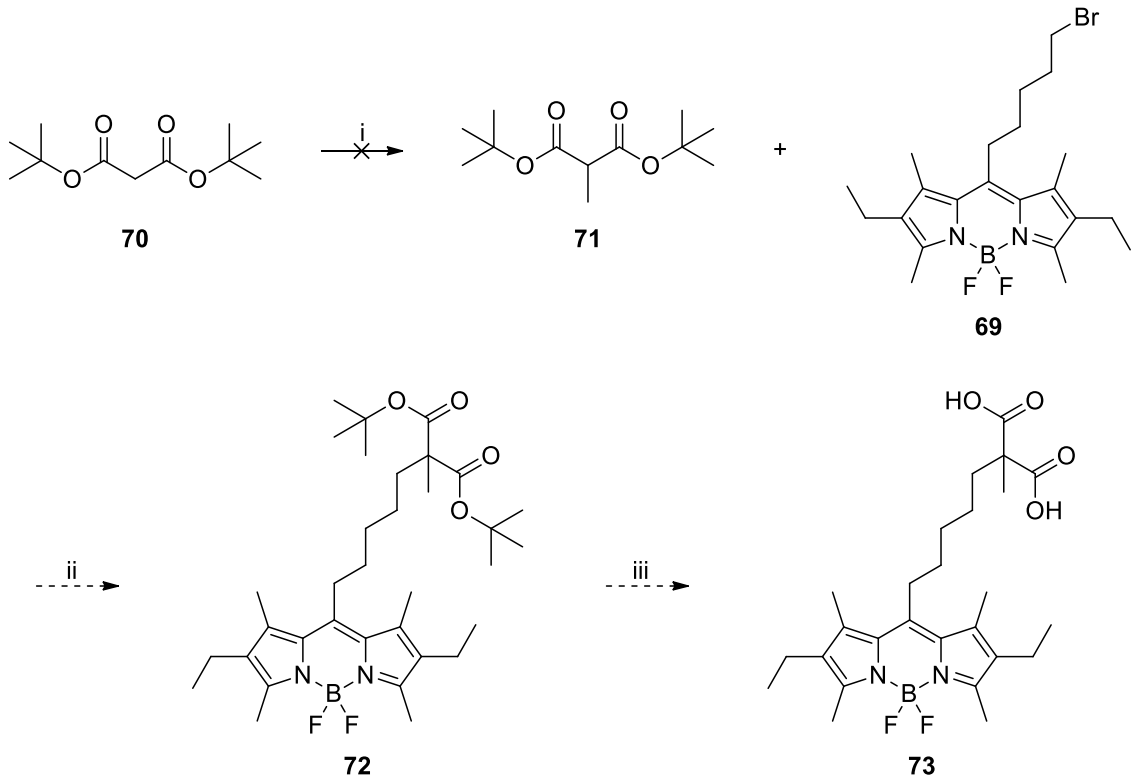

Scheme 22: Proposed route for the synthesis of **73**. Reagents and conditions: i) Under argon, NaH, THF, MeI, 3 h, RT; ii) KI, K_2CO_3, DMF, RT; iii) TFA.

An attempt to synthesize **71** was unsuccessful. The second method that was considered involved substitution of the bromine with the commercially available methylated Meldrum's acid (**74**) which could later be ring opened to form the malonate.

This was achieved by first stirring **69** with potassium iodide in DMF at RT for 1 h. This would allow halogen exchange to take place; Br on **69** needed to be swapped with I in order to increase reactivity. A test reaction with no potassium iodide was carried out and resulted in no product being formed. A mass spectrum of the reaction mixture proved that a halogen exchange had indeed taken place (**Figure 53**).

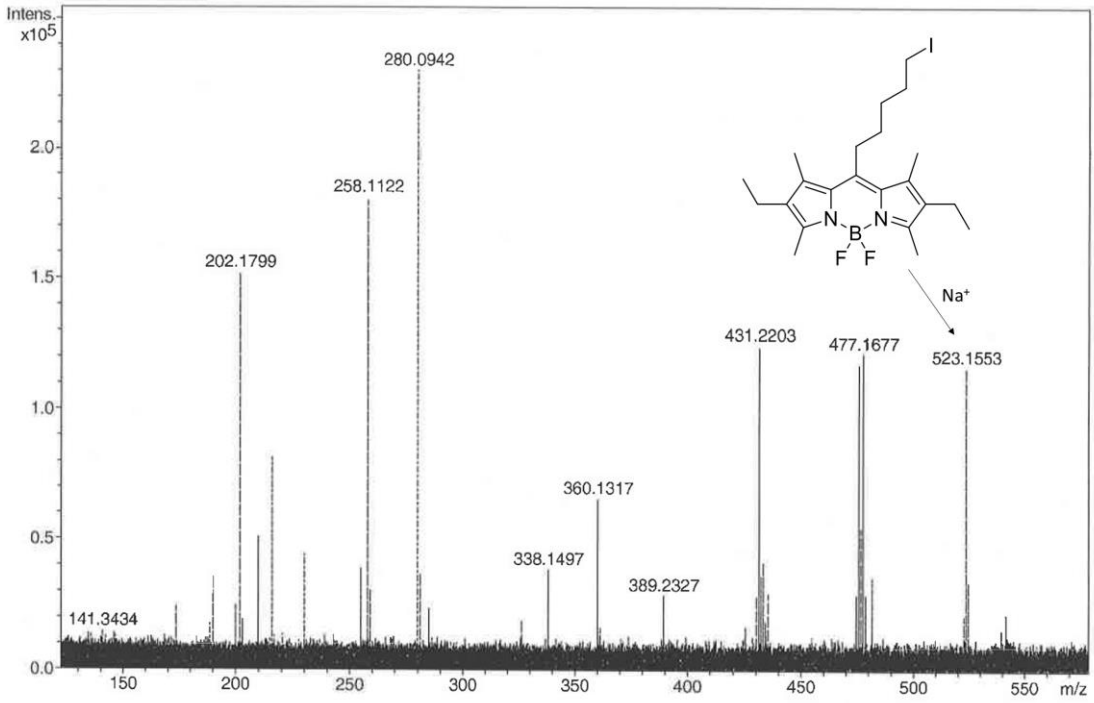

Figure 53: Mass spectrum proving that halogen exchange had occurred.

Separately, methylated Meldrum's acid (**74**) was treated with potassium carbonate in DMF at room temperature, allowing for a deprotonation of **74** to take place. The mixture containing **69**, having undergone halogen exchange, was added to the mixture containing **74** and the combined reaction mixture was then heated to 50 °C and stirred for 48 h. The progress of the reaction was determined by TLC analysis. After aqueous work up, the product was purified by flash chromatography on silica gel using a solvent gradient of 100% hexane to 40% ethyl acetate in hexane. The product was achieved in a good yield of 59% (**Scheme 23**).

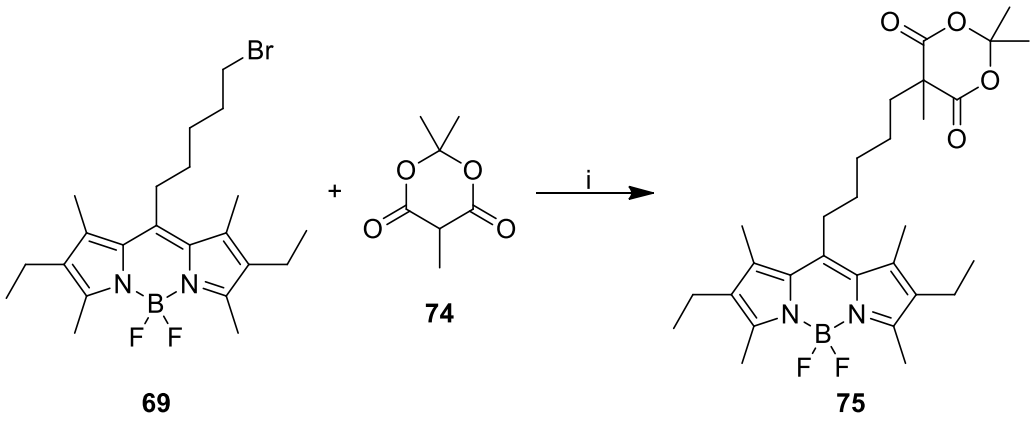

Scheme 23: Formation of **75**. Reagents and conditions: i) Under argon, **69** and K_2CO_3 in DMF added to **74** and KI in DMF, 50 °C, 48 h, 59%.

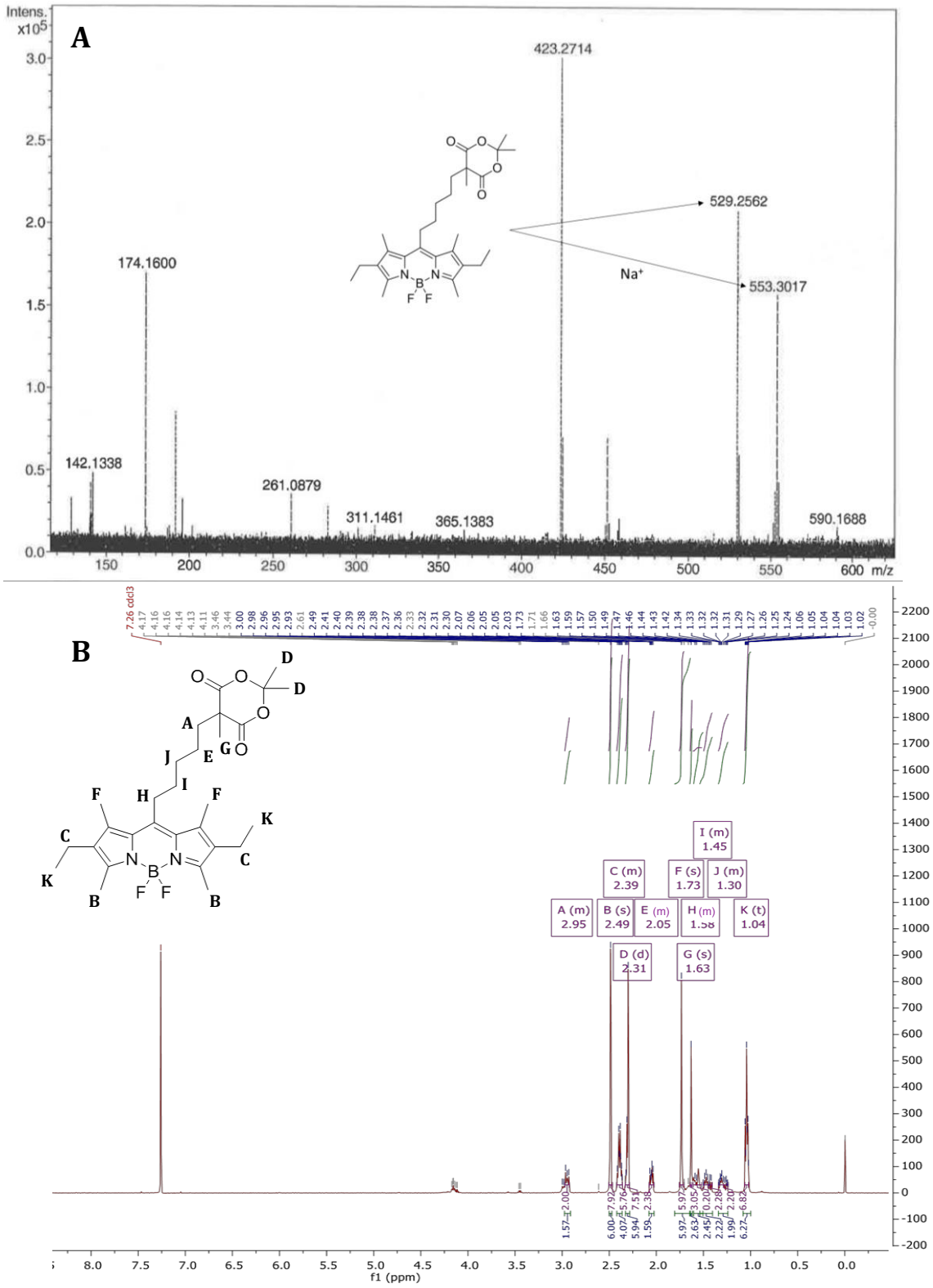

Figure 54: Analysis of **75**. **A**: Mass spectrum showing *m/z* of **75**. **B**: ^{1}H NMR spectrum showing peaks consistent with the presence of product **75**.

The sharp melting point, 187.4 – 189.2°C, indicated a relatively high degree of purity and the ^{1}H NMR spectrum showed there were negligible impurities present (**Figure 54**).

The ring opening of the methylated Meldrum's acid was achieved by dissolving **75** and lithium hydroxide in a 1:1 mixture of THF and water. The mixture was stirred at room temperature and the reaction monitored by TLC analysis until reaction completion was indicated after 72 h. The solvent was removed and the aqueous reaction mixture was acidified to pH 2 using HCl (1 M). The product could then be extracted. The product was obtained in 25% yield (**Scheme 24**).

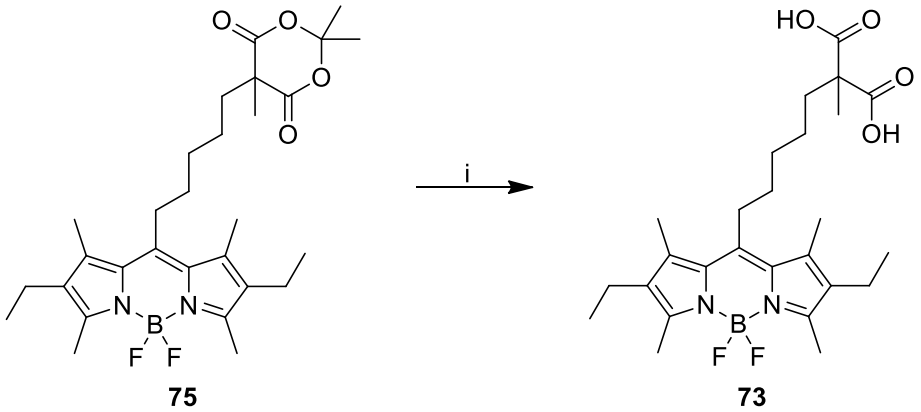

Scheme 24: Formation of **73**. Reagents and conditions: i) LiOH, THF-H_2O (1:1), 72 h, RT, 25%.

^{1}H NMR spectroscopic analysis showed peaks consistent with the presence of **73** and a mass spectrum confirmed that the *m/z* of **73** was present (**Figure 55**).

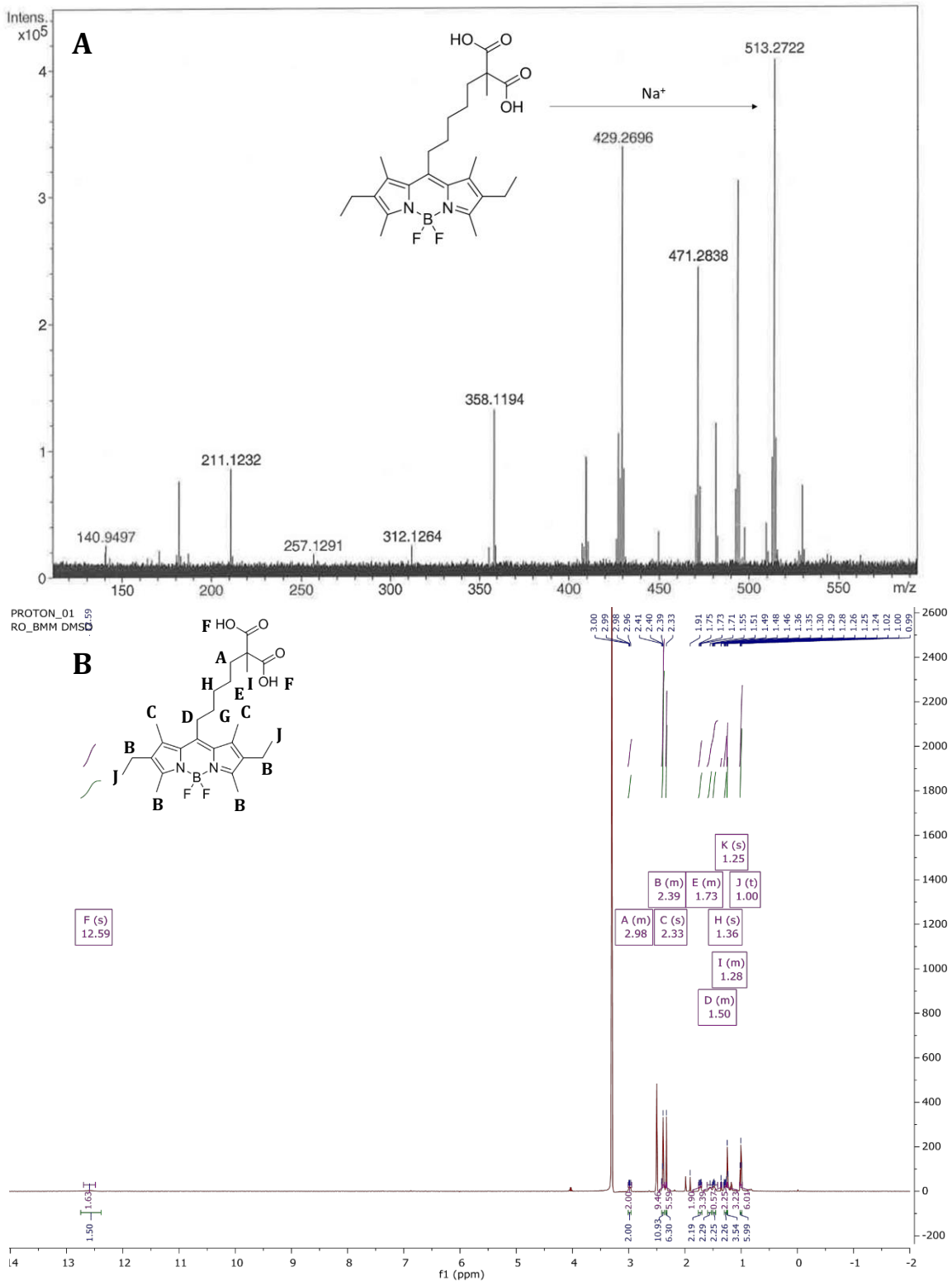

Figure 55: Analysis of **73**. **A**: Mass spectrum showing *m/z* of **73**. **B**: ^{1}H NMR spectrum showing peaks consistent with the presence of product **73**.

Once the product was obtained it could be tested in cells for its ability to preferentially enter apoptotic cells. At this point it was found that **73** seemed to be fairly stable in solution and could be stored for long periods of time without showing signs of degradation such as discolouration. Dr. Karen Marshall and Professor Louise Serpell investigated the behaviour of **73** using neurons from the hippocampus of a 1-day old rat that were cultured on a layer of astrocytes. The cells were treated with a dose of staurosporine (STS) at either 1 μM or 0.5 μM concentration for 5 hours for apoptosis to be induced. **73** was added at 50 μM concentration and the cells were incubated for 30 minutes then observed under a fluorescence microscope.[i]

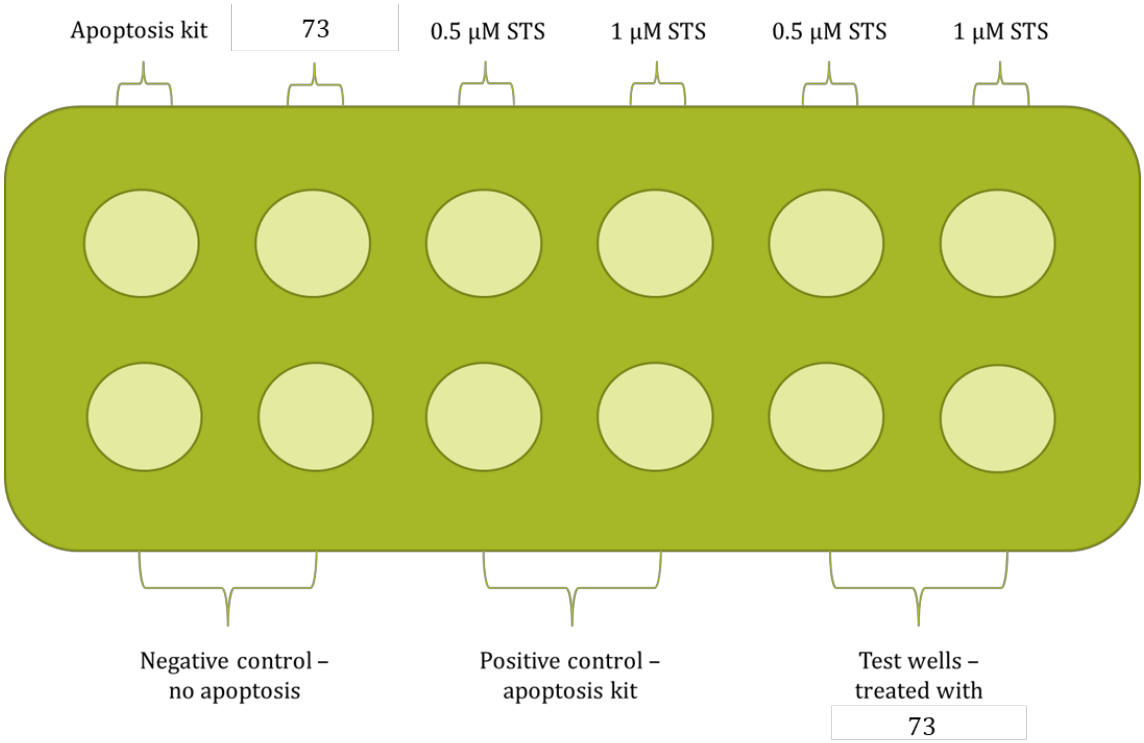

Figure 56: Cartoon representation of well plate containing cells treated with STS and/or a fluorescent dye.

To observe how **73** was acting, a picture of the well was taken under normal lighting conditions referred to as "brightfield", then another picture was taken of the same

[i] Experiments and analysis of results completed by K. Marshall, L. Serpell, University of Sussex, 2015, unpublished.

well under UV light. The two pictures were merged and a clear picture of healthy, apoptotic and dead cells along with the fluorescent stain was visible (**Figure 57**). Annexin was used as a control as a commonly used apoptosis imaging agent.

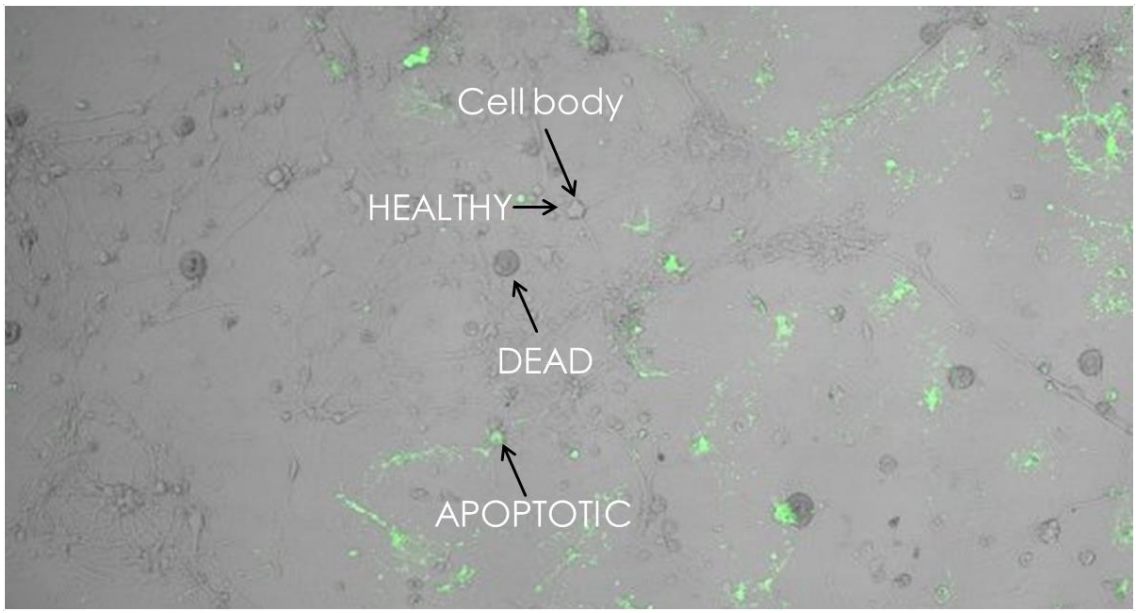

Figure 57: A composite image showing healthy, apoptotic and dead cells along with the fluorescent apoptotic imaging agent, in this case annexin. The healthy cells are seen as light grey and have taken up none of the annexin. The apoptotic cells have been stained green by annexin. The dead cells appear dark grey and have taken up none of the annexin.

The first wells to be imaged were the positive controls. These wells contained cells that had been treated with STS (1 or 0.5 μM) and stained with annexin to ensure that apoptosis had taken place in order to compare the difference between the different concentrations of STS. As observed in **Figure 58** apoptosis had been induced and it appeared that the wells that received the higher dose of STS had a higher proportion of cells undergoing apoptosis, as would be expected.

The next set of wells to be imaged were the wells that had been treated with STS and stained using **73** (**Figure 59**). The wells that received the higher dose of STS again appeared to contain a higher proportion of cells stained with the BODIPY dye than the wells that received a lower dose. However, it also appeared that **73** had started to stain the media which is made up of astrocytes, leading to the conclusion that **73** may not be able to specifically enter cells going through apoptosis.

Lastly, the negative control wells were imaged (**Figure 60**). These wells contained cells that were not treated with STS. One set of wells was treated with annexin and one set was treated with **73**. The cells treated with annexin showed almost no cells undergoing apoptosis, whereas the wells treated with **73** showed some staining.

Results of positive controls

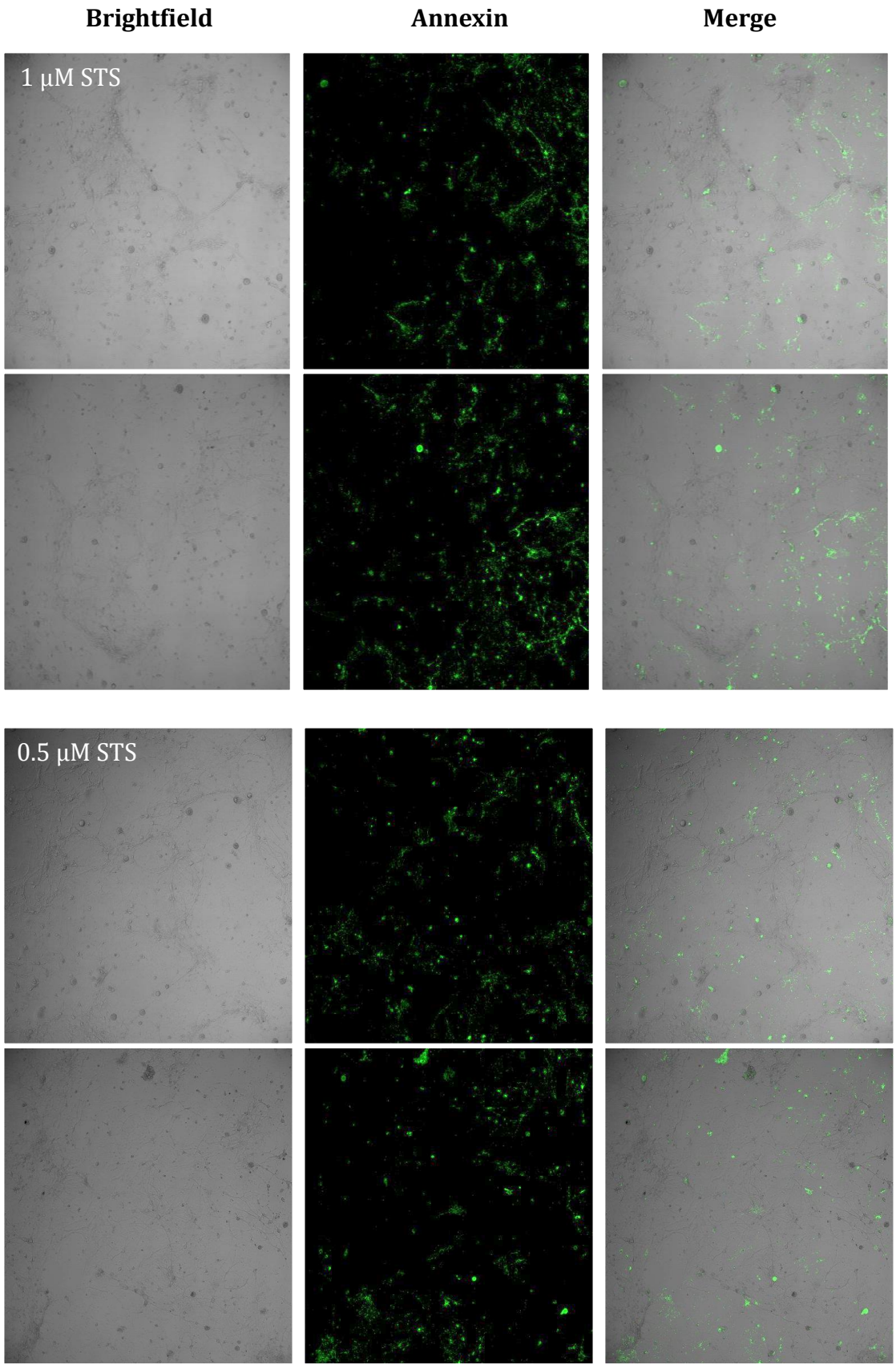

Figure 58: Positive control images. Top: cells treated with 1 µM STS; bottom: cells treated with 0.5 µM STS.

*Results of treatment with **73***

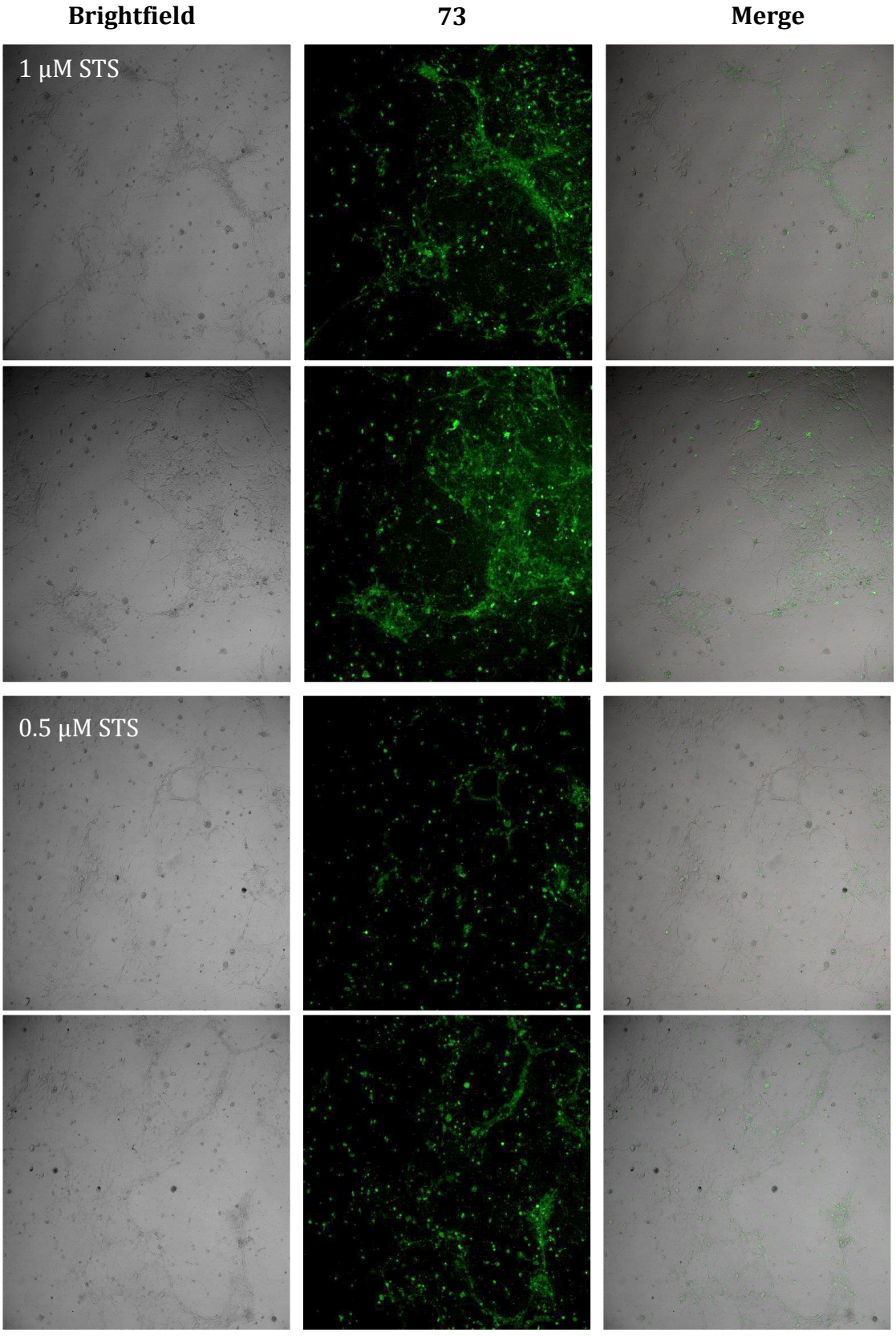

Figure 59: Images of cells treat with **73**. Top: cells treated with 1 µM STS; bottom: cells treated with 0.5 µM STS.

Results of negative controls

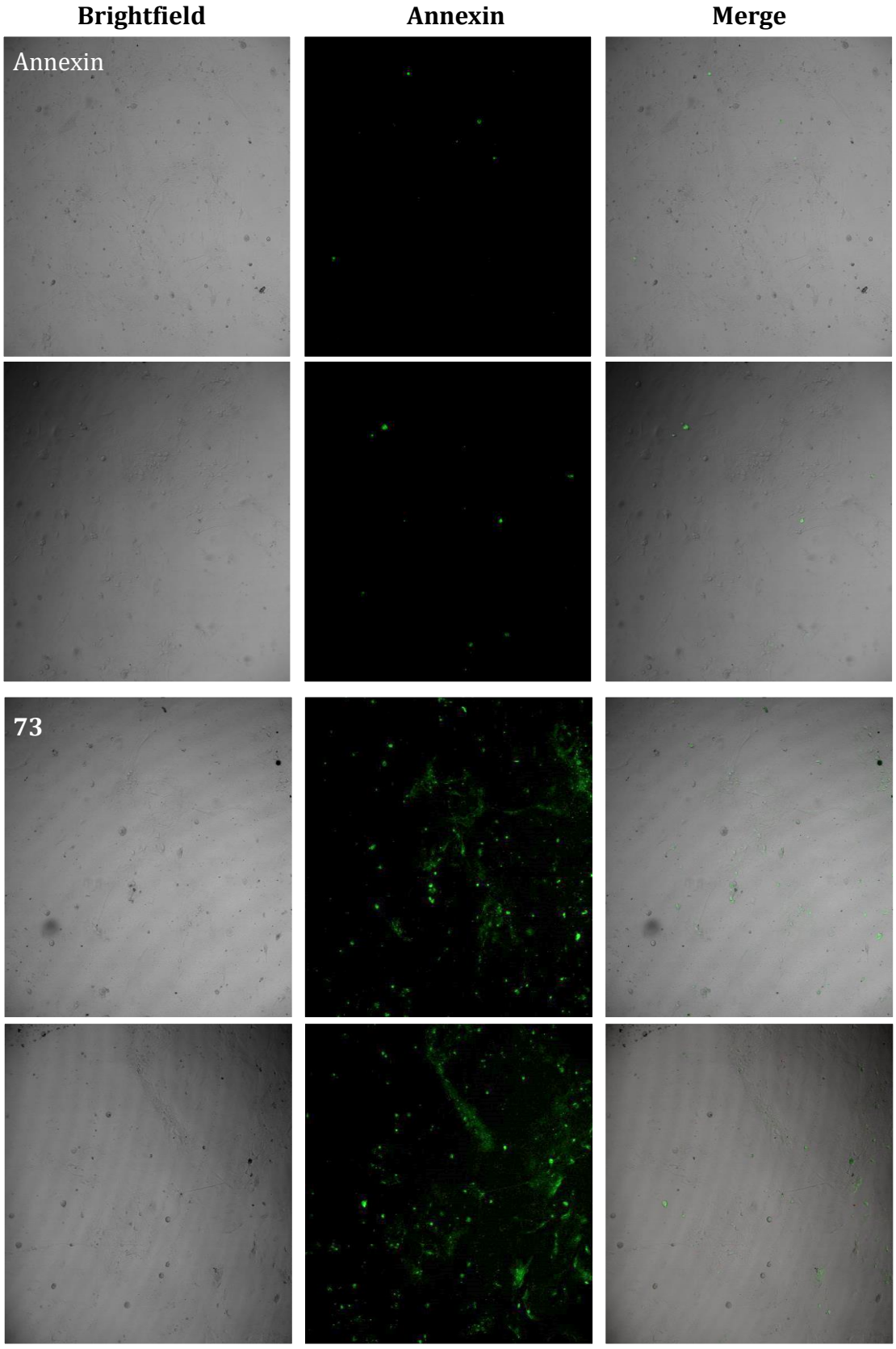

Figure 60: Negative control images. Top: cells treated with 1 µM STS; bottom: cells treated with 0.5 µM STS.

The results from the negative controls led to the conclusion that **73** was not the specific apoptosis imaging agent it was designed to be. However, the apparent differences in the amount of staining in each of the resultant images provided some hope that perhaps there was some degree of specificity and so perhaps the structure could be altered to improve the results. It was therefore hypothesized that the addition of the fluorophore to the ML10 core structure had increased the lipophilicity, which had led to **73** staining the membranes of both healthy and apoptotic cells indiscriminately.

The hypothesis was explored further with the use of Marvin Sketch to calculate the logP of **73** and logP of ML10. It should be noted that when using predictive software that the values obtained are purely an estimation and are taken to be a general guide and not an accurate representation of the true values. When generating a clogP, it is also necessary to take into account the p*K*a of **73** and the pH of the cell culture medium which was around pH 7. At this pH, the malonate group would likely only be half protonated, which meant analyzing the conjugate base of **73**. This provided a space filling diagram along with an evaluation of approximate values for each group's contribution to the overall clogP. In **Figure 61** it is shown that the clogP for **73** had been calculated as 2.17. This was then compared with the clog P of ML10 which was determined by the software to be -1.57 (**Figure 62**).

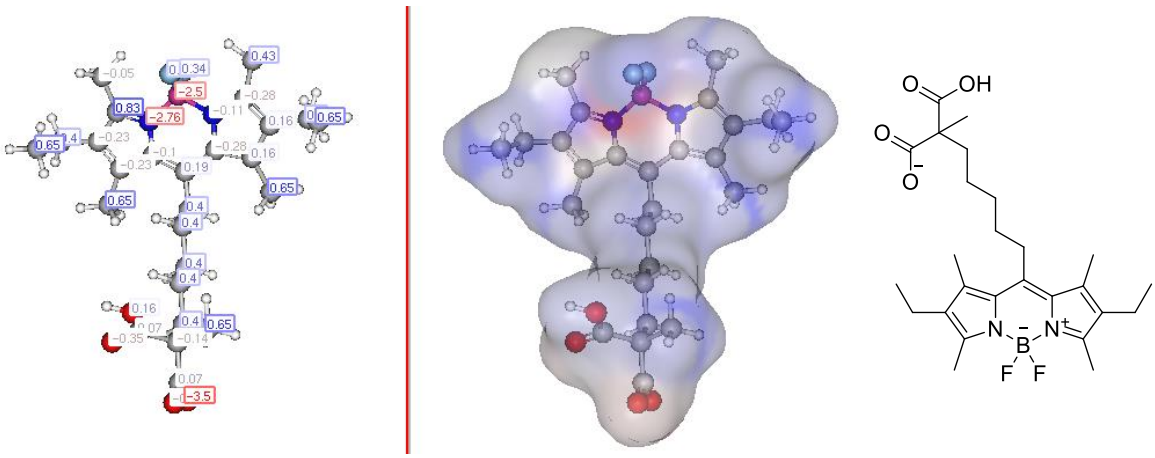

Figure 61: Marvin Sketch generated images of **73** for deducing the clogP.

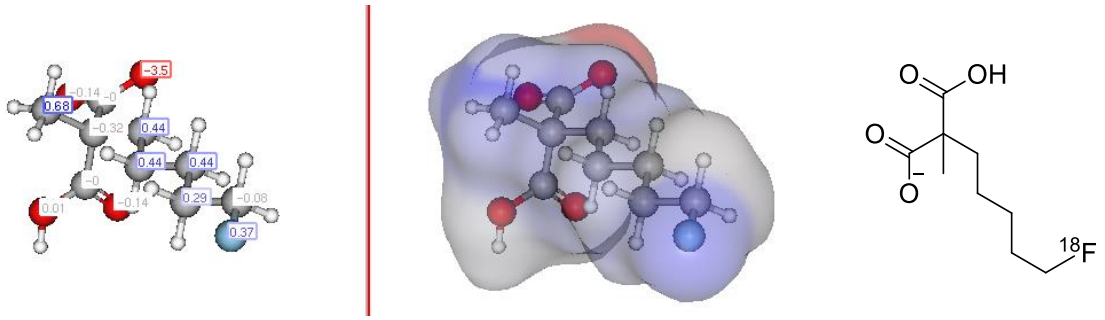

Figure 62: Marvin Sketch generated images of ML10 for deducing the clogP.

Since a lower number indicates a lower degree of lipophilicity this would indicate that there is quite a large discrepancy between the lipophilicity of ML10 and **73**. Therefore, structural modifications of **73** were considered in order to lower the clogP and thus optimize the properties of a new series of derivatives. The most obvious way to lower the clogP would be to reduce the carbon chain length.

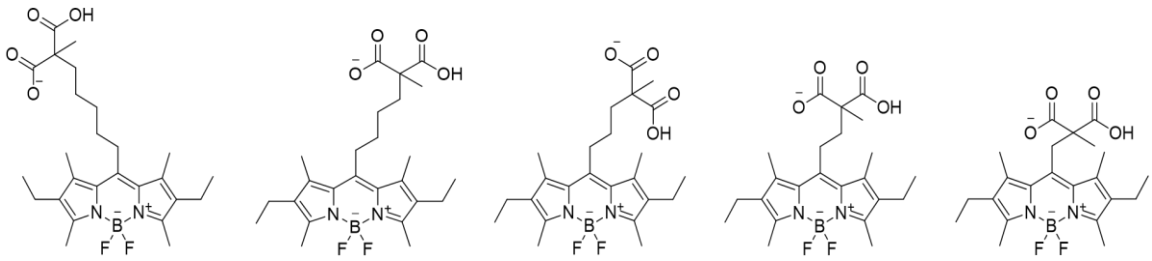

Figure 63: Marvin Sketch generated clogPs of potential BODIPY-ML10 structures.

From **Figure 63** it was apparent that with a trisubstituted pyrrole for the formation of the BODIPY core, the clogP would not be reduced low enough to match that of ML10. These values were compared with comparative structures derived from an unsubstituted pyrrole-based BODIPY core. From **Figure 64** it was apparent that pyrrole substituents contribute significantly to the lipophilicity of the structure. Investigations into unsubstituted pyrrole based BODIPY dyes were carried out but hit a dead end (**section 2.1.2.3.1.**) and so it was decided to investigate commercially available monosubstituted pyrroles (**section 2.1.2.3.3.**).

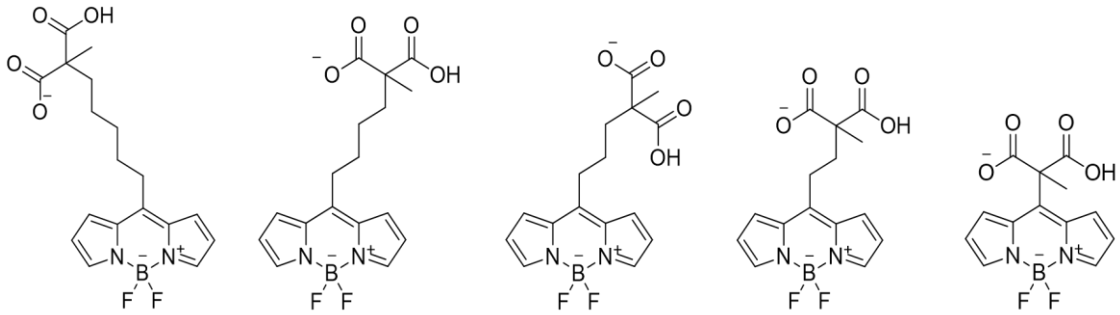

Figure 64: Marvin Sketch generated clogPs of potential BODIPY-ML10 structures.

Since reducing the carbon chain length would be an easy modification, and since bromoacyl chlorides of varying carbon chain length are commercially available, it was decided to apply the conditions already established for the formation of **73** to developing a small library of BODIPY derivatives using the trisubstituted pyrrole (**68**). This decision was made as it was unconfirmed how much of an effect, if any, the lipophilicity of a structure would have on the structure's ability to specifically stain apoptotic cells.

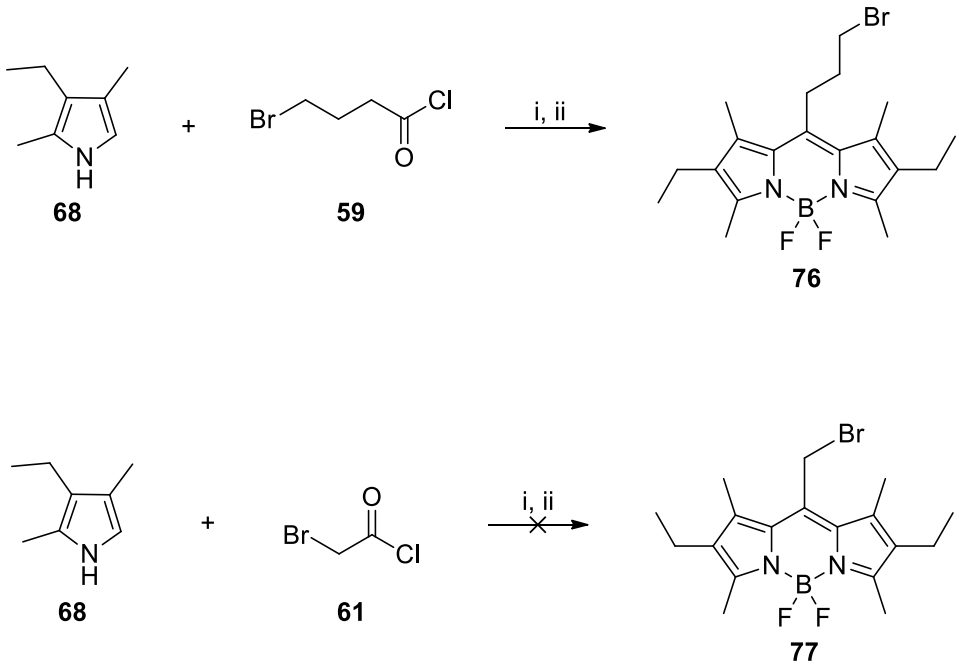

Scheme 25: BODIPY analogues with shorter alkyl chains. Reagents and conditions: i) Inert atmosphere, 1,2-dichloroethane, RT, 12 h; ii) NEt_3, $BF_3.Et_2O$, 50 °C, overnight, 34% (**76**).

Bromide **76** was successfully produced in a 34% yield, whilst **77** could not be isolated from the crude reaction mixture (**Scheme 25**). Attempts to attach the methylated Meldrum's acid (**74**) to **76** failed (**Scheme 26**).

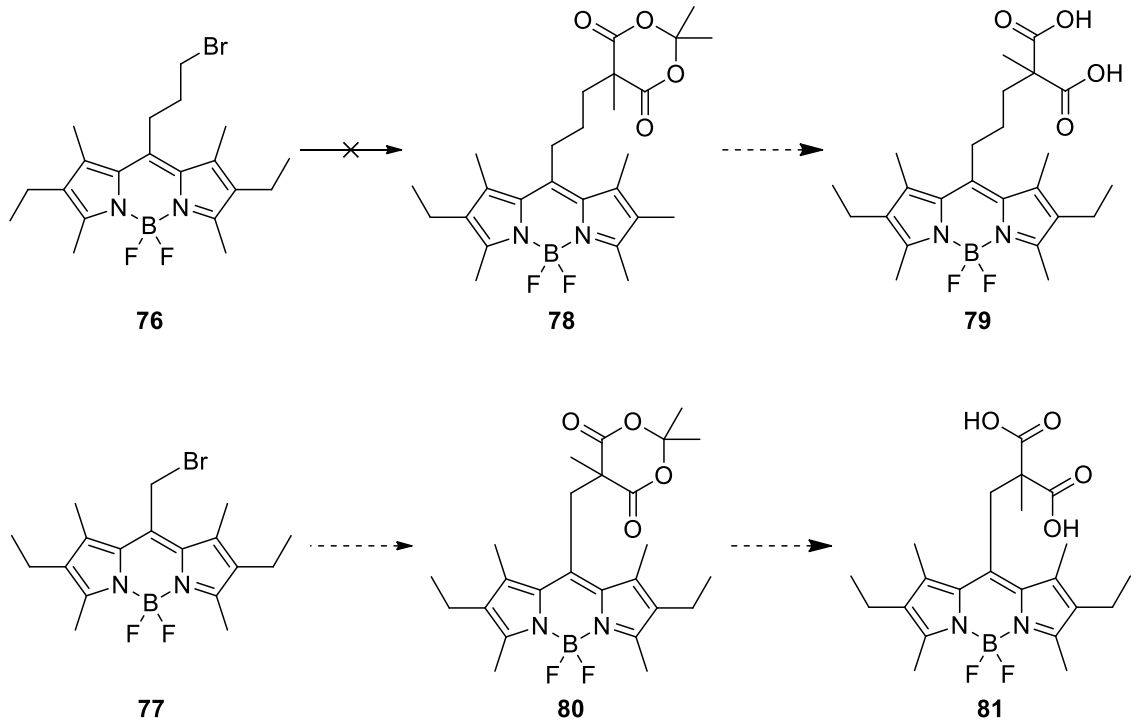

Scheme 26: Proposed routes to trisubstituted pyrrole based BODIPY dyes with shorter carbon chain lengths.

Considering the bulk of the trisubstituted pyrrole and the Meldrum's acid, it is not unreasonable to assume that a steric clash between the groups could be the reason for the reaction not proceeding. Therefore, it was decided that a less hindered pyrrole should be sought.

2.3.2.3. Monosubstituted Pyrrole

To overcome the steric hindrance problem, it was decided to investigate the synthesis of an alternative BODIPY series starting from a commercially available monosubstitued pyrrole, 2-methylpyrrole (**82**, **Figure 65**).

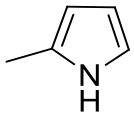

82

Figure 65: 2-methylpyrrole.

The lipophilicity of the final structures was analyzed by Marvin Sketch to determine their clogP values with varying carbon chain lengths. This indicated that the clogP of the 3,5-dimethyl-BODIPY derivative **85** was almost identical to the clogP of ML10 (**Figure 66**).

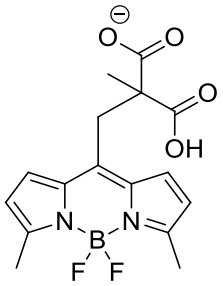

clogP = -1.58

85

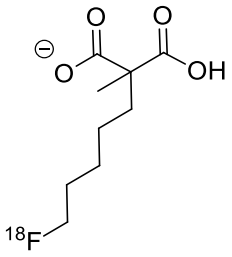

clogP = -1.57

Figure 66: Comparison of clogPs of **85** and ML10.

Based upon these findings, it was decided to proceed with the formation of this BODIPY derivative **85** with a one carbon linking chain (**Scheme 27**).

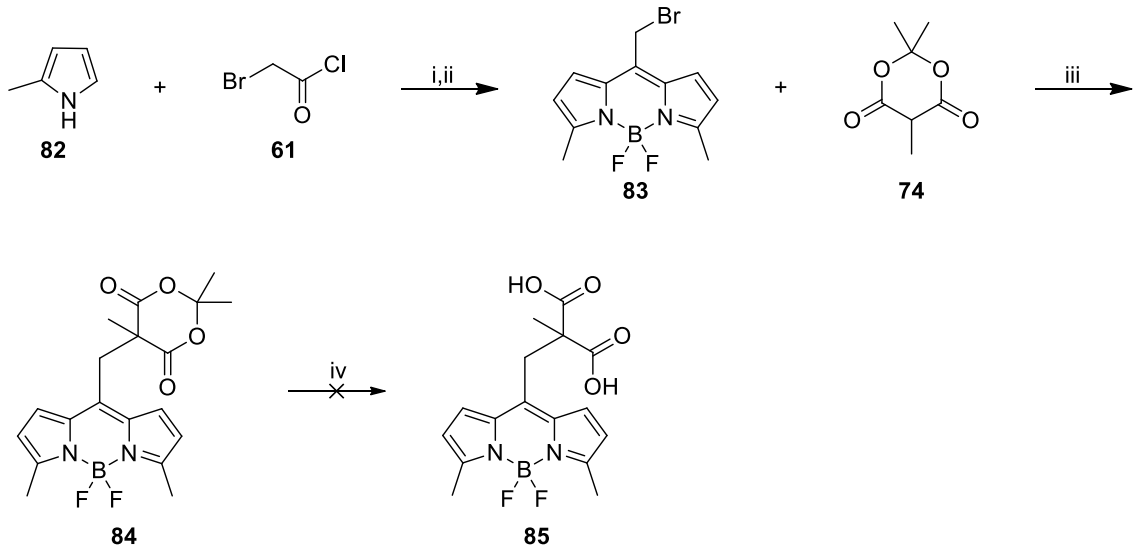

Scheme 27: Formation of **85**. Reagents and conditions: i) Inert atmosphere, 1,2-dichloroethane, RT, 12 h; ii) NEt_3, $BF_3.Et_2O$, 50 °C, overnight, 20%; iii) Inert atmosphere, **74** and K_2CO_3 in DMF added to **83** and KI in DMF, 50 °C, 48 h, 17%; iv) LiOH, THF-H_2O (1:1), 72 h, RT.

For step 1 the yield was comparable to the yields achieved when using the unsubstituted pyrrole as a starting material. The melting point of **83**, 175.3 – 177.2 °C, suggested a reasonable level of purity, however ^{1}H NMR spectroscopic analysis suggested the presence of some minor impurities (**Figure 67**).

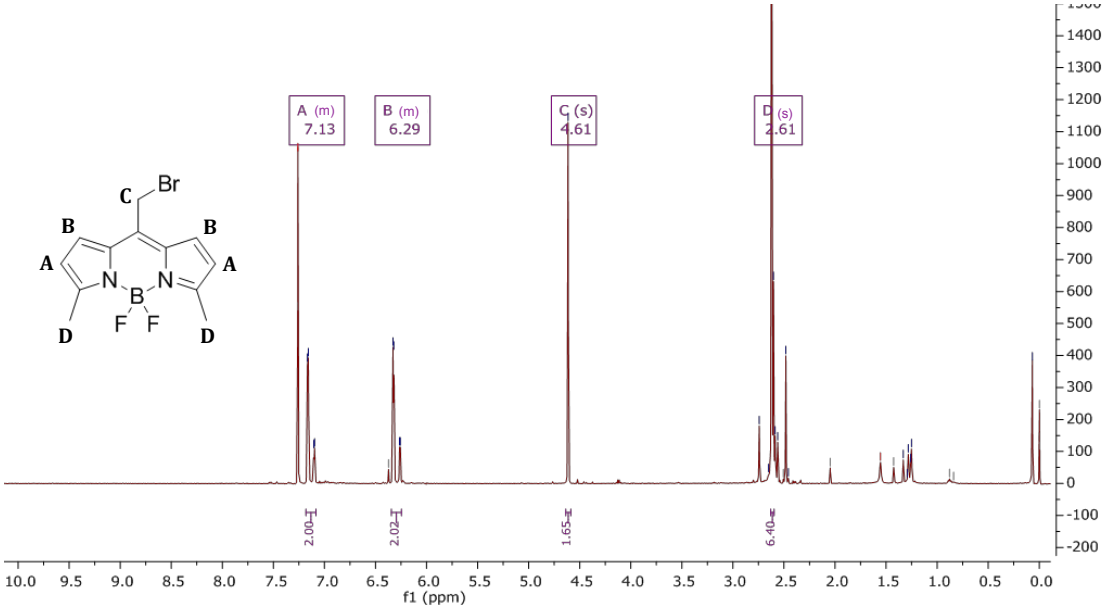

Figure 67: Analysis of **83**. ^{1}H NMR spectrum showing peaks consistent with the presence of product **83**, as well as some minor impurities.

The yield from step 2 at 17% was much lower than the only other successful example of Meldrum's acid-BODIPY attachment, which proceeded in 59% yield. This could mean that steric interactions between the Meldrum's acid and the BODIPY core were still affecting the reaction. With a melting point of 210.2 – 213.0°C, the degree of purity seemed to be reasonable, whereas the ^{1}H NMR spectrum of the product indicated the presence of minor impurities (**Figure 68**).

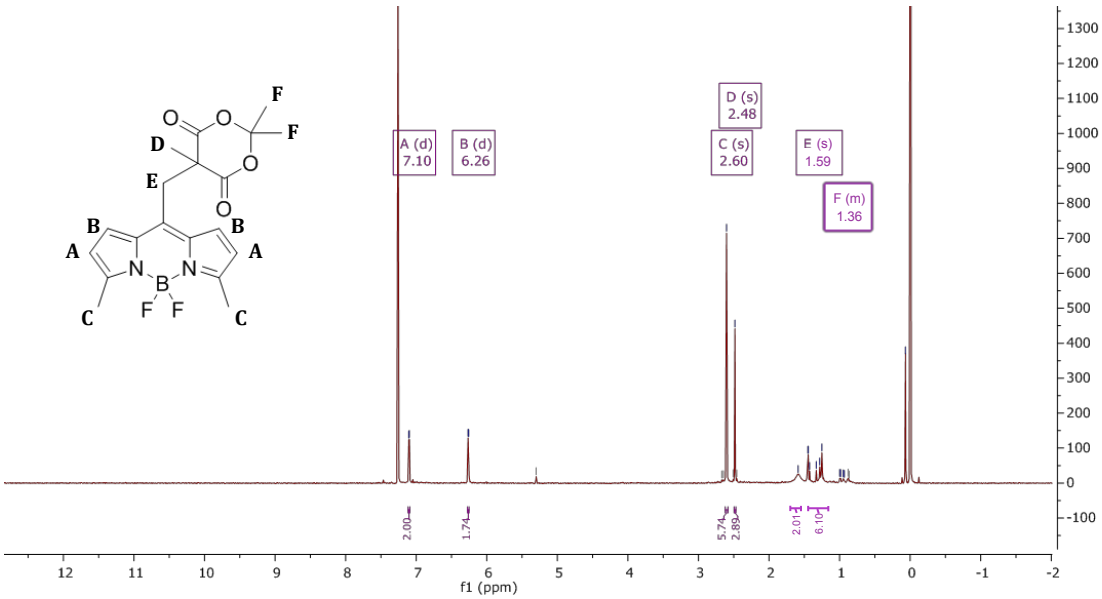

Figure 68: Analysis of **84**. ^{1}H NMR spectrum showing peaks consistent with the presence of product **84**, as well as some minor impurities.

Unfortunately, an attempt to carry out the final step and ring open the Meldrum's acid resulted in no final product being isolated. This could be due to the fact that this reaction was carried out on a small-scale due to the small yield achieved from step 2, and since the final step might also be a low yielding reaction, any final product made could have been lost during purification.

2.3.3. Towards a drug-like structure

Once tests have been completed using the BODIPY-ML10 fluorescent model, then it would be time to move onto testing small drug-like molecules needed to deliver a

molecular cargo into apoptotic cells. The molecular cargo in question would contain iodine-131 (^{131}I) due to its ability to destroy tissue by short range beta radiation.

Since the C-I bond is quite a weak bond, it would be necessary to incorporate a ring to provide metabolic stability. Keeping to the theory that lipophilicity plays a role in the structure's ability to preferentially enter apoptotic cells, the clogP of varying chain lengths was considered (**Figure 69**). Reducing the carbon chain length would not lower the clogP sufficiently to match that of ML10 but the addition of a H-bond acceptor to the ring would result in clogP values that approximate ML10 (**Figure 69**).

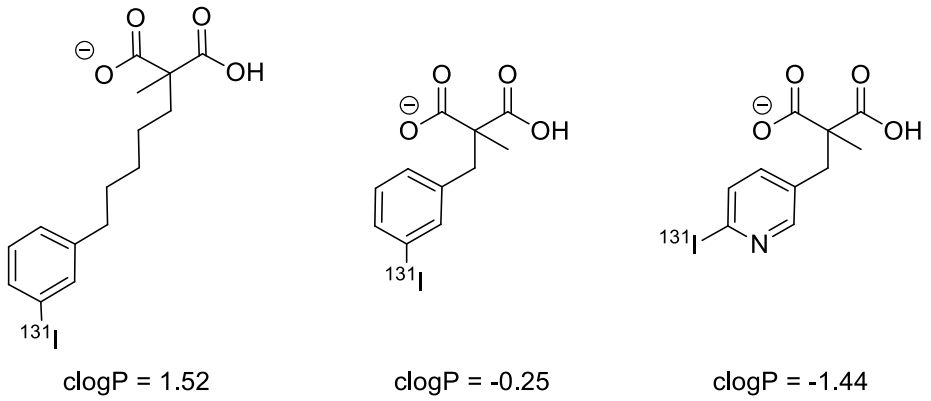

Figure 69: Results of investigation into clogP of potential structures for drug development.

A method for the synthesis of a similar structure had been developed by Zhu *et al*. in 2005 to access an intermediate towards the formation of an insecticidal *N*-substituted sulfoximine.[205] Following a similar method in a two-step process, the first step proceeded by the addition of a dimethylated malonate group to 3-chloromethyl-6-chloropyridine by stirring at RT overnight in the presence of potassium *tert*-butoxide in THF. The solvent was removed from the mixture and the residue triturated with boiling hexane to give the alkylated product **88** as a colourless solid in 41% yield (**Scheme 28**).

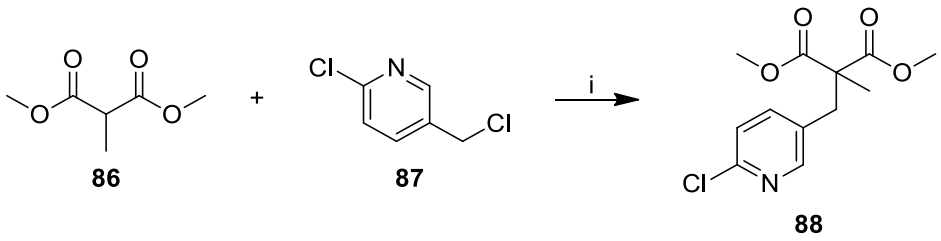

Scheme 28: Preparation of **88**. Reagents and conditions: i) Under argon, potassium *tert*-butoxide, THF, RT, overnight, purification by trituration with boiling hexane, 41%.

The second step involved the hydrolysis of the ester groups by adding lithium hydroxide monohydrate in water to **88** in THF. The mixture was left to stir overnight at RT then acidified with HCl to give the product as a colourless solid in 85% yield with no further purification required (**Scheme 29**).

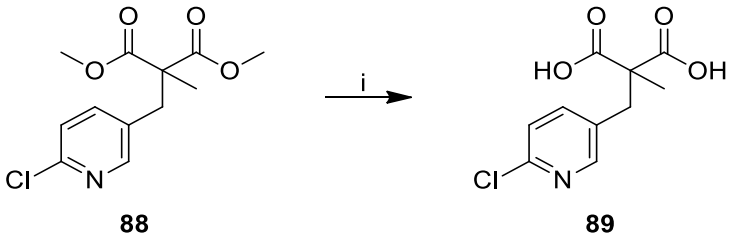

Scheme 29: Preparation of **89**: i) $LiOH{\cdot}H_2O$ in water, THF, RT, overnight, acidify with HCl, 85%.

The final step required halogen exchange to be carried out (**Scheme 30**). However, since the halogen that needed to be substituted was attached to a pyridine ring, a simple Finklestein reaction was not appropriate. Therefore, another method was sought.

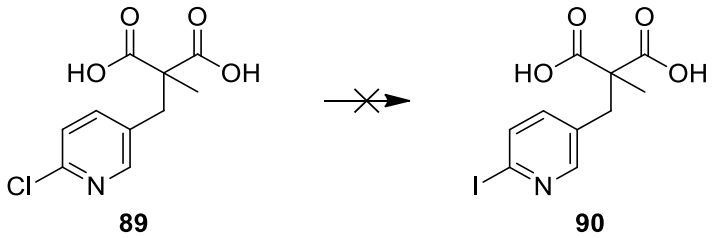

Scheme 30: Attempted halogen exchange of Cl to I using a method developed by Bissember and Banwell.[206]

A plausible method was found that had been developed by Bissember and Banwell in 2009.[206] This method required the addition of acetyl chloride to a stirred mixture

of **89** and sodium iodide in acetonitrile. The mixture was then subjected to microwave irradiation in a microwave reactor and heated for 3 hours at 80 °C. After this time, the mixture was treated with potassium carbonate (10% w/v aqueous solution), sodium sulphite (5% w/v aqueous solution), sodium thiosulfate (saturated aqueous solution) and the aqueous solutions washed with dichloromethane. Unfortunately, no product was recovered by this method, potentially due to the solubilizing effect of the dicarboxylic acid allowing the product to be water soluble. Thus, it was considered that the methyl protecting groups should not be removed until after the halogen exchange.

2.4. Future perspectives

To finish the library of BODIPY fluorophores it would be necessary to complete the formation of **85** (**Scheme 31**).

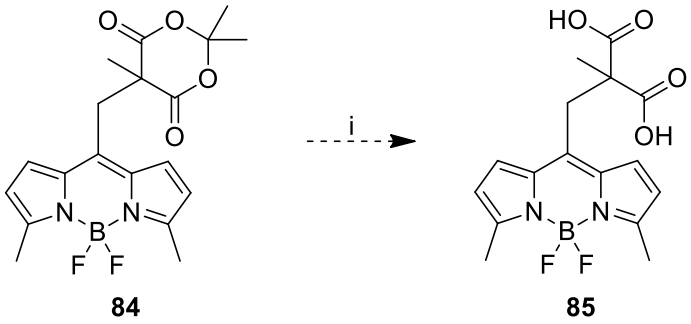

Scheme 31: Proposed reaction scheme for the formation of **85**. Reagents and conditions: i) LiOH, THF-H_2O (1:1), 72 h, RT.

Once **85** had been made it would be necessary to test it in a cell line, thus proving whether or not logP is a factor in the structure's ability to preferentially enter apoptotic cells. If it was found that **85** was unable to do this then it may well be necessary to abandon this fluorophore project in favour of continuing work on developing the radiolabelled "drug-like" molecule, since the fluorophore development was only meant to be a model of how the radiolabelled molecule might behave.

The development of **90** was also not completed during this project. This could be achieved using a procedure developed by Bissember and Banwell (**Scheme 32**).[206]

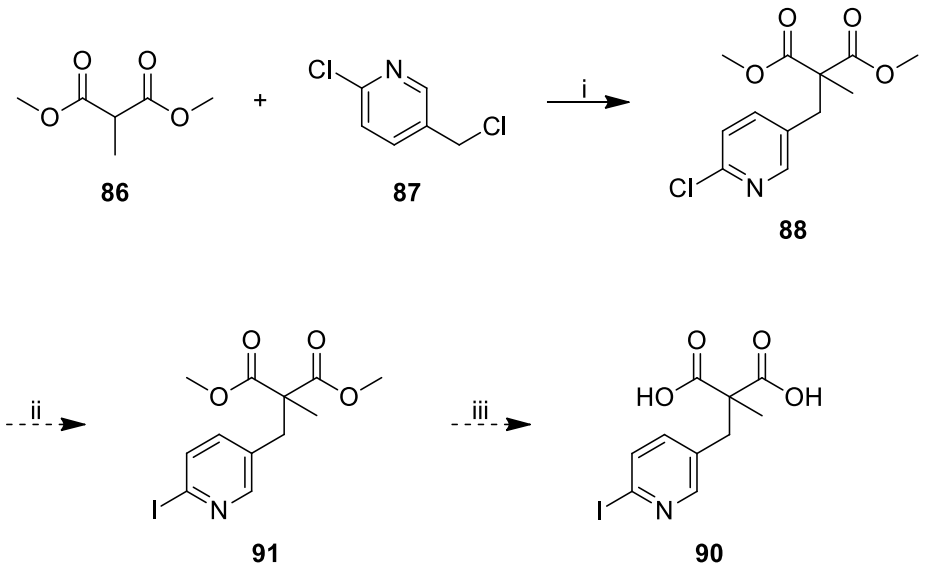

Scheme 32: Proposed scheme for the formation of **90**. Reagents and conditions: i) Under argon, potassium *tert*-butoxide, THF, RT, overnight, purification by trituration with boiling hexane; ii) acetyl chloride, NaI, irradiation at 80 °C for 3 h in a pressure-rated glass vial using a CEM Discover microwave synthesiser; iii) $LiOH \cdot H_2O$ in water, THF, RT, overnight, acidify with HCl.

Since mono- and dialkylpyridines do display a weak fluorescence at about 300 nm[207], it may be possible to observe **90** under a fluorescence microscope, though since that lies below the range of the on-site fluorescence microscope (**section 2.2.1.**), it would be necessary to outsource that part of the project.

As part of future work, it would be prudent to investigate further development of **90**. There are many ways in which the structure could be altered in the event that the molecule didn't quite do the job it had been designed for. For example, the pyridine ring could easily be swapped for a benzene ring and a variety of solubilizing groups added to the ring to adjust the clogP. In short, a whole library of compounds could be designed to be tested.

2.5. Conclusion

Due to time constraints, it was not possible to finish all lines of enquiry within this project. There is still plenty of work that could be done to see the project through to completion, including developing a library of small molecules to be tested for their ability to accumulate in apoptotic cells. A lack of a biological collaborator meant that testing of the BODIPY fluorophores would not be possible. It was also found towards the end of the project that a contaminated argon cylinder may have played a role in the low yielding BODIPY reactions, the various side reactions and may explain the difficulty in reproducing results of earlier experiments. It may also be the reason behind the violent reaction described in **section 2.2.2.3.2.**, though this cannot be proven and it is not recommended to try this particular method again.

Briefly, novel BODIPY structures were synthesized with varying levels of success. Through a continued investigation, and perhaps ignoring the goals set out by this thesis, many more novel BODIPYs could be made through the simple variation of starting materials used i.e. pyrroles with varying R groups and different acyl chlorides forming the *meso* position. Though not novel, **89** is a small molecule with lots of potential to be further developed into, hopefully one day, a therapeutic to assist existing cancer therapies.

Chapter 3: Inhibitory tools

3.1. Background and aims

The aim of this project was to further investigate synthetic routes already developed in the Bagley group for the synthesis of the MK2 inhibitor PF-3644022 (**33**; **Figure 70**). This involved testing a new catalyst that it was hoped would aid the formation of the quinoline ring within the molecule and so establish a rapid efficient route to the inhibitor.

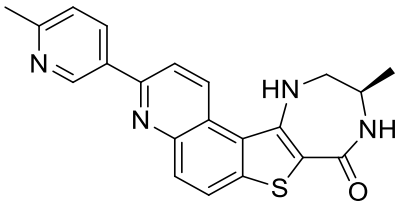

33

Figure 70: PF-3644022.

Studies carried out by the Bagley group and others into the effects of p38 inhibitors in WS cells revealed a reversal of the accelerated ageing phenotype, suggesting the possibility of therapeutic intervention.[147,208] However, p38 inhibitors have exhibited poor kinase selectivity and high toxicity.[148,209,210] Therefore, as discussed in **Chapter 1**, it was necessary to consider targeting the downstream kinase MK2. The MK2 inhibitor PF-3644022 (**33**), which was first developed by Anderson *et al.* at Pfizer[142], exhibited good selectivity for MK2 and nanomolar potency (IC_{50} 5 nM)[142,166], though it was found to induce hepatotoxicity in dogs.[142,166,174] However, the encouraging preliminary data indicating use of **33** could correct the stressed morphology and increase the replicative lifespan of WS cells, made a compelling case to improve the synthetic route towards **33** and so facilitate further biological study.[211]

3.1.1. Background of PF-3644022 (33)

PF-3644022 (**33**) was first described by Anderson *et al*. in 2010 as an ATP-competitive MK2 inhibitor and was developed at Pfizer for therapeutic intervention

of rheumatoid arthritis. This was because MK2 knockout mice were shown to be resistant to developing arthritis.[160] The authors declared PF-3644022 (**33**) to be "the first MK2 inhibitor described with oral efficacy in both acute and chronic models of inflammation".[142] As previously mentioned, **33** was shown to potently inhibit and have good selectivity for MK2 and in streptococcal cell wall induced arthritic mouse models, **33** exhibited good pharmacokinetic properties and efficacy.[142]

The hit-to-lead investigation into the development of an MK2 inhibitor was started in 2007[212], with a high-throughput screen identifying a hit that was then modified to create a series of 2-arylpyridyl pyrroles. Crystallographic analysis of the inhibitors when complexed with both MK2 and CDK2 allowed the researchers to identify areas for modification that would provide the inhibitor with greater selectivity towards MK2, most notably by placing a rigid aryl group at the 2-postion of the quinoline ring. Around the same time, other groups had also been working on developing MK2 inhibitors and had identified carbolines with a fused lactam ring as potentially potent compounds[160,165,212,213], leading to a scaffold Pfizer had modified during SAR studies in 2009 to fuse benzothiophene and lactam moieties (**Figure 71**).[163] The hypothesis was that the 7-methoxy group would form a hydrogen bond to the hinge region (Leu141 backbone NH) and the lactam portion would bind to the conserved catalytic Lys93 and Asp207 in the active site of MK2. During studies to try and improve the kinase selectivity and cell potency, a series of lactam-fused benzothiophenes was produced with an extra aryl group in order to provide a rigid attachment for selectivity in the hinge-binding region.[163] This study led to the development of PF-3644022 (**33**).[163]

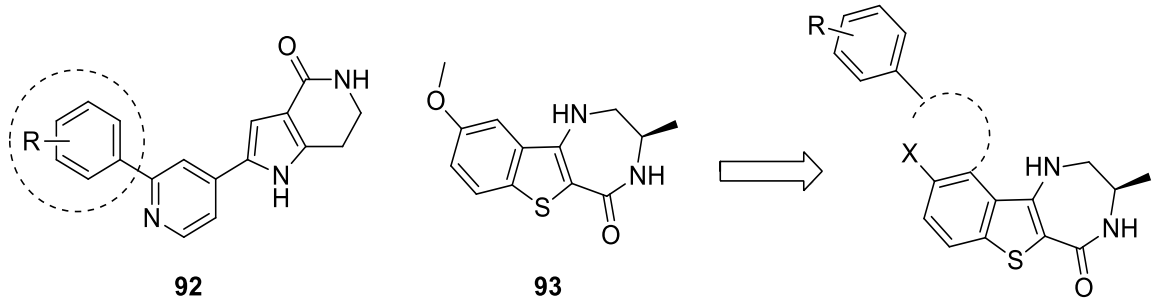

Figure 71: Anderson *et al.*'s combination of MK2 inhibitors which later led to the formation of PF-3644022 (**33**).[163]

Anderson *et al.*'s total synthesis (**Scheme 33**) started from a commercially-available nitroquinoline **94** that was converted to aminocyanoquinoline **95** by treatment with ethyl cyanoacetate and KOH in DMF. Diazotization converted the amino group to a bromide to provide **96**. The bromide was treated with methyl thioglycolate to produce **97** via nucleophilic aromatic substitution and subsequent aminothiophene formation. Diazotization and subsequent substitution converted the amino group of **97** to bromide **98**. The bromide then underwent a Buchwald coupling with (*R*)-propane-1,2-diamine to produce diazapene **99**. Boc protecting groups were used to doubly protect **99** and the pyridine was oxidized to form *N*-oxide **100**. Treatment with oxalyl chloride and removal of the Boc protecting groups produced intermediate **101**, which provided a late stage intermediate for convenient analogue synthesis via Suzuki coupling. The proposal by the Bagley group was to streamline this total synthesis.

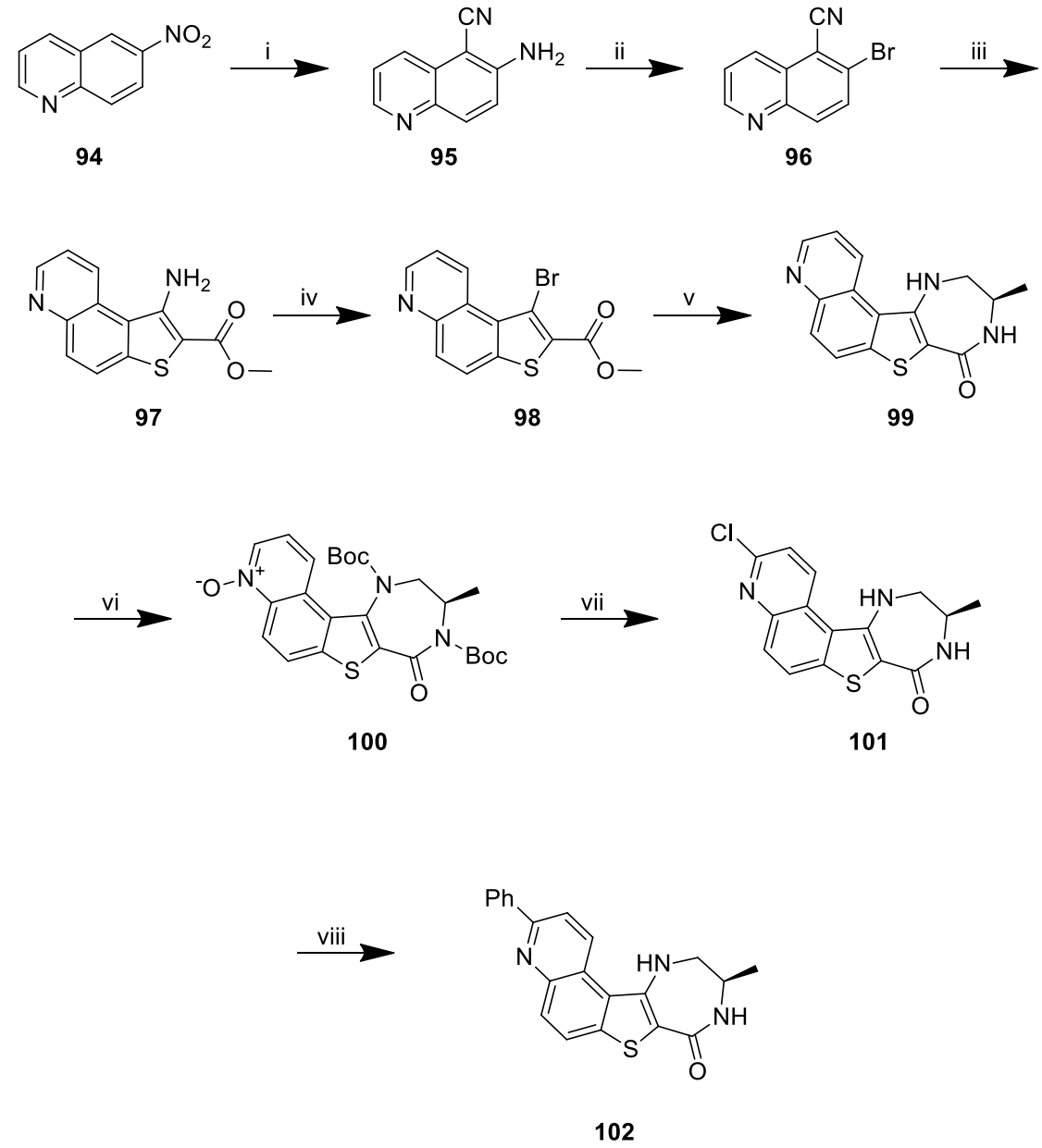

Scheme 33: Anderson *et al.* total synthesis of PF-3644022 (33).[163] Reagents and conditions: i) ethyl cyanoacetate, KOH, DMF then HCl, ii) $NaNO_2$ then HBr; iii) methyl mercaptoacetate, NaOMe, MeOH; iv) t-BuONO, $CuBr_2$; v) (*R*)-propane-1,2-diamine, $Pd_2(dba)_3$ (5 mol%), (±)-BINAP (10 mol%), Cs_2CO_3 (2 equiv.) toluene, 110 °C, 24 h, then TFA/CH_2Cl_2, then NaOMe/MeOH; vi) Boc_2O, DMAP, TEA; then *m*-CPBA, vii) $(COCl)_2$, DMF, then HCl; viii) $PhB(OH)_2$, $Pd(PPh_3)_4$, Na_2CO_3, 80 °C.

3.2. Synthetic routes

The total synthesis of PF-3644022 (**33**) was investigated by previous members of the Bagley group with varying degrees of success. Almost all steps in an alternative 8-step process were optimized to give 75–100% yield but the very last step proved to be difficult, with only a 6% yield obtained. **Sections 3.2.1–3.2.5** describe the processes developed within the group and **section 3.2.6** will discuss efforts made as part of this thesis to improve the yield of the final step for quinoline formation.

3.2.1. Formation of 5-nitrobenzo[*b*]thiophene-2-carboxylic acid (106)

Bagley *et al.* hypothesised that PF-3644022 (**33**) could be prepared from a benzothiophene core motif that could be further functionalized to produce a range of MK2 inhibitors, rather than starting from 6-nitroquiloline as reported by Anderson *et al.*[163,214]

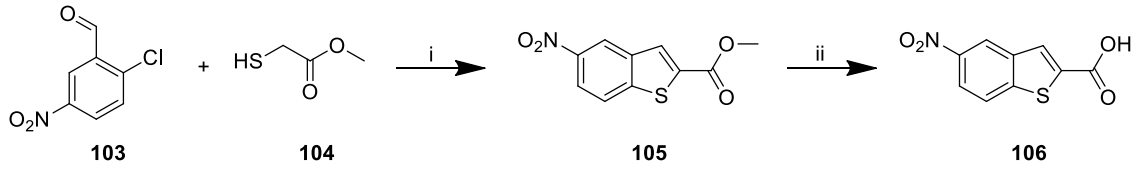

103 **104** **105** **106**

Scheme 34: Formation of benzothiophene **106**. Reagents and conditions: i) K_2CO_3, DMF, irradiated at 90 °C for 15 min in a pressure-rated glass vial using a CEM Discover microwave synthesizer; ii) NaOH (1 M), MeOH, irradiated at 100 °C for 3 min in a pressure-rated glass vial (35 mL) using a CEM Discover microwave synthesizer; H_2O; HCl (aq).

This rapid route towards a benzothiophene scaffold was developed by Bagley *et al*. and has been used towards the synthesis of the thieno[2,3-*b*]pyridine core motif of LIMK1 inhibitors, the benzo[4,5]thieno[3,2-*e*][1,4]diazepin-5(2*H*)-one scaffold of MK2 inhibitors and a benzo[4,5]thieno[3,2-*d*]-pyrimidin-4-one inhibitor of the PIM kinases.[174] The annulation based method allowed the highly efficient preparation of 3-halo- and 3-amino-2-substituted benzo[*b*]thiophenes using microwave irradiation, producing the products in relatively high (>58%) yields.

Previous synthetic routes towards 3-halobenzo[*b*]thiophenes employed before this study were deemed problematic. For example, direct ring halogenation suffers from the low reactivity of heteroaryl units as well as poor compatibility with functional

groups,[215–218] and methods involving the 5-*endo-dig* halocyclization of *ortho*-alkynylaryl thiophenol derivatives,[219–223] which requires installation of an alkyne by metal-catalyzed cross-coupling followed by cyclization mediated by a halogen-containing electrophile, have a number of inherent disadvantages.

The Bagley *et al.* method was applied to step (i) and (ii) and yields of 79% and 95% were achieved, respectively (**Scheme 34**).

3.2.1.1. Methyl 3-Aminobenzo[b]thiophene-2-carboxylate (107)

A method for the rapid synthesis of this core motif was developed in collaboration with Dr. Dwyer, whose goal it was to introduce functionality suitable for subsequent elaboration to the target inhibitor. Using a microwave synthesizer and the conditions and reagents listed in **Scheme 35**, the results listed in **Table 1** were achieved. This method appears to be superior to other routes which rely upon halogenations.

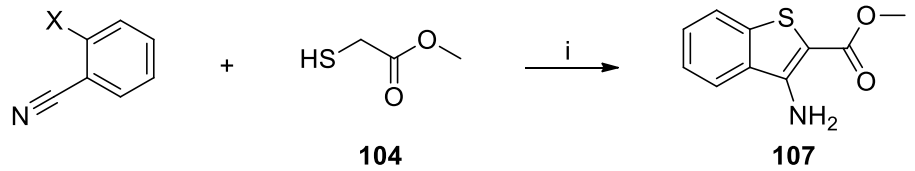

Scheme 35: Formation of benzothiophene **107**. Reagents and conditions: i) DMSO, NEt_3, microwave irradiation 15 min at 130 °C using a CEM discover microwave synthesizer. Yields: X = F, 65%; X = Br, 23%; X = I, 47%.

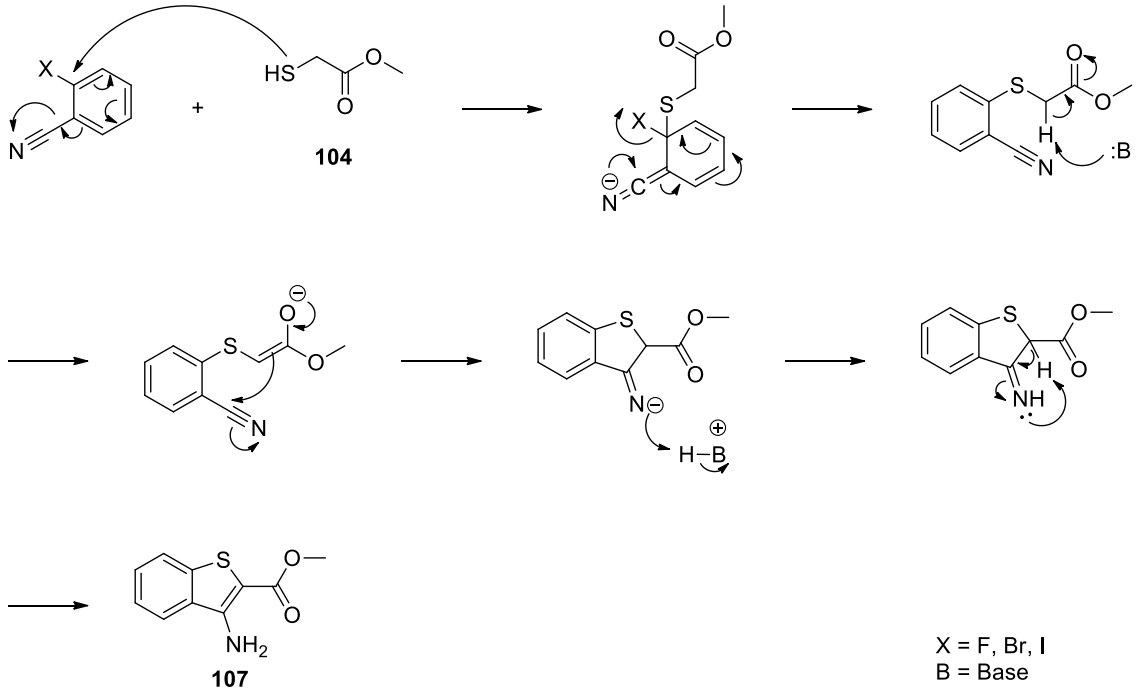

Scheme 36: Proposed mechanism for the formation of benzothiophene **107**.

Table 1: Optimization of microwave conditions for synthesis of **107**

Entry	Method[a]	X	Temp. °C	Time (min)[b]	Yield (%)[c]
1	A	F	130	11	56
2	**A**	**F**	**130**	**15**	**65**
3	A	F	130	30	56
4	B	I	130	15	47
5	C	Br	130	15	23

[a]See experimental section for method details. [b]Hold time at the given temperature, as measured by the in-built IR sensor, by modulation of the initial microwave power. [c]Isolated yield of product **107** after reaction according to **Scheme 35**, cooling in a stream of compressed air and pouring the reaction mixture into iced water.

From **Table 1** it is evident that entry 2, using the fluorinated benzonitrile as the starting material, provided the best yield. Therefore, this method was used to test other halogenated benzonitriles with varying degrees of success. This result is to be expected due to the fact it is an S_NAr reaction. Due to the electronegativity of fluorine and its *ortho* postion on the aromatic ring, the transition state is stabilized during

the addition stage (the rate determining step), allowing acceptance of electrons followed by elimination of fluoride.[224]

3.2.1.2. Methyl 3-Aminothieno[2,3-*b*]pyridine-2-carboxylate (108)

Due to the success of the reaction in **Scheme 35** in forming the benzothiophene derivatives for the MK2 inhibitor, the method was applied to a pyridine analogue, which is the core motif of a series of LIMK inhibitors (**Scheme 37**).

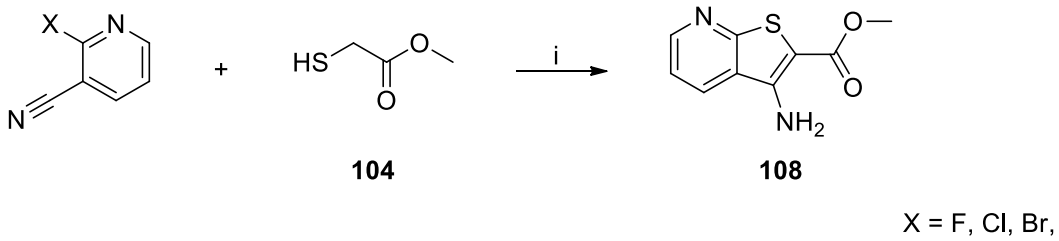

Scheme 37: Formation of thienopyridine **108**. Reagents and conditions: i) DMSO, NEt_3, microwave irradiation 15 min at 130 °C using a CEM discover microwave synthesizer. Yields: X = F, 66%; X = Br, 51%; X = Cl, 69%

Table 2: Results of microwave method applied to pyridine analogue, **108**

Entry	Method	X	Temp. °C	Time (min)	Yield (%)
1	A	F	130	15	66
2	B	Br	130	15	51
3	**C**	**Cl**	**130**	**15**	**69**

[a]See experimental section for method details. [b]Hold time at the given temperature, as measured by the in-built IR sensor, by modulation of the initial microwave power. [c]Isolated yield of product **107** after reaction according to **Scheme 35**, cooling in a stream of compressed air and pouring the reaction mixture into iced water.

Table 2 shows better yields than the benzothiophene derivatives. This is presumably due to the electronegative nitrogen and delocalization around the ring stabilizing the intermediate anion, so the leaving group doesn't have to be such a good leaving group.[224] However, the chloropyridine produced the best yield, though the yields of all three substrates are similar.

3.2.2. Formation of 3-bromo-5-nitrobenzo[*b*]thiophene-2-carboxylate (110)

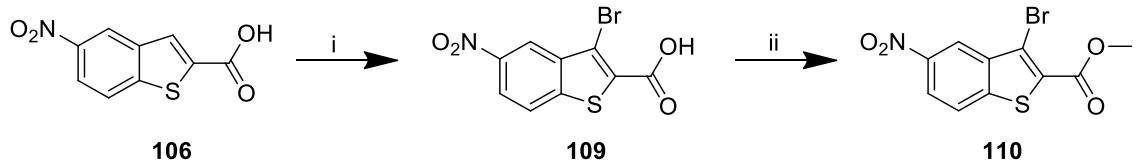

Scheme 38: Formation of **110**. Reagents and conditions: i) anhydrous NaOAc, glacial AcOH, Br_2, 55 °C, 27 h; ii) MeI, K_2CO_3, DMF, 3 h, RT, then NH_4Cl (aq.), 87%.

For the synthesis of **110** a procedure originally developed by Mbere *et al.* was modified.[174,225] Mbere *et al.* described a method for the synthesis of a new ring fused benzo[*b*]thieno derivative with an embedded nine-membered ring system which was achieved by a ring closing metathesis methodology and catalyzed by a palladium mediated oxidative cyclisation. The modified method, published by Bagley *et al.* does not require the use of a palladium catalyst.[174] The modified method was employed in this project and produced a product yield of 87% (**Scheme 38**).

3.2.3. Formation of (*R*)-methyl 3((2-((*tert*-butoxycarbonyl)amino)propyl-amino-5-nitrobenzo[*b*]thiophene-2-carboxylate (112)

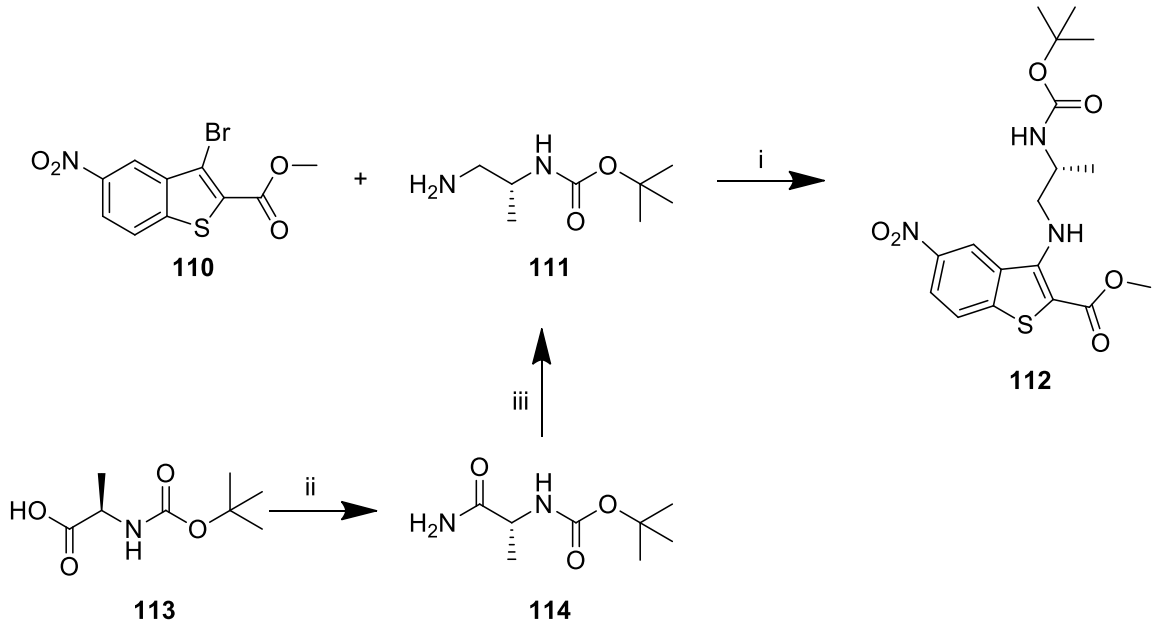

Scheme 39: Formation of **112**. Reagents and conditions: i) Cs_2CO_3, (±)-BINAP, $Pd(OAc)_2$, dry toluene, irradiated at 150 °C, 75 min in a pressure-rated glass vial using a CEM Discover microwave synthesizer by moderating the initial power (200 W); ii) EDCI·HCl, HOBt·H_2O, DCM, 0 °C; RT, 30 min;

aq. NH_3 (18 M), 0°C; RT, 30 min; iii) BH_3•SMe_2, THF, Ar, 0 °C; 18 h, RT; ion exchange, SCX-2, MeOH; NH_3, MeOH.

The reaction conditions used for the formation of (*R*)-methyl 3((2-((*tert*-butoxycarbonyl)amino)propyl-amino-5-nitrobenzo[*b*]thiophene-2-carboxylate (**112**) were adapted from the Buchwald-Hartwig *N*-arylation studies carried out by Queiroz *et al*. for the coupling of aryl amines and electron-rich and electron-poor 3-halogenated benzo[*b*]thiophenes. Queiroz *et al.* developed the palladium catalyzed amination of benzothiphenes.[226] Bagley *et al.* modified the procedure to include microwave irradiation, shortening the reaction times to 1-1.25 h from the 24 h necessary with the conventional heating employed by Queiroz *et al.*[174] whilst achieving similar yields. The amount of base required was also reduced when using microwave irradiation, which reduced the amount of transesterification side products. **112** was achieved in a 70% yield (**Scheme 39**).

For the formation of (*R*)-*tert*-butyl (2-aminopropyl)carbamate (**111**), there were two possible methods that could be used. The first method for conversion of the carboxylic acid to the amide used a mixed anhydride method and reaction with ethyl chloroformate under basic conditions followed by substitution with ammonia to give amide (**111**), which when carried out produced a yield of 40% (**Scheme 39**).[227]

The second method was based on peptide coupling using EDCI·HCl and HOBt·H_2O with DIEA and ammonia followed by a reduction of the amide group using the Lewis acidic borane dimethylsulfide (BH_3•SMe_2) at 0 °C under an inert atmosphere, which was then allowed to warm to room temperature overnight. Reaction completion was determined by TLC analysis, and the excess BH_3•SMe_2 was removed under reduced pressure and the residues washed with MeOH to decomplex borane.[228] The product (**111**) was purified by SCX-2 chromatography to give a high yield of 82% (**Scheme 39**).

3.2.3.1. Buchwald-Hartwig *N*-arylation – palladium catalysis and cyclisation

During the mid-1990s, Buchwald and Hartwig simultaneously conducted studies into the use of palladium in forming carbon-heteroatom bonds. Palladium had

already been widely investigated as a successful catalyst for a range of C-C bond forming reactions. The studies conducted by Buchwald and Hartwig showed successful application of palladium catalysts to promote nucleophilic substitution reactions at a vinylic or aromatic centre. Before these studies, it had been necessary to use harsh reaction conditions such as copper-mediated nucleophilic displacement reactions of aryl halides using various nitrogen nucleophiles,[229] strongly acidic nitration and subsequent reduction to the aniline, and radical nucleophilic aromatic substitution ($S_{RN}1$) using alkali metals and ammonia, which could return a mixture of products through benzyne formation.[230]

However, Buchwald and Hartwig were not the first to carry out studies into using palladium as a catalyst for carbon-heteroatom bond forming reactions; in 1983 Migita *et al.* used catalytic amounts of $PdCl_2[P(o\text{-tolyl})_3]_2$ to mediate aryl C-N bond formation and in 1984 Boger and Panek published an intramolecular palladium(0) mediated aryl C-N bond formation in the synthesis of the natural product lavendamycin.[231,232] Migita *et al.* coupled aryl bromides and diethylaminotributyltin and screened a number of palladium complexes and found that catalytic amounts of $PdCl_2[P(o\text{-tolyl})_3]_2$ was much more efficient than $Pd(PPh_3)_4$ or $PdCl_2(PPh_3)_2$.[231] Boger and Panek used stoichiometric amounts of $Pd(PPh_3)_4$ in THF for the coupling and cyclisation of a linked aryl amine and aryl bromide, proposing the formation of a 6-membered σ-bonded palladacycle intermediate that resulted in the formation of a β-carboline.[232]

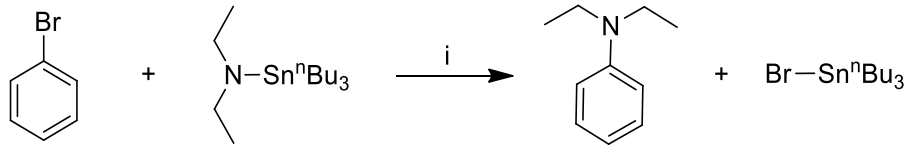

Scheme 40: Migita et al.[231] Reagents and conditions: i) $PdCl_2[P(o\text{-tolyl})_3]_2$ (1 mol%), toluene, 100 °C, Ar, 33-79%.

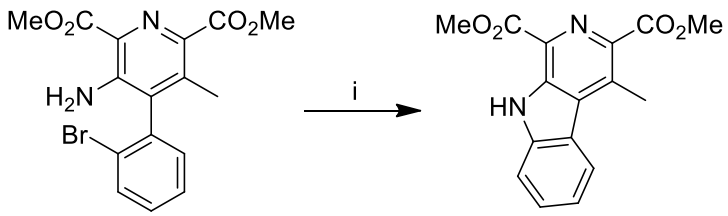

Scheme 41: Boger and Panek.[232] Reagents and conditions: i) $Pd(PPh_3)_4$ (1.5 equiv.), THF, 80 °C, 21 h, 84%.

The simultaneous publication in 1994 of studies conducted by Buchwald and Hartwig extended the scope of carbon-heteroatom coupling using palladium catalysts. Hartwig *et al.* noted the similarity between Migita *et al.*'s studies and Stille coupling; both coupling reactions involving stannanes and halides, the former for C-N bond formation, the latter for C-C bond formation. Hartwig *et al.* continued with the study of coupling stannanes to halides but set out to identify the active species in the catalytic cycle by isolating intermediates from several stages of the cycle and conducted crystallographic characterization of these intermediates in order to gain insight to the mechanistic pathway. Through these studies, the group was able to isolate and identify the Pd(II) dimer complex $[PdArBr(P(o\text{-tolyl})_3)]_2$, which was formed after the oxidative addition of ArBr to $Pd^0[P(o\text{-tolyl})_3]$.[233] They proposed that transmetallation would occur on the monomer or dimer of the complex,[233] however a later study by Driver and Hartwig showed that the reductive elimination step proceeds by a dissociative process and forms the three-coordinate species to give the coupled arylamine.[234]

The studies conducted by Buchwald *et al*. again recognized the importance of Migita *et al*.'s work and noted the lack of applicability of the route to the general synthesis of arylamines was probably due to the instability of aminostannanes.[235] Buchwald *et al.*'s study aimed to extend the scope of Migita *et al.*'s work in order to apply the method to coupling a wider variety of amines, including primary and secondary alkyl and aryl amines. The group were able to demonstrate that this was possible by an *in situ* transamination reaction that could be applied more generally. The group also tested other $PdCl_2L_2$ catalysts (where L = $(PPh_3)_2$, DPPF or $Ph_2P(CH_2)_3PPh_2$) and determined that the original catalyst used by Migita *et al*. gave superior results. The study also showed that reactions of lithium amides with *n*-Bu_3SnCl in ether, as was

the conventional route to produce aminostannanes, was unsuccessful, possibly due to the production of LiCl or BuLi poisoning the active species. In order to avoid poisoning, *in situ* generation of aminostannanes was done by reacting an aminostannane derived from a volatile amine with a higher boiling amine in toluene with subsequent removal of the volatile amine by purging the vessel with argon.[235]

In 1995, Buchwald and Hartwig concurrently published methods for C-N bond formation that were tin free. Whilst tin-mediated methods were high yielding, they required long reaction times and removal of the tin-amide side products, which would pose a problem to the applicability of the methods to the large-scale preparation of arylamines for pharmaceutical purposes due to toxicity. Through the addition of a bulky base, the need for tin was eliminated. Buchwald *et al*. used a slight excess of sodium *tert*-butoxide (NaO^tBu) alongside [$PdCl_2(P(o\text{-tolyl})_3)$] and [$Pd(dba)_2$]/2 $P(o\text{-tolyl})_3$ to couple primary and secondary amines with aryl bromides, followed by an aqueous workup and column chromatography producing pure arylamines.[236] Hartwig *et al*. used lithium silylamide ($LiN(SiMe_3)_2$) as a base to successfully produce arylamines, though noted that slower reaction times were achieved with NaO^tBu.[237] The study also proposed that the mechanism proceeded by addition of the amine to a monophosphine complex after the break-down of the Pd(II) complex, leading to an enhancement of the amine acidity. This would then be followed by deprotonation of the bulky silyl amide base to form the amido complex, which would then rapidly undergo reductive elimination of the arylamine product.[237] **Scheme 7** shows the widely accepted Buchwald-Hartwig catalytic cycle.[238]

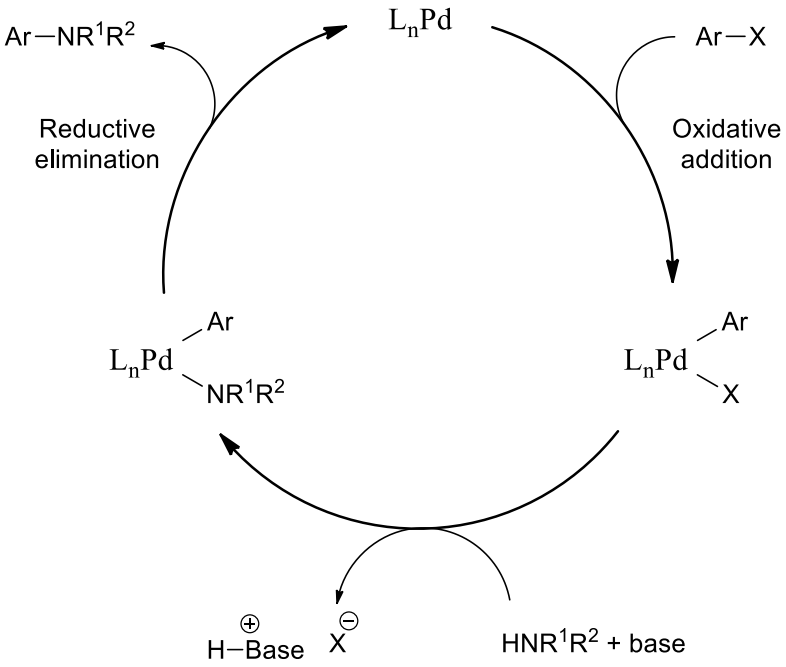

Scheme 42: Buchwald-Hartwig *N*-arylation proposed catalytic cycle.[238]

3.2.4. Formation of (3*R*)-3-methyl-9-nitro-1,2,3,4-tetrahydro-5*H*-[1]benzothieno[3,2-*e*][1,4]diazepin-5-one (115)

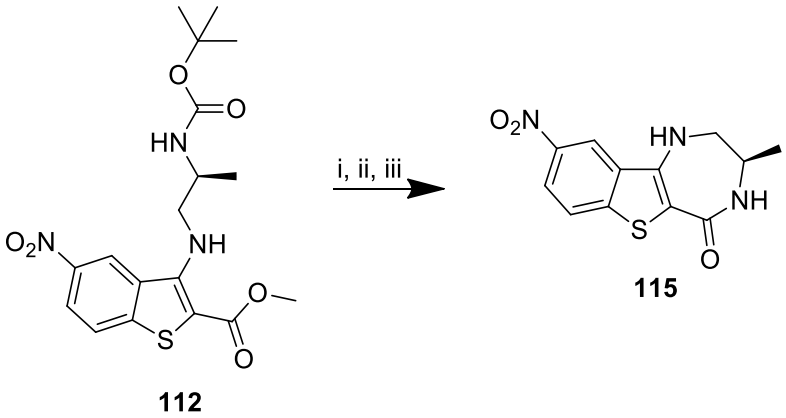

Scheme 43: Formation of **115**. Reagents and conditions: i) TFA (10% v/v in DCM), RT, NaOMe in MeOH, 50 °C, 2 h; ii) reflux, 2 h; iii) 0°C, HCl (1 M), 30 min 100%.

For the ring closing reaction to take place, first a general Boc deprotection was carried out by stirring **112** at room temperature overnight with 10% TFA in DCM, with reaction completion confirmed by TLC analysis. The volatile components were then carefully removed. The cyclization step was carried out under basic conditions, as per a procedure detailed by Khatana *et al*. for similar benzothieno-1,4-diazepin-

5-one compounds.[239] The reaction mixture was stirred with NaOMe in MeOH and heated to 50 °C for 2 h, then heated to reflux for 2 h. The crude mixture was then poured into iced water and neutralized using 1 M HCl aqueous solution. The product (**115**) was isolated by vacuum filtration as a red powder in quantitative yield (**Scheme 43**).

3.2.5. Formation of (3*R*)-9-amino-3-methyl-1,2,3,4-tetrahydro-5*H*-[1]benzothieno[3,2-*e*][1,4]diazepin-5-one (116)

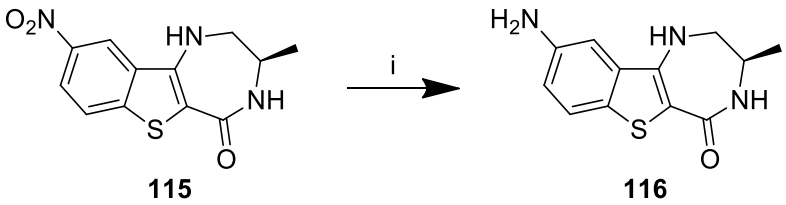

115 **116**

Scheme 44: Formation of **116**. Reagents and conditions: i) DBU, $Mo(CO)_6$, EtOH, irradiated at 150 °C, 30 min, 92%.

The procedure employed for this step was originally developed by Spencer *et al*. for the reduction of poly-functionalised nitroaromatic compounds using microwave irradiation, molybdenum hexacarbonyl ($Mo(CO)_6$) and 1,8-diazabicyclo[5.4.0]undec-7-ene (DBU) in ethanol.[240,241] The reaction is thought to proceed by the formation of metal nitrenes, which are formed when the nitro group is deoxygenated, resulting in the loss of carbon dioxide (CO_2) via metal carbonyl mediated carbonylation, leading to the formation of the primary amine by protonolysis of the nitrogen.[242] DBU is added as a non-nucleophilic base as it is known to facilitate CO liberation from $Mo(CO)_6$.[243]

The conversion of nitrobenzothiophene **115** to amine **116** was carried out with one equivalent of $Mo(CO)_6$ and three equivalents of DBU in EtOH in a sealed vessel irradiated at 150 °C at 30 minutes. Amine **116** was purified by flash column chromatography to give the isolated product in high yield (92%, see **Scheme 44**).

3.2.6. Formation of (*R*)-10-methyl-3-(6-methylpyridin-3-yl)-9-10-11-12-tetrahydro-8*H*-[1,4]diazepino[5',6':4,5]thieno[3,2-*f*]quinoline-8-one. PF-3644022 (33)

The final step in the total synthesis of PF-3644022 (**33**) was investigated by previous members of the group with limited success. One of the avenues explored was based on work published by Wang *et al.* who developed a route to fused quinoline systems via a Doebner type multicomponent reaction (MCR).[244–248] A Doebner MCR would usually be carried out using an aniline, a functionalized aldehyde and pyruvic acid, the product of which (a 2-substituted-quinoline-4-carboxylate) can be decarboxylated to give a 2-substituted quinoline.[249,250] Instead, Wang *et al.* used an alkyl aldehyde, butyl vinyl ether (n-BVE) and molecular iodine (10 mol%) as a mild Lewis acid catalyst.[251] The proposal was that an alkyl aldehyde should be in equilibrium with the enol form; the enol would immediately react with an I_2-activated Schiff base, followed by an intramolecular Friedel-Crafts cyclization, with subsequent dehydration and oxidation producing an aromatized benzo[*f*]quinoline (**Scheme 45**).

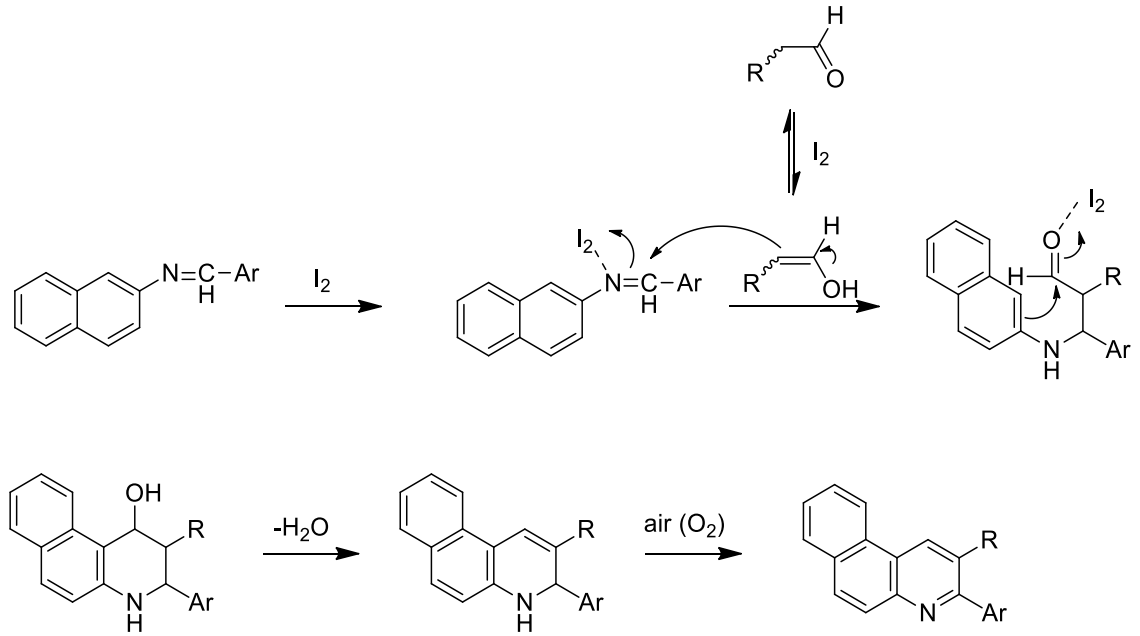

Scheme 45: Wang *et al.*'s proposed mechanism for I_2-catalysed reaction of a Schiff base and alkyl aldehyde towards benzo[*f*]quinoline derivatives.[251]

It was therefore proposed that this system could be adapted for the final step in the synthesis of PF-3644022 (**33**), using amine **116**, 6-methylpyridine-3-carboxaldehyde, n-BVE and a Lewis acid in a one-pot system. A trial system was

developed and investigated by Lorna Brigham, a summer student in the research group.[ii] Brigham's test reaction involved using pyridine-3-carboxaldehyde and aniline (**117**) to promote cyclization and to test the scope of Wang *et al.'s* published methods.

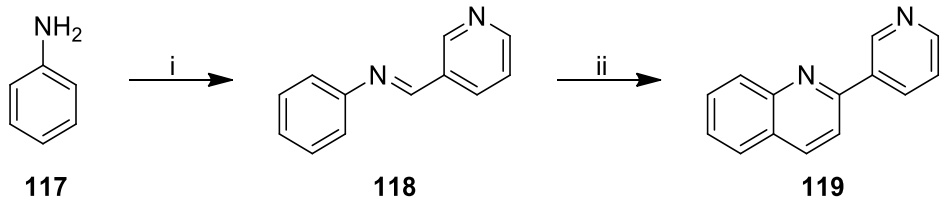

Scheme 46: Brigham's trial multi-component quinoline synthesis. Reagents and conditions: i) pyridine-3-carboxaldehyde, solvent; ii) n-BVE, Lewis acid, Δ, 20 h, or MW 100 °C, 1 h.

Brigham found that a much higher quantity of molecular iodine was required for the reaction to proceed (50 mol%) and produce quinoline **119**. Different Lewis acids were also tested but ultimately I_2 produced the best results. It was also found that a pre-stir of aniline and aldehyde for 1 h at room temperature was required to first form the Schiff base before the addition of the Lewis acid. This minimized the formation of side products, which otherwise hampered purification techniques. Microwave irradiation also reduced the extent of side product formation.

The project was then handed over to Dr. Dwyer who conducted a solvent screening, leading to a change from Wang *et al.*'s procedure, which used THF, to MeCN which was found to be the optimum solvent. The modified method was applied to the final step in PF-3644022 (**33**) synthesis (**Scheme 47**).[214]

[ii] Experiments and analysis of results completed by Lorna Brigham, M.C. Bagley, University of Sussex, 2015, unpublished.

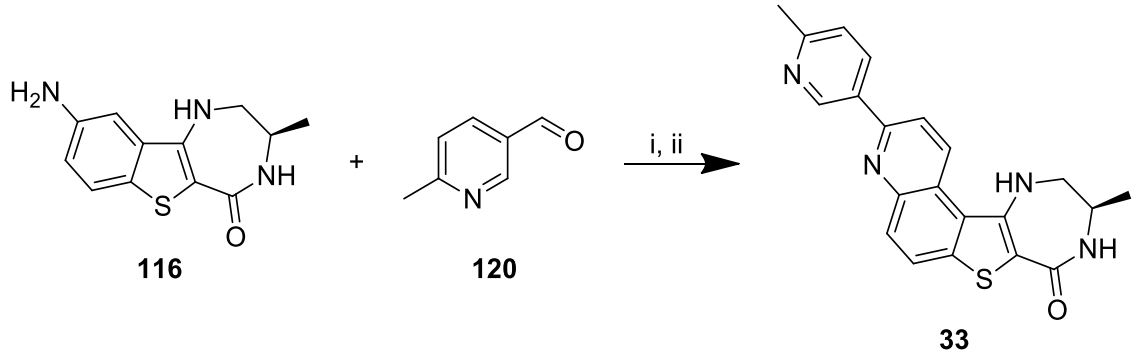

Scheme 47: Final step in PF-3644022 (**33**) synthesis. Reagents and conditions: i) MeCN, RT, 1 h; ii) n-BVE, I_2 (50 mol%), MW 100 °C, 3 h, 6%.[214]

3.2.6.1. Formation of 6-methylpyridin-3-carboxaldehyde (120)

The final step in the synthesis towards PF-3644022 (**33**) required the formation of 6-methylpyridin-3-carboxaldehyde (**120**). Initially, Dr. Dwyer had tried to oxidize **121** using Dess-Martin periodinane (DMP) as this is usually a mild and highly efficient method of oxidation; however, on this occasion long reaction times resulted in poor yields. Therefore, Swern oxidation conditions were employed whereby oxalyl chloride was reacted with DMSO in dry DCM at −78 °C, followed by the dropwise addition of **121** and then the addition of NEt_3 as base to form the sulfur ylide and facilitate the oxidation. Purification by flash chromatography gave aldehyde **120** in high yield (75%) (**Scheme 48**).

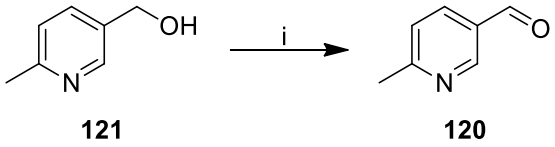

Scheme 48: Formation of **120**. Reagents and conditions: i) $(COCl)_2$, DMSO, NEt_3, CH_2Cl_2, −78 °C, 75%.

3.2.6.2. A new method for the final step in the synthesis of PF-3644022 (33)

Since previous efforts in the Bagley group to carry out the final step in the synthesis of PF-3644022 had only resulted in low yields (6%), the requirement for further investigation was obvious. Since test reactions carried out by Brigham and Bagley had shown promising results it was decided that a new type of Lewis acid catalyst may help improve the yield, since so far only iodine and $SnCl_2{\cdot}H_2O$ had been investigated. A new Lewis acid catalyst had been developed at the University of

Sussex by Kostakis *et al*. This Zn/4f coordination cluster (CC) had been successfully employed in Friedel-Crafts reactions and in the Petasis borono-Mannich multicomponent reaction,[252–254] with the full scope of its capabilities yet to be investigated. Therefore, it was of great interest to both the Bagley group and the Kostakis group to apply the catalyst to the Doebner-type MCR of the final step in our synthesis.

3.2.6.2.1. Isoskeletal tetranuclear Zn/4f coordination cluster as a new catalyst

The Kostakis group at the University of Sussex developed an isoskeletal tetranuclear Zn/4f coordination cluster (CC) that had been proven to be a highly efficient catalyst in Friedel-Crafts alkylation of indoles and nitrostyrenes, as well as in the Petasis borono-Mannich multicomponent reaction.[252–254] Only a few recent examples of polynuclear CCs, which are made up of organic ligands, transition metals (3d) and/or lanthanides (4f), have been reported as useful catalysts.[255–257] However, catalysts that contain zinc or lanthanides have been extensively used in Friedel-Craft reactions.[258,259] Having had previous success with a series of isoskeletal CCs catalyzing domino reactions at room temperature,[255,260] and with the knowledge that lanthanide and zinc/Schiff base compounds had been used as catalysts in reactions involving indole derivatives with aldehydes and ketones,[261,262] the Kostakis group set out to synthesize and test a novel isoskeletal tetranuclear Zn/4f (CC) in the Friedel-Crafts reaction (**Scheme 49**).

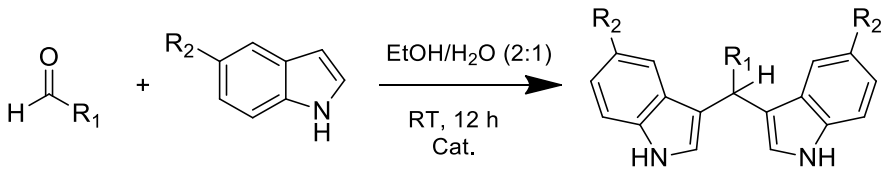

Scheme 49: Friedel-Crafts acylation tested by Kostakis group with novel catalyst.[252]

The catalyst the group designed is bimetallic, containing zinc and yttrium, and has a rigid, defective, dicubane topology, which remains intact in organic solvents—a feature which allows both metal centers to coordinate to substrates and promote coupling reactions efficiently due to the proximity of the metal centers to one another.[252] During a solvent screen it was also found that the catalyst's mode of

action was homogeneous, because reactions in low polarity solvents yielded no conversion of substrates to products.

Friedel-Crafts reactions

Friedel-Crafts reactions have become some of the most important organic chemistry reactions. They are carbon-carbon bond forming reactions that involve the introduction of an alkyl or acyl group onto an aromatic substrate by treating the substrate with an alkyl halide or alkene for alkylation, or an acyl halide or anhydride for acylation, in the presence of a Lewis acid.

To test the scope of the new catalyst, the Kostakis group chose to synthesize bisindolylmethane via the nucleophilic addition of benzaldehyde to indole. Bisindolylmethane derivatives have shown great promise as pharmacophores; however, the existing catalytic systems and metal salts employed for their synthesis are expensive, and require toxic reagents, high temperatures and high catalytic loadings, and in the case of silver salts, they suffer from photosensitivity.[263–266] Therefore there is a need to improve their synthetic process. The indole ring system is a class of heterocyclic subunit found extensively in nature and as such has extensive biological activity, which has been of great interest to the drug development community in the development of scaffolds.[267,268]

The conditions of the reaction were optimized and found that the optimum reaction time was 12 h and the ideal solvent system was ethanol-water (2:1), though DMF, acetonitrile or ethanol could also be used though with lower yields. The low yields when ethanol had been used indicated that water was needed to promote the reaction.[252] At a 2.5 mol% loading, the reactants were converted to the desired product in quantitative yields, and at 1 mol% the product was obtained at a slightly lower yield of 96%, which was still a vast improvement on existing systems.[262,264,265] The reaction conditions were then tested further with a variety of aldehydes and substituted indoles, which were reported as achieving excellent yields.[252] However, when the reaction conditions were tried using ketones instead of aldehydes, even with longer reaction times and higher temperatures, there was no product formation. Further tests were carried out, reacting indoles with an aliphatic

aldehyde instead of an aromatic aldehyde, which resulted in low yields even after 72 h. The optimized conditions were then applied to the reaction of substituted indoles with benzaldehyde, which had varying success; 2-methyl-indole gave a quantitative yield in only 2 h, but swapping the $-CH_3$ group for the electron withdrawing $-CF_3$ group resulted in only a 16% yield, and reactions with indole-3-acetic acid and *N*-methylindole resulted in no product formation. This lack of reactivity was postulated by Kostakis *et al.* to be due to the carboxylic acid group of indole-3-acetic acid being in competition with benzaldehyde to coordinate to the Y centre and that the nitrogen atom, blocked by a $-CH_3$ group in *N*-methylindole, needed to coordinate to the catalyst in order for the reaction to proceed.

The mechanism proposed by the Kostakis group is shown in **Scheme 50.** First, the nitrogen atom of the indole coordinates to the Zn(II) centre and the oxygen atom of the aldehyde coordinates to the Y centre. This leads to the indole being deprotonated, leaving a negative charge at C-3 promoting the formation of a benzaldehyde-indole hemiaminal. Another indole is then alkylated and finally a proton exchange leads to the release of the bis-adduct.

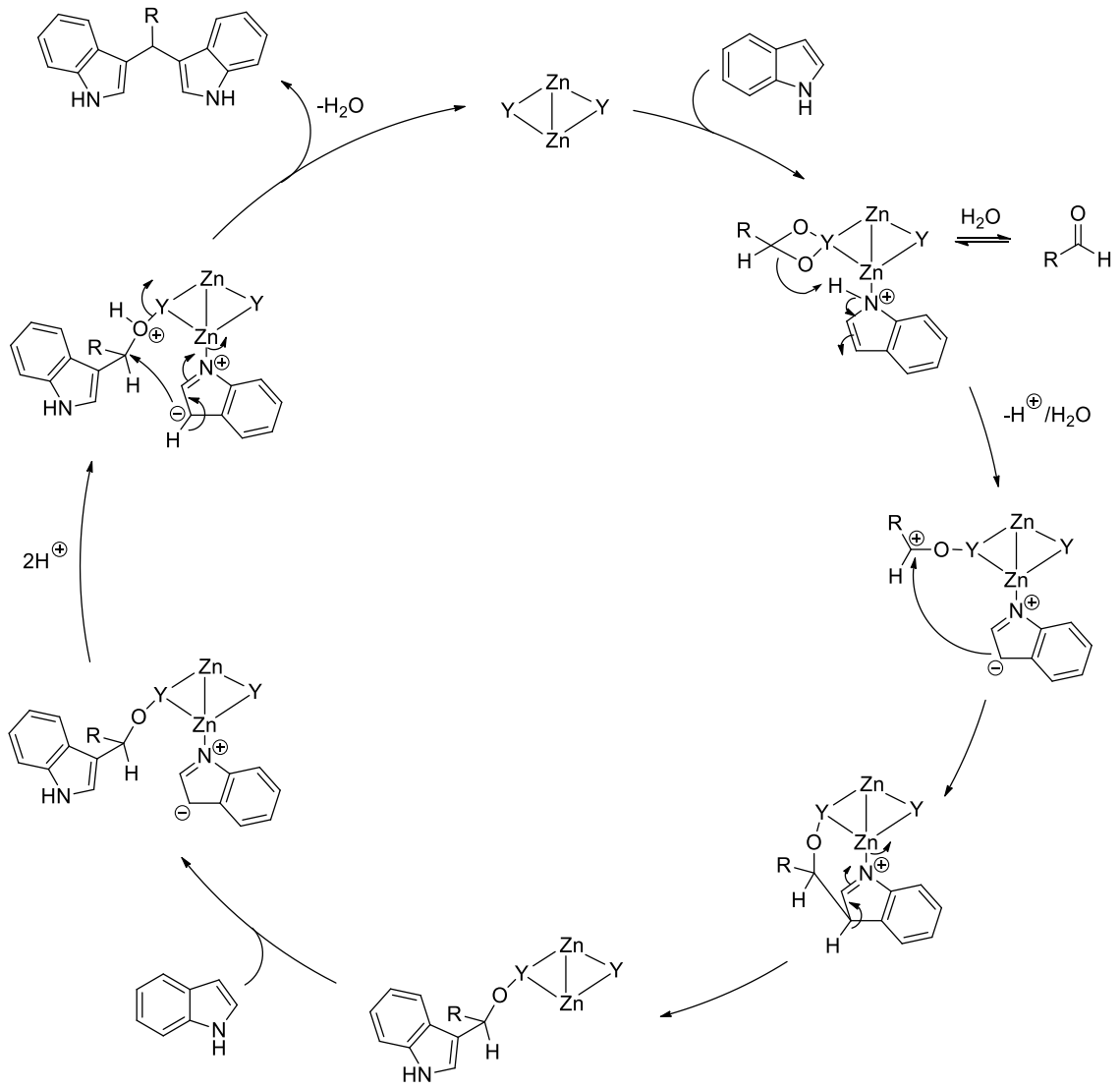

Scheme 50: Mechanism of Friedel-Crafts alkylation proposed by Kostakis *et al.*[252]

The catalyst was also proven to be highly efficient for the conversion of *trans*-β-nitrostyrene and indole to an indolylnitroalkane, with the product being obtained in a 94% yield after 24 h at room temperature using ethanol as a solvent (**Scheme 51**).[254]

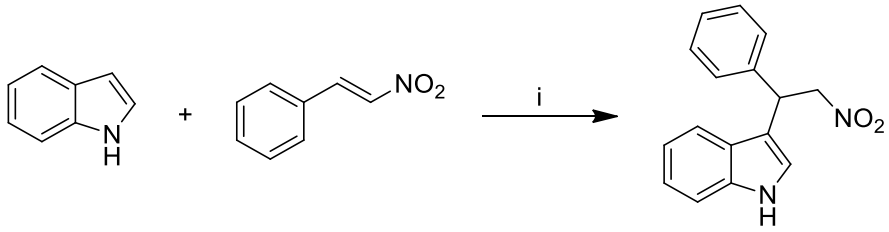

Scheme 51: Conversion of *trans*-β-nitrostyrene and indole to an indolylnitroalkane.[254] Reagents and conditions: i) EtOH, 24 h, RT, $Zn_2Y_2L_4$ (1 mol%), 94%.

Petasis borono-Mannich multicomponent reaction

The Petasis borono-Mannich reaction is a multicomponent reaction (MCR) that involves amines, aldehydes and boronic acids[269] to prepare amines and their derivatives such as α-amino acids, heterocycles and alkylaminophenols via a Mannich-type condensation.[270] MCRs are incredibly useful in organic synthesis as they involve simple starting materials that can be converted into products in fewer steps and in shorter time periods; however, most existing methods still suffer from requiring high catalyst loads, high temperatures and long reaction times.[271–281]

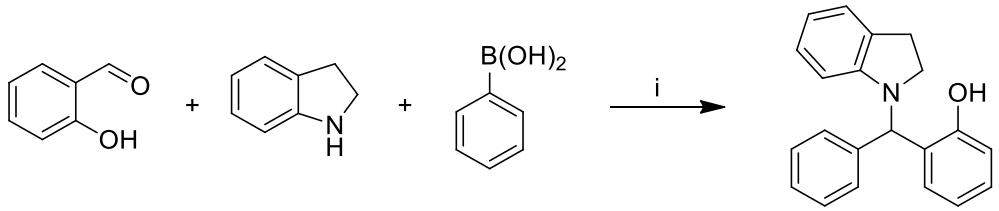

Scheme 52: Trial reaction carried out by Kostakis *et al*. to test the scope of the $Zn_2Y_2L_4$ catalyst.[253] Reagents and conditions: i) DME, RT, 12–16 h, $Zn_2Y_2L_4$ (1 mol%).

A trial reaction was carried out by Kostakis *et al*. and conditions optimized for the reaction of salicylic aldehyde, indoline and phenylboronic acid (1:1:1) (**Scheme 52**).[253] The ideal solvent was found to be DME, and catalyst loading was trialled at 1 mol% because of the previous success of this loading in the Friedel-Crafts reaction,[252,254] and when carried out at room temperature the reaction resulted in a yield of 74% after 12-16 h.[253]

3.2.6.2.2. Results of the application of Zn/4f coordination cluster as a new catalyst for the final step in the synthesis of PF-3644022 (33)

The catalyst provided for testing by the Kostakis group has the general formula $Zn_2Y_2L_4$, where L = $C_{21}H_{25}NO_3$ (**Figure 72**).

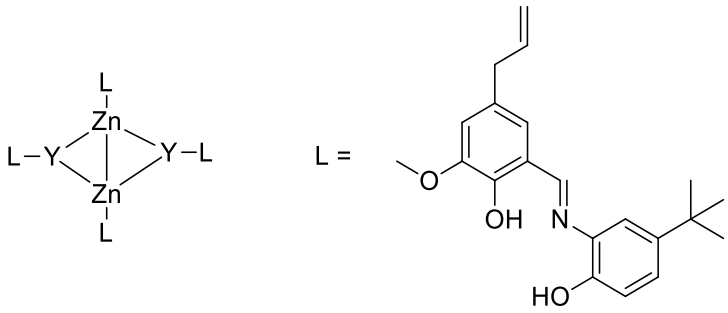

Figure 72: Simplified structure of $Zn_2Y_2L_4$ catalyst.

There are two different ways that the ligands coordinate to the metal centres, which is illustrated in **Figure 73**.

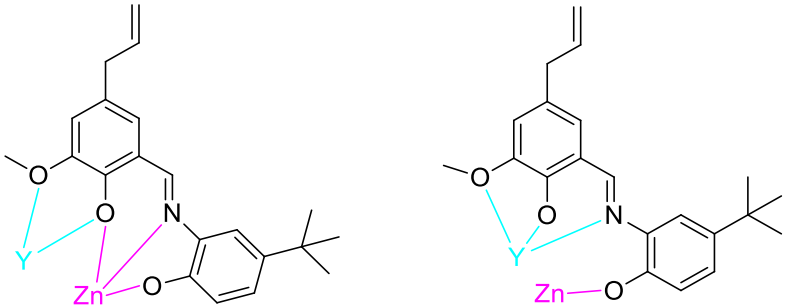

Figure 73: Coordination points of the ligands to the metal centres; two ligands coordinate as per the structure shown on the left with the other two ligands coordinating to the metal centres as per the structure shown on the right.

For the final reaction step the same conditions were employed for testing the new catalyst as were developed by Wang *et al.* and modified by Dr. Dwyer.[251] Since previous publications by Kostakis *et al.* had reported high catalyst efficiency at quantities as low as 1 mol%,[252–254] it was decided that the test reactions would be completed at 1 and 10 mol% catalyst loading. Using the catalyst in 50 mol%, as per the previous attempts using molecular iodine, was deemed inappropriate as the purpose of this investigation was to ascertain whether the catalyst would work in catalytic amounts not stoichiometric, as well as increase the yield from 6%.

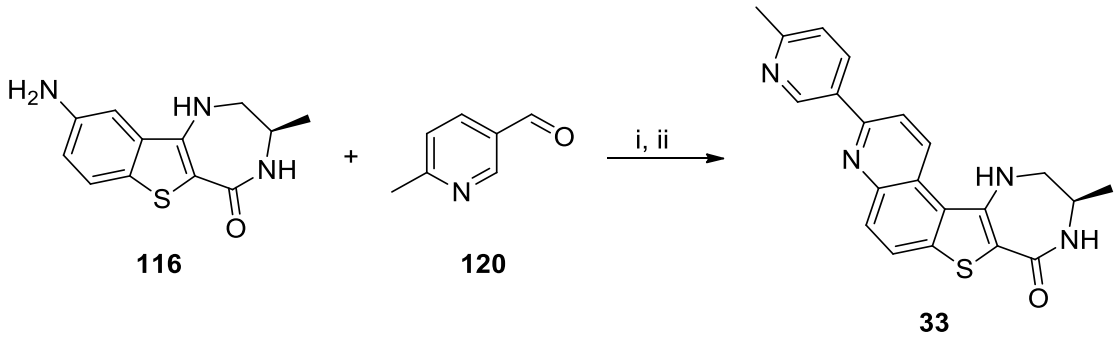

Scheme 53: Final step in PF-3644022 synthesis. Reagents and conditions: i) MeCN, RT, 1 h; ii) n-BVE (10 mol%), $Zn_2Y_2(C_{21}H_{25}NO_3)_4$ (1 mol%/10 mol%), MW 100 °C, 3 h.

Reactions were run in MeCN at room temperature for 1 h before adding n-BVE and the catalyst, and then the reaction vessels were placed in a microwave reactor for 3 h at 100 °C. TLC analysis showed that there were several species present. Purification by flash chromatography could not cleanly separate the product from the side products formed. Mass spectrometry suggested that the product had been formed; however, the product was not clearly discernible from ^{1}H NMR spectroscopic analysis with the broad peaks indicating that zinc from the catalyst could still be present in the crude product (**Figure 74**).

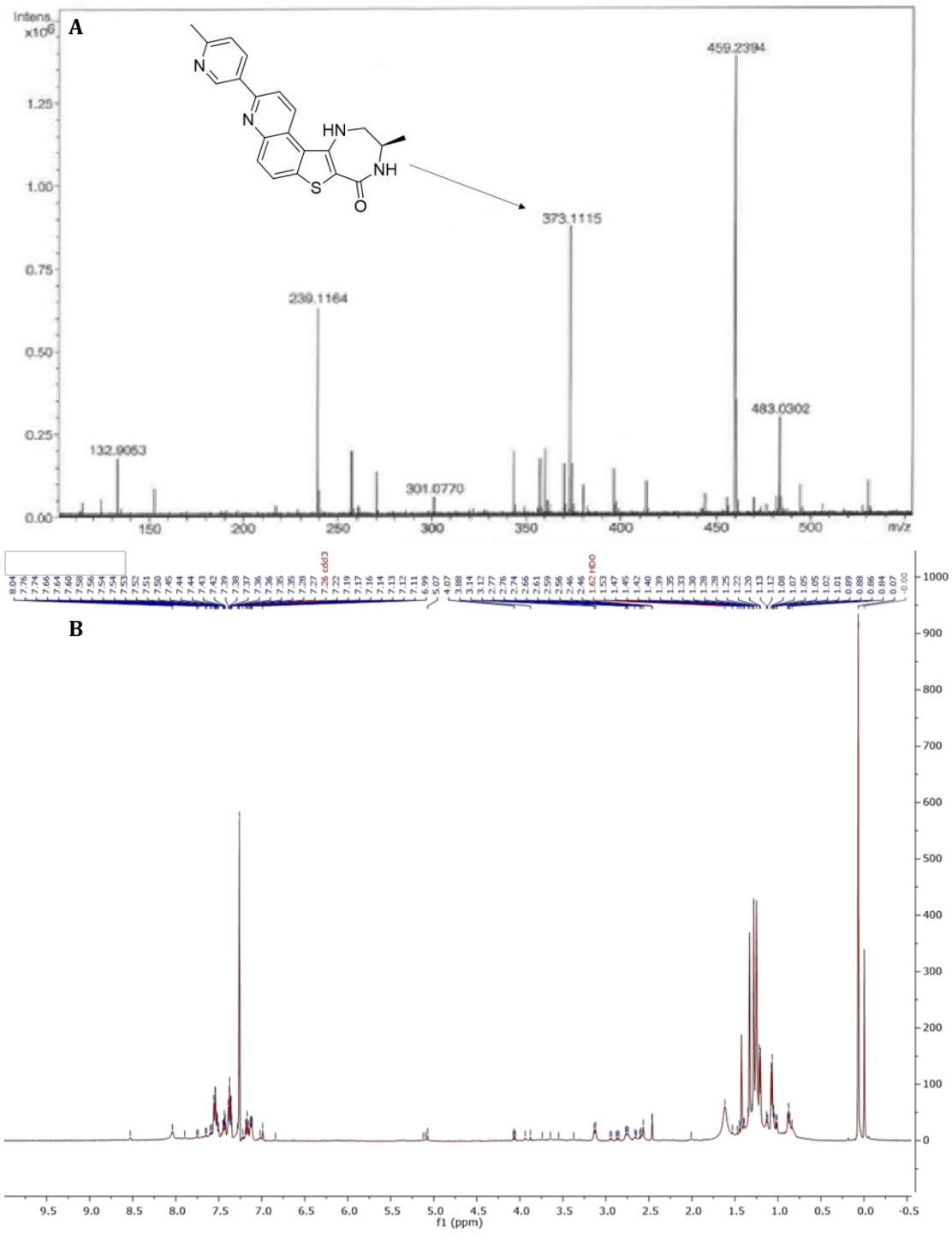

Figure 74: Analysis of **33**. **A**: Mass spectrum showing mass of **33**. **B**: NMR showing no discernible peaks consistent with the presence of product **33**, with broadened peaks suggesting presence of Zn.

Also, the catalyst was not recovered after any of the reactions. From the reaction containing 10 mol% catalyst, a crude yield of 63% was achieved, whilst the reaction containing 1 mol% catalyst had a crude yield of 10%. Because the analysis carried out on the crude products was inconclusive, it is unknown how much, if any, of the

yield was actually the desired product, PF-3644022. Analytical data of both crude products was identical.

A TLC plate indicated the presence of multiple side products which were formed during the reaction, though, despite the mass spectrum, it cannot be assumed that PF-3644022 was one of the products. It could also be possible that the catalyst was not reformed at the end of the reaction and the ligands were present in the crude product, though there appears to be no mass ion peak for the ligand (339.43), the metal complex (308.57) or the catalyst (1717.46).

3.3. Future perspectives

As has been discussed, the catalyst $Zn_2Y_2L_4$ has not been fully investigated for its applicability to the Doebner-type MCR described in this chapter. If it is assumed that the product PF-3644022 was made during the reactions described above, then it can also be assumed that those reaction conditions are not optimal for the catalyst. Whilst the reaction conditions that were set by previous group members were adhered to for the sake of a fair comparison of results, these were different conditions to those deemed as optimal when the catalyst had been used previously during the Friedel-Crafts or Petasis borono-Mannich reactions. For instance, solvent screens carried out by Kostakis *et al.* found that EtOH produced the best results for Friedel-Crafts reactions and DME produced the best results for the Petasis borono-Mannich reaction.

The method of heating could also play a role. For this study microwave-assisted dielectric heating was used but the Kostakis group studies all relied upon conventional heating. Perhaps the catalyst is not suited to microwave irradiation and so conventional heating methods should be tested.

The Kostakis group have also developed several other isoskeletal coordination cluster catalysts, all of which have the formula Zn_2Ln_2, where Ln=Y, Sm, Eu, Gd, Dy, Tb or Yb. Whilst it may not be possible to test all of these catalysts, some have shown quite promising results (yields >90%) at low catalyst loadings (2.5 and 1 mol%).

It may also be beneficial to investigate other Lewis acids, because investigations by the Bagley group have been somewhat limited.

Also, the Skraup method used by Anderson *et al.*, and suggested by Dr. Dwyer in her doctoral thesis, has yet to be examined. This would require forming the unsubstituted quinoline **99**, followed by functionalizing the pyridine ring to the *N*-oxide **100**, which would then be chlorinated to form **101**. From there a Suzuki coupling of **101** with 2-methylpyridinyl-5-boronic acid would result in formation of PF-3644022 (**Scheme 19**).

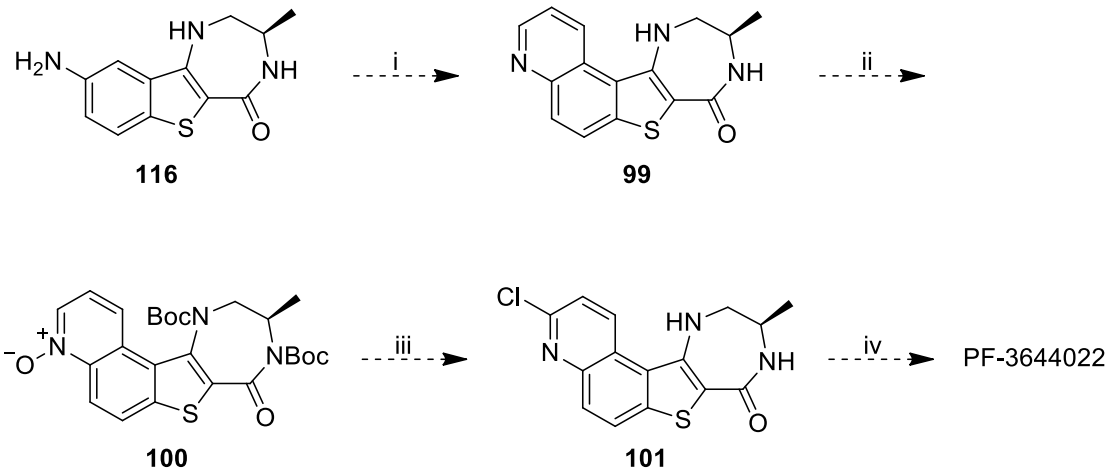

Scheme 54: Alternative route to PF-3644022 proposed by Dr. Dwyer.[214] Reagents and conditions: i) glycerol, H_2SO_4, $B(OH)_3$, Ac_2O, $Fe_2(SO_4)_3$;[282] ii) Boc_2O, DMAP, NEt_3 then mCPBA; iii) $(COCl)_2$, DMF, then HCl; (iv) 2-methylpyridinyl-5-boronic acid, $Pd(PPh_3)_4$, Na_2CO_3, 80 °C.[163]

3.4. Conclusion

The results from testing the new catalyst $Zn_2Y_2L_4$ were unfortunately inconclusive. Though there was a small amount of evidence to support the hypothesis that the product, PF-3644022, was formed during the reaction (mass spectrometry) it was not possible to determine with confidence that this was in fact the case by spectroscopic methods. The amount of product obtained from the reactions containing 10 mol% and 1 mol% catalyst were 19 mg and 3 mg, respectively, making further purification attempts almost impossible. Due to time constraints, it was not possible to carry out the synthetic route again in order to further investigate the catalyst.

Though the results are inconclusive at this time, exploring different catalysts has opened up new collaborations and there is great scope for further work to be explored with this chemistry.

Chapter 4 – Conclusions

Chapter 2 of this thesis saw the formation of several novel BODIPY compounds (**Figure 75**).

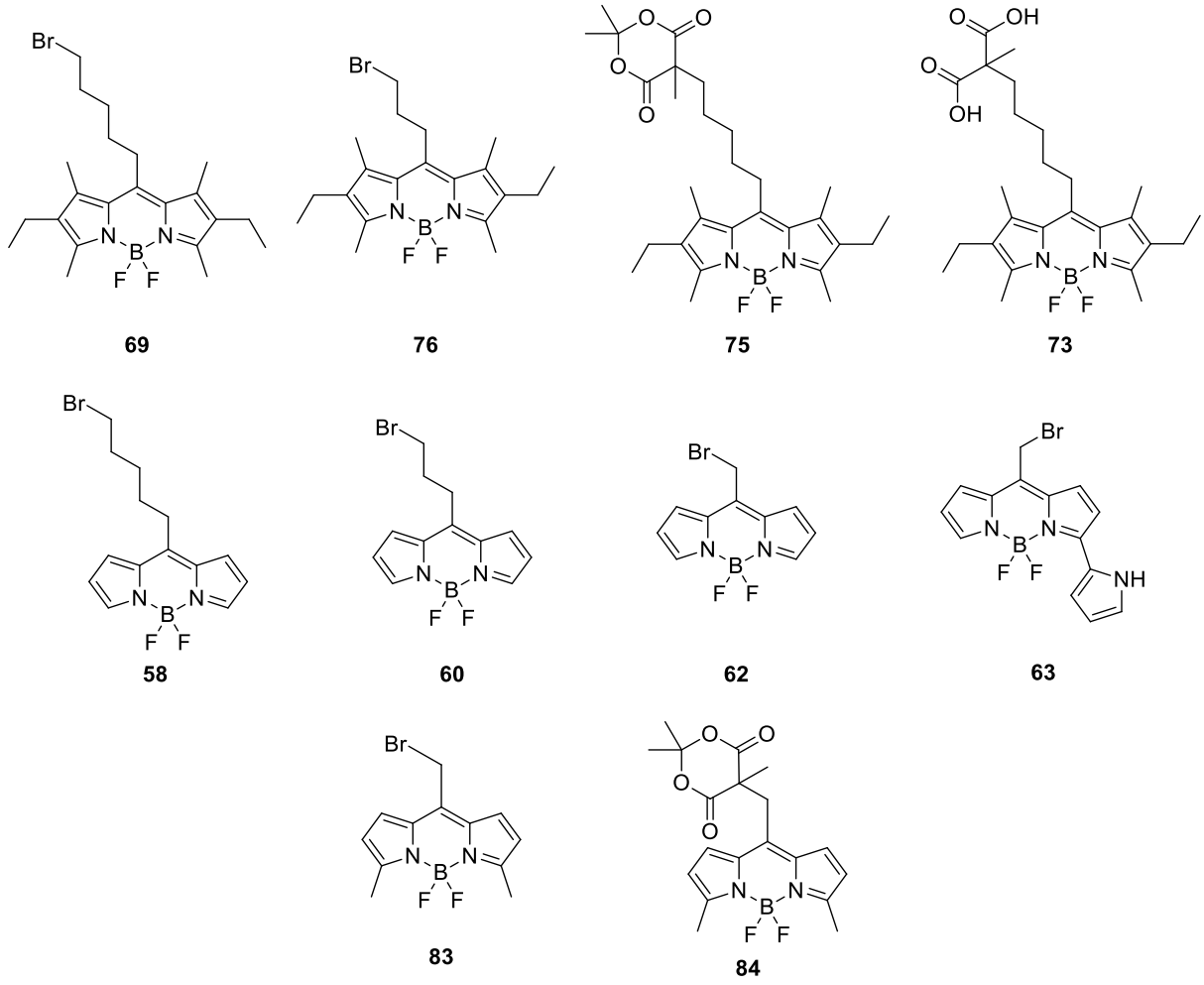

Figure 75: BODIPY fluorophores synthesized during this project.

To finish the library of BODIPY fluorophores it would be necessary to complete the formation of **85** (**Scheme 55**).

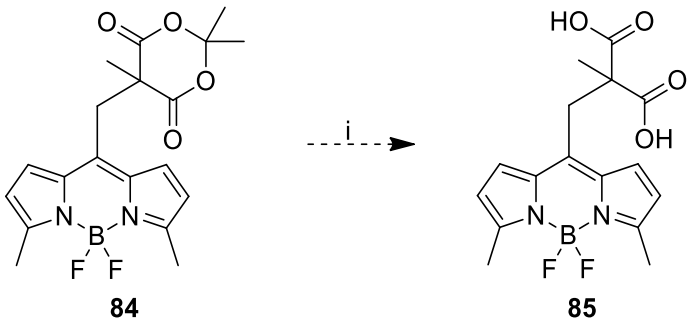

Scheme 55: Proposed reaction scheme for the formation of **85**. Reagents and conditions: i) LiOH, THF-H_2O (1:1), 72 h, RT.

Once **85** has been made it would be necessary to test its properties in a cell line, thus proving whether or not logP is a factor in the structure's ability to preferentially enter apoptotic cells. If it was found that **85** did not specifically target apoptotic cells then it would be necessary to instead focus work on developing the radiolabelled "drug-like" molecule, since the fluorophore development was only meant to provide a model and evidence on how the radiolabelled molecule might behave.

The development of **90** was also attempted in this thesis, though not realized. It is thought that this could be achieved using a procedure developed by Bissember and Banwell (**Scheme 56**).[206]

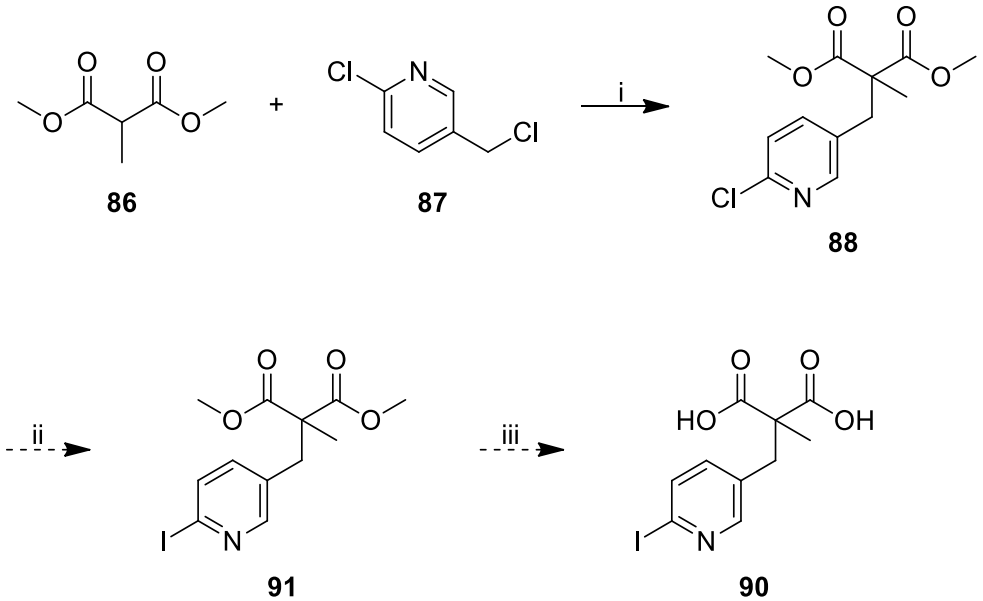

Scheme 56: Proposed scheme for the formation of **90**. Reagents and conditions: i) Under argon, potassium *tert*-butoxide, THF, RT, overnight, purification by trituration with boiling hexane; ii) acetyl

chloride, NaI, irradiation at 80 °C for 3 h in a pressure-rated glass vial using a CEM Discover microwave synthesiser; iii) $LiOH{\cdot}H_2O$ in water, THF, RT, overnight, acidify with HCl.

It would be necessary to establish a good procedure for the development of **90** before the project can be handed to a collaborator proficient in handling radioactive material for the insertion of iodine-131. It would also be prudent to develop a library of small molecules, perhaps by further investigating the development of **90** in a trial and error process of finding the most stable combination of structures, rings and solubilizing groups to adjust for the clogP. Whilst it may be possible to still observe the structures behaviour under a fluorescence microscope (mono- and dialkylpyridines display a weak fluorescence at about 300 nm[207]), the limitations of on-site equipment would make it necessary to outsource this part of the project.

Chapter 3 of this thesis set out to investigate the catalyst $Zn_2Y_2(C_{21}H_{25}NO_3)_4$ for its applicability to the Doebner-type MCR that would lead to the formation of PF-3644022 (**33**).

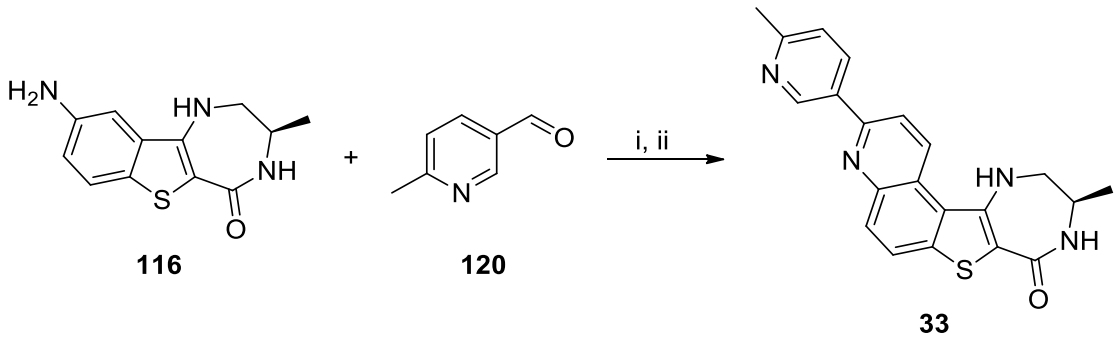

Scheme 57: Final step in PF-3644022 synthesis. Reagents and conditions: i) MeCN, RT, 1 h; ii) n-BVE (10 mol%), $Zn_2Y_2(C_{21}H_{25}NO_3)_4$ (1 mol%), MW 100 °C, 3 h.

It was not conclusively proven that PF-3644022 (**33**) was in fact made during the reactions described in **Scheme 57** but it has been assumed that these reaction conditions were not optimum for this catalyst. Whilst the reaction conditions that were set by previous group members were adhered to for the sake of a fair comparison of results, none of the optimum reaction conditions used during the employment of the catalyst during the Friedel-Crafts or Petasis borono-Mannich reactions were retained. Solvent screens carried out by Kostakis *et al.* found that

EtOH produced the best results for Friedel-Crafts reactions and DME produced the best results for the Petasis borono-Mannich reaction and it would sensible to involve a solvent screen during a full test of this catalyst.

The Kostakis group also reported on several other isoskeletal coordination cluster catalysts they had developed, all of which have the formula Zn_2Ln_2, where Ln is Y, Sm, Eu, Gd, Dy, Tb and Yb. Whilst it may not be possible to test all of these catalysts, some have shown quite promising results (yields >90%) at low catalyst loadings (2.5 and 1 mol%) and may find application in the formation of quinoline synthesis.

A method suggested by Dr. Dwyer in her doctoral thesis has yet to be examined – the Skraup reaction would mimic methods developed by Anderson *et al.*[163] This would require forming the unsubstituted quinoline, followed by functionalizing the pyridine ring to the *N*-oxide which would then be chlorinated. From there a Suzuki coupling would result in PF-3644022 (**Scheme 58**).

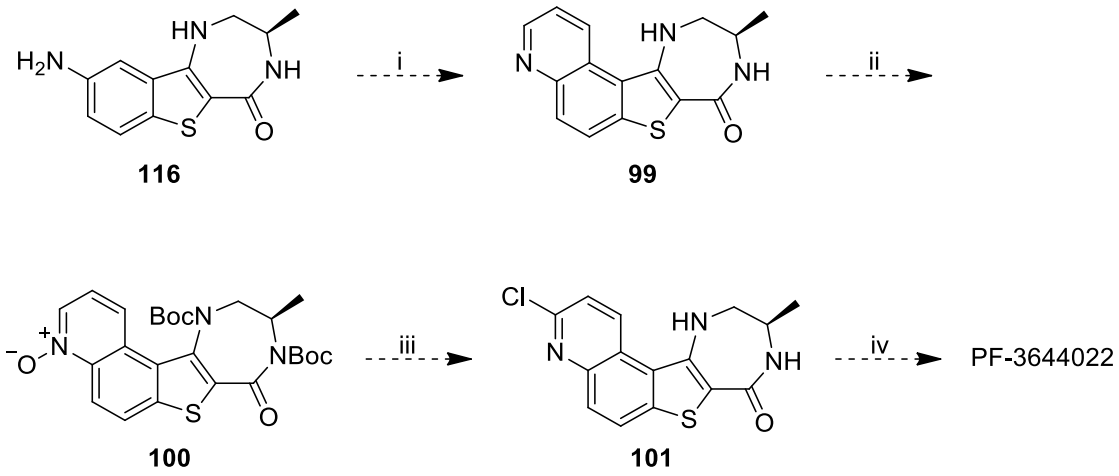

Scheme 58: Alternative route to PF-3644022 proposed by Dr. Dwyer[214] Reagents and conditions: i) glycerol, H_2SO_4, $B(OH)_3$, Ac_2O, $Fe_2(SO_4)_3$;[282] ii) Boc_2O, DMAP, NEt_3 then *m*CPBA; iii) $(COCl)_2$, DMF, then HCl; (iv) 2-methylpyridinyl-5-boronic acid, $Pd(PPh_3)_4$, Na_2CO_3, 80 °C.[163]

Chapter 5 – Experimental

All procedures were completed in air unless otherwise stated. Commercially available reagents were used throughout without purification unless otherwise stated, with solvents dried by standard procedures. Analytical thin layer chromatography was carried out using aluminium-backed plates coated with Merck TLC Silicagel 60 F254. Plates were visualised under UV light (at 254 and/or 360 nm), and/or with ninhydrin and potassium permanganate solutions. Microwave-assisted reactions were carried out using a CEM Discover™, CEM Explorer at the given temperature using the instrument's in-built IR temperature measuring device, by varying the irradiation power (initial power given in parentheses). Column chromatography was carried out on a Biotage Isolera Prime flash purification system. SCX-2 ion exchange chromatography was carried out using Biotage Isolute SPE SCX-2 flash columns. Fully characterised compounds were chromatographically homogeneous. Melting points were determined using a Stanford Research Systems Optimelt and are uncorrected. IR spectra were recorded in the range 4000-600 cm-1 using a Perkin Trans FT-IR Spectrum. NMR spectra were recorded using a Varian VNMRS instrument operating at 600, 500 or 400 MHz. J values were recorded in Hz and multiplicities were expressed in the usual conventions. ESI mass spectra were obtained using a Bruker Daltonics Apex III, with ESI source Apollo ESI, using methanol as the spray solvent. For EI mass spectra a Fissons VG Autospec instrument was used at 70 eV and were captured by Dr. Alla K. Abdul-Sada of the University of Sussex Mass Spectroscopy Centre.

Chapter 2

3,3'-disulfanediylbis(2-(5-(dimethylamino)naphthalene-1-

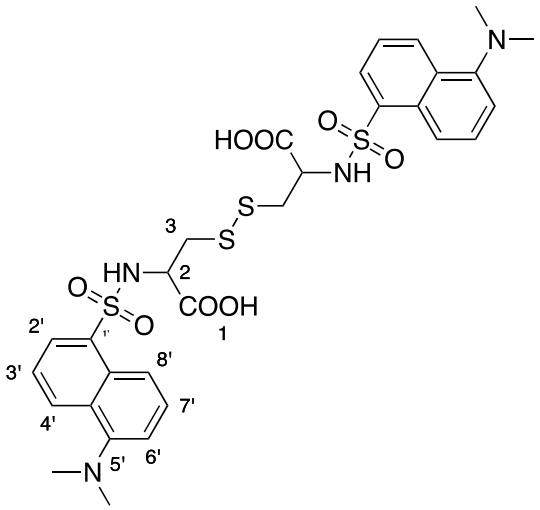

sulfonamido)propanoic acid) (26)

Chemical formula: $C_{30}H_{34}N_4O_8S_4$
Mr: 706.87

According to a procedure developed by Shirvan *et al.*[126] L-cystine (96 mg, 0.4 mmol) and potassium carbonate (221 mg, 1.6 mmol) was dissolved in a solution of water and acetone (50/50). Dansyl chloride (270 mg, 1 mmol) was added and the mixture stirred for 1.5 h at RT. After this time, the acetone was removed under reduced pressure and the remaining solution acidified to pH 3 with citric acid (2 M). The solid was filtered under vacuum and dried in air to give the *title compound* (280 mg, 99%) as a pale yellow solid, mp. 133.6 – 134.2 °C (Found (ES^+): 707.1338. $C_{30}H_{35}N_4O_8S_4$ [*MH*] requires 707.1332); IR (neat) ν_{max}/cm^{-1} 3681.8, 3569.8, 3074.4, 1720.7, 1574.7, 1452.9, 1323.9, 1144.5, 923.9, 785.4, 626.2, 587.5, 576.5; ^1H NMR (500 MHz, DMSO-d_6) δ_H/ppm 12.81 (s, 2H, N*H*), 8.53 (d, 2H, *J* = 8.5), 8.43 (d, 2H, *J* = 8.4), 8.25 (d, 2H, *J* = 8.2) 8.10 (d, 2H, *J* = 8.0), 7.52 (m, 4H), 7.23 (d, 2H, *J* = 7.2), 3.85 (m, 2H), 2.82 (s, 12H, $4CH_3$), 2.77 (m, 2H); ^{13}C NMR (126 MHz, DMSO-d_6) δ_C/ppm: 171.5, 151.7, 136.7, 129.9, 129.6, 129.5, 128.7, 128.1, 123.7, 119.9, 115.4, 55.3, 45.5. One quaternary carbon not visible.

General Procedure for BODIPY Synthesis

Following a procedure developed by Jiao *et al.*[283] under inert atmosphere, bromo-acyl chloride (1 equiv.) in THF (1 mL) was added dropwise to a mixture of freshly distilled pyrrole (10 equiv.) in 1,2-dichloroethane (100 mL). NEt_3 (5 equiv.) was added followed by $BF_3.Et_2O$, the mixture was heated to 50 °C and left to stir overnight. Reaction mixture was concentrated under reduced pressure and diluted with DCM. Organic layer washed with water, dried over Na_2SO_4 and solvent removed. Purification by flash chromatography.

10-(5-bromopentyl)-2,8-diethyl-5,5-difluoro-1,3,7,9-tetramethyl-5H-dipyrrolo[1,2-c:2',1'-f][1,3,2]diazaborinin-4-ium-5-uide (69)

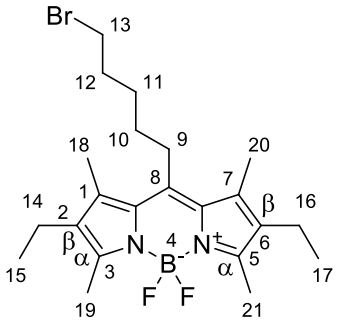

Chemical formula: $C_{22}H_{32}BBrF_2N_2$

Mr: 453.21

Purified by flash chromatography on SiO_2 (dry load), gradient eluting from hexane to hexane/ethyl acetate (80:20) to give the *title compound* (243.19 mg, 54%) as red crystals, mp. 150.5 – 151.3 °C; (Found (ESI$^+$): 475.1695 $C_{10}H_{10}ClNO_4Na$ [*MNa*] requires 475.1702) ^{1}H NMR (500 MHz, $CDCl_3$) δ 3.44 (t, J = 6.6 Hz, 2H, 13-C*H*$_2$), 3.02 – 2.99 (m, 2H, 9-C*H*$_2$), 2.49 (s, 6H, 19/21-C*H*$_3$), 2.40 (q, J = 7.6 Hz, 4H, 14/16-C*H*$_2$), 2.33 (s, 6H, 18/20-C*H*$_3$), 1.96 – 1.91 (m, 2H, 12-C*H*$_2$), 1.69 – 1.64 (m, 4H, 10/11-C*H*$_2$), 1.05 (t, J = 7.6 Hz, 6H, 15/17-C*H*$_3$); ^{13}C NMR (126 MHz, $CDCl_3$) δ 152.2 (α-*C*), 144.2 (*meso*-*C*), 135.5 (7α-*C*), 132.6 (β-*C*), 130.8 (1-*C*), 33.4 (*C*H$_2$), 32.3 (*C*H$_2$), 30.8 (*C*H$_2$), 28.5 (*C*H$_2$), 28.3 (*C*), 17.2 (CH$_2$*C*H$_3$), 14.8 (*C*H$_2$CH$_3$), 13.4 (*C*H$_3$), 12.4 (*C*H$_3$); *m/z* (EI) 452 (M$^•$, 87%), 454 (83), 408 (100), 500 (66), 287 (87), 393 (47).

10-(3-bromopropyl)-2,8-diethyl-5,5-difluoro-1,3,7,9-tetramethyl-5H-dipyrrolo[1,2-c:2',1'-f][1,3,2]diazaborinin-4-ium-5-uide (76)

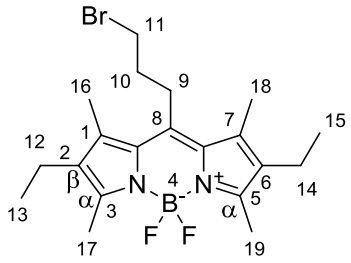

Chemical formula: $C_{20}H_{28}BBrF_2N_2$

Mr: 425.16

Purified by flash chromatography on SiO_2 (dry load), gradient eluting from hexane to hexane/ethyl acetate (80:20) to give the *title compound* (286 mg, 34%) as a red solid, mp. 203.4 – 205.1°C; ^{1}H NMR (500 MHz, $CDCl_3$) δ 3.81 (t, J = 6.0 Hz, 2H, 11-C*H*$_2$), 3.14 – 3.06 (m, 2H, 9-C*H*$_2$), 2.50 (s, 6H, 17/19-C*H*$_3$), 2.39 (t, J = 7.6 Hz, 4H, 12/14-C*H*$_2$), 2.34 (s, 6H, 16/18-C*H*$_3$), 1.90 – 1.87 (m, 2H, 10-C*H*$_2$), 1.04 (t, J = 7.6 Hz, 6H, 13/15-C*H*$_3$). ^{13}C NMR (126 MHz, $CDCl_3$) δ 152.2 (α-*C*), 144.3 (*meso*-*C*), 135.7 (7α-*C*), 132.6 (β-*C*), 130.9 (1*C*), 62.6 (C*H*$_2$), 34.4 (C*H*$_2$), 25.0 (C*H*$_2$), 17.2 (*C*H$_2$CH$_3$), 14.8 (CH$_2$*C*H$_3$), 13.4 (*C*H$_3$), 12.4 (*C*H$_3$); *m/z* (EI) 312 (M•, 21%), 313 (17), 311 (5), 232 (100), 231 (97), 94 (91) 211 (61), 206 (52), 203 (49) 69 (51).

10-(5-bromopentyl)-5,5-difluoro-5H-dipyrrolo[1,2-c:2',1'-f][1,3,2]diazaborinin-4-ium-5-uide (58)

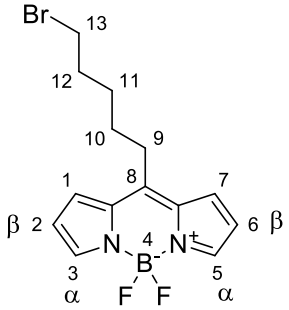

Chemical formula: $C_{14}H_{16}BBrF_2N_2$

Mr: 341.00

Purified by flash chromatography on SiO_2 (dry load), gradient eluting from hexane to hexane/ethyl acetate (90:10) to give the *title compound* (256.5 mg, 43% mixed products. Yield of **58** 9%) as a red sticky solid, (Found (ES^+): 341.0624 $C_{14}H_{16}BBrF_2N_2$ [*MH*] requires 341.0631); ^1H NMR (500 MHz, $CDCl_3$) δ 7.06 – 7.04 (m, 2H, 3/5-C*H*), 6.94 – 6.92 (m, 2H, 1/7-C*H*), 6.28 (dt, J = 4.3, 2.5 Hz, 2H, 2/6-C*H*), 3.42 (t, J = 6.7 Hz, 2H, 13-C*H₂*), 2.80 (d, J = 7.4 Hz, 2H, 9-C*H₂*), 2.39 (s, 2H, 12-C*H₂*), 1.93 – 1.86 (m, 2H, 10-C*H₂*), 1.51 (dt, J = 8.8, 3.8 Hz, 2H, 11-C*H₂*); ^{13}C NMR (126 MHz, $CDCl_3$) δ 190.8 (α-*C*), 178.3 (*meso*-*C*), 131.8 (7α-*C*), 124.8 (β-*C*), 116.5 (1-*C*), 110.7 (*C*H_2), 37.6 (*C*H_2), 33.6 (*C*H_2), 32.3 (*C*H_2), 27.6 (*C*H_2).

10-(3-bromopropyl)-5,5-difluoro-5H-dipyrrolo[1,2-c:2',1'-f][1,3,2]diazaborinin-4-ium-5-uide (60)

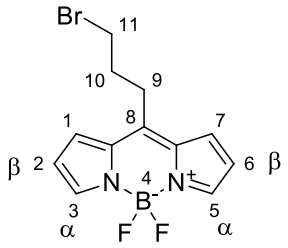

Chemical formula: $C_{12}H_{12}BBrF_2N_2$
Mr: 312.95

Purified by flash chromatography on SiO_2 (dry load), gradient eluting from hexane to hexane/ethyl acetate (90:10) to give the *title compound* (197 mg, 18%) as a dark orange sticky solid; (Found (ESI^+): 312.0215 $C_{12}H_{12}BBrF_2N_2$ [*MH*] requires 312.0239); ^1H NMR (500 MHz, $CDCl_3$) δ 7.04 (m, 4H, 1,3,5,7-C*H*), 6.30 (m, 2H, 2/6-C*H*), 2.45 (m, 2H, 11-C*H₂*), 1.19 (m, 2H, 9-C*H₂*), 0.96 (m, 2H, 10-C*H₂*); ^{13}C NMR (126 MHz, $CDCl_3$) δ 190.5 (α-*C*), 132.7 (*meso*-*C*), 124.3 (7α-*C*), 116.04 (β-*C*), 110.77 (1-*C*), 27.81 (*C*H_2), 17.11 (*C*H_2), 10.70 (*C*H_2).

10-(bromomethyl)-5,5-difluoro-5H-dipyrrolo[1,2-c:2',1'-f][1,3,2]diazaborinin-4-ium-5-uide (62)

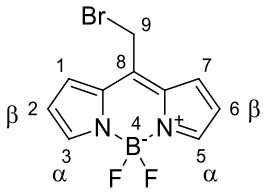

Chemical formula: $C_{10}H_8BBrF_2N_2$
Mr: 284.90

Purified by flash chromatography on SiO_2 (dry load), gradient eluting from hexane to hexane/ethyl acetate (90:10) to give the *title compound* (150 mg, 15%) as a dark orange solid, mp 115.8 – 118.9 °C; ^{1}H NMR (500 MHz, $CDCl_3$) δ 7.85 (s, 2H, 3/5-C*H*), 7.31 (d, J = 4.2 Hz, 2H, 1/7-C*H*), 6.57 – 6.52 (m, 2H, 2/6-C*H*), 2.64 (s, 2H, 9-C*H*$_2$); ^{13}C NMR (126 MHz, $CDCl_3$) δ 143.6 (α-*C*), 128.2 (*meso*-*C*), 118.1 (7α-*C*), 91.7 (β-*C*), 88.4 (1-*C*), 16.3 (*C*H_2).

10-(bromomethyl)-5,5-difluoro-3-(1H-pyrrol-2-yl)-5H-dipyrrolo[1,2-c:2',1'-f][1,3,2]diazaborinin-4-ium-5-uide (63)

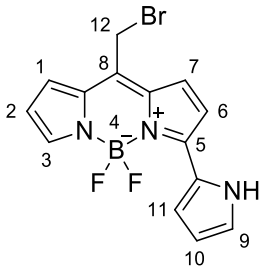

Chemical formula: $C_{14}H_{11}BBrF_2N_3$
Mr: 349.97

Purified by flash chromatography on SiO_2 (dry load), gradient eluting from hexane to hexane/ethyl acetate (90:10) to give the *title compound* (130 mg, 11%) as a purple solid, mp 124.6 – 130.9 °C; ^{1}H NMR (500 MHz, $CDCl_3$) δ 10.48 (s, 1H, N*H*), 7.60 (s, 1H, 3-C*H*), 7.34 (d, J = 4.7 Hz, 1H, 9-C*H*), 7.16 (d, J = 3.5 Hz, 1H, 10-C*H*), 7.03-

6.99 (m, 2H, 1/7-C*H*), 6.91 (d, J = 4.7 Hz, 1H, 11-C*H*), 6.49 – 6.44 (m, 1H, 6-C*H*), 6.40-6.36 (m, 1H, 2-C*H*), 2.54 (s, 2H, 12-CH_2).

10-(Bromomethyl)-5,5-difluoro-3,7-dimethyl-5H-dipyrrolo[1,2-c:2',1'-f][1,3,2]diazaborinin-4-ium-5-uide (83)

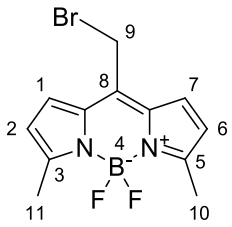

Chemical formula: $C_{12}H_{12}BBrF_2N_2$
Mr: 312.95

Purified by flash chromatography on SiO_2 (dry load), gradient eluting from hexane to hexane/ethyl acetate (60:40) to give the *title compound* (125 mg, 20%) as a dark red solid, mp. 175.3 – 177.2 °C; ^{1}H NMR (500 MHz, $CDCl_3$) δ 7.17 – 7.10 (m, 2H, 2/6-C*H*), 6.33 – 6.26 (m, 2H, 1/7-C*H*), 4.61 (s, 2H, 9-CH_2), 2.61 (s, 6H, 10/11-CH_3); ^{13}C NMR (126 MHz, $CDCl_3$) δ 159.4 (α-*C*), 135.7 (*meso*-*C*), 134.2 (7α-*C*), 127.2 (β-*C*), 120.1 (1-*C*), 37.7 (*C*H_2), 15.2 (CH_3); ·*m/z* (EI) 312 (M•, 70%), 268 (92), 233 (100), 213 (93).

General Procedure for Attachment of Methylated Meldrum's Acid to BODIPY
Under an inert atmosphere, methylated Meldrum's acid (1 equiv.) and potassium carbonate (1 equiv.) was dissolved in DMF. To this was added a solution of BODIPY (1 equiv.) and KI (1 equiv.) dissolved in DMF. The mixture was heated to 50 °C and stirred for 48 h. Mixture was washed with water and extracted with EtOAc. Organic extracts were combined and washed with brine, dried over Na_2SO_4 and solvent removed *in vacuo*. Purified by recrystallization from hexane.

2,8-diethyl-5,5-difluoro-1,3,7,9-tetramethyl-10-(5-(2,2,5-trimethyl-4,6-dioxo-1,3-dioxan-5-yl)pentyl)-5H-dipyrrolo[1,2-c:2',1'-f][1,3,2]diazaborinin-4-ium-5-uide (75)

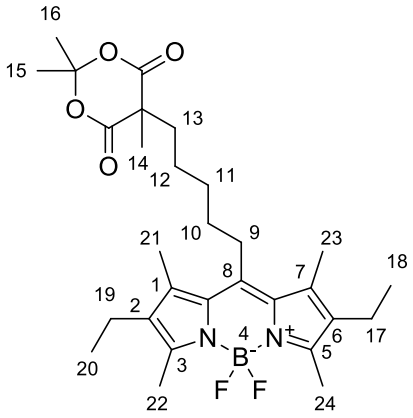

Chemical formula: $C_{29}H_{41}BF_2N_2O_4$

Mr: 530.45

(310.5 mg, 59%) as a red solid, mp. 187.4 – 189.2°C ; (Found (ES^+): 553.3017 $C_{29}H_{41}BF_2N_2O_4Na$ [*MH*] requires 553.3020); ^1H NMR (500 MHz, $CDCl_3$) δ 2.97 – 2.92 (m, 2H, 13-C*H*$_2$), 2.49 (s, 6H, 22/24-C*H*$_3$), 2.42 – 2.36 (m, 4H, 17/19-C*H*$_2$), 2.31 (d, J = 6.6 Hz, 6H, 15/16-C*H*$_3$), 2.06 – 2.03 (m, 2H, 12-C*H*$_2$), 1.73 (s, 6H, 21/23-C*H*$_3$), 1.63 (s, 3H, 14-C*H*$_3$), 1.59 – 1.57 (m, 2H, 9-C*H*$_2$), 1.50 – 1.41 (m, 2H, 10-C*H*$_2$), 1.34 – 1.24 (m, 2H, 11-C*H*$_2$), 1.04 (t, J = 7.5 Hz, 6H, 18/20-C*H*$_3$); m/z (EI+): 530 (M^+, 69), 428 (100), 413 (20), 287 (26).

5,5-difluoro-3,7-dimethyl-10-((2,2,5-trimethyl-4,6-dioxo-1,3-dioxan-5-yl)methyl)-5H-dipyrrolo[1,2-c:2',1'-f][1,3,2]diazaborinin-4-ium-5-uide (84)

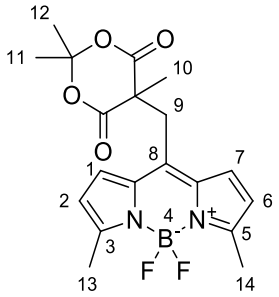

Chemical formula: $C_{19}H_{21}BF_2N_2O_4$

Mr: 390.19

(20 mg, 17%) as a dark red solid, mp. 210.2 – 213.0 °C; ^{1}H NMR (500 MHz, $CDCl_3$) δ 7.10 (d, J = 4.1 Hz, 2H, 2/6-C*H*$_2$), 6.26 (d, J = 4.1 Hz, 2H, 1/7-C*H*$_2$), 2.60 (s, 6H, 13/14-C*H*$_3$), 2.48 (s, 3H, 10-C*H*$_3$), 1.59 (s, 2H), 1.46 – 1.23 (m, 6H, 11/12-C*H*$_3$).

General Procedure for Ring Opening Meldrum's Acid

BODIPY (1 equiv.) and LiOH (4 equiv.) dissolved in THF-H_2O (1:1) mixture and stirred for 72 h at r.t. Mixture concentrated under reduced pressure and residue dissolved in water and extracted with ether. Aqueous layer acidified to pH 2 with HCl (1 M) and extracted with EtOAc. Organic layers were combined and dried over Na_2SO_4 and solvent removed. Residue dissolved in basic water, washed with ether and reacidified to pH 2 and extracted with EtOAc.

10-(6,6-dicarboxyheptyl)-2,8-diethyl-5,5-difluoro-1,3,7,9-tetramethyl-5H-dipyrrolo[1,2-c:2',1'-f][1,3,2]diazaborinin-4-ium-5-uide (73)

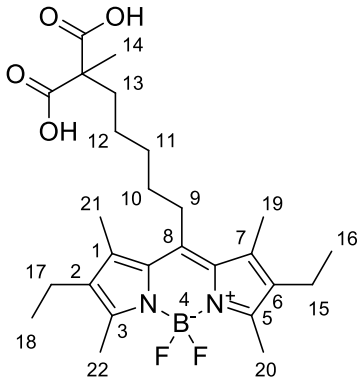

Chemical formula: $C_{26}H_{37}BF_2N_2O_4$

Mr: 490.39

to give the *title compound* (49.04 mg, 25%) as a red solid, mp. 150.1-152.2 °C (Found (ESI$^+$): 513.2722 $C_{26}H_{37}BF_2N_2O_4Na$ [*MH*] requires 513.2707); ^{1}H NMR (500 MHz, DMSO-*d*$_6$) δ 12.59 (s, 2H, O*HOH*), 3.01 – 2.95 (m, 2H, 13-C*H*$_2$), 2.41 – 2.37 (m, 10H, overlapping 15/17-C*H*$_2$ and 20/22-C*H*$_3$), 2.33 (s, 6H, 19/21-C*H*$_3$), 1.76 – 1.70 (m, 2H, 9-C*H*$_2$), 1.57 – 1.54 (m, 2H, 12-C*H*$_2$), 1.51 – 1.46 (m, 2H, 10-C*H*$_2$), 1.31 – 1.26 (m, 2H, 11-C*H*$_2$), 1.25 (s, 3H, 14-C*H*$_3$), 1.00 (t, J = 7.5 Hz, 6H, 16/18-C*H*$_3$).

Dimethyl 2-((6-chloropyridin-3-yl)methyl)-2-methylmalonate (88)

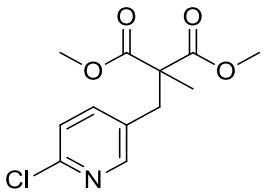

Chemical formula: $C_{12}H_{14}ClNO_4$
Mr: 271.70

According to a procedure developed by Zhu *et al.*[205] under argon, potassium tert-butoxide (450 mg) in THF (10 mL) was added dropwise to dimethyl malonate (0.6 mL) and stirred at RT for 10 min. 3-Chloromethyl-6-chloropyridine (650 mg) was added and the mixture stirred overnight at RT. The mixture was then poured into water (40 mL) and extracted with diethyl ether (3 x 20 mL). The organic extracts were combined, washed with brine (1 x 30 mL) and dried over $MgSO_4$, filtered and the solvent was removed *in vacuo* and the residue triturated with boiling hexane. Hexane was decanted from the insoluble oil, the extracts combined and solvent removed *en vacuo* to give the *title compound* (448.1 mg, 41%) as a white solid, mp. 84.1 – 86.0°C (Found (ES^+): 272.0690 [*MNa*] requires 294.0504); ^1H NMR (500 MHz, $CDCl_3$) δ_H/ppm 8.16 (s, 1H, CH), 7.46 – 7.44 (m, 1H, CH), 7.25 – 7.23 (m, 1H, CH), 3.73 (d, J = 1.3 Hz, 6H, CH_3), 3.19 (s, 2H, CH_2), 1.37 (s, 3H, CH_3); ^{13}C NMR (126 MHz, $CDCl_3$) δ 171.82, 151.12, 149.45, 140.54, 130.83, 124.58, 54.71, 37.93, 20.04.

2-((6-Chloropyridin-3-yl)methyl)-2-methylmalonic acid (89)

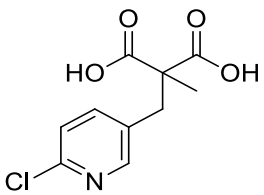

Chemical formula: $C_{10}H_{10}ClNO_4$
Mr: 243.64

According to a procedure developed by Zhu *et al.*[205] lithium hydroxide monohydrate (220 mg) in water (2 mL) was added to 2-[(6-chloropyridine-3-yl)methyl]-2-methyl

malonate (400 mg) in THF (3 mL) and the mixture was stirred overnight at RT. Mixture was poured into water (15 mL) and pH adjusted to <2 with HCl. Mixture extracted with diethyl ether, organic extracts combined, washed with water and dried over $MgSO_4$, filtered and solvent removed *in vacuo* to give the *title compound* (310.3 mg, 85%) as a white solid, mp. 82.7 – 84.0°C (Found (ESI^+): 244.0368 $C_{10}H_{10}ClNO_4$ [*MH*] requires 244.0371); ^1H NMR (500 MHz, DMSO-d_6) δ 13.00 (s, 2H), 8.18 (s, 1H), 7.64- 7.62 (m, 1H), 7.44 – 7.41 (m, 1H), 3.06 (s, 2H), 1.14 (s, 3H).); ^{13}C NMR (126 MHz, DMSO-d_6) δ 165.27, 142.45, 133.25, 124.14, 115.53, 110.50, 46.07, 29.09, 10.82; m/z (EI+): 245 (M•+, 19), 234 (56), 128 (40), 126 (100).

Chapter 3

Methyl 3-Aminobenzo[*b*]thiophene-2-carboxylate (107)

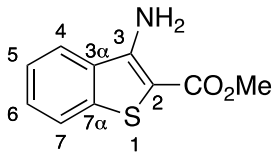

Chemical formula: $C_{10}H_9NO_2S$

Mr: 207.25

Method A

A solution of 2-fluorobenzonitrile (0.16 mL, 1.5 mmol), DMSO (0.75 mL), methyl thioglycolate (0.135 mL, 1.5 mmol) and triethylamine (0.63 mL, 4.5 mmol) was irradiated in a pressure-rated glass tube (10 mL) for 15 min at 130 °C using a CEM discover microwave synthesiser. The reaction mixture was cooled in a stream of compressed air then poured into ice water and stirred for 5 min. The solid was vacuum filtered, washed with water until the filtrate was colourless and dried in air to give the *title compound* (203 mg, 65%) as a purple solid.

Method B

A solution of 2-iodobenzonitrile (34.0 mg, 1.5 mmol), DMSO (0.75 mL), methyl thioglycolate (0.135 mL, 1.5 mmol) and triethylamine (0.63 mL, 4.5 mmol) was irradiated in a pressure-rated glass tube (10 mL) for 15 min at 130 °C using a CEM discover microwave synthesiser. The reaction mixture was cooled in a stream of compressed air then poured into ice water and stirred for 5 min. The solid was vacuum filtered, washed with water until the filtrate was colourless and dried in air to give the *title compound* (148 mg, 47%) as a purple solid.

Method C

A solution of 2-bromobenzonitrile (27.0 mg, 1.5 mmol), DMSO (0.75 mL), methyl thioglycolate (0.135 mL, 1.5 mmol) and triethylamine (0.63 mL, 4.5 mmol) was irradiated in a pressure-rated glass tube (10 mL) for 15 min at 130 °C using a CEM discover microwave synthesiser. The reaction mixture was cooled in a stream of compressed air then poured into ice water and stirred for 5 min. The solid was

vacuum filtered, washed with water until the filtrate was colourless and dried in air to give the *title compound* (72 mg, 23%) as a purple solid.

Analysis

mp 107.6–107.8 °C (MeOH–H_2O) (lit.[284] mp 110–111) (Found [ES^+]: 208.0434. $C_{10}H_{10}NO_2S$ [*MH*] requires 208.0432); IR (neat) ν_{max}/cm^{-1} 3434 (N-H), 3337 (N-H), 1659 (C=O), 1520, 1289 (C-O), 1257, 1127, 1064, 756, 738; ^1H NMR (500 MHz, DMSO-d_6) δ_H/ppm 8.13 (1H, d, *J* = 8.1 Hz, 4-CH), 7.82 (1H, d, *J* = 8.1 Hz, 7-CH), 7.50 (1H, m, 6-CH), 7.39 (1H, m, 5-CH), 7.15 (2H, bs, NH_2), 3.78 (3H, s, Me); ^{13}C NMR (101 MHz, DMSO-d_6) δ_C/ppm 164.8 (C=O), 149.8 (3-C), 138.8 (7α-C), 131.4 (3α-C), 128.5 (6-CH), 123.8 (5-CH), 123.1 (4-CH), 123.1 (7-CH), 94.4 (2-C), 51.2 (Me); *m/z* (EI) 207 ($M^{\bullet+}$, 93%), 176 (30), 175 (100), 147 (34), 146 (37).

Methyl 3-Aminothieno[2,3-*b*]pyridine-2-carboxylate (108)

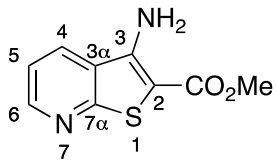

Chemical formula: $C_9H_8N_2O_2S$
Mr: 208.24

Method A

2-chloro-3-pyridinecarbonitrile (34.64 mg, 0.25 mmol), DMSO (1 mL), methyl thioglycolate (0.22 mL, 0.25 mmol) and triethylamine (0.10 mL, 0.75 mmol) was irradiated in a pressure-rated glass tube (10 mL) for 15 min at 130 °C using a CEM discover microwave synthesiser. The reaction mixture was cooled in a stream of compressed air then poured into ice water and stirred for 5 min. The solid was vacuum filtered, washed with water until the filtrate was colourless and dried in air to give the *title compound* (36 mg, 69%) as a yellow solid.

Method B

2-fluoro-3-pyridinecarbonitrile (30.5 mg, 0.25 mmol), DMSO (1 mL), methyl thioglycolate (0.22 mL, 0.25 mmol) and triethylamine (0.10 mL, 0.75 mmol) was

irradiated in a pressure-rated glass tube (10 mL) for 15 min at 130 °C using a CEM discover microwave synthesiser. The reaction mixture was cooled in a stream of compressed air then poured into ice water and stirred for 5 min. The solid was vacuum filtered, washed with water until the filtrate was colourless and dried in air to give the *title compound* (34 mg, 66%) as a yellow solid.

Method C

2-bromo-3-pyridinecarbonitrile (45.8 mg, 0.25 mmol), DMSO (1 mL), methyl thioglycolate (0.22 mL, 0.25 mmol) and triethylamine (0.10 mL, 0.75 mmol) was irradiated in a pressure-rated glass tube (10 mL) for 15 min at 130 °C using a CEM discover microwave synthesiser. The reaction mixture was cooled in a stream of compressed air then poured into ice water and stirred for 5 min. The solid was vacuum filtered, washed with water until the filtrate was colourless and dried in air to give the *title compound* (27 mg, 51%) as a yellow solid.

Analysis

mp 191 °C (dec.) (lit.[285] mp 194–196 °C) (Found [ES$^+$]: 209.0380. $C_9H_9N_2O_2S$ [*MH*] requires 209.0385); IR (neat) ν_{max}/cm^{-1} 3417 (N-H), 3314, 3202, 2943, 1679 (C=O), 1291 (C-O), 1127 (C-O), 755 (C-H), 738 (C-H), 712 (C-H); ^{1}H NMR (500 MHz, DMSO-*d*$_6$) δ_H/ppm 8.68 (1H, dd, *J* = 4.6, 1.6 Hz, 6-CH), 8.54 (1H, dd, *J* = 8.1, 1.6 Hz, 4-CH), 7.46 (1H, dd, *J* = 8.1, 4.6 Hz, 5-CH), 7.30 (2H, bs, NH_2), 3.80 (3H, s, Me); ^{13}C NMR (101 MHz, DMSO-*d*$_6$) δ_C/ppm 164.7 (C=O), 159.7 (7α-C), 150.7 (6-CH), 147.7 (3-C), 131.4 (4-CH), 125.5 (3α-C), 119.4 (5-CH), 93.2 (2-C), 51.4 (Me); *m/z* (EI) 208 ($M^{\bullet+}$, 100%), 177 (28), 176 (93), 148 (60).

Methyl 5-nitrobenzo[*b*]thiophene-2-carboxylate (105)

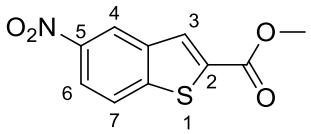

Chemical Formula: $C_{10}H_7NO_4S$

Mr: 237.23

A mixture of 2-chloro-5-nitrobenzaldehyde (1.50 g, 8.0 mmol), methyl thioglycolate (0.90 mL, 10 mmol) and K_2CO_3 (1.34 g, 9.6 mmol) in DMF (9.0 mL) was irradiated at 90 °C for 15 min in a pressure-rated glass vial (35 mL) using a CEM Discover microwave synthesizer. After cooling in a flow of compressed air, the mixture was poured into water and the solid filtered off under reduced pressure. Solid was washed with water and dried in air to give the *title compound* (1.5 g, 79%) as an off-white solid, mp 214.3-216.1 °C (lit[286] 211-212); ^{1}H NMR (500 MHz, $CDCl_3$) δH/ppm 8.79 (d, J = 2.2 Hz, 1H), 8.31 (dd, J = 8.9, 2.2 Hz, 1H), 8.19 (d, J = 0.9 Hz, 1H), 8.00 (dt, J = 8.9, 0.8 Hz, 1H), 3.99 (s, 3H); ^{13}C NMR (126 MHz, $CDCl_3$) δ 162.4, 147.5, 146.1, 138.5, 137.4, 130.8, 123.7, 121.3, 121.1, 53.1. (Me); m/z (EI+): 237 (M•+, 100), 206 (75), 160 (41).

5-Nitrobenzo[b]thiophene-2-carboxylic acid (106)

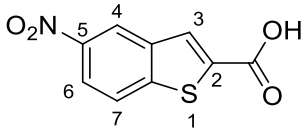

Chemical Formula: $C_9H_5NO_4S$
Mr: 223.21

A mixture of methyl 5-nitrobenzo[b]thiophene-2-carboxylate (1.0 g, 4.2 mmol), aqueous NaOH solution (1M; 12.5 mL) and MeOH (17.5 mL) was irradiated at 100 °C for 3 min in a pressure-rated glass vial (35 mL) using a CEM Discover microwave synthesizer. After cooling in a flow of compressed air, the reaction mixture was poured into water and acidified with 1M HCl. The solid was filtered under reduced pressure, washed with water and dried in air to give the *title compound* (889 g, 95%) as an off-white powder, mp 241.8 - 243.2 °C, (lit.[287] 239-241); ^{1}H NMR (500 MHz, Methanol-d4) δ 8.84 (d, J = 2.2 Hz, 1H), 8.26 (dd, J = 9.0, 2.3 Hz, 1H), 8.20 (s, 1H), 8.11 (d, J = 9.0 Hz, 1H); ^{13}C NMR (126 MHz, CD_3OD) δ 164.7, 148.8, 147.3, 140.1, 139.79, 131.9, 124.9, 122.2, 121.7, 49.5, 49.3, 49.2, 49.0, 48.8, 48.7, 48.5; m/z (EI+): 223 (M•+, 100), 177 (29), 89 (27).

3-Bromo-5-nitrobenzo[b]thiophene-2-carboxylic acid (109)

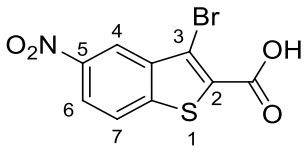

Chemical Formula: $C_9H_4BrNO_4S$
Mr: 302.10

According to a modified procedure,[225] to a mixture of 5-nitrobenzo[b]thiophene-2-carboxylic acid (500 mg, 2.25 mmol) and anhydrous NaOAc (565 mg, 6.5 mmol) in glacial AcOH (14 mL), bromine (0.7 mL, 13.5 mmol) was added dropwise under an inert atmosphere. The solution was refluxed at 55 °C for 27 h. The solution was allowed to cool to RT then poured into iced water and the solid isolated by vacuum filtration and dried in air to give the *title compound* (591 mg, 87%) as an off white solid, mp 308.4 – 310.5 °C (lit.[215] 307-309); ^{1}H NMR (500 MHz, Methanol-d4) δ 8.79 (d, J = 2.2 Hz, 1H), 8.36 (dd, J = 8.9, 2.2 Hz, 1H), 8.18 (d, J = 8.9 Hz, 1H).; m/z (EI+): 303 (MBr •$^+$, 100), 301 (M79Br •+, 94), 273 (18), 257 (30), 223 (26).

Methyl 3-bromo-5-nitrobenzo[b]thiophene-2-carboxylate (110)

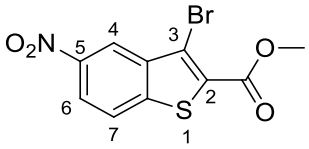

Chemical Formula: $C_{10}H_6BrNO_4S$
Mr: 316.13

From 3-bromo-5-nitrobenzo[b]thiophene-2-carboxylic acid
According to a modified procedure,[225,288] iodomethane (0.2 mL, 3.22 mmol) was added to a solution of 3-bromo-5-nitrobenzo[*b*]thiophene-2-carboxylic acid (500 mg, 1.66 mmol) and K_2CO_3 (575 mg, 4.15 mmol) in DMF (7.5 mL) and the solution stirred for 3 h at RT. The solution was quenched with NH_4Cl (sat.aq.), poured into

water and filtered under reduced pressure. Solid washed on filter paper with water and air dried to give the *title compound* (485 mg, 92%) as an off-white powder, mp 210.2-212.3 °C (lit.[215] 211-212); ^{1}H NMR (500 MHz, $CDCl_3$) δ 8.88 (d, J = 2.1 Hz, 1H), 8.37 (dd, J = 9.0, 2.1 Hz, 1H), 7.99 (d, J = 8.9 Hz, 1H), 4.01 (s, 3H).); ^{13}C NMR (126 MHz, $CDCl_3$) δ 161.1, 146.6, 144.8, 139.0, 131.1, 123.9, 122.3, 121.5, 115.8, 77.4, 77.4, 77.2, 76.9, 53.2; m/z (EI+): 317 (M81Br $\bullet^+$, 100), 286 (67), 284 (65).

(R)-Methyl 3-((2-((tert-butoxycarbonyl)amino)propyl)amino)-5-nitrobenzo[b]thiophene-2-carboxylate (112)

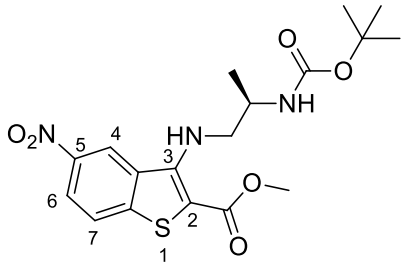

Chemical Formula: $C_{18}H_{23}N_3O_6S$
Mr: 409.46

According to a modified procedure,[226] under argon, *tert*-butyl([2R]-1-aminopropan-2-yl)carbamate (131 mg, 0.75 mmol) was added to a mixture of methyl 3-bromo-5-nitrobenzo[*b*]thiophene-2-carboxylate (200 mg, 0.6 mmol), Cs_2CO_3 (261 mg, 0.8 mmol), (±)-BINAP (37 mg, 0.06 mmol) and $Pd(OAc)_2$ (1.8 mg, 8.0 µmol) in dry toluene (4 mL). Mixture irradiated at 150 °C for 75 min in a pressure rated glass vial (10 mL) using a CEM Discover microwave synthesizer by moderating the initial power (200 W). After cooling in a flow of compressed air, the reaction mixture was diluted with water (20 mL) and extracted with ethyl acetate (3 x 30 mL). The organic extracts were combined, washed with brine, dried over Na_2SO_4, filtered and the solvent removed *in vacuo*. Purification by flash chromatography on SiO_2, gradient eluting with pet. Ether 40/60 to diethyl ether (50:50) to give the title compound (160 mg, 65%) as a red solid, mp 179.3-181.5 °C, (Found [ESI+]: 432.1207 $C_{18}H_{24}N_3O_6SNa$ [MNa] requires 432.1200); ^{1}H NMR (500 MHz, DMSO-d_6) δ 3.81 (s, 3H), 3.78 – 3.71 (m, 1H), 3.56 (dt, J = 13.7, 7.3 Hz, 1H), 1.31 (s, 9H), 1.11 (d, J = 6.6

Hz, 3H), 8.97 (d, J = 2.1 Hz, 1H), 8.30 (dd, J = 8.9, 2.0 Hz, 1H), 8.17 (d, J = 9.0 Hz, 1H), 7.58 (s, 1H), 6.91 (d, J = 8.1 Hz, 1H); ^{13}C NMR (126 MHz, DMSO-*d*$_6$) δ 163.7, 154.6, 150.2, 146.7, 144.4, 135.4, 124.8, 121.7, 120.6, 117.3, 87.8, 51.8, 50.6, 46.3, 40.1, 40.2, 28.1, 18.4.

(3R)-3-Methyl-9-nitro-1,2,3,4-tetrahydro-5H-[1]benzothieno[3,2-e][1,4]diazepin-5-one (115)

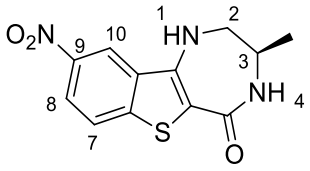

Chemical Formula: $C_{12}H_{11}N_3O_3S$
Mr: 277.30

According to a modified procedure,[239,289] a solution of (R)-methyl 3-((2-((tert-butoxycarbonyl)amino)propyl)amino)-5-nirtobenzo[*b*]thiophene-2-carboxylate (100 mg, 0.24 mmol) in TFA (10% v/v in DCM) (2 mL) stirred at RT until salt formation confirmed by TLC (Rf 0.3; MeOH-DCM [10:90]), then volatiles removed *in vacuo*. Residue dissolved in a solution of NaOMe (25 wt. % in MeOH; 0.3 mL, 1.5 mmol) in MeOH (2 mL) then heated to 50 °C for 2 h, then heated to reflux for 2 h. The mixture was allowed to cool to RT then cooled in an ice bath and neutralized by addition of HCl (1M) and stirred for 30 min at 0 °C. Solid isolated by vacuum filtration, washed on the filter paper with water and allowed to air dry to give the *title compound* (65 mg, 98%) as a red powder, mp 330.8-343.1 (dec.); ^{1}H NMR (500 MHz, DMSO-*d*$_6$) δ 9.04 (d, J = 2.2 Hz, 1H), 8.22 (dd, J = 8.8, 2.2 Hz, 1H), 8.05 (d, 1H), 8.00 (d, J = 4.6 Hz, 1H), 3.64 – 3.57 (m, 1H), 3.38 (d, J = 4.3 Hz, 2H), 1.16 (d, J = 6.7 Hz, 3H), ^{13}C NMR (126 MHz, DMSO-*d*$_6$) δ 164.2, 145.4, 144.3, 141.8, 132.9, 123.9, 120.9, 118.6, 108.6, 50.7, 47.6, 18.6; *m/z* (EI+): 277 (M, 100), 262 (M-CH3, 26), 234 (31), 206 (26).

(3R)-9-Amino-3-methyl-1,2,3,4-tetrahydro-5H-[1]benzothieno[3,2-e][1,4]diaepin-5-one (116)

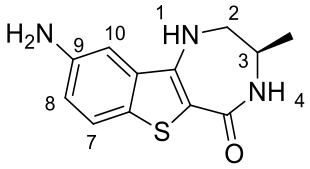

Chemical Formula: $C_{12}H_{13}N_3OS$
Mr: 247.32

According to a modified procedure,[240] in a pressure-rated glass vial (10 mL), DBU (0.1 mL, 0.7 mmol) was added to a solution of (3R)-3-mehtyl-9-nitro-1,2,3,4-tetrahydro-5H-[1]benzothieno[3,2-e][1,4]diazepin-5-one (60 mg, 0.22 mmol) and $Mo(CO)_6$ (58 mg, 0.22) in ethanol (3 mL). The mixture was irradiated at 150 °C for 30 min using a CEM Discover microwave synthesizer by moderating the initial power (300 W). After cooling in a flow of compressed air the volatiles were removed in vacuo. Purification by flash chromatography on SiO_2 gradient eluting with DCM to MeOH-DCM (10:90) to give the *title compound* (51 mg, 94%) as a brown solid, mp 150.8-161.1 °C (dec.) (Found [ESI+]: 248.0860. $C_{12}H_{14}N_3OS$ [MH] requires 248.0852); ^{1}H NMR (500 MHz, DMSO-d_6) δ 7.60 (d, J = 4.5 Hz, 1H), 7.37 (d, J = 8.5 Hz, 1H), 7.14 (t, J = 4.4 Hz, 1H), 6.98 (d, J = 2.1 Hz, 1H), 6.79 (dt, J = 8.5, 1.7 Hz, 1H), 5.04 (s, 2H), 3.53 (q, J = 6.1 Hz, 1H), 3.31 (d, J = 4.7 Hz, 2H), 1.13 (d, J = 6.7 Hz, 3H). ^{13}C NMR (126 MHz, DMSO-d_6) δ 164.8, 145.4, 141.2, 134.1, 126.7, 122.7, 117.1, 106.6, 104.9, 50.9, 47.7, 18.6.

tert-Butyl ([2R]-1-aminopropan-2-yl)carbamate (111)

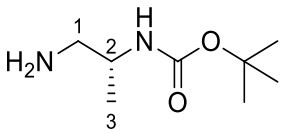

Chemical Formula: $C_8H_{18}N_2O_2$
Mr: 174.24

According to modified procedures,[290,291] at 0 °C EDCI.HCl (1.16 g, 6.0 mmol) was added to a solution of Boc-D-Ala-OH (1.0 g, 5.3 mmol) and HOBt.H_2O (0.8 g, 6.0 mmol) in CH_2Cl_2 (40 mL). The solution was allowed to warm to RT and stirred for 30 min then cooled back down to 0 °C for aqueous NH_3 solution (18.1 M; 1.2 mL) to be added drop-wise and stirred for 30 min whilst being allowed to warm to RT. Resulting solids were removed by filtration under reduced pressure and the filtrate was washed with water (2 x 20 mL) and brine (3 x 30 mL), dried over $MgSO_4$, filtered and evaporated *in vacuo*. Under Ar at 0 °C a solution of BH_3•SMe_2 in THF (2 M; 27 mL, 54 mmol) was added portion-wise to a solution of (R)-tert-butyl-(1-amino-1-oxopropan-2-yl)carbamate (1 g, 5.4 mmol) in dry THF (18 mL). The reaction mixture was stirred for 18 h once it had been allowed to warm to RT. The reaction mixture was concentrated *in vacuo* and the residue treated with MeOH (3 x 20 mL), stirring and concentrating to dryness *in vacuo*. Purification by SCX-2 ion exchange chromatography, gradient eluting with MeOH to 2 M NH_3 in MeOH, gave the title compound (0.75 g, 81%) as a colourless oil, (Rf 0.3; MeOH-CH2Cl2 [10:90]); (Found [ESI+]: 174.1598. $C_8H_{18}N_2O_2$ [MH] requires 174.1601); ^{1}H NMR (500 MHz, $CDCl_3$) δ 4.77 (d, J = 8.4 Hz, 1H), 3.64 – 3.55 (m, 1H), 2.69 (dd, J = 13.0, 4.9 Hz, 1H), 2.58 (dd, J = 13.0, 6.5 Hz, 1H), 1.39 (s, 9H), 1.07 (d, J = 6.7 Hz, 3H). ^{13}C NMR (126 MHz, $CDCl_3$) δ 155.9, 79.3, 77.4, 76.9, 48.7, 47.5, 28.5, 18.6; m/z (EI+): 174 (M•, 12), 173 (67), 86 (93), 58 (100).

6-Methylpyridine-3-carboxaldehyde (120)

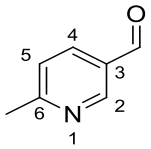

Chemical Formula: C_7H_7NO
Mr: 121.14

Under argon at -78 °C, DMSO (1 mL) in dry DCM (7 mL) was added dropwise over a period of 20 min to a solution of $COCl_2$ (3.5 mL, 7 mmol) in dry DCM (12 mL) and the mixture stirred for 20 min. Over a period of 20 min (6-Methylpyridin-3-yl)methanol

(400 mg, 3.25 mmol) in dry DCM (3 mL) was added dropwise to the mixture. Triethylamine (5 mL, 36 mmol) was added dropwise over a period of 10 min and the solution stirred while being allowed to warm to RT for 30 min. The solution was poured into water (30 mL), extracted with DCM (2 x 30 mL), the organic extracts combined, dried over Na_2SO_4, filtered and the solvent removed *in vacuo*. Purification by flash chromatography on SiO_2, gradient eluting from ethyl acetate/hexane (50:50) to ethyl acetate/hexane (70:30) to give the *title compound* (295 mg, 75%) as a brown oil, ^{1}H NMR (500 MHz, $CDCl_3$) δ 10.06 (s, 1H), 8.94 (d, J = 2.1 Hz, 1H), 8.06 (dd, J = 8.1, 2.1 Hz, 1H), 7.33 (d, J = 8.0 Hz, 1H), 2.66 (s, 3H); ^{13}C NMR (126 MHz, $CDCl_3$) δ 190.7 (CHO), 165.1, 152.2, 136.0, 129.4, 123.9, 25.2 (Me); m/z (EI+): 121 (M•+, 72), 120 (52), 92 (100). Data matches literature values.[292,293]

Chapter 6 – Bibliography

1 G. Melino, *Nature*, 2001, **412**, 23–23.

2 G. Kroemer, L. Galluzzi, P. Vandenabeele, J. Abrams, E. S. Alnemri, E. H. Baehrecke, M. V Blagosklonny, W. S. El-Deiry, P. Golstein, D. R. Green, M. Hengartner, R. A. Knight, S. Kumar, S. a Lipton, W. Malorni, G. Nuñez, M. E. Peter, J. Tschopp, J. Yuan, M. Piacentini, B. Zhivotovsky and G. Melino, *Cell Death Differ.*, 2009, **16**, 3–11.

3 C. B. Thompson, *Science*, 1995, **267**, 1456–1462.

4 S. Elmore, *Toxicol. Pathol.*, 2007, **35**, 495–516.

5 E. Ulukaya, C. Acilan and Y. Yilmaz, *Cell Biochem. Funct.*, 2011, **29**, 468–480.

6 J. F. Kerr, A. H. Wyllie and A. R. Currie, *Br. J. Cancer*, 1972, **26**, 239–57.

7 J. M. Adams and S. Cory, *Curr. Opin. Immunol.*, 2007, **19**, 488–496.

8 D. R. Green and J. C. Reed, *Science*, 1998, **281**, 1309–1312.

9 R. S. Hotchkiss, A. Strasser, J. E. McDunn and P. E. Swanson, *N. Engl. J. Med.*, 2009, **361**, 1570–1583.

10 D. S. Schwarz and M. D. Blower, *Cell. Mol. Life Sci.*, 2016, **73**, 79–94.

11 J. B. Oliveira and S. Gupta, *J. Clin. Immunol.*, 2008, **28**, 20–28.

12 S. W. Lowe, E. Cepero and G. Evan, *Nature*, 2004, **432**, 307–315.

13 G. Evan, *Science*, 1998, **281**, 1317–1322.

14 D. M. Ferriero, *N. Engl. J. Med.*, 2004, **351**, 1985–1995.

15 C. Ikonomidou, M. T. Price, V. Stefovska and F. Ho, *Science*, 2000, **287**, 1056–1060.

16 A. W. Loepke, G. K. Istaphanous, J. J. McAuliffe, L. Miles, E. A. Hughes, J. C. McCann, K. E. Harlow, C. D. Kurth, M. T. Williams, C. V. Vorhees and S. C. Danzer, *Anesth. Analg.*, 2009, **108**, 90–104.

17 C. Piot, P. Croisille and P. Staat, *N. Engl. J. Med.*, 2008, 473–481.

18 M. Aziz, A. Jacob and P. Wang, *Cell Death Dis.*, 2014, **5**, e1526.

19 D. J. Stearns-Kurosawa, M. F. Osuchowski, C. Valentine, S. Kurosawa and D. G. Remick, *Annu. Rev. Pathol. Mech. Dis.*, 2011, **6**, 19–48.

20 H. Bantel and K. Schulze-Osthoff, *Crit. Care*, 2009, **13**, 173.

21 T. van der Poll, F. L. van de Veerdonk, B. P. Scicluna and M. G. Netea, *Nat. Rev. Immunol.*, 2017, **17**, 407–420.

22 T. Inaba, T. Inukai, T. Yoshihara, H. Seyschab, R. A. Ashmun, C. E. Canman, S. J. Laken, M. B. Kastan and A. T. Look, *Lett. to Nat.*, 1996, **382**, 541–544.

23 H. L. Tang, K. L. Yuen, H. M. Tang and M. C. Fung, *Br. J. Cancer*, 2009, **100**, 118–122.

24 H. Lam, H. Man, K. Hou, S. Hu, S. Shan, K. Man, H. M. L. Tang, H. M. L. Tang, K. H. Mak, S. Hu, S. S. Wang, K. M. Wong, C. S. Wong, H. Y. Wu, H. T. Law, K. Liu, C. C. Talbot Jr., W. K. Lau, D. J. Montell and M. C. Fung, *Mol. Biol. Cell*, 2012, **23**, 2240–2252.

25 D. J. Klionsky, *Nat. Rev. Mol. Cell Biol.*, 2007, **8**, 931–937.

26 P. Jiang and N. Mizushima, *Cell Res.*, 2014, **24**, 69–79.

27 B. Levine, G. Kroemer and I. G. Roussy, *Cell*, 2008, **132**, 27–42.

28 L. Eckhart, S. Lippens, E. Tschachler and W. Declercq, *Biochim. Biophys. Acta - Mol. Cell Res.*, 2013, **1833**, 3471–3480.

29 M. Conrad, J. P. F. Angeli, P. Vandenabeele and B. R. Stockwell, *Nat. Rev. Drug Discov.*, 2016, **15**, 348–366.

30 L. Galluzzi, I. Vitale, J. M. Abrams, E. S. Alnemri, E. H. Baehrecke, M. V Blagosklonny, T. M. Dawson, V. L. Dawson, W. S. El-Deiry, S. Fulda, E. Gottlieb, D. R. Green, M. O. Hengartner, O. Kepp, R. A. Knight, S. Kumar, S. A. Lipton, X. Lu, F. Madeo, W. Malorni, P. Mehlen, G. Nuñez, M. E. Peter, M. Piacentini, D. C. Rubinsztein, Y. Shi, H.-U. Simon, P. Vandenabeele, E. White, J. Yuan, B. Zhivotovsky, G. Melino and G. Kroemer, *Cell Death Differ.*, 2012, **19**, 107–120.

31 L. Hayflick, *Exp. Cell Res.*, 1965, **37**, 614–636.

32 J. Campisi and F. d'Adda di Fagagna, *Nat. Rev. Mol. Cell Biol.*, 2007, **8**, 729–740.

33 A. J. Ruben and E. Biology, 2000, **1**, 72–76.

34 P. L. J. de Keizer, *Trends Mol. Med.*, 2017, **23**, 6–17.

35 M. P. Baar, R. M. C. Brandt, D. A. Putavet, J. D. D. Klein, K. W. J. Derks, B. R. M. Bourgeois, S. Stryeck, Y. Rijksen, H. van Willigenburg, D. A. Feijtel, I. van der Pluijm, J. Essers, W. A. van Cappellen, W. F. van IJcken, A. B. Houtsmuller, J. Pothof, R. W. F. de Bruin, T. Madl, J. H. J. Hoeijmakers, J. Campisi and P. L. J. de Keizer, *Cell*, 2017, **169**, 132–147.

36 G. Evan, *Science*, 1998, **281**, 1317–1322.

37 D. Hanahan and R. A. Weinberg, *Cell*, 2000, **100**, 57–70.

38 D. Hanahan and R. A. Weinberg, *Cell*, 2011, **144**, 646–674.

39 N. Cheng, A. Chytil, Y. Shyr, A. Joly and H. L. Moses, *Mol. Cancer Res.*, 2008, **6**, 1521–1533.

40 N. A. Bhowmick, E. G. Neilson and H. L. Moses, *Nature*, 2004, **432**, 332–337.

41 D. L. Burkhart and J. Sage, *Nat. Rev. Cancer*, 2008, **8**, 671–682.

42 A. Deshpande, P. Sicinski and P. W. Hinds, *Oncogene*, 2005, **24**, 2909–2915.

43 C. J. Sherr and F. McCormick, *Cancer Cell*, 2002, **2**, 103–112.

44 M. A. Blasco, *Nat Rev Genet*, 2005, **6**, 611–622.

45 J. W. Shay and W. E. Wright, *Nat. Rev. Mol. Cell Biol.*, 2000, **1**, 72–6.

46 D. Hanahan and J. Folkman, *Cell*, 1996, **86**, 353–364.

47 A. Wicki and G. Christofori, *Tumor Angiogenes. Basic Mech. Cancer Ther.*, 2008, **19**, 67–88.

48 G. Bergers and L. E. Benjamin, *Nat. Rev. Cancer*, 2003, **3**, 401–410.

49 G. Berx and F. van Roy, *Cold Spring Harb. Perspect. Biol.*, 2009, **1**, 1–27.

50 U. Cavallaro and G. Christofori, *Nat. Rev. Cancer*, 2004, **4**, 118–132.

51 J. E. Talmadge and I. J. Fidler, *Cancer Res.*, 2010, **70**, 5649–5669.

52 J. J. Li, *Laughing Gas, Viagra and Lipitor: the human stories behind the drugs we use*, Oxford University Press, 2006.

53 P. G. Corrie, *Medicine (Baltimore).*, 2007, **36**, 24–28.

54 B. W. Lash and P. B. Gilman, *Cancer Immunother. Immune Suppr. Tumor Growth Second Ed.*, 2013, **39**, 167–185.

55 K. Cheung-Ong, G. Giaever and C. Nislow, *Chem. Biol.*, 2013, **20**, 648–659.

56 N. Hosoya and K. Miyagawa, *Cancer Sci.*, 2014, **105**, 370–388.

57 M. J. Lind, *Syst. Ther.*, 2007, 19–23.

58 D. K. Armstrong, B. Bundy, L. Wenzel, H. Q. Huang, R. Baergen, S. Lele, L. J. Copeland, J. L. Walker, R. A. Burger and Gynecologic Oncology Group, *N. Engl. J. Med.*, 2006, **354**, 34–43.

59 T. A. Greenhalgh and R. P. Symonds, *Obstet. Gynaecol. Reprod. Med.*, 2014, **24**, 259–265.

60 K. A. Camphausen and L. R. Coia, Principles of Radiation Therapy, http://www.cancernetwork.com/articles/principles-radiation-therapy-1, (accessed 4 April 2017).

61 J. W. Snider and M. Mehta, *Handb. Clin. Neurol.*, 2016, **134**, 131–147.

62 C. M. Pfeffer and A. T. K. Singh, *Int. J. Mol. Sci.*, 2018, **19**, 448.

63 I. M. Ghobrial, T. E. Witzig and A. A. Adjei, *CA A Cancer J. Clin.*, 2005, **55**, 178–194.

64 E. A. Havell, W. Fiers and R. J. North, *J. Exp. Med.*, 1988, **167**, 1067–1085.

65 J. Ogasawara, R. Watanabe-Fukunaga, M. Adachi, A. Matsuzawa, T. Kasugai, Y. Kitamura, N. Itoh, T. Suda and S. Nagata, *Nature*, 1993, **364**, 806–809.

66 I. N. Lavrik, *Cell Death Dis.*, 2014, **5**, e1259.

67 D. De Miguel, J. Lemke, A. Anel, H. Walczak and L. Martinez-Lostao, *Cell Death Differ.*, 2016, **23**, 733–747.

68 S. Baig, I. Seevasant, J. Mohamad, A. Mukheem, H. Z. Huri and T. Kamarul, *Cell Death Dis.*, 2016, **7**, e2058.

69 H. N. LeBlanc and A. Ashkenazi, *Cell Death Differ.*, 2003, **10**, 66–75.

70 A. W. Tolcher, *Hematol. Oncol. Clin. North Am.*, 2002, **16**, 1255–1267.

71 C. G. Ferreira, M. Epping, F. A. E. Kruyt and G. Giaccone, *Clin. Cancer Res.*, 2002, **8**, 2024–2034.

72 A. El-Zawahry, J. McKillop and C. Voelkel-Johnson, *BMC Cancer*, 2005, **5**, 1–9.

73 O. Micheau, S. Shirley and F. Dufour, *Br. J. Pharmacol.*, 2013, **169**, 1723–1744.

74 R. S. Herbst, S. G. Eckhardt, R. Kurzrock, S. Ebbinghaus, P. J. O'Dwyer, M. S. Gordon, W. Novotny, M. A. Goldwasser, T. M. Tohnya, B. L. Lum, A. Ashkenazi, A. M. Jubb and D. S. Mendelson, *J. Clin. Oncol.*, 2010, **28**, 2839–2846.

75 J. C. Soria, E. Smit, D. Khayat, B. Besse, X. Yang, C. P. Hsu, D. Reese, J. Wiezorek and F. Blackhall, *J. Clin. Oncol.*, 2010, **28**, 1527–1533.

76 L. Y. Dimberg, C. K. Anderson, R. Camidge, K. Behbakht and H. L. Ford, 2015, **32**, 1341–1350.

77 L. Zhang and B. Fang, *Cancer Gene Ther.*, 2005, **12**, 228–237.

78 M. M. Lovric and C. J. Hawkins, *Oncogene*, 2010, **29**, 5048–5060.

79 A. Thorburn, K. Behbakht and H. Ford, *Drug Resist. Updat.*, 2008, **11**, 17–24.

80 M. Siegemund, N. Pollak, O. Seifert, K. Wahl, K. Hanak, A. Vogel, A. K. Nussler, D. Göttsch, S. Münkel, H. Bantel, R. E. Kontermann and K. Pfizenmaier, *Cell Death Dis.*, 2012, **3**, e295.

81 J. Milton Harris and R. B. Chess, *Nat. Rev. Drug Discov.*, 2003, **2**, 214–221.

82 V. M. Ukrainskaya, A. V Stepanov, I. S. Glagoleva, V. D. Knorre, A. A. J. Belogurov and A. G. Gabibov, *Acta Naturae*, 2017, **9**, 55–63.

83 F. A. Greco, P. Bonomi, J. Crawford, K. Kelly, Y. Oh, W. Halpern, L. Lo, G. Gallant and J. Klein, *Lung Cancer*, 2008, **61**, 82–90.

84 T. Doi, H. Murakami, A. Ohtsu, N. Fuse, T. Yoshino, N. Yamamoto, N. Boku, Y. Onozawa, C. P. Hsu, K. S. Gorski, G. Friberg, T. Kawaguchi and T. Sasaki, *Cancer Chemother. Pharmacol.*, 2011, **68**, 733–741.

85 A. Jin, T. Ozawa, K. Tajiri, Z. Lin, T. Obata, I. Ishida, H. Kishi and A. Muraguchi, *Eur. J. Immunol.*, 2010, **40**, 3591–3593.

86 NIH National Cancer Institute, CAR T Cells: Engineering Patients' Immune Cells to Treat Their Cancers, https://www.cancer.gov/about-cancer/treatment/research/car-t-cells, (accessed 21 April 2018).

87 E. Kobayashi, H. Kishi, T. Ozawa, H. Hamana, H. Nakagawa, A. Jin, Z. Lin and A. Muraguchi, *Biochem. Biophys. Res. Commun.*, 2014, **453**, 798–803.

88 J. L. Dine, C. C. O'Sullivan, D. Voeller, Y. E. Greer, K. J. Chavez, C. M. Conway, S. Sinclair, B. Stone, L. Amiri-Kordestani, A. S. Merchant, S. M. Hewitt, S. M. Steinberg, S. M. Swain and S. Lipkowitz, *Breast Cancer Res. Treat.*, 2016, **155**, 235–251.

89 H. Inoue and K. Tani, *Cell Death Differ.*, 2014, **21**, 39–49.

90 S. N. Willis and J. M. Adams, *Mol. Cell*, 2010, **17**, 617–625.

91 M. Giam, D. C. S. Huang and P. Bouillet, *Oncogene*, 2008, **27**, S128–S136.

92 V. Labi, M. Erlacher, S. Kiessling and A. Villunger, *Cell Death Differ.*, 2006, **13**, 1325–1338.

93 A. Letai, M. C. Bassik, L. D. Walensky, M. D. Sorcinelli, S. Weiler and S. J. Korsmeyer, *Cancer Cell*, 2002, **2**, 183–192.

94 S. N. Willis, L. Chen, G. Dewson, A. Wei, E. Naik, J. I. Fletcher, J. M. Adams and D. C. S. Huang, *Genes Dev.*, 2005, **19**, 1294–1305.

95 K. Papadopoulos, *Semin. Oncol.*, 2006, **33**, 449–456.

96 N. Dias and C. a Stein, *Mol. Cancer Ther.*, 2002, **1**, 347–355.

97 T. A. Bacon, F. Morvan, B. Rayner, J. L. Imbach and E. Wickstrom, *J. Biochem. Biophys. Methods*, 1988, **16**, 311–318.

98 S. Akhtar, R. Kole and R. L. Juliano, *Life Sci.*, 1991, **49**, 1793–1801.

99 E. Wickstrom, *J. Biochem. Biophys. Methods*, 1986, **13**, 97–102.

100 a P. Simões-Wüst, S. Hopkins-Donaldson, B. Sigrist, L. Belyanskaya, R. a Stahel and U. Zangemeister-Wittke, *Oligonucleotides*, 2004, **14**, 199–209.

101 T. Oltersdorf, S. W. Elmore, A. R. Shoemaker, R. C. Armstrong, D. J. Augeri, B. A. Belli, M. Bruncko, T. L. Deckwerth, J. Dinges, P. J. Hajduk, M. K. Joseph, S. Kitada, S. J. Korsmeyer, A. R. Kunzer, A. Letai, C. Li, M. J. Mitten, D. G. Nettesheim, S. C. Ng, P. M. Nimmer, J. M. O'Connor, A. Oleksijew, A. M. Petros, J. C. Reed, W. Shen, S. K. Tahir, C. B. Thompson, K. J. Tomaselli, B. Wang, M. D. Wendt, H. Zhang, S. W. Fesik and S. H. Rosenberg, *Nature*, 2005, **435**, 677–681.

102 R. S. Herbst, *Clin. Cancer Res.*, 2004, **10**, 4245S–4248S.

103 M. H. Kang and C. P. Reynolds, *Clin. Cancer Res.*, 2009, **15**, 1126–1132.

104 A. Kamal, S. Faazil and M. S. Malik, *Expert Opin. Ther. Patents*, 2014, **24**, 339–354.

105 C. M. Rudin, R. Salgia, X. Wang, L. D. Hodgson, G. A. Masters, M. Green and E. E. Vokes, *J. Clin. Oncol.*, 2008, **26**, 870–876.

106 A. Y. Bedikian, M. Millward, H. Pehamberger, R. Conry, M. Gore, U. Trefzer, A. C. Pavlick, R. DeConti, E. M. Hersh, P. Hersey, J. M. Kirkwood and F. G. Haluska, *J. Clin. Oncol.*, 2006, **24**, 4738–4745.

107 M. Certo, V. D. G. Moore, M. Nishino, G. Wei, S. Korsmeyer, S. A. Armstrong and A. Letai, *Cancer Cell*, 2006, **9**, 351–365.

108 E. Gavathiotis, M. Suzuki, M. L. Davis, K. Pitter, G. H. Bird, S. G. Katz, H. Tu, H. Kim, E. H.-Y. Cheng, N. Tjandra and L. D. Walensky, *Nature*, 2008, **455**, 1076–1081.

109 H. Kim, M. Rafiuddin-Shah, H. C. Tu, J. R. Jeffers, G. P. Zambetti, J. J. D. Hsieh and E. H. Y. Cheng, *Nat. Cell Biol.*, 2006, **8**, 1348–1358.

110 M. S. Lee, J. H. Ha, H. S. Yoon, C. K. Lee and S. W. Chi, *Biochem. Biophys. Res. Commun.*, 2014, **445**, 120–125.

111 L. M. Lindqvist, M. Heinlein, D. C. S. Huang and D. L. Vaux, *Proc. Natl. Acad. Sci.*, 2014, **111**, 8512–8517.

112 W. J. Fairbrother and A. Ashkenazi, *Cell*, 2014, **157**, 1506–1508.

113 T. Moldoveanu, A. V. Follis, R. W. Kriwacki and D. R. Green, *Trends Biochem. Sci.*, 2014, **39**, 101–111.

114 G. Polier, M. Giaisi, R. Köhler, W. W. Müller, C. Lutz, E. C. Buss, P. H. Krammer

and M. Li-Weber, *Int. J. Cancer*, 2015, **136**, 688–698.

115 T. T. Renault, R. Elkholi, A. Bharti and J. E. Chipuk, *J. Biol. Chem.*, 2014, **289**, 26481–26491.

116 C. A. Hassig, F. Zeng, P. Kung, M. Kiankarimi, S. Kim, P. W. Diaz, D. Zhai, K. Welsh, S. Morshedian, Y. Su, B. O'Keefe, D. J. Newman, Y. Rusman, H. Kaur, C. E. Salomon, S. G. Brown, B. Baire, A. R. Michel, T. R. Hoye, S. Francis, G. I. Georg, M. A. Walters, D. B. Divlianska, G. P. Roth, A. E. Wright and J. C. Reed, *J. Biomol. Screen.*, 2014, **19**, 1201–1211.

117 K. H. Khan, M. Blanco-Codesido and L. R. Molife, *Crit. Rev. Oncol. Hematol.*, 2014, **90**, 200–219.

118 Q. L. Deveraux, N. Roy, H. R. Stennicke, T. Van Arsdale, Q. Zhou, S. M. Srinivasula, E. S. Alnemri, G. S. Salvesen and J. C. Reed, *EMBO J.*, 1998, **17**, 2215–2223.

119 F. Bunz, P. M. Hwang, C. Torrance, T. Waldman, Y. Zhang, L. Dillehay, J. Williams, C. Lengauer, K. W. Kinzler and B. Vogelstein, *J. Clin. Invest.*, 1999, **104**, 263–269.

120 Y. M. Rustum, *Front. Biosci.*, 2004, **9**, 2467–2473.

121 R. M. Schultz, V. F. Patel, J. F. Worzalla and C. Shih, *Anticancer Res.*, **19**, 437–443.

122 R. Mannhold, S. Fulda and E. Carosati, *Drug Discov. Today*, 2010, **15**, 210–219.

123 B. Valeur and M. N. Berberan-Santos, *J. Chem. Educ.*, 2011, **88**, 731–738.

124 A. U. Acuña, F. Amat-Guerri, P. Morcillo, M. Liras and B. Rodríguez, *Org. Lett.*, 2009, **11**, 3020–3023.

125 J. R. Lakowicz, *Principles of Fluorescence Spectroscopy*, Springer US, Boston, MA, 2006, vol. 40.

126 M. Damianovich, I. Ziv, S. N. Heyman, S. Rosen, A. Shina, D. Kidron, T. Aloya, H. Grimberg, G. Levin, A. Reshef, A. Bentolila, A. Cohen and A. Shirvan, *Eur. J. Nucl. Med. Mol. Imaging*, 2006, **33**, 281–291.

127 C. M. M. Lahorte, C. van de Wiele, K. Bacher, B. van den Bossche, H. Thierens, S. van Belle, G. Slegers and R. a Dierckx, *Nucl. Med. Commun.*, 2003, **24**, 871–880.

128 I. Akushevich, J. Kravchenko, S. Ukraintseva, K. Arbeev, A. Kulminski and A. I.

Yashin, *Exp. Gerontol.*, 2013, **48**, 1395–1401.

129 M. K. Drews, Werner's Syndrome; A Genetic Disease that Mimics Premature Aging, http://www.pathology.washington.edu/research/werner/, (accessed 18 May 2015).

130 J. Regan, C. A. Pargellis, P. F. Cirillo, T. Gilmore, E. R. Hickey, G. W. Peet, A. Proto, A. Swinamer and N. Moss, *Bioorg. Med. Chem. Lett.*, 2003, **13**, 3101–3104.

131 J. Regan, S. Breitfelder, P. Cirillo, T. Gilmore, A. G. Graham, E. Hickey, B. Klaus, J. Madwed, M. Moriak, N. Moss, C. Pargellis, S. Pav, A. Proto, A. Swinamer, L. Tong and C. Torcellini, *J. Med. Chem.*, 2002, **45**, 2994–3008.

132 S. Schreiber, B. Feagan, G. D'Haens, J.-F. Colombel, K. Geboes, M. Yurcov, V. Isakov, O. Golovenko, C. N. Bernstein, D. Ludwig, T. Winter, U. Meier, C. Yong and J. Steffgen, *Clin. Gastroenterol. Hepatol.*, 2006, **4**, 325–334.

133 S. Iwano, Y. Asaoka, H. Akiyama, S. Takizawa, H. Nobumasa, H. Hashimoto and Y. Miyamoto, *J. Appl. Toxicol.*, 2011, **31**, 671–677.

134 O. J. Broom, B. Widjaya, J. Troelsen, J. Olsen and O. H. Nielsen, *Clin. Exp. Immunol.*, 2009, **158**, 272–280.

135 Y. J. Feng and Y. Y. Li, *J. Dig. Dis.*, 2011, **12**, 327–332.

136 A. D. Bachstetter and L. J. Van Eldik, *Aging Dis.*, 2010, **1**, 199–211.

137 Y. Kuma, G. Sabio, J. Bain, N. Shpiro, R. Márquez and A. Cuenda, *J. Biol. Chem.*, 2005, **280**, 19472–194729.

138 P. Gomez-Gutierrez, P. M. Campos, M. Vega and J. J. Perez, *PLoS One*, 2016, **11**, e0167379.

139 S. Schreiber, B. Feagan, G. D'Haens, J.-F. Colombel, K. Geboes, M. Yurcov, V. Isakov, O. Golovenko, C. N. Bernstein, D. Ludwig, T. Winter, U. Meier, C. Yong and J. Steffgen, *Clin. Gastroenterol. Hepatol.*, 2006, **4**, 325–334.

140 A. Shiryaev and U. Moens, *Cell. Signal.*, 2010, **22**, 1185–1192.

141 J. C. Lee, A. M. Badger, D. E. Griswold, D. Dunnington, A. Truneh, B. Votta, J. R. White, P. R. Young and P. E. Bender, *Ann. N. Y. Acad. Sci.*, 1993, **696**, 149–170.

142 R. Mourey and B. Burnette, *J. Pharmacol. Exp. Ther.*, 2010, **333**, 797–807.

143 N. Ronkina, A. Kotlyarov and M. Gaestel, *Front. Biosci.*, 2008, **13**, 5511–5521.

144 a Kotlyarov, a Neininger, C. Schubert, R. Eckert, C. Birchmeier, H. D. Volk and M. Gaestel, *Nat. Cell Biol.*, 1999, **1**, 94–97.

145 R. Winzen, M. Kracht, B. Ritter, A. Wilhelm, C. a Chen, A. Shyu, M. Mu, M. Gaestel, K. Resch and H. Holtmann, *EMBO J.*, 1999, **18**, 4969–4980.

146 J. C. Lee, J. T. Laydon, P. C. McDonnell, T. F. Gallagher, S. Kumar, D. Green, D. McNulty, M. J. Blumenthal, J. R. Heys, S. W. Landvatter, J. R. Keys, S. W. Land vatter, J. E. Strickler, M. M. McLaughlin, I. R. Siemens, S. M. Fisher, G. P. Livi, J. R. White, J. L. Adams and P. R. Young, *Nature*, 1994, **372**, 739–746.

147 M. C. Bagley, T. Davis, P. G. S. Murziani, C. S. Widdowson and D. Kipling, *Pharmaceuticals*, 2010, **3**, 1842–1872.

148 M. C. Genovese, *Arthritis Rheum.*, 2009, **60**, 317–320.

149 Kyriakis and Avruch, *Physiol. Rev.*, 2001, **81**, 807–869.

150 L. Xing, *MAP Kinase*, 2016, **4**, 24–30.

151 P. Norman, in *Investigational Drugs*, 2002, pp. 530–537.

152 C. Ding, *Investig. Drugs*, 2006, **7**, 1020–1025.

153 R. J. Hill, K. Dabbagh, D. Phippard, C. Li, R. T. Suttmann, M. Welch, E. Papp, K. W. Song, K. -c. Chang, D. Leaffer, Y.-N. Kim, R. T. Roberts, T. S. Zabka, D. Aud, J. D. Porto, A. M. Manning, S. L. Peng, D. M. Goldstein and B. R. Wong, *J. Pharmacol. Exp. Ther.*, 2008, **327**, 610–619.

154 S. B. Cohen, T.-T. Cheng, V. Chindalore, N. Damjanov, R. Burgos-Vargas, P. DeLora, K. Zimany, H. Travers and J. P. Caulfield, *Arthritis Rheum.*, 2009, **60**, 335–344.

155 M. Fiore, S. Forli and F. Manetti, *J. Med. Chem.*, 2016, **59**, 3609–3634.

156 P. Cohen, *Curr. Opin. Cell Biol.*, 2009, **21**, 317–324.

157 A. Schlapbach and C. Huppertz, *Future Med. Chem.*, 2009, **1**, 1243–1257.

158 M. Guma, D. Hammaker, K. Topolewski, M. Corr, D. L. Boyle, M. Karin and G. S. Firestein, *Arthritis Rheum.*, 2012, **64**, 2887–2895.

159 A. Kotlyarov, Y. Yannoni and S. Fritz, *Mol. Cell. Biol.*, 2002, **22**, 4827–4835.

160 D. R. Anderson, M. J. Meyers, W. F. Vernier, M. W. Mahoney, R. G. Kurumbail, N. Caspers, G. I. Poda, J. F. Schindler, D. B. Reitz and R. J. Mourey, *J. Med. Chem.*, 2007, **50**, 2647–2654.

161 A. L. Ray, E. F. Castillo, K. T. Morris, R. A. Nofchissey, L. L. Weston, V. G. Samedi, J. A. Hanson, M. Gaestel, I. V. Pinchuk and E. J. Beswick, *Int. J. Cancer*, 2016, **138**, 770–775.

162 D. R. Anderson, M. J. Meyers, R. G. Kurumbail, N. Caspers, G. I. Poda, S. a. Long,

B. S. Pierce, M. W. Mahoney and R. J. Mourey, *Bioorganic Med. Chem. Lett.*, 2009, **19**, 4878–4881.

163 D. R. Anderson, M. J. Meyers, R. G. Kurumbail, N. Caspers, G. I. Poda, S. a. Long, B. S. Pierce, M. W. Mahoney, R. J. Mourey and M. D. Parikh, *Bioorg. Med. Chem. Lett.*, 2009, **19**, 4882–4884.

164 T. Davis, M. C. Bagley, M. C. Dix, P. G. S. Murziani, M. J. Rokicki, C. S. Widdowson, J. M. Zayed, M. A. Bachler and D. Kipling, *Bioorganic Med. Chem. Lett.*, 2007, **17**, 6832–6835.

165 J. P. Wu, J. Wang, A. Abeywardane, D. Andersen, M. Emmanuel, E. Gautschi, D. R. Goldberg, M. A. Kashem, S. Lukas, W. Mao, L. Martin, T. Morwick, N. Moss, C. Pargellis, U. R. Patel, L. Patnaude, G. W. Peet, D. Skow, R. J. Snow, Y. Ward, B. Werneburg and A. White, *Bioorganic Med. Chem. Lett.*, 2007, **17**, 4664–4669.

166 J. S. Daniels, Y. Lai, S. South, P.-C. Chiang, D. Walker, B. Feng, R. Mireles, L. O. Whiteley, J. W. McKenzie, J. Stevens, R. Mourey, D. Anderson and J. W. Davis Ii, *Drug Metab. Lett.*, 2013, **7**, 15–22.

167 X. Ge, P. Lyu, Y. Gu, L. Li, J. Li, Y. Wang, L. Zhang, C. Fu and Z. Cao, *Biochem. Biophys. Res. Commun.*, 2015, **464**, 862–868.

168 X. Huang, G. W. Shipps, C. C. Cheng, P. Spacciapoli, X. Zhang, M. A. McCoy, D. F. Wyss, X. Yang, A. Achab, K. Soucy, D. K. Montavon, D. M. Murphy and C. E. Whitehurst, *ACS Med. Chem. Lett.*, 2011, **2**, 632–637.

169 X. Huang, X. Zhu, X. Chen, W. Zhou, D. Xiao, S. Degrado, R. Aslanian, J. Fossetta, D. Lundell, F. Tian, P. Trivedi and A. Palani, *Bioorganic Med. Chem. Lett.*, 2012, **22**, 65–70.

170 J. Qin, P. Dhondi, X. Huang, R. Aslanian, J. Fossetta, F. Tian, D. Lundell and A. Palani, *ACS Med. Chem. Lett.*, 2012, **3**, 100–105.

171 D. Xiao, A. Palani, X. Huang, M. Sofolarides, W. Zhou, X. Chen, R. Aslanian, Z. Guo, J. Fossetta, F. Tian, P. Trivedi, P. Spacciapoli, C. E. Whitehurst and D. Lundell, *Bioorganic Med. Chem. Lett.*, 2013, **23**, 3262–3266.

172 D. Xiao, X. Zhu, M. Sofolarides, S. Degrado, N. Shao, A. Rao, X. Chen, R. Aslanian, J. Fossetta, F. Tian, P. Trivedi, D. Lundell and A. Palani, *Bioorganic Med. Chem. Lett.*, 2014, **24**, 3609–3613.

173 A. U. Rao, D. Xiao, X. Huang, W. Zhou, J. Fossetta, D. Lundell, F. Tian, P.

Trivedi, R. Aslanian and A. Palani, *Bioorganic Med. Chem. Lett.*, 2012, **22**, 1068–1072.

174 M. C. Bagley, J. E. Dwyer, M. D. B. Molina, A. W. Rand, H. L. Rand and N. C. O. Tomkinson, *Org. Biomol. Chem.*, 2015, **13**, 6814–6824.

175 P. Lidström, J. Tierney, B. Wathey and J. Westman, *Tetrahedron*, 2001, **57**, 9225–9283.

176 F. Mavandadi and Å. Pilotti, *Drug Discov. Today*, 2006, **11**, 165–174.

177 S. Caddick and R. Fitzmaurice, *Tetrahedron*, 2009, **65**, 3325–3355.

178 T. Terai and T. Nagano, *Pflugers Arch. Eur. J. Physiol.*, 2013, **465**, 347–359.

179 J. F. William Herschel, *R. Soc. London*, 1845, **135**, 143–145.

180 G. G. Stokes, *Philos. Trans. R. Soc. London*, 1852, **142**, 463–562.

181 S. von Prowazek, *Kleinwelt*, 1914, 37–40.

182 A. Baeyer, *Ber Dtsch Chem Ges*, 1871, 555–558.

183 US Patent 377,349, 1888.

184 A. Cohen, A. Shirvan, G. Levin, H. Grimberg, A. Reshef and I. Ziv, *Cell Res.*, 2011, **21**, 1642–1642.

185 N. J. Yang and M. J. Hinner, *Methods Mol. Biol.*, 2015, **1266**, 29–53.

186 E. S. Schweikhard and C. M. Ziegler, *Amino acid secondary transporters: Toward a common transport mechanism*, Elsevier, 2012, vol. 70.

187 O. Mitsunobu and M. Yamada, *Bull. Chem. Soc. Jpn.*, 1967, **40**, 2380–2382.

188 S. Fletcher, *Org. Chem. Front.*, 2015, **2**, 739–752.

189 S. Manna, J. R. Falck and C. Mioskowski, *Synth. Commun.*, 1985, **15**, 663–668.

190 T. K. M. Shing, L. Li and K. Narkunan, *J. Org. Chem.*, 1997, **62**, 1617–1622.

191 A. Loudet and K. Burgess, *Chem. Rev.*, 2007, **107**, 4891–4932.

192 G. Ulrich, R. Ziessel and A. Harriman, *Angew. Chemie - Int. Ed.*, 2008, **47**, 1184–1201.

193 H. Lu, J. Mack, Y. Yang and Z. Shen, *Chem. Soc. Rev.*, 2014, **43**, 4778–4823.

194 Y. Ni and J. Wu, *Org. Biomol. Chem.*, 2014, **12**, 3774–3791.

195 K. Umezawa, D. Citterio and K. Suzuki, *Anal. Sci.*, 2014, **30**, 327–349.

196 L. Yuan, W. Lin, K. Zheng, L. He and W. Huang, *Chem. Soc. Rev.*, 2013, **42**, 622–661.

197 J. O. Escobedo, O. Rusin, S. Lim and R. M. Strongin, *Curr. Opin. Chem. Biol.*, 2010, **14**, 64–70.

198 K. E. Sapsford, L. Berti and I. L. Medintz, *Angew. Chemie - Int. Ed.*, 2006, **45**, 4562–4588.

199 A. P. Silva, H. Q. N. Gunaratne, T. Gunnlaugsson, A. J. M. Huxley, C. P. McCoy, J. T. Rademacher and T. E. Rice, *Chem. Rev.*, 1997, **97**, 1515–1566.

200 H. Sunahara, Y. Urano, H. Kojima and T. Nagano, *J. Am. Chem. Soc.*, 2007, **129**, 5597–5604.

201 H. Koutaka, J. Kosuge, N. Fukasaku, T. Hirano, K. Kikuchi, Y. Urano, H. Kojima and T. Nagano, *Chem. Pharm. Bull. (Tokyo).*, 2004, **52**, 700–703.

202 A. Treibs and F. ???H Kreuzer, *Justus Liebigs Ann. Chem.*, 1968, **718**, 208–223.

203 T. E. Wood and A. Thompson, *Chem. Rev.*, 2007, **107**, 1831–1861.

204 M. Zhang, E. Hao, Y. Xu, S. Zhang, H. Zhu, Q. Wang, C. Yu and L. Jiao, *RSC Adv.*, 2012, **2**, 11215.

205 United States Patent Application Publication, US 2005/0228027, 2005.

206 A. C. Bissember and M. G. Banwell, *J. Org. Chem.*, 2009, **74**, 4893–4895.

207 T. Handa, Y. Utena, H. Yajima, T. Ishii and H. Morita, *J. Phys. Chem.*, 1986, **90**, 2589–2596.

208 T. Davis, D. M. Baird, M. F. Haughton, C. J. Jones and D. Kipling, *J Gerontol A Biol Sci Med Sci*, 2005, **60**, 1386–1393.

209 T. Force, K. Kuida, M. Namchuk, K. Parang and J. M. Kyriakis, *Circulation*, 2004, **109**, 1196–1205.

210 D. M. Goldstein, A. Kuglstatter, Y. Lou and M. J. Soth, *J. Med. Chem.*, 2010, **53**, 2345–2353.

211 M. C. Bagley, M. Baashen, I. Chuckowree, J. E. Dwyer, D. Kipling and T. Davis, *Pharmaceuticals*, 2015, **8**, 257–276.

212 J. I. Trujillo, M. J. Meyers, D. R. Anderson, S. Hegde, M. W. Mahoney, W. F. Vernier, I. P. Buchler, K. K. Wu, S. Yang, S. J. Hartmann and D. B. Reitz, *Bioorganic Med. Chem. Lett.*, 2007, **17**, 4657–4663.

213 D. R. Goldberg, Y. Choi, D. Cogan, M. Corson, R. DeLeon, A. Gao, L. Gruenbaum, M. H. Hao, D. Joseph, M. A. Kashem, C. Miller, N. Moss, M. R. Netherton, C. P. Pargellis, J. Pelletier, R. Sellati, D. Skow, C. Torcellini, Y. C. Tseng, J. Wang, R. Wasti, B. Werneburg, J. P. Wu and Z. Xiong, *Bioorganic Med. Chem. Lett.*, 2008, **18**, 938–941.

214 J. E. Dwyer, University of Sussex, 2016.

215 M. Martin-Smith and S. T. Reid, *J. Chem. Soc.*, 1960, 938.

216 M. Martin-Smith and M. Gates, *J. Am. Chem. Soc.*, 1956, **5939**, 5351–5357.

217 M. Martin-Smith and M. Gates, *J. Am. Chem. Soc.*, 1956, **78**, 6177–6180.

218 J. F. Dit Chabert, L. Joucla, E. David and M. Lemaire, *Tetrahedron*, 2004, **60**, 3221–3230.

219 K. O. Hessian and B. L. Flynn, *Org. Lett.*, 2003, **5**, 4377–4380.

220 B. L. Flynn, P. Verdier-Pinard and E. Hamel, *Org. Lett.*, 2001, **3**, 651–653.

221 D. Yue and R. C. Larock, *J. Org. Chem.*, 2002, **67**, 1905–1909.

222 S. Kim, N. Dahal and T. Kesharwani, *Tetrahedron Lett.*, 2013, **54**, 4373–4376.

223 V. Guilarte, M. A. Fernández-Rodríguez, P. García-García, E. Hernando and R. Sanz, *Org. Lett.*, 2011, **13**, 5100–5103.

224 J. Clayden, N. Greeves and S. Warren, *Organic Chemistry*, Oxford University Press, 2nd edn., 2012.

225 J. M. Mbere, J. B. Bremner, B. W. Skelton and A. H. White, *Tetrahedron*, 2011, **67**, 6895–6900.

226 M. J. R. P. Queiroz, A. Begouin, I. C. F. R. Ferreira, G. Kirsch, R. C. Calhelha, S. Barbosa and L. M. Estevinho, *European J. Org. Chem.*, 2004, 3679–3685.

227 M. C. Bagley, R. T. Buck, S. L. Hind and C. J. Moody, *J. Chem. Soc. Perkin Trans. 1*, 1998, 591–600.

228 H. S. Chong, X. Sun, P. Dong and C. S. Kang, *European J. Org. Chem.*, 2011, 6641–6648.

229 J. Lindley, *Tetrahedron*, 1984, **40**, 1433–1456.

230 J. F. Bunnett, *Acc. Chem. Res.*, 1978, **11**, 413–420.

231 M. Kosugi, M. Kameyama and T. Migita, *Chem. Lett.*, 1983, 927–928.

232 L. Dale Boger and J. S. Panek, *Tetrahedron Lett.*, 1984, **25**, 3175–3178.

233 F. Paul, J. Patt and J. F. Hartwig, *J. Am. Chem. Soc.*, 1994, **116**, 5969–5970.

234 M. S. Driver and J. F. Hartwig, *J. Am. Chem. Soc.*, 1995, **117**, 4708–4709.

235 A. S. Guram and S. L. Buchwald, *J. Am. Chem. Soc.*, 1994, **116**, 7901–7902.

236 A. S. Guram, R. A. Rennels and S. L. Buchwald, *Angew. Chemie Int. Ed. English*, 1995, **34**, 1348–1350.

237 J. Louie and J. F. Hartwig, *Tetrahedron Lett.*, 1995, **36**, 3609–3612.

238 J. F. Hartwig, *Nature*, 2008, **455**, 314–322.

239 S. S. Khatana, D. H. Boschelli, J. B. Kramer, D. T. Connor, H. Barth and P. Stoss,

J. Org. Chem., 1996, **61**, 6060–6062.

240 J. Spencer, N. Anjum, H. Patel, R. P. Rathnam and J. Verma, *Synlett*, 2007, 2557–2558.

241 J. Spencer, R. P. Rathnam, H. Patel and N. Anjum, *Tetrahedron*, 2008, **64**, 10195–10200.

242 S. Iyer and G. M. Kulkarni, *Synth. Commun.*, 2004, **34**, 721–725.

243 J. Wannberg and M. Larhed, *J. Org. Chem.*, 2003, **68**, 5750–5753.

244 X. Li, Z. Mao, Y. Wang, W. Chen and X. Lin, *Tetrahedron*, 2011, **67**, 3858–3862.

245 X. S. Wang, Q. Li, J. R. Wu, Y. L. Li, C. S. Yao and S. J. Tu, *Synthesis (Stuttg).*, 2008, 1902–1910.

246 X.-S. Wang, Q. Li, C.-S. Yao and S.-J. Tu, *European J. Org. Chem.*, 2008, **2008**, 3513–3518.

247 X. S. Wang, Q. Li, J. R. Wu and S. J. Tu, *J. Comb. Chem.*, 2009, **11**, 433–437.

248 X. S. Wang, J. Zhou, M. Y. Yin, K. Yang and S. J. Tu, *J. Comb. Chem.*, 2010, **12**, 266–269.

249 O. Doebner, *Justus Liebig's Ann. der Chemie*, 1887, **242**, 265–289.

250 J. J. Li and E. J. Corey, *Name Reactions in Heterocyclic Chemistry*, John Wiley & Sons, Inc., Hoboken, NJ, USA, 2005.

251 Q. Li, C. Yao, M. Zhang, S. Tu and X. Wang, *J. Heterocycl. Chem.*, 2008, **45**, 1027–1031.

252 K. Griffiths, P. Kumar, G. R. Akien, N. F. Chilton, A. Abdul-Sada, G. J. Tizzard, S. J. Coles and G. E. Kostakis, *Chem. Commun.*, 2016, **52**, 7866–7869.

253 P. Kumar, K. Griffiths, S. Lymperopoulou and G. E. Kostakis, *RSC Adv.*, 2016, **6**, 79180–79184.

254 P. Kumar, S. Lymperopoulou, K. Griffiths, S. Sampani and G. Kostakis, *Catalysts*, 2016, **6**, 140.

255 K. Griffiths, C. W. D. Gallop, A. Abdul-Sada, A. Vargas, O. Navarro and G. E. Kostakis, *Chem. - A Eur. J.*, 2015, **21**, 6358–6361.

256 F. Evangelisti, R. Moré, F. Hodel, S. Luber and G. R. Patzke, *J. Am. Chem. Soc.*, 2015, **137**, 11076–11084.

257 K. Liu, W. Shi and P. Cheng, *Coord. Chem. Rev.*, 2015, **289–290**, 74–122.

258 G. K. Veits and J. Read De Alaniz, *Tetrahedron*, 2012, **68**, 2015–2026.

259 Y. Hui, L. Lin, X. Liu and X. Feng, in *Zinc Catalysis*, Wiley-VCH Verlag GmbH & Co. KGaA, 2015, pp. 57–82.

260 K. Griffiths, P. Kumar, J. D. Mattock, A. Abdul-Sada, M. B. Pitak, S. J. Coles, O. Navarro, A. Vargas and G. E. Kostakis, *Inorg. Chem.*, 2016, **55**, 6988–6994.

261 D. Chen, L. Yu and P. G. Wang, *Tetrahedron Lett.*, 1996, **37**, 4467–4470.

262 Y. H. Hui, Y. C. Chen, H. W. Gong and Z. F. Xie, *Chinese Chem. Lett.*, 2014, **25**, 163–165.

263 C. Karami, H. Ahmadian, M. Nouri, F. Jamshidi, H. Mohammadi, K. Ghodrati, A. Farrokhi and Z. Hamidi, *Catal. Commun.*, 2012, **27**, 92–96.

264 S. Khaksar, M. Tajbakhsh and M. Gholami, *Comptes Rendus Chim.*, 2014, **17**, 30–34.

265 M. A. Zolfigol, P. Salehi, M. Shiri and Z. Tanbakouchian, *Catal. Commun.*, 2007, **8**, 173–178.

266 J. Beltrá, M. C. Gimeno and R. P. Herrera, *Beilstein J. Org. Chem.*, 2014, **10**, 2206–2214.

267 M. Inman and C. J. Moody, *Chem. Sci.*, 2013, **4**, 29–41.

268 T. V. Sravanthi and S. L. Manju, *Eur. J. Pharm. Sci.*, 2016, **91**, 1–10.

269 N. A. Petasis and I. Akritopoulou, *Tetrahedron Lett.*, 1993, **34**, 583–586.

270 N. R. Candeias, F. Montalbano, P. M. S. D. Cal and P. M. P. Gois, *Chem. Rev.*, 2010, **110**, 6169–6193.

271 B. H. Rotstein, S. Zaretsky, V. Rai and A. K. Yudin, *Chem. Rev.*, 2014, **114**, 8323–8359.

272 R. Kakuchi, *Angew. Chemie - Int. Ed.*, 2014, **53**, 46–48.

273 M. Shiri, *Chem. Rev.*, 2012, **112**, 3508–3549.

274 A. Domling, W. Wang and K. Wang, *Chem. Rev.*, 2012, **112**, 3083–3135.

275 E. Ruijter, R. Scheffelaar and R. V. A. Orru, *Angew. Chemie - Int. Ed.*, 2011, **50**, 6234–6246.

276 N. Isambert, M. del M. S. Duque, J.-C. Plaquevent, Y. Génisson, J. Rodriguez and T. Constantieux, *Chem. Soc. Rev.*, 2011, **40**, 1347–1357.

277 C. Kalinski, M. Umkehrer, L. Weber, J. Kolb, C. Burdack and G. Ross, *Mol. Divers.*, 2010, **14**, 513–522.

278 M. Varyani, P. K. Khatri and S. L. Jain, *Catal. Commun.*, 2016, **77**, 113–117.

279 T. Flagstad, M. T. Petersen and T. E. Nielsen, *Angew. Chemie - Int. Ed.*, 2015,

54, 8395–8397.

280 S. Roy and O. Reiser, *Angew. Chemie - Int. Ed.*, 2012, **51**, 4722–4725.

281 I. Ibrahem, P. Breistein and A. Córdova, *Chem. - A Eur. J.*, 2012, **18**, 5175–5179.

282 H. Fujiwara and K. Kitagawa, *Heterocycles*, 2000, **53**, 409.

283 J. Park, W.-J. J. Song and K. C. Chung, *Cell. Mol. Life Sci.*, 2009, **66**, 3235–3240.

284 R. Beck, *J. Org. Chem.*, 1972, **37**, 3224–3226.

285 R. Romagnoli, P. G. Baraldi, M. Kimatrai Salvador, D. Preti, M. Aghazadeh Tabrizi, M. Bassetto, A. Brancale, E. Hamel, I. Castagliuolo, R. Bortolozzi, G. Basso and G. Viola, *J. Med. Chem.*, 2013, **56**, 2606–2618.

286 V. G. Matassa, F. J. Brown, P. R. Bernstein, H. S. Shapiro, T. P. Maduskuie, L. A. Cronk, E. P. Vacek, Y. K. Yee and D. W. Snyder, *J. Med. Chem.*, 1990, **33**, 2621–2629.

287 L. Fieser and R. Kennelly, *J. Am. Chem. Soc.*, 1935, **57**, 1611–1616.

288 World Intellectual Property Organization, WO 2006125324 A1, 2006.

289 World Intellectual Property Organization, WO 2005/018568 A2, 2005.

290 W. Wu, Z. Li, G. Zhou and S. Jiang, *Tetrahedron Lett.*, 2011, **52**, 2488–2491.

291 A. L. Marquart, B. L. Podlogar, E. W. Huber, D. A. Demeter, N. P. Peet, H. J. R. Weintraub and M. R. Angelastro, *J. Org. Chem.*, 1994, **59**, 2092–2100.

292 WO 2008040934 A1, 2008, 28.

293 E. P. Kyba, S. T. Liu, K. Chockalingam and B. R. Reddy, *J. Org. Chem.*, 1988, **53**, 3513–3521.

Appendix

Neuron cultures (plated on an astrocyte feeder layer)

Note the following:

- All solution volumes are enough for 24 wells of cells plated in 24 well plates (8 wells each in 3 plates – see step I)
- Astrocytes will be required as a feeder layer for neurons. Therefore, on the initial dissection plate astrocytes only. It will take approx. 14 days for a T25 to become confluent. Once astrocytes are plated on coverslips (step II), neurons can be prepared
- Pregnant rats are delivered fortnightly on a Tuesday, along with a litter of P1 pups. The pregnant rat will deliver her pups the following Monday, normally around midday. Thus, dissections can only be carried out on a Monday, Tuesday, or at the latest early Weds (for rats delivered on Tuesday only). Bear this in mind when planning out the procedure
- Make up fresh media every week and HBSS on the day of dissection.

Media/Reagents required (prepare just before use)

Stock concentrations given in brackets

20 µg/ml Poly-D-lysine (Sigma/cat no.)

- 125 µl PDL (4 mg/ml – dissolved in sterile water and stored at -20 C in 5ml tubes)
- 24 ml sterile water

	Astrocyte media	**Hippocampal (neuron) media**
BME (1X)	43 ml	45.5 ml
Glucose (45 %)	440 µl	440 µl
FCS	5 ml	1 ml
Na-pyruvate (100 mM)	500 µl	500 µl
HEPES (1 M, pH 7.35)	500 µl	500 µl
Pen/Strep (100X)	500 µl	500 µl

B27 (50X)	-	1 ml
Glutamax (100X)	-	500 µl

Hanks Balanced salt solution (HBSS) (for dissection)

- 1.5 ml HBSS (containing calcium and magnesium) (10X)
- 150 µl HEPES (1 M, pH 7.35)
- 13.5 ml H2O

HEPES buffer solution (100X/1 M)

- Make up from powder and pH to 7.3 with NaOH

Ara-C (Company/cat. No.)

- 13 µl Ara-C (stock conc.5mM)
- 7.5 ml hippocampal media (from above)

Procedure

I. Preparation of PDL coated plates (day 0 - Wed)

1. Add around 0.5 ml sterile water to the outer 16 wells in a sterile 24 well plate (helps prevent evaporation of media)
2. Sterilise coverslips in IMS, take out and allow to dry then place in the middle 8 wells using sterilised tweezers
3. Add 1 ml PDL to each of the 8 wells. Make sure no coverslips are floating, if they are gently push down with tweezers
4. Incubate overnight at 37C (if you forget, you can incubate for around 4h before plating astrocytes)

II. Plating astrocytes on PDL coated coverslips (day 1 - Thurs)

1. Aspirate PDL from coverslip. Add ~1 ml sterile water to wash and aspirate. Allow to dry while preparing astrocytes
2. Astrocytes should be confluent in a T25. Wash with sterile 1x PBS

3. Trypsinise with 1 ml trypsin (the entire aliquot) and leave at RT until detached. Check the cells are shrunken on the microscope and gently return to hood. Aspirate residual trypsin then add 2 ml of astrocyte media, bash flask, check cells are dislodged and transfer to 15ml tube. Triturate (~30times)
4. Add 200-300 ul cell suspension (perhaps even less ~150 if you want to have just astro islands, which is better for imaging) to 17.3-17.2 ml astrocyte media (17.5 ml needed). Add 0.7 ml of diluted cell suspension to each well.
5. Label plates with todays date and the date on the flask that contained the astrocytes. Ensure no coverslips are floating. Return the remaining cell suspension to T25 and add 5-6ml of astro media. Label the flask with the date when it was used.

III. Dissection (day 6 - Tues)

Bench preparation

1. Turn on the water bath to 37C (always on in our lab) and warm hippocampal and astrocyte media
2. Bring plenty of ice in ice bucket and keep the following on ice: Petri dish, sterile Pasteur pipette, 15 ml sterile polypropylene tube with ice cold HBSS and dissection kit
3. Clean the work bench and dissecting microscope thoroughly with Dettol
4. Take out all the instruments from sterile container, wipe with Dettol and let them air dry completely before use
5. Add most but not all (leave around 2 ml) ice cold and sterile dissection medium (HBSS) in petri dish and leave on ice

Protocol

1. Keep animal covered during transport from room 4.04 to prep room (4.34)
2. Kill the P0-P1 rats by cervical dislocation using a blunt instrument and remove the head
3. Dissect the skull cap with forceps and scissors cutting above the ear towards the nose through the eye on both sides. Holding down the nose, gently peel

back the skull. Remove the brain at the olfactory bulb and ensure it is detached all the way round before gently scooping out with a spatula and place in the petri dish containing ice cold HBSS. Keep petri dish on ice. The tissue must be always kept submerged in the dissection medium. (Alternatively, to open up the skull, cut the skin with the scalpel through the middle. Cut the skull through the middle and make diagonal cuts with the curved scissors more or less at the level of olfactory bulbs. Remove two halves of the skull will the forceps.)

4. Cut the brain in half and move to the microscope. Dissect out the hippocampus by firstly making a horizontal cut along the bottom, then up along the curved edge and finally rolling out the hippocampus. Ensure most of the cortex and all meninges and patches of blood vessels are removed (BE TIMELY). Once clean, using the Pasteur pipette move the hippocampus to the 15 ml tube containing the remaining HBSS and keep on ice. Repeat for other side of the brain.
5. Clean work area and tools thoroughly
6. In the hood, gently remove HBSS with a sterile transfer pipet, leaving hippocampi at the bottom of the tube
7. Gently add 2 ml hippocampal medium. Remove and repeat x3 to wash. On the 4th addition, leave the media in the tube. Transfer the contents of this tube to a fresh tube to ensure no traces of HBSS remain
8. Dissociate the cortices thoroughly by gently triturating up and down with a 1 ml pipette until no lumps remain. Avoid making any bubbles
9. Count the total number of cells: Put 10 µl of cell suspension in an eppendorf. In another eppendorf add 2.5 ul trypan blue to 7.5 ul media then add this 10 ul to the 10 ul of cells, mix them well, leave for 30 seconds to ensure deads cells pick up the trypan and load 10 ul onto a Neubauer chamber slide. Count number of live (white) cells in each corner square (each comprised of 16 smaller squares).
10. Work out the average number per corner square and calculate total number of cells per ml using the formula (avg. no. cells in one corner square x 2 (dilution factor) x 10,000 (volume conversion factor)).

11. Work out how much cell suspension to add per well in the 24 well plate if plating 40,000 cells/well in a total volume of 0.7 ml made up with hippocampal media.

For example, if plating 25 wells (8 wells in 3 plates + 1 extra) will need a total of 1,000,000 cells. If you have e.g. 700,000 cells/ml then you need 1.43 ml of cell suspension and 16.07 ml of hippocampal media (0.7 x 25 = 17.5 ml less 1.43 = 16.07 ml).

Remove the media already on the cells (the astro media) Add 0.7 ml of this diluted cell suspension to each well onto the astrocyte feeder layer. The no. of cells plated may change depending on application and density required. Plate the remaining cells in a T25 in astrocyte media (400-500 ul per flask + 6 ml media)

IV. Ara-C (day 8 - Thurs)

1. Remove 200 µl media and replace with 300 µl hippocampal media containing ara-c to curb glial cell proliferation

Neurons will mature in 12-14 days from plating. Check your cells after about a week. They will still be quite young, but you should clearly see established neuronal networks. Monitor the colour of the media, do partial exchange (200-300ul) if media appears quite yellowish.

26 April 2016 ML10 experiment

Cells: Neurons from the hippocampus of a 1-day old rat, cultured in media on a layer of astrocytes.

Treated with staurosporine (1 uM or 0.5 uM) for 5 hours to induce apoptosis – lower concentration was intended to slow down the process to capture early events.

Final concentration of ML10 = 50 uM
Incubation time = 30 min

Positive control was Kinetic Apoptosis kit from Abcam – marks apoptotic cells, similar to Annexin (green)

Green brightness setting in FIJI 10/200, ML10 10/100
Two examples of each are shown
10x dry objective

Organic & Biomolecular Chemistry

PAPER

View Article Online
View Journal | View Issue

Cite this: *Org. Biomol. Chem.*, 2015, **13**, 6814

Microwave-assisted synthesis of 3-aminobenzo[*b*]-thiophene scaffolds for the preparation of kinase inhibitors†

Mark C. Bagley,*[a] Jessica E. Dwyer,[a] Maria D. Beltran Molina,[b] Alexander W. Rand,[a] Hayley L. Rand[a] and Nicholas C. O. Tomkinson[b]

Received 23rd April 2015,
Accepted 11th May 2015

DOI: 10.1039/c5ob00819k

www.rsc.org/obc

Microwave irradiation of 2-halobenzonitriles and methyl thioglycolate in the presence of triethylamine in DMSO at 130 °C provides rapid access to 3-aminobenzo[*b*]thiophenes in 58–96% yield. This transformation has been applied in the synthesis of the thieno[2,3-*b*]pyridine core motif of LIMK1 inhibitors, the benzo[4,5]thieno[3,2-e][1,4]diazepin-5(2*H*)-one scaffold of MK2 inhibitors and a benzo[4,5]thieno[3,2-*d*]-pyrimidin-4-one inhibitor of the PIM kinases.

Introduction

Benzothiophenes are naturally-occurring heterocycles, found in petroleum deposits in their simplest form but also discovered recently as a motif in more complex glycosides isolated from the roots of *E. grijissii*.[1] Benzothiophenes are important components of organic semiconductors due to their potential for elongated and highly delocalised electronic structures.[2,3] Substituted benzothiophenes have also found application in drug discovery as highly-privileged structures and valuable building blocks in medicinal chemistry, being incorporated into tubulin polymerisation inhibitors,[4,5] acetyl-CoA carboxylase inhibitors,[6] antidepressants,[7] and as estrogen receptor modulators.[8,9] Benzothiophenes are present in a number of clinical agents, including Raloxifene,[10] a selective estrogen receptor modulator, Zileuton,[11] an inhibitor of 5-lipoxygenase and leukotriene biosynthesis used for the treatment of asthma, and the antifungal agent Sertaconazole, which inhibits the synthesis of ergosterol.[12]

Scaffolds based upon 2- or 3-aminobenzo[*b*]thiophenes have enormous potential for further derivatization and have shown great promise in fragment-based drug discovery and in hit identification or lead development, including approaches towards antimitotic agents[5,13] and in the development of inhibitors of kinase targets, such as the LIMK protein family,[14] PIM-kinases[15] and MAPK-2 kinase (MK2) (Fig. 1).[16,17] A number of 3-aminothieno[2,3-*b*]pyridine-2-carboxamide hits, such as **1**, were identified from high throughput screening (HTS) as inhibitors of LIMK1, leading to the development of tricyclic derivatives such as **2a** and the benzothieno[3,2-*d*]pyri-

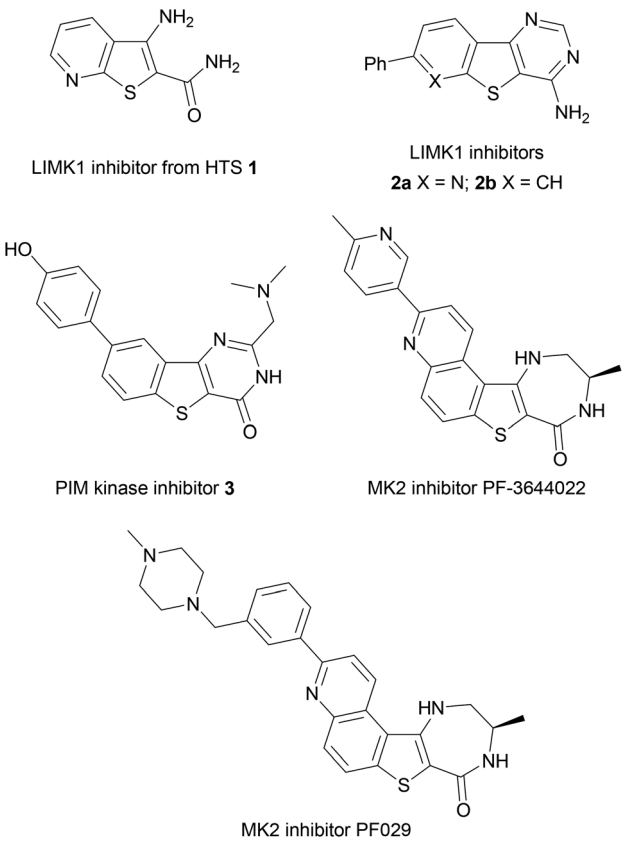

Fig. 1 Aminobenzothiophene scaffolds in drug discovery.

[a]Department of Chemistry, School of Life Sciences, University of Sussex, Falmer, Brighton, East Sussex, BN1 9QJ, UK. E-mail: m.c.bagley@sussex.ac.uk
[b]WestCHEM, Department of Pure and Applied Chemistry, University of Strathclyde, Glasgow, G1 1XL, UK

†Electronic supplementary information (ESI) available. See DOI: 10.1039/c5ob00819k

midine **2b** as a LIMK1 inhibitor lead candidate, to disrupt actin polymerisation and thus prevent the metastatic potential of tumour cells where LIMK is over-expressed.[14]

Benzothienopyrimidinones have been investigated as PIM kinase inhibitors.[15] The PIM kinases (PIM1, PIM2 and PIM3) have been implicated in tumourigenesis and simultaneous targeting of all three isoforms has presented itself as a promising approach in cancer therapy, with PIM triple knockout mice found to be viable and fertile.[18] The benzothiophene scaffold was again identified from an initial HTS hit,[15] leading to the development of a range of potent and selective benzo[*b*]thiophene-derived inhibitors such as **3** with nM activity (K_i values of 2, 3 and 0.5 nM against PIM1, PIM2 and PIM3, respectively) with oral bioavailability in mouse models.

Examples of aminobenzothiophene derivatives are also found amongst inhibitors of the mitogen activated protein kinase (MAPK) family of enzymes. These enzymes are essential for inflammatory cell signalling events and contain historically popular drug targets for inflammatory diseases, including rheumatoid arthritis and Crohn's disease because of their involvement in the production of pro-inflammatory cytokines,[19] as well as being implicated in accelerated cellular ageing in Werner syndrome (WS) *via* p38.[20–23] MAPK-activated protein kinase (MK2) is a rate-limiting kinase downstream of p38 in the MAPK pathway and has been the subject of many studies in recent years,[24] as MK2 knock-out mice possess normal healthy phenotypes whereas p38 knock-out mice are lethal.[25] The aminobenzo[*b*]thiophene derivative PF-3644022 shows excellent kinase selectivity for MK2, *in vivo* potency on a nanomolar scale and projected ADME characteristics that suggested it was suitable for oral human dosing.[17,26,27] However, PF-3644022 was found to result in hepatotoxicity in dogs[27] and so the analogue PF029 was developed and exhibited an improved toxicological profile with no loss of cellular potency. This was rationalized through installation of a metabolic shunt onto the reactive diazepinone ring and extension of the biaryl ring section to increase the compound's cationic character, thus reducing its molecular affinity for transporter proteins.

As part of our interest in the synthesis of MAPK inhibitors for the study of cellular ageing in Werner syndrome,[20,28–33] the benzothiophene scaffold, and its selectivity and cellular activity profile for MK2 exemplified by PF-3644022, made it an attractive target for synthesis. We have shown that treating young WS cell cultures with p38 MAPK inhibitors can bring about a complete reversal of the ageing phenotype, giving increased replicative life-span, growth rates comparable to normal young cells and a reduction in levels of F-actin stress fibres.[20,23] These findings suggested that WS could be amenable to therapeutic intervention, but with high toxicity and poor kinase selectivity exhibited *in vivo* by many p38 inhibitors,[34–36] an inhibitor scaffold that targeted the downstream kinase MK2 would offer a promising alternative target.[20,37]

With such a range of biological properties, there is a continuing interest in the search for new methods to access substituted benzothiophenes.[38] One approach, with the potential to incorporate diversity into a target library, would be to employ transition metal-mediated processes from the corresponding 3-halobenzo[*b*]thiophenes.[39] However, methods for the synthesis of 3-halobenzo[*b*]thiophenes are currently fairly limited. In particular, routes can be problematic when using ring halogenation due to the low reactivity of the heteroaryl unit and its functional group compatibility.[40–43] The 5-*endo-dig* halocyclisation of *ortho*-alkynylaryl thiophenol derivatives offers an alternative approach,[44–48] but this requires installation of an alkyne by metal-catalyzed cross-coupling followed by cyclisation, mediated by a halogen-containing electrophile, so can exhibit a number of inherent disadvantages.

Herein, we present an annulation-based method for the rapid preparation of 3-halo and 3-amino-2-substituted benzo[*b*]thiophenes suitable for elaboration to a range of kinase inhibitors.[49] It employs microwave irradiation as a convenient platform for fast reaction kinetics, and to improve reaction efficiency, and avoids the need for metal-catalyzed processes to establish the parent heterocycle. This method is shown to be suitable to access the pharmacophore of a range of biologically-active scaffolds for application in medicinal chemistry and drug discovery.

Results and discussion

The benzothiophene-containing chemotypes appearing in recent drug discovery programmes (Fig. 1) feature, or could in principle be derived from, electron-poor aminobenzothiophene intermediates or their 7-aza analogues (Scheme 1). For

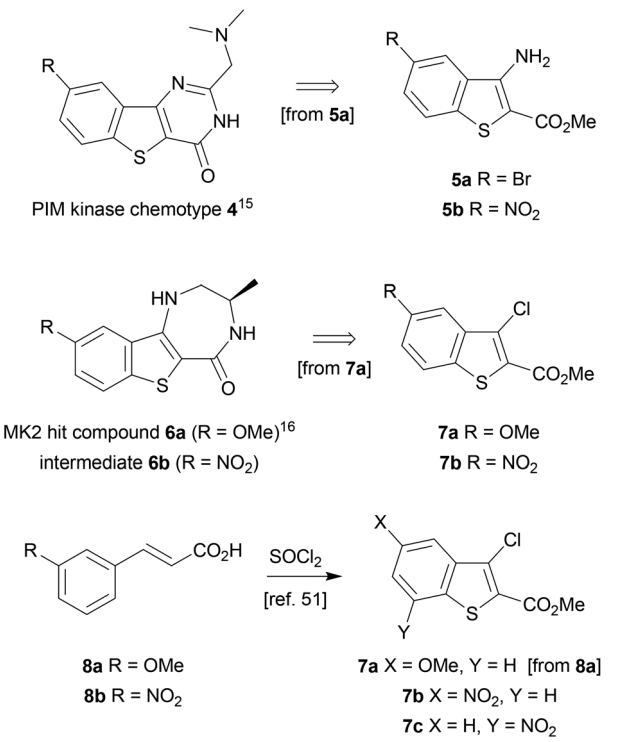

Scheme 1 Benzothiophene precursors to kinase inhibitors.

example, the PIM kinase inhibitor scaffold **4** has been accessed from 5-bromobenzothiophene **5a**, using the halogen as a handle for library diversification in a late-stage Suzuki coupling.[15] Similarly, it could be hypothesized that inhibitors of MK2 for study in WS cells, such as PF-3644022 (Fig. 1), could be prepared from the same core motif **5**, using 5-nitrobenzothiophene **5b**, rather than by the functionalization of 6-nitroquinoline as reported by Anderson *et al.*[17] This approach would enable the synthesis of a range of diverse chemical tools from a single common template. The original route to MK2 hit compound **6a**, prior to the development of PF-3644022,[16] employed cinnamic acid **8a** in reaction with thionyl chloride in chlorobenzene at 120 °C to establish the 3-chlorobenzothiophene scaffold **7a** (Scheme 1).[50] Unfortunately this route would be wholly inappropriate for the synthesis of benzothiophene **7b** for elaboration to the desired intermediate **6b** on route to PF-3644022, as altering the substituent-directing effects to a nitro group results in poor yields and inseparable mixtures of **7b** and **7c** in the benzothiophene synthesis, as well as giving other side products, as reported by Higa.[51] Hence an alternative route had to be sought.

Our first approach towards scaffold **6b** used an alternative and established method to access 3-halobenzothiophenes by halogenation of the corresponding benzothiophene.[40] The condensation of methyl thioglycolate with 2-chloro-5-nitrobenzaldehyde (**9**) under basic conditions gave methyl 5-nitrobenzo[*b*]-thiophene-2-carboxylate (**10**) in high yield (Scheme 2). We have shown in previous work how microwave dielectric heating can be used to dramatically reduce reaction times in the synthesis of inhibitor scaffolds.[30,32,33,37,52] Given that elevated temperature has promoted this,[53,54] and a closely-related process for the synthesis of 2-acetylbenzothiophenes,[55] we carried out this transformation under microwave irradiation at 90 °C to give the benzothiophene **10** in good yield, whilst shortening the reaction time from 17 h to 15 min. Selective halogenation at C-3 of **10** was facilitated in a convoluted sequence of reactions *via* the carboxylic acid **11** to overcome poor heterocycle reactivity.[40] Saponification, again conducted by microwave dielectric heating, under basic conditions was complete in 3 min at 100 °C and gave the carboxylic acid **11** in excellent yield. Subsequent heating with excess bromine and sodium acetate in glacial acetic acid did give 3-bromobenzothiophene **13** in good yield after esterification using methyl iodide on a number of occasions. However, the bromination was found to be highly variable and efforts to develop an alternative process using microwave heating were constantly frustrated[56] and so a more reliable and efficient route was sought. The poor yield of this bromination reaction is catalogued in a recent report.[57]

In an alternative approach, our success in the microwave-assisted synthesis of **10** was adapted to incorporate an amino group at C-3, amenable by diazotization chemistry to provide efficient access to 3-bromobenzothiophene **13**. The cyclocondensation of methyl thioglycolate with 2-nitrobenzonitriles under basic conditions has been established by Beck,[58–60] and adapted methods with halide displacement have also been reported.[61–64] By switching the base from NaOMe[61] to Et_3N[63] and heating either 5-bromo-2-fluorobenzonitrile (**14a**) or 2-fluoro-5-nitrobenzonitrile (**14b**) and methyl thioglycolate gave the corresponding 3-aminobenzothiophene **5a,b** in very high yield (Scheme 3), *e.g.* for **5b** either at 100 °C in DMSO for 2 h using conductive heating (95% yield) or under microwave irradiation at 130 °C for 11 min (94% yield), after simply pouring the reaction mixture into ice-water and collecting the product by filtration. Subsequent deaminative bromination[60] of aminobenzo[*b*]thiophene **5b** using *tert*-butyl nitrite in acetonitrile in the presence of copper(II) bromide gave the target bromobenzothiophene **13** in excellent yield by this much more direct route.

The scope of this method was further explored by investigating a number of substrates (Scheme 4, Table 1), suitable for

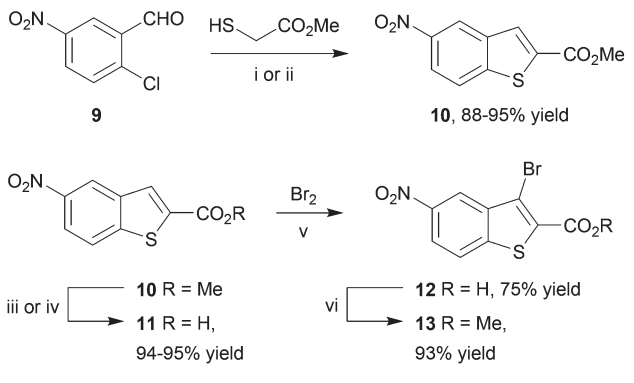

Scheme 2 Reagents and conditions: (i) K_2CO_3, DMF, RT, 17 h; (ii) K_2CO_3, DMF, microwaves, 90 °C, 15 min; (iii) NaOH, MeOH–H_2O, reflux, 3 h; (iv) NaOH, MeOH–H_2O, microwaves, 100 °C, 3 min; (v) Br_2, AcOH, NaOAc, 55 °C, 48 h; (vi) MeI, K_2CO_3, DMF, RT, 3 h.

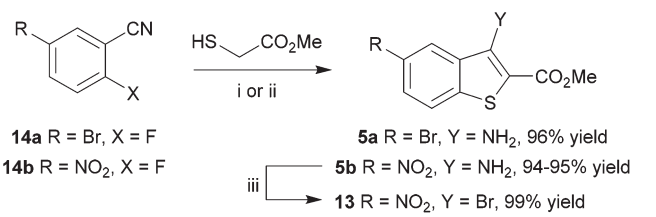

Scheme 3 Reagents and conditions: (i) Et_3N, DMSO, 100 °C, 2 h; H_2O; (ii) Et_3N, DMSO, microwaves, 130 °C, 11 min; H_2O; (iii) *tert*-BuONO, $CuBr_2$, MeCN, 0 °C; RT, 2 h; HCl (aq.).

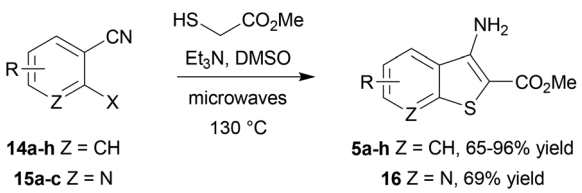

Scheme 4 Synthesis of benzothiophenes **5a–h** and 7-aza–**16**.

Table 1 Scope of the microwave-assisted synthesis of 3-amino benzothiophenes **5a–h** (Y = NH_2) and the 7-aza analogue **16**

Entry	Substrate	R	X	Z	Time/ min[a]	Product	Yield[b] (%)
1	**14a**	5-Br	F	CH	11	**5a**	96
2	**14b**	5-NO_2	F	CH	11	**5b**	94
3	**14c**	5-Cl	F	CH	11	**5c**	92
4	**14d**	4-CF_3	F	CH	18	**5d** (R = 6-CF_3)	80
5	**14e**	4-NO_2	F	CH	35	**5e** (R = 6-NO_2)	67
6[c]	**14f**	5-Ph	F	CH	15	**5f**	85
7	**14g**	H	F	CH	15	**5g**	65
8	**14g**	H	Br	CH	15	**5g**	23
9	**14g**	H	I	CH	15	**5g**	47
10	**14h**	5-CF_3	F	CH	20	**5h**	88
11	**15a**	H	F	N	15	**16**	66
12	**15b**	H	Cl	N	15	**16**	69
13	**15c**	H	Br	N	15	**16**	51

[a] Hold time at the given temperature, as measured by the in-built IR sensor, by modulation of the initial microwave power. [b] Isolated yield of product **5** or **16** after reaction according to Scheme 4, cooling in a stream of compressed air and pouring the reaction mixture into iced water. [c] Product was isolated by aqueous work up, followed by purification by column chromatography on silica gel.

elaboration to a range of benzothiophene-containing scaffolds found in drug discovery (Fig. 1).

It was found that the process was most efficient for highly electron-poor precursors, such as **14a–d** (entries 1–4), and was generally most effective with 2-fluorides, but could also accommodate bromides and iodides albeit with reduced efficiency (Table 1, entries 8 and 9). In most cases a very simple work up procedure was effective, providing benzothiophenes **5a–h** in 65–96% yield in reaction times varying between 11 and 35 min, depending upon substrate. The efficiency compared well to other available methods (*cf.* Table 1, entry 7, with Beck synthesis of **5g**,[58] 52% yield after 20 h), and so this method was adopted as the route of choice to access the benzothiophene scaffold. Furthermore, it was possible to apply the procedure to the synthesis of 7-azabenzothiophene **16** using 2-halonicotinonitriles **15a–c**. Interestingly, the choice of halogen as substrate did not cause much variation in the yield of azabenzothiophene product **16** (entries 11–13), which represents the core heterocyclic motif of the 3-aminothieno[2,3-*b*]-pyridine-2-carboxamide inhibitors[14] of LIMK1.

Having developed this rapid microwave-assisted method to prepare benzothiophenes, the 5-nitro analogue **13** was further elaborated to the benzo[4,5]thieno[3,2-*e*][1,4]diazepin-5(2*H*)-one MK2 inhibitor scaffold **6b**. Buchwald–Hartwig coupling of (*R*)-*tert*-butyl (1-aminopropan-2-yl)carbamate (**17**) and bromobenzothiophene **13** gave a good yield of the *N*-arylated product **18** under microwave irradiation at 150 °C after 75 min (Scheme 5). Subsequent Boc-deprotection using TFA and lactamization by treatment with NaOMe using a modified procedure of Boschelli[65] under conductive heating gave the MK2 inhibitor scaffold **6b**, bearing suitable functionality for further elaboration, in essentially quantitative yield.

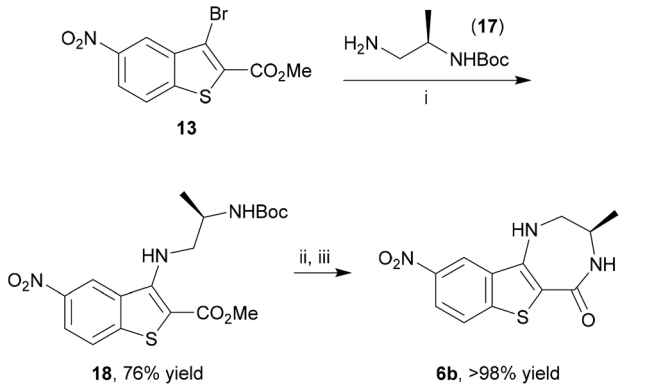

Scheme 5 Reagents and conditions: (i) $Pd(OAc)_2$ (5 mol%), Cs_2CO_3, (±)-BINAP (13 mol%), PhMe, microwaves, 150 °C, 75 min; (ii) TFA, CH_2Cl_2, RT, 4.5 h; (iii) NaOMe, MeOH, 50 °C, 2 h; reflux, 2 h; HCl (aq.).

Finally, an application of our microwave-assisted method to access a pre-functionalized benzothiophene **5i** for direct transformation to a benzo[4,5]thieno[3,2-*d*]pyrimidin-4-one scaffold **21** as a chemical tool for PIM kinase inhibition[15,66] was investigated. This inhibitor exhibits subnanomolar to single-digit nanomolar K_i values against all three PIM kinases and has been co-crystallised with PIM1, guiding subsequent SAR studies. It was postulated that rather than introducing the cyclopropylvinyl group by a late-stage Suzuki coupling, in accordance with the original diversification study, this group could be incorporated from the start in order to access **20** directly. To that end, 2-fluorobenzonitrile **14i** was prepared by the Pd-catalyzed Suzuki–Miyaura coupling of 5-bromo-2-fluorobenzonitrile (**14a**) and the corresponding boronate ester at 80 °C,[15] and heated with methyl thioglycolate in the presence

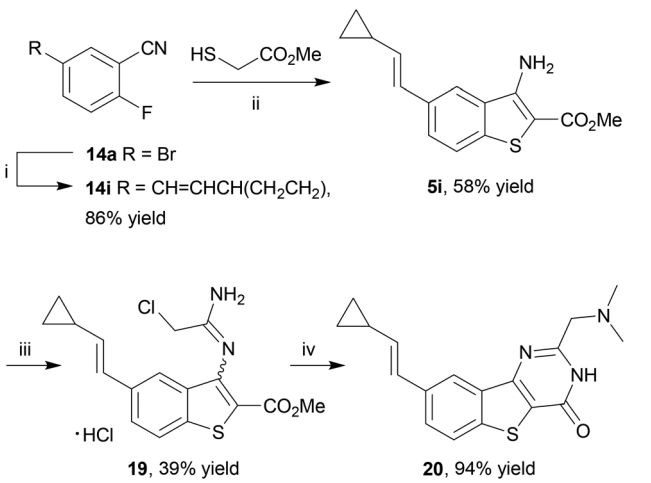

Scheme 6 Reagents and conditions: (i) *trans*-2-cyclopropylvinylboronic acid pinacol ester, $Pd(Ph_3)_2Cl_2$ (10 mol%), 1 M Na_2CO_3, DME/EtOH/H_2O, 80 °C, 16 h; (ii) Et_3N, DMSO, microwaves, 130 °C, 35 min; (iii) 2-chloroacetonitrile, HCl, dioxane, RT, 16 h; (iv) Me_2NH, EtOH, RT, 16 h; SCX column, MeOH/CH_2Cl_2; NH_3, MeOH.

of Et_3N in DMSO at 130 °C for 35 min under microwave irradiation to give the corresponding benzothiophene **5i** in reasonable yield after purification by column chromatography (Scheme 6). The cyclopropylvinyl group was found to be compatible with the subsequent chemistry: reaction of **5i** with chloroacetonitrile in 4 N HCl in dioxane gave chloromethyl derivative **19** which, on reaction with dimethylamine, underwent further cyclization to give the thienopyrimidinone scaffold **20** after purification by immobilization on an acidic resin. Thus the method delivered this known PIM kinase inhibitor by an extremely rapid route, suitable for biological study.

Experimental

Materials and methods

Commercially available reagents were used without further purification; solvents were dried by standard procedures. Light petroleum refers to the fraction with bp 40–60 °C and ether refers to diethyl ether. Unless otherwise stated, reactions were performed under an atmosphere of air. Flash chromatography was carried out using Merck Kieselgel 60 H silica or Matrex silica 60. Analytical thin layer chromatography was carried out using aluminium-backed plates coated with Merck Kieselgel 60 GF_{254} that were visualised under UV light (at 254 and/or 360 nm). Microwave irradiation experiments were performed in a sealed Pyrex tube using a self-tunable CEM Discover, CEM Explorer or Biotage Initiator 2.5 EXP EU focused monomodal microwave synthesizer at the given temperature using the instrument's in-built IR temperature measuring device, by varying the irradiation power (initial power given in parentheses).

Fully characterized compounds were chromatographically homogeneous. Melting points were determined on a Kofler hot stage apparatus or Stanford Research Systems Optimelt and are uncorrected. Specific rotations were measured at the indicated temperature (in °C) using a ADP440 polarimeter (Bellingham + Stanley) at the sodium D line and are given in deg cm^{-3} g^{-1} dm^{-1} with concentration c in 10^{-2} g cm^{-3}. Infra-red spectra were recorded in the range 4000–600 cm^{-1} on a Perkin-Elmer 1600 series FTIR spectrometer using an ATR probe or a Shimadzu IRAffinity-1 equipped with an ATR accessory and are reported in cm^{-1}. NMR spectra were recorded using a Varian VNMRS instrument operating at 400 or 500 MHz or a Bruker Avance III 400 MHz or Bruker Avance DRX 500 MHz for ^1H spectra and 100 or 126 MHz for ^{13}C spectra; J values were recorded in Hz and multiplicities were expressed by the usual conventions. Low resolution mass spectra were determined using a Waters Q-TOF Ultima using electrospray positive ionization, A Waters LCT premier XE using atmospheric pressure chemical ionization (APcI), an Agilent 6130 single quadrupole with an APcI/electrospray dual source, a Fisons Instrument VG Autospec using electron ionization at 70 eV (low resolution) or a ThermoQuest Finnigan LCQ DUO electrospray, unless otherwise stated. TOFMS refers to time-of-flight mass spectrometry, ES refers to electrospray ionization, CI refers to chemical ionization (ammonia), FTMS refers to Fourier transform mass spectrometry, NSI refers to nano-electrospray ionization and EI refers to electron ionization. A number of high resolution mass spectra were obtained courtesy of the EPSRC Mass Spectrometry Service at University College of Wales, Swansea, UK using the ionization methods specified.

Synthetic procedures

General procedure for synthesis of 3-aminobenzo[*b*]thiophenes 5 from benzonitriles 14. A mixture of the benzonitrile **14** (1.0 equiv.), methyl thioglycolate (1.05 equiv.) and triethylamine (3.1 equiv.) in dry DMSO (2 M) was irradiated in a Biotage Initiator 2.5 EXP EU or CEM Discover microwave synthesizer at 130 °C for the time specified (hold time) by modulating the initial microwave power. After cooling to room temperature in a stream of compressed air, the reaction mixture was poured into ice-water and the resulting solid collected, washed with water and dried *in vacuo* to give the desired product.

Methyl 3-amino-5-bromobenzo[*b*]thiophene-2-carboxylate (5a). 5-Bromo-2-fluorobenzonitrile (**14a**) (0.50 g, 2.50 mmol), methyl thioglycolate (0.22 mL, 2.60 mmol) and triethylamine (1.10 mL, 7.75 mmol) were reacted according to the above general procedure for 11 min to give the *title compound* (700 mg, 96%) as a brown solid, mp 170–171 °C (Found [ES^+]: 285.9535. $C_{10}H_9{}^{79}BrNO_2S$ [*MH*] requires 285.9532); IR (neat) ν_{max}/cm^{-1} 3477 (N–H), 3363 (N–H), 2954 (C–H), 1681 (C═O); ^1H NMR (400 MHz, d_6-DMSO) δ_H/ppm 8.44 (1H, d, J = 1.9 Hz, 4-CH), 7.82 (1H, d, J = 8.6 Hz, 7-CH), 7.64 (1H, dd, J = 8.6, 1.9 Hz, 6-CH), 7.17 (2H, bs, NH_2), 3.79 (3H, s, Me); ^{13}C NMR (101 MHz, d_6-DMSO) δ_C/ppm 164.6 (C), 148.6 (C), 137.7 (C), 133.2 (C), 131.0 (C), 125.7 (CH), 125.2 (CH), 117.1 (CH), 96.1 (C), 51.4 (Me); m/z (ES) 286 (M[^{79}Br]H^+, 100%).

Methyl 3-amino-5-nitrobenzo[*b*]thiophene-2-carboxylate (5b). 2-Fluoro-5-nitrobenzonitrile (**14b**) (0.50 g, 3.0 mmol), methyl thioglycolate (0.30 mL, 3.3 mmol) and triethylamine (1.3 mL, 9.3 mmol) were reacted according to the above general procedure for 11 min to give the *title compound* (0.71 g, 94%) as an orange solid, mp 243.4–244.1 °C (acetone) (lit.,[67] mp 244–246 °C) (Found [FTMS]: 253.0280. $C_{10}H_9N_2O_4S$ [*MH*] requires 253.0278); IR (neat) ν_{max}/cm^{-1} 3445 (N–H), 3342 (N–H), 1681 (C═O), 1572 (NO_2), 1432 (C–C), 1328 (NO_2), 1276 (C–O), 1093 (C–O); ^1H NMR (500 MHz, d_6-DMSO) δ_H/ppm 9.24 (1H, d, J = 2 Hz, 4-CH), 8.29 (1H, dd, J = 9, 2 Hz, 6-CH), 8.12 (1H, d, J = 9 Hz, 7-CH), 7.47 (2H, bs, NH_2), 3.82 (3H, s, Me); ^{13}C NMR (100 MHz, d_6-DMSO) δ_C/ppm 164.2 (C), 149.6 (C), 144.9 (C), 144.5 (C), 131.4 (C), 124.3 (CH), 122.0 (CH), 119.4 (CH), 96.8 (C), 51.4 (Me); m/z (EI) 252 ($M^{\bullet+}$, 100%), 219 (72). ^1H and ^{13}C NMR spectroscopic analyses were in good agreement with literature data.[67]

Methyl 3-amino-5-chlorobenzo[*b*]thiophene-2-carboxylate (5c). 5-Chloro-2-fluorobenzonitrile (**14c**) (0.50 g, 3.2 mmol), methyl thioglycolate (0.30 mL, 3.36 mmol) and triethylamine (1.38 mL, 9.92 mmol) were reacted according to the above general procedure for 11 min to give the *title compound* (710 mg, 92%) as a colourless solid, mp 170–172 °C (Found [ES^+]: 242.0039. $C_{10}H_9{}^{35}ClNO_2S$ [*MH*] requires 242.0037); IR (neat) ν_{max}/cm^{-1} 3477 (N–H), 3365 (N–H), 1681 (C═O), 1278

(C–O); ^{1}H NMR (500 MHz, d_6-DMSO) δ_H/ppm 8.30 (1H, d, J = 2.1 Hz, 4-CH), 7.88 (1H, d, J = 8.6 Hz, 7-CH), 7.53 (1H, dd, J = 8.6, 2.1 Hz, 6-CH), 7.17 (2H, bs, NH_2), 3.79 (3H, s, Me); ^{13}C NMR (126 MHz, d_6-DMSO) δ_C/ppm 164.6 (C), 148.7 (C), 137.3 (C), 132.7 (C), 129.1 (C), 128.4 (CH), 125.0 (CH), 122.7 (CH), 96.2 (C), 51.4 (Me); m/z (ES) 242 (M[^{35}Cl]H$^+$, 100%). ^{1}H NMR spectroscopic analyses were in good agreement with literature data.[15]

Methyl 3-amino-6-(trifluoromethyl)benzo[*b*]thiophene-2-carboxylate (5d). 2-Fluoro-4-(trifluoromethyl)benzonitrile (**14d**) (0.50 g, 2.64 mmol), methyl thioglycolate (0.24 mL, 2.73 mmol) and triethylamine (1.14 mL, 8.20 mmol) were reacted according to the above general procedure for 20 min to give the *title compound* (580 mg, 80%) as a colourless solid, mp 159–161 °C (Found [ES$^+$]: 298.0120. $C_{11}H_8F_3NNaO_2S$ [*MNa*] requires 298.0124); IR (neat) ν_{max}/cm^{-1} 3471 (N–H), 3344 (N–H), 2964 (C–H), 1664 (C=O); ^{1}H NMR (400 MHz, d_6-DMSO) δ_H/ppm 8.38–8.32 (2H, 5-CH and 7-CH), 7.72 (1H, d, J = 8.7 Hz, 4-CH), 7.26 (2H, bs, NH_2), 3.82 (3H, s, Me); ^{13}C NMR (126 MHz, d_6-DMSO) δ_C/ppm 164.5 (C), 148.8 (C), 138.9 (C), 134.1 (C), 128.4 (q, $^2J_{C-F}$ = 31.8 Hz, C), 124.2 (q, $^1J_{C-F}$ = 272.7 Hz, C), 124.1 (CH), 121.0–120.7 (m, CH), 120.3–120.0 (m, CH), 97.4 (C), 51.5 (Me); m/z (ES) 276 (MH$^+$, 100%).

Methyl 3-amino-6-nitrobenzo[*b*]thiophene-2-carboxylate (5e). 2-Fluoro-4-nitrobenzonitrile (**14e**) (0.50 g, 3.00 mmol), methyl thioglycolate (0.28 mL, 3.15 mmol) and triethylamine (1.29 mL, 9.30 mmol) were reacted according to the above general procedure for 35 min to give the *title compound* (510 mg, 67%) as a colourless solid, mp 228–231 °C (lit.,[58] mp 229–231 °C) (Found [ES$^+$]: 275.0101. $C_{10}H_8N_2NaO_4S$ [*MNa*] requires 275.0097); IR (neat) ν_{max}/cm^{-1} 3489 (N–H), 3367 (N–H), 1697 (C=O), 1624 (C–O); ^{1}H NMR (400 MHz, d_6-DMSO) δ_H/ppm 8.90 (1H, d, J = 2.1 Hz, 7-CH), 8.37 (1H, d, J = 8.7 Hz, 4-CH), 8.19 (1H, dd, J = 8.7, 2.1 Hz, 5-CH), 7.30 (2H, bs, NH_2), 3.83 (3H, s, Me); ^{13}C NMR (101 MHz, d_6-DMSO) δ_C/ppm 164.3 (C), 148.4 (C), 147.0 (C), 138.8 (C), 135.6 (C), 124.2 (CH), 119.8 (CH), 118.5 (CH), 99.8 (C), 51.7 (Me); m/z (ES) 253 (MH$^+$, 20%), 252 (M$^{\bullet+}$, 100). ^{1}H NMR spectroscopic analyses were in good agreement with literature data.[63]

Methyl 3-amino-5-phenylbenzo[*b*]thiophene-2-carboxylate (5f). 4-Fluoro-[1,1′-biphenyl]-3-carbonitrile (**14f**) (0.30 g, 1.52 mmol), methyl thioglycolate (0.14 mL, 1.59 mmol) and triethylamine (0.65 mL, 4.74 mmol) were reacted according to a modified general procedure for 15 min. After cooling in a stream of compressed air, EtOAc (25 mL) was added and the solution was washed sequentially with water (3 × 25 mL) and brine (3 × 25 mL), dried over $MgSO_4$ and evaporated *in vacuo*. Purification by flash chromatography on silica gel, eluting with light petroleum–EtOAc (4 : 1), gave the *title compound* (380 mg, 85%) as a colourless solid, mp 96–97 °C (Found [ES$^+$]: 284.0741. $C_{16}H_{14}NO_2S$ [*MH*] requires 284.0740); IR (neat) ν_{max}/cm^{-1} 3439 (N–H), 3338 (N–H), 2949 (C–H), 1658 (C=O); ^{1}H NMR (400 MHz, d_6-DMSO) δ_H/ppm 8.54 (1H, s, 4-CH), 7.91 (1H, d, J = 8.5 Hz, 7-CH), 7.84 (1H, d, J = 8.5 Hz, 6-CH), 7.78 (2H, d, J = 7.5 Hz, 2′,6′-Ph*H*), 7.51 (2H, app t, J = 7.5 Hz, 3′,5′-Ph*H*), 7.39 (1H, t, J = 7.5 Hz, 4′-Ph*H*), 7.26 (2H, bs, NH_2), 3.80 (3H, s, Me); ^{13}C NMR (101 MHz, d_6-DMSO) δ_C/ppm 164.8 (C), 149.9 (C), 139.6 (C), 138.0 (C), 136.2 (C), 132.2 (C), 129.0 (CH), 127.5 (CH), 127.2 (CH), 126.7 (CH), 123.6 (CH), 121.0 (CH), 95.0 (C), 51.2 (Me); m/z (ES) 284 (MH$^+$, 100%).

Methyl 3-aminobenzo[*b*]thiophene-2-carboxylate (5g). 2-Fluorobenzonitrile (**14g**) (0.16 mL, 1.5 mmol), methyl thioglycolate (0.135 mL, 1.5 mmol) and triethylamine (0.63 mL, 4.5 mmol) were reacted according to the above general procedure for 15 min to give the *title compound* (203 mg, 65%) as a purple solid, mp 107.6–107.8 °C (MeOH–H_2O) (lit.,[58] mp 110–111 °C) (Found [ES$^+$]: 208.0434. $C_{10}H_{10}NO_2S$ [*MH*] requires 208.0432); IR (neat) ν_{max}/cm^{-1} 3434 (N–H), 3337 (N–H), 1659 (C=O), 1520, 1289 (C–O); ^{1}H NMR (500 MHz, d_6-DMSO) δ_H/ppm 8.13 (1H, d, J = 8.1 Hz, 4-CH), 7.82 (1H, d, J = 8.1 Hz, 7-CH), 7.50 (1H, m, 6-CH), 7.39 (1H, m, 5-CH), 7.15 (2H, bs, NH_2), 3.78 (3H, s, Me); ^{13}C NMR (101 MHz, d_6-DMSO) δ_C/ppm 164.8 (C=O), 149.8 (3-C), 138.8 (7α-C), 131.4 (3α-C), 128.5 (6-CH), 123.8 (5-CH), 123.1 (4-CH), 123.1 (7-CH), 94.4 (2-C), 51.2 (Me); m/z (ES) 207 (M$^{\bullet+}$, 93%), 176 (30), 175 (100), 147 (34), 146 (37). NMR spectroscopic analyses were in good agreement with literature data.[59,68]

Methyl 3-amino-5-(trifluoromethyl)benzo[*b*]thiophene-2-carboxylate (5h). 2-Fluoro-5-(trifluoromethyl)benzonitrile (**14h**) (0.50 g, 2.6 mmol), methyl thioglycolate (0.24 mL, 2.73 mmol) and triethylamine (1.14 mL, 8.20 mmol) were reacted according to the above general procedure for 20 min to give the *title compound* (640 mg, 88%) as a colourless solid, mp 140–141 °C (Found [ES$^+$]: 298.0121. $C_{11}H_8F_3NNaO_2S$ [*MNa*] requires 298.0120); IR (neat) ν_{max}/cm^{-1} 3468 (N–H), 3335 (N–H), 1664 (C=O); ^{1}H NMR (400 MHz, d_6-DMSO) δ_H/ppm 8.67 (1H, bs, 4-CH), 8.09 (1H, d, J = 8.5 Hz, 7-CH), 7.79 (1H, dd, J = 8.5, 1.5 Hz, 6-CH), 7.34 (2H, s, NH_2), 3.82 (3H, s, Me); ^{13}C NMR (101 MHz, d_6-DMSO) δ_C/ppm 164.5 (C), 149.3 (C), 142.5 (C), 131.3 (C), 124.9 (q, $^2J_{C-F}$ = 32.7 Hz, C), 124.5 (q, $^1J_{C-F}$ = 272.1 Hz, C), 124.4 (C–H), 124.1 (m, C–H), 120.7 (m, C–H), 96.2 (C), 51.4 (Me); m/z (ES) 276 (MH$^+$, 100%).

Methyl (*E*)-3-amino-5-(2-cyclopropylvinyl)benzo[*b*]thiophene-2-carboxylate (5i). (*E*)-5-(2-Cyclopropylvinyl)-2-fluorobenzonitrile (**14i**) (0.25 g, 1.33 mmol), methyl thioglycolate (0.12 mL, 1.39 mmol) and triethylamine (0.57 mL, 4.12 mmol) were reacted according to a modified general procedure for 35 min. After cooling in a stream of compressed air, EtOAc (25 mL) was added and the solution was washed sequentially with water (3 × 25 mL) and brine (3 × 25 mL), dried over $MgSO_4$ and evaporated *in vacuo*. Purification by flash chromatography on silica gel, eluting with light petroleum–EtOAc (4 : 1), gave the *title compound* (210 mg, 58%) as a colourless solid, mp 131–132 °C (Found [ES$^+$]: 274.0899. $C_{15}H_{16}NO_2S$ [*M*] requires 274.0896); IR (neat) ν_{max}/cm^{-1} 3481 (N–H), 3365 (N–H), 1672 (C=O); ^{1}H NMR (400 MHz, d_6-DMSO) δ_H/ppm 8.12 (1H, d, J = 1.6 Hz, 4-CH), 7.71 (1H, d, J = 8.5 Hz, 7-CH), 7.50 (1H, dd, J = 8.5, 1.6 Hz, 6-CH), 7.12 (2H, bs, NH_2), 6.53 (1H, d, J = 15.8 Hz, CH), 5.93 (1H, dd, J = 15.8, 9.1 Hz, CH), 3.78 (3H, s, Me), 1.69–1.55 (1H, m, CH), 0.86–0.80 (2H, m, C*H*H), 0.56–0.49 (2H, m, CH*H*); ^{13}C NMR (101 MHz, d_6-DMSO) δ_C/ppm 164.8 (C), 149.7 (C), 136.9 (C), 135.2 (C), 133.7 (CH), 131.9 (C), 126.4 (CH), 126.4 (CH), 123.1 (CH), 119.4 (CH),

94.9 (C), 51.2 (Me), 14.4 (CH), 7.1 (CH_2); *m*/*z* (ES) 274 (MH^+, 100%).

(3*R*)-3-Methyl-9-nitro-1,2,3,4-tetrahydro-5*H*-[1]benzothieno-[3,2-*e*][1,4]diazepin-5-one (6b). A solution of (*R*)-methyl 3-((2-((*tert*-butoxycarbonyl)amino)propyl)amino)-5-nitrobenzo[*b*]-thiophene-2-carboxylate (**18**) (0.30 g, 0.73 mmol) in TFA (10% *v*/*v* in CH_2Cl_2) (5.7 mL, 7.3 mmol) was stirred at room temperature for 4.5 h. When salt formation was confirmed by TLC analysis [R_f 0.3 in MeOH–CH_2Cl_2 (1 : 9)] the mixture was evaporated *in vacuo*. The residue was dissolved in a mixture of MeOH (5 mL) and NaOMe (25 wt% in MeOH; 1 mL, 4.4 mmol) and warmed to 50 °C for 2 h before heating at reflux for 2 h. The reaction mixture was then allowed to cool to room temperature, cooled in an ice bath, neutralized by the addition of hydrochloric acid (1 M) and stirred at 0 °C for 30 min. The resulting solid was isolated by filtration under reduced pressure, washed with water and dried in air to give the *title compound* (0.18 g, 100%) as a red powder, mp 337.4–342.4 °C (dec.) (Found [ES^+]: 278.0590. $C_{12}H_{1s}N_3O_3S$ [*MH*] requires 278.0594); $[\alpha]_D^{24}$ +110.6 (*c* 0.04, MeOH); IR (neat) ν_{max}/cm^{-1} 3307 (N–H), 1598 (C═O), 1501 (NO_2), 1438 (C–C), 1318 (NO_2), 1102 (C–N), 736 (N–H); ^1H NMR (500 MHz, d_6-DMSO) δ_H/ppm 9.03 (1H, d, *J* = 2 Hz, 10-CH), 8.22 (1H, dd, *J* = 9, 2 Hz, 8-CH), 8.05 (1H, d, *J* = 9 Hz, 7-CH), 8.02 (1H, m, 1-NH), 7.95 (1H, d, *J* = 3 Hz, 4-NH), 3.60 (1H, m, 3-CH), 3.39 (2H, m, 2-CH_2), 1.16 (3H, d, *J* = 7 Hz, Me); ^{13}C NMR (125 MHz, d_6-DMSO) δ_C/ppm 164.2 (5-C), 145.3 (C), 144.2 (C), 141.8 (C), 132.9 (C), 123.8 (7-CH), 120.8 (8-CH), 118.6 (10-CH), 108.6 (C), 50.6 (2-CH_2), 47.6 (3-CH), 18.6 (Me); *m*/*z* (ES) 277 ($M^{\bullet+}$, 87%), 262 (24), 234 (29), 206 (30).

Methyl 5-nitrobenzo[*b*]thiophene-2-carboxylate (10), prepared under ambient conditions. Methyl thioglycolate (0.48 mL, 5.4 mmol) and K_2CO_3 (0.89 g, 6.5 mmol) were added sequentially to a solution of 2-chloro-5-nitrobenzaldehyde (1.01 g, 5.4 mmol) in DMF (6.5 mL) and the mixture was stirred at room temperature for 17 h. The reaction was then quenched in ice-water and the resulting solid collected, washed with water and dried *in vacuo* to give the *title compound* (1.22 g, 95%) as an off-white solid, mp 213.3–217.6 °C (lit.,[69] mp 213–215 °C) (Found [FTMS + p NSI]: 255.0435. $C_{10}H_{11}N_2O_4S$ [MNH_4] requires 255.0434); IR (neat) ν_{max}/cm^{-1} 3093 (C–H), 1701 (C═O), 1528 (NO_2), 1439 (C–C), 1342 (NO_2), 1302 (C–O); ^1H NMR (500 MHz, $CDCl_3$) δ_H/ppm 8.80 (1H, d, *J* = 2 Hz, 4-CH), 8.32 (1H, dd, *J* = 9, 2 Hz, 6-CH), 8.20 (1H, s, 3-CH), 8.01 (1H, d, *J* = 9 Hz, 7-CH), 4.00 (3H, s, Me); ^{13}C NMR (125 MHz, $CDCl_3$) δ_C/ppm 162.2 (C), 147.4 (C), 145.9 (C), 138.3 (C), 137.2 (C), 130.7 (3-CH), 123.6 (7-CH), 121.2 (9-CH), 120.9 (7-CH), 52.9 (Me); *m*/*z* (EI) 237 ($M^{\bullet+}$, 100%), 206 (63), 160 (25). ^1H NMR spectroscopic analyses were in good agreement with literature data.[53,70]

Methyl 5-nitrobenzo[*b*]thiophene-2-carboxylate (10), using microwave-assisted conditions. A mixture of 2-chloro-5-nitrobenzaldehyde (0.75 g, 4.0 mmol), methyl thioglycolate (0.45 mL, 5 mmol) and K_2CO_3 (0.67 g, 4.8 mmol) in DMF (4.5 mL) was irradiated at 90 °C for 15 min (hold time) in a pressure-rated glass tube (35 mL) using a CEM Discover microwave synthesizer by moderating the initial power (100 W). After cooling in a flow of compressed air, the reaction mixture was poured into water and the resulting solid filtered under reduced pressure, washed with water and dried in air to give the *title compound* (0.84 g, 88%) as an off-white solid, mp 216.8–218.5 °C (lit.,[69] mp 213–215 °C), with identical spectroscopic properties.

5-Nitrobenzo[*b*]thiophene-2-carboxylic acid (11), using conductive heating. A solution of aqueous NaOH (1 M; 5 mL, 5 mmol) was added to a solution of methyl 5-nitrobenzo[*b*]-thiophene-2-carboxylate (**10**) (0.40 g, 1.7 mmol) in MeOH (5.5 mL) and the mixture was heated at reflux for 3 h. After cooling to room temperature, the solution was acidified with 1 M HCl (aq.) and the resulting solid filtered under reduced pressure and dried in air to give the *title compound* (0.36 g, 95%) as an off-white powder, mp 241.4–242.7 °C (lit.,[71] mp 239–241 °C) (Found [TOFMS]: 224.0020. $C_9H_6NO_4S$ [*MH*] requires 224.0018); IR (neat) ν_{max}/cm^{-1} 2844 (br, O–H), 1670 (C═O), 1600 (C–C), 1511 (NO_2), 1344 (NO_2), 1313 (C–O); ^1H NMR (500 MHz, CD_3OD) δ_H/ppm 8.87 (1H, d, *J* = 2 Hz, 4-CH), 8.30 (1H, dd, *J* = 9, 2 Hz, 6-CH), 8.24 (1H, s, 3-CH), 8.15 (1H, d, *J* = 9 Hz, 7-CH); ^{13}C NMR (125 MHz, CD_3OD) δ_C/ppm 164.8 (C), 148.9 (5-C), 147.5 (C), 140.3 (C), 140.0 (C), 132.0 (3-CH), 125.1 (7-CH), 122.3 (4-CH), 121.9 (6-CH); *m*/*z* (EI) 223 ($M^{\bullet+}$, 100%), 195 (38), 149 (37). ^1H NMR spectroscopic analyses were in good agreement with literature data.[53]

5-Nitrobenzo[*b*]thiophene-2-carboxylic acid (11), using microwave-assisted heating. A mixture of methyl 5-nitrobenzo-[*b*]thiophene-2-carboxylate (**10**) (0.20 g, 0.84 mmol), aqueous NaOH solution (1 M; 2.5 mL) and MeOH (3.5 mL) was irradiated at 100 °C for 3 min (hold time) in a pressure-rated glass tube (10 mL) using a CEM Discover microwave synthesizer by moderating the initial power (100 W). After cooling in a flow of compressed air, the reaction mixture was diluted with water, acidified with 1 M HCl and the resulting solid was filtered under reduced pressure, washed with water and dried in air to give the *title compound* (0.16 g, 94%) as an off-white powder, mp 241.3–242.1 °C (lit.,[71] mp 239–241 °C), with identical spectroscopic properties.

3-Bromo-5-nitrobenzo[*b*]thiophene-2-carboxylic acid (12). According to a modified literature procedure,[57] bromine (1.4 mL, 27 mmol) was added portion-wise to a solution of 5-nitrobenzo[*b*]thiophene-2-carboxylic acid (**11**) (1.0 g, 4.5 mmol) and anhydrous sodium acetate (1.13 g, 13 mmol) in glacial acetic acid (28 mL) under N_2. A reflux condenser was fitted and the solution heated at 55 °C for 27 h. After cooling to room temperature, the solution was poured into ice-water and the resulting solid isolated by vacuum filtration and dried in air to give the *title compound* (1.02 g, 75%) as a yellow powder, mp 309.5–316.8 °C (lit.,[40] mp 307–309 °C) (Found [TOF MS]: 301.9126. $C_9H_5{}^{79}BrNO_4S$ [*MH*] requires 301.9123); IR (neat) ν_{max}/cm^{-1} 2961 (br, O–H), 1701 (C═O), 1600 (C–C), 1511 (NO_2), 1347 (NO_2), 1270 (C–O), 620 (C–Br); ^1H NMR (500 MHz, CD_3OD) δ_H/ppm 8.83 (1H, d, *J* = 2 Hz, 4-CH), 8.39 (1H, dd, *J* = 9, 2 Hz, 6-CH), 8.21 (1H, d, *J* = 9 Hz, 7-CH); *m*/*z* (EI) 303 ($M[^{81}Br]^{\bullet+}$, 98%), 301 ($M[^{79}Br]^{\bullet+}$, 96), 293 (17), 291 (13).

Methyl 3-bromo-5-nitrobenzo[*b*]thiophene-2-carboxylate (13), from acid 12. According to a modified literature pro-

cedure,[57] iodomethane (0.46 mL, 7.4 mmol) was added to a solution of 3-bromo-5-nitrobenzo[*b*]thiophene-2-carboxylic acid (**12**) (1.12 g, 3.7 mmol) and K_2CO_3 (1.28 g, 9.2 mmol) in DMF (15 mL). After stirring at room temperature for 3 h, the reaction mixture was quenched with saturated aqueous NH_4Cl solution, poured into excess water and filtered under reduced pressure. The collected solid was washed with water and dried in air to give the *title compound* (1.09 g, 93%) as an off-white powder, mp 211.5–212.5 °C (lit.,[40] mp 211–212 °C) (Found [TOF MS]: 315.9279. $C_{10}H_7{}^{79}BrNO_4S$ [*MH*] requires 315.9279); IR (neat) ν_{max}/cm^{-1} 3101 (C–H), 1691 (C═O), 1600 (C–C), 1514 (NO_2), 1347 (NO_2), 1089 (C–O), 1052 (C–O), 617 (C–Br); ^1H NMR (500 MHz, $CDCl_3$) δ_H/ppm 8.90 (1H, d, J = 2 Hz, 4-CH), 8.38 (1H, dd, J = 9, 2 Hz, 6-CH), 8.00 (1H, d, J = 9 Hz, 7-CH), 4.02 (3H, s, Me); ^{13}C NMR (125 MHz, $CDCl_3$) δ_c/ppm 161.0 (C), 146.5 (5-C), 144.6 (C), 138.9 (C), 131.0 (3α-C), 123.8 (7-CH), 122.2 (6-CH), 121.3 (4-CH), 115.6 (3-CH), 53.0 (Me); *m*/*z* (EI) 317 ($M[^{81}Br]^{\bullet+}$, 100%), 315 ($M[^{79}Br]^{\bullet+}$, 94), 286 (58), 284 (55).

Methyl 3-bromo-5-nitrobenzo[*b*]thiophene-2-carboxylate (13), from 3-aminobenzothiophene 5b. Following the procedure of Iaroshenko *et al.*,[60] $CuBr_2$ (0.94 g, 4.2 mmol) was added to a solution of *tert*-butyl nitrite (0.45 mL, 3.8 mmol) in dry MeCN (11 mL) at 0 °C under argon. Methyl 3-amino-4-nitrobenzo[*b*]thiophene-2-carboxylate (**5b**) (0.69 g, 2.7 mmol) was then added portion-wise and the solution kept at 0 °C until nitrogen evolution ceased. The reaction mixture was allowed to warm to room temperature, stirred for 2 h and then poured into dilute hydrochloric acid (10%; 25 mL). The aqueous mixture was extracted with EtOAc (3 × 30 mL) and the organic extracts were combined, dried (Na_2SO_4) and evaporated *in vacuo* to give the *title compound* (0.86 g, 99%) as an orange solid, mp 212.3–213.0 °C (acetone) (lit.,[40] mp 211–212 °C), with identical spectroscopic and spectrometric properties.

(*E*)-5-(2-Cyclopropylvinyl)-2-fluorobenzonitrile (14i). To a solution containing 5-bromo-2-fluorobenzonitrile (**14a**) (3.0 g, 15.0 mmol), $Pd(PPh_3)_2Cl_2$ (1.0 g, 1.5 mmol) and *trans*-2-cyclopropylvinylboronic acid pinacol ester (3.7 mL, 18 mmol) in DME/EtOH/H_2O (7 : 2 : 3) (50 mL) was added aqueous Na_2CO_3 solution (1 M; 27 mL). The resulting mixture was placed under an atmosphere of nitrogen and heated at 80 °C for 16 h after which time the reaction was cooled to room temperature and filtered through Celite. Purification by flash column chromatography on silica gel, eluting with light petroleum–EtOAc (9 : 1), gave the *title compound* (2.4 g, 86%) as a yellow oil (Found [ES^+]: 188.0868. $C_{12}H_{11}NF$ [*MH*] requires 188.0870); IR (neat) ν_{max}/cm^{-1} 3007 (C–H), 2496 (CN), 1672 (C═C); ^1H NMR (400 MHz, $CDCl_3$) δ_H/ppm 7.53–7.46 (2H, m), 7.16–7.08 (1H, m), 6.39 (1H, d, J = 15.7 Hz), 5.71 (1H, dd, J = 15.7, 9.0 Hz), 1.65–1.53 (1H, m), 0.92–0.84 (2H, m), 0.59–0.52 (2H, m); ^{13}C NMR (101 MHz, $CDCl_3$) δ_C/ppm 161.7 (d, J = 258.2 Hz), 137.9, 135.3 (d, J = 3.5 Hz), 131.8 (d, J = 7.9 Hz), 130.0, 124.2, 116.5 (d, J = 20.3 Hz), 101.5 (d, J = 15.7 Hz), 77.2, 14.7, 7.6; *m*/*z* (ES) 188 (MH^+, 100%).

Methyl 3-aminothieno[2,3-*b*]pyridine-2-carboxylate (16). 2-Chloro-3-pyridinecarbonitrile (**15b**) (35 mg, 0.25 mmol), methyl thioglycolate (0.22 mL, 0.25 mmol) and triethylamine (0.10 mL, 0.72 mmol) were reacted according to the above general procedure for 15 min to give the *title compound* (36 mg, 69%) as a yellow solid, mp 191 °C (dec.) (lit.,[13] mp 194–196 °C) (Found [ES^+]: 209.0380. $C_9H_9N_2O_2S$ [*MH*] requires 209.0385); IR (neat) ν_{max}/cm^{-1} 3417 (N–H), 3314, 3202, 2943, 1679 (C═O), 1291 (C–O), 1127 (C–O); ^1H NMR (500 MHz, d_6-DMSO) δ_H/ppm 8.68 (1H, dd, J = 4.6, 1.6 Hz, 6-CH), 8.54 (1H, dd, J = 8.1, 1.6 Hz, 4-CH), 7.46 (1H, dd, J = 8.1, 4.6 Hz, 5-CH), 7.30 (2H, bs, NH_2), 3.80 (3H, s, Me); ^{13}C NMR (101 MHz, d_6-DMSO) δ_C/ppm 164.7 (C═O), 159.7 (7α-C), 150.7 (6-CH), 147.7 (3-C), 131.4 (4-CH), 125.5 (3α-C), 119.4 (5-CH), 93.2 (2-C), 51.4 (Me); *m*/*z* (EI) 208 ($M^{\bullet+}$, 100%), 177 (28), 176 (93), 148 (60). ^1H NMR spectroscopic analyses were in good agreement with literature data.[13]

***tert*-Butyl [(2*R*)-1-aminopropan-2-yl]carbamate (17).** According to a modified literature procedure,[72] a solution of Boc-D-Ala-OH (0.50 g, 2.64 mmol) and HOBt·H_2O (0.41 g, 3.0 mmol) in CH_2Cl_2 (20 mL) was cooled to 0 °C and EDCI·HCl (0.58 g, 3.0 mmol) was added. The solution was allowed to warm to room temperature and stirred for 30 min. The solution was then cooled to 0 °C, aqueous NH_3 (18.1 M; 0.6 mL) was added drop-wise and the mixture was stirred at room temperature for 30 min. Any solid residue was removed by filtration and the filtrate was washed sequentially with water (20 mL) and brine (2 × 20 mL), dried ($MgSO_4$) and evaporated *in vacuo*. Purification by flash column chromatography on SiO_2, gradient eluting with MeOH–CH_2Cl_2 (from 3–7% MeOH), gave Boc-D-Ala-NH_2 (0.37 g, 75%) as colourless crystals, mp 127.5–128.2 °C (lit.,[73] mp 120–121 °C). According to a modified literature procedure,[74] BH_3·SMe_2 (2 M in THF; 13.5 mL, 27 mmol) was added portion-wise to a solution Boc-D-Ala-NH_2 (0.5 g, 2.7 mmol) in dry THF (9 mL) under N_2 at 0 °C. The reaction mixture was allowed to warm to room temperature, stirred for 18 h, evaporated *in vacuo* and treated with MeOH (3 × 15 mL), stirring and evaporating *in vacuo* each time. Purification by ion exchange chromatography using an Isolute SPE SCX-2 flash column, eluting first with MeOH and then with a solution of NH_3 in MeOH (2 M), gave the *title compound* (0.39 g, 84%) as a colourless oil [R_f 0.3 in MeOH–CH_2Cl_2 (1 : 9)] (Found [ES^+]: 175.1443. $C_8H_{19}N_2O_2$ [*MH*] requires 175.1441); $[\alpha]_D^{24}$ −5.7 (*c* 1.1, MeOH); IR (neat) ν_{max}/cm^{-1} 2973 (C–H), 1685 (C═O), 1521 (N–H), 1364 (CH_3 deformation), 1247 (C–O), 1165 (C–N), 1045 (C–O), 872 (N–H); ^1H NMR (500 MHz, $CDCl_3$) δ_H/ppm 4.78 (1H, m, N*H*Boc), 3.60 (1H, m, 2-CH), 2.70 (1H, m, 1-C*H*H), 2.59 (1H, m, 1-CH*H*), 1.40 (9H, s, CMe_3), 1.08 (3H, d, J = 7 Hz, 3-Me); ^{13}C NMR (125 MHz, $CDCl_3$) δ_C/ppm 155.7 (C), 79.1 (C), 48.6 (2-CH), 47.4 (4-CH_2), 28.4 (CMe_3), 18.5 (Me). ^1H NMR spectroscopic analyses were in good agreement with literature data.[75]

(*R*)-Methyl 3-((2-((*tert*-butoxycarbonyl)amino)propyl)amino)-5-nitrobenzo[*b*]thiophene-2-carboxylate (18). According to a modified literature procedure,[76] (*R*)-*tert*-butyl (1-aminopropan-2-yl)carbamate (**17**) (35 mg, 0.20 mmol) was added to a stirred mixture of methyl 3-bromo-5-nitrobenzo[*b*]thiophene-2-carboxylate (**13**) (50 mg, 0.16 mmol), Cs_2CO_3 (73 mg, 0.22 mmol), (±)-BINAP (13 mg, 0.02 mmol) and $Pd(OAc)_2$ (2.0 mg, 8.0 μmol) in dry toluene (1.0 mL) under N_2 and the mixture was irra-

diated at 150 °C for 75 min (hold time) in a pressure-rated glass tube (10 mL) using a CEM Discover microwave synthesizer by moderating the initial power (200 W). After cooling in a flow of compressed air, the reaction mixture was partitioned between water (20 mL) and EtOAc (30 mL). The aqueous layer was further extracted with EtOAc (2 × 30 mL) and the organic extracts were combined, washed with brine (30 mL), dried (Na_2SO_4) and evaporated. Purification by flash column chromatography on SiO_2 (dry load), gradient eluting with light petroleum to Et_2O–light petroleum (1 : 1), gave the *title compound* (50 mg, 76%) as a red solid, mp 182.9–184.0 °C (Found [ES^+]: 410.1378. $C_{18}H_{24}N_3O_6S$ [*MH*] requires 410.1380); $[\alpha]_D^{24}$ +55.3 (*c* 0.1, MeOH); IR (neat) ν_{max}/cm^{-1} 3355 (N–H), 2954 (C–H), 1672 (C═O), 1588 (NO_2) 1508 (C–C), 1325 (NO_2), 1230 (C–O), 1060 (C–N); ^1H NMR (500 MHz, d_6-DMSO) δ_H/ppm 8.94 (1H, m, 4-CH), 8.27 (1H, d, *J* = 9 Hz, 6-CH), 8.15 (1H, d, *J* = 9 Hz, 7-CH), 7.54 (1H, m, 3-NH), 6.87 (1H, d, *J* = 6 Hz, 2′-NH), 3.81 (4H, m, 1′-C*H*H and OMe), 3.76 (1H, m, 2′-CH), 3.57 (1H, m, 1′-CH*H*), 1.32 (9H, s, CMe_3), 1.12 (1H, d, *J* = 6 Hz, 3′-Me); ^{13}C NMR (125 MHz, d_6-DMSO) δ_C/ppm 164.0 (C), 155.1 (C), 150.3 (3-C), 145.2 (C), 144.3 (C), 131.1 (3α-C), 124.7 (7-CH), 121.6 (6-CH), 120.5 (4-CH), 99.5 (2-C), 77.6 (*C*Me_3), 51.7 (OMe), 50.5 (1′-CH_2), 46.2 (2′-CH), 28.1 (C*Me*$_3$), 18.3 (3′-Me); *m*/*z* (EI) 410 (MH^+, 100%), 409 ($M^{\bullet+}$, 70).

Methyl 3-((1-amino-2-chloroethylidene)amino)-5-((*E*)-2-cyclopropylvinyl)benzo[*b*]thiophene-2-carboxylate hydrochloride (19). Methyl (*E*)-3-amino-5-(2-cyclopropylvinyl)benzo[*b*]thiophene-2-carboxylate (**5i**) (200 mg, 0.73 mmol) was suspended in a solution of HCl in 1,4-dioxane (4 M; 3 mL) and chloroacetonitrile (91 μL, 1.43 mmol) was added drop-wise. The reaction mixture was stirred at room temperature for 16 h and the suspension was filtered under reduced pressure, washed with light petroleum (60 mL) and dried *in vacuo* for 6 h to give the *title compound* (110 mg, 39%) as a colourless solid, mp 195–197 °C (dec.) (Found [ES^+]: 317.0512. $C_{16}H_{14}{}^{35}ClN_2OS$ [*MH* − *MeOH*] requires 317.0515); IR (neat) ν_{max}/cm^{-1} 3332 (br, N–H), 3001 (C–H), 2675 (C–H), 1676 (C═O), 1620 (C═C); ^1H NMR (400 MHz, CD_3OD) δ_H/ppm 7.91 (1H, d, *J* = 8.6 Hz, 7-CH), 7.72 (1H, d, *J* = 1.5 Hz, 4-CH), 7.67 (1H, dd, *J* = 8.6, 1.5 Hz, 6-CH), 6.60 (1H, d, *J* = 15.8 Hz, CH), 5.96 (1H, dd, *J* = 15.8, 9.1 Hz, CH), 4.73 (2H, s, CH_2), 3.94 (3H, s, Me), 1.65–1.55 (1H, m, CH), 0.87–0.79 (2H, m, C*H*H), 0.59–0.48 (2H, m, CH*H*); ^{13}C NMR (101 MHz, CD_3OD) δ_C/ppm 166.3 (C), 162.4 (C), 138.9 (C), 138.3 (CH), 138.0 (C), 135.8 (C), 130.5 (C), 130.4 (C), 127.7 (CH), 127.3 (CH), 124.6 (CH), 119.6 (CH), 53.4 (Me), 40.1 (CH), 15.5 (CH), 7.8 (CH_2, CH_2); *m*/*z* (ES) 349 (M[^{35}Cl]H^+, 100%).

(*E*)-8-(2-Cyclopropylvinyl)-2-((dimethylamino)methyl)benzo[4,5]thieno[3,2-*d*]pyrimidin-4(3*H*)-one (20). Compound **19** (70 mg, 0.18 mmol) was added to a solution of dimethylamine in ethanol (33%; 3 mL) and the reaction mixture was stirred at room temperature for 16 h. The solvent was evaporated *in vacuo* and the resulting colourless solid was dissolved in MeOH–CH_2Cl_2 (1 : 1; 5 mL) and loaded onto an SCX cartridge (1 g). The cartridge was flushed with MeOH (3 × 5 mL) and then eluted with a solution of NH_3 in MeOH (2 M; 8 mL) to give the *title compound* as a colourless solid (55 mg, 94%), mp 202–203 °C (dec.) (Found [ES^+]: 326.1324 $C_{18}H_{20}N_3OS$ [*MH*] requires 326.1322); IR (neat) ν_{max}/cm^{-1} 2873 (br, C–H), 1672 (C═O), 1587 (C═C); ^1H NMR (400 MHz, d_6-DMSO) δ_H/ppm 12.41 (1H, bs, NH), 8.09 (1H, d, *J* = 1.5 Hz, 4-CH), 8.03 (1H, d, *J* = 8.5 Hz, 7-CH), 7.69 (1H, dd, *J* = 8.5, 1.5 Hz, 6-CH), 6.68 (1H, d, *J* = 15.8 Hz, CH), 6.01 (1H, dd, *J* = 15.8, 9.2 Hz, CH), 3.52 (2H, s, CH_2), 2.29 (6H, s, Me), 1.66–1.56 (1H, m, CH), 0.85–0.78 (2H, m, C*H*H), 0.61–0.54 (2H, m, CH*H*); ^{13}C NMR (101 MHz, d_6-DMSO) δ_C/ppm 158.5 (C), 157.2 (C), 152.7 (C), 138.3 (C), 136.2 (CH), 135.2 (CH), 134.6 (C), 126.5 (C), 126.2 (CH), 123.9 (CH), 122.0 (C), 119.7 (CH), 61.3 (CH_2), 45.1 (Me, Me), 14.7 (CH), 7.2 (CH_2, CH_2); *m*/*z* (ES) 326 (MH^+, 100%). ^1H NMR spectroscopic analyses were in good agreement with literature data for the corresponding HCl salt.[15]

Conclusions

This method for the microwave-assisted synthesis of 3-aminobenzo[*b*]thiophenes is rapid, simple to carry out and generally high yielding. It has been applied in the synthesis of a range of functional benzothiophenes and their 7-aza analogues and constitutes a very efficient route to the corresponding 3-halobenzothiophenes using diazonium chemistry. Applications of this process have been shown in the synthesis of the thieno[2,3-*b*]pyridine core motif of LIMK1 inhibitors using 2-halopyridine-3-carbonitriles, the benzo[4,5]thieno[3,2-*e*][1,4]diazepin-5(2*H*)-one scaffold of MK2 inhibitors with functionality suitable for subsequent modification using Buchwald–Hartwig chemistry, and a benzo[4,5]thieno[3,2-*d*]pyrimidin-4-one target as a chemical tool for inhibition of PIM kinases. In the case of inhibitors of MK2, the use of this approach has been shown to be superior to traditional bromination chemistry using the parent benzothiophene heterocycle. Given the speed, efficiency and reliability of these methods, and their ability to incorporate a wide range of functionality, these approaches are likely to find application in providing chemical tools, rapidly, reliably and efficiently, for advancing studies in chemical biology, as well as to access targets in medicinal chemistry.

Acknowledgements

We thank the EPSRC-BBSRC-MRC sponsored network SMS-Drug (EP/I037229/1; award to MCB and NCOT), EPSRC (studentship awards to JED and HLR) and the R M Phillips Trust (award to MCB) for support of this work and Dr Alaa Abdul-Sada at the University of Sussex and the EPSRC Mass Spectrometry Service at the University of Wales, Swansea UK for mass spectra.

Notes and references

1 K. Koike, Z. Jia, T. Nikaido, Y. Liu, Y. Zhao and D. Guo, *Org. Lett.*, 1999, **1**, 197.

2 J. Huang, H. Luo, L. Wang, Y. Guo, W. Zhang, H. Chen, M. Zhu, Y. Liu and G. Yu, *Org. Lett.*, 2012, **14**, 3300.
3 Y. Ni, K. Nakajima, K. Kanno and T. Takahashi, *Org. Lett.*, 2009, **11**, 3702.
4 K. G. Pinney, a. D. Bounds, K. M. Dingeman, V. P. Mocharla, G. R. Pettit, R. Bai and E. Hamel, *Bioorg. Med. Chem. Lett.*, 1999, **9**, 1081.
5 R. Romagnoli, P. G. Baraldi, M. D. Carrion, C. L. Cara, D. Preti, F. Fruttarolo, M. G. Pavani, M. A. Tabrizi, M. Tolomeo, S. Grimaudo, A. Di Cristina, J. Balzarini, J. A. Hadfield, A. Brancale and E. Hamel, *J. Med. Chem.*, 2007, **50**, 2273.
6 T. Chonan, D. Wakasugi, D. Yamamoto, M. Yashiro, T. Oi, H. Tanaka, A. Ohoka-Sugita, F. Io, H. Koretsune and A. Hiratate, *Bioorg. Med. Chem.*, 2011, **19**, 1580.
7 L. Berrade, B. Aisa, M. J. Ramirez, S. Galiano, S. Guccione, L. R. Moltzau, F. O. Levy, F. Nicoletti, G. Battaglia, G. Molinaro, I. Aldana, A. Monge and S. Perez-Silanes, *J. Med. Chem.*, 2011, **54**, 3086.
8 K. C. Lee, B. S. Moon, J. H. Lee, K.-H. Chung, J. A. Katzenellenbogen and D. Y. Chi, *Bioorg. Med. Chem.*, 2003, **11**, 3649.
9 C. D. Jones, M. G. Jevnikar, A. J. Pike, M. K. Peters, L. J. Black, A. R. Thompson, J. F. Falcone and J. A. Clemens, *J. Med. Chem.*, 1984, **27**, 1057.
10 Editorial, *Lancet Oncol.*, 2006, **7**, 443; V. G. Vogel, J. P. Costantino, D. L. Wickerham, W. M. Cronin, R. S. Cecchini, J. N. Atkins, T. B. Bevers, L. Fehrenbacher, E. R. Pajon, J. L. Wade, A. Robidoux, R. G. Margolese, J. James, S. M. Lippman, C. D. Runowicz, P. A. Ganz, S. E. Reis, W. McCaskill-Stevens, L. G. Ford, V. C. Jordan and N. Wolmark, *JAMA*, 2006, **295**, 2727.
11 P. Lu, M. L. Schrag, D. E. Slaughter, C. E. Raab, M. Shou and A. D. Rodrigues, *Drug Metab. Dispos.*, 2003, **31**, 1352.
12 J. D. Croxtall and G. L. Plosker, *Drugs*, 2009, **69**, 339.
13 R. Romagnoli, P. G. Baraldi, M. K. Salvador, D. Preti, M. A. Tabrizi, M. Bassetto, A. Brancale, E. Hamel, I. Castagliuolo, R. Bortolozzi, G. Basso and G. Viola, *J. Med. Chem.*, 2013, **56**, 2606.
14 B. E. Sleebs, A. Levit, I. P. Street, H. Falk, T. Hammonds, A. C. Wong, M. D. Charles, M. F. Olson and J. B. Baell, *Med. Chem. Commun.*, 2011, **2**, 977.
15 Z.-F. Tao, L. A. Hasvold, J. D. Leverson, E. K. Han, R. Guan, E. F. Johnson, V. S. Stoll, K. D. Stewart, G. Stamper, N. Soni, J. J. Bouska, Y. Luo, T. J. Sowin, N.-H. Lin, V. S. Giranda, S. H. Rosenberg and T. D. Penning, *J. Med. Chem.*, 2009, **52**, 6621.
16 D. R. Anderson, M. J. Meyers, R. G. Kurumbail, N. Caspers, G. I. Poda, S. A. Long, B. S. Pierce, M. W. Mahoney and R. J. Mourey, *Bioorg. Med. Chem. Lett.*, 2009, **19**, 4878.
17 D. R. Anderson, M. J. Meyers, R. G. Kurumbail, N. Caspers, G. I. Poda, S. A. Long, B. S. Pierce, M. W. Mahoney, R. J. Mourey and M. D. Parikh, *Bioorg. Med. Chem. Lett.*, 2009, **19**, 4882.
18 H. Mikkers, M. Nawijn, J. Allen, C. Brouwers, E. Verhoeven, J. Jonkers and A. Berns, *Mol. Cell. Biol.*, 2004, **24**, 6104.
19 S. Kumar, J. Boehm and J. C. Lee, *Nat. Rev. Drug Discovery*, 2003, **2**, 717.
20 M. C. Bagley, T. Davis, P. G. S. Murziani, C. S. Widdowson and D. Kipling, *Pharmaceuticals*, 2010, **3**, 1842.
21 D. Kipling, T. Davis, E. L. Ostler and R. G. Faragher, *Science*, 2004, **305**, 1426.
22 T. Davis, M. F. Haughton, C. J. Jones and D. Kipling, *Ann. N. Y. Acad. Sci.*, 2006, **1067**, 243.
23 T. Davis, D. M. Baird, M. F. Haughton, C. J. Jones and D. Kipling, *J. Gerontol., Ser. A*, 2005, **60**, 1386.
24 A. Schlapbach and C. Huppertz, *Future Med. Chem.*, 2009, **1**, 1243.
25 N. Ronkina, A. Kotlyarov and M. Gaestel, *Front. Biosci.*, 2008, **13**, 5511.
26 R. J. Mourey, B. L. Burnette, S. J. Brustkern, J. S. Daniels, J. L. Hirsch, W. F. Hood, M. J. Meyers, S. J. Mnich, B. S. Pierce, M. J. Saabye, J. F. Schindler, S. A. South, E. G. Webb, J. Zhang and D. R. Anderson, *J. Pharmacol. Exp. Ther.*, 2010, **333**, 797.
27 J. S. Daniels, Y. Lai, S. South, P.-C. Chiang, D. Walker, B. Feng, R. Mireles, L. O. Whiteley, J. W. McKenzie, J. Stevens, R. Mourey, D. Anderson and J. W. Davis II, *Drug Metab. Lett.*, 2013, **7**, 15.
28 T. Davis, M. J. Rokicki, M. C. Bagley and D. Kipling, *Chem. Cent. J.*, 2013, **7**, 18.
29 M. C. Bagley, M. Baashen, J. Dwyer, P. Milbeo, D. Kipling and T. Davis, in *Microwaves in Drug Discovery and Development: Recent Advances*, ed. J. Spencer and M. C. Bagley, Future Science Ltd., 2014, ch. 5, pp. 86–104.
30 M. C. Bagley, M. Baashen, V. L. Paddock, D. Kipling and T. Davis, *Tetrahedron*, 2013, **69**, 8429.
31 T. Davis, M. C. Dix, M. J. Rokicki, C. S. Widdowson, A. J. C. Brook, D. Kipling and M. C. Bagley, *Chem. Cent. J.*, 2011, **5**, 83.
32 M. C. Bagley, T. Davis, M. C. Dix, V. Fusillo, M. Pigeaux, M. J. Rokicki and D. Kipling, *J. Org. Chem.*, 2009, **74**, 8336.
33 M. C. Bagley, T. Davis, M. C. Dix, C. S. Widdowson and D. Kipling, *Org. Biomol. Chem.*, 2006, **4**, 4158.
34 T. Force, K. Kuida, M. Namchuk, K. Parang and J. M. Kyriakis, *Circulation*, 2004, **109**, 1196.
35 D. M. Goldstein, A. Kuglstatter, Y. Lou and M. J. Soth, *J. Med. Chem.*, 2010, **53**, 2345.
36 M. C. Genovese, *Arthritis Rheum.*, 2009, **60**, 317.
37 T. Davis, M. C. Bagley, M. C. Dix, P. G. S. Murziani, M. J. Rokicki, C. S. Widdowson, J. M. Zayed, M. A. Bachler and D. Kipling, *Bioorg. Med. Chem. Lett.*, 2007, **17**, 6832.
38 C. Hou, Q. He and C. Yang, *Org. Lett.*, 2014, **16**, 5040.
39 E. David, J. Perrin, S. Pellet-Rostaing, J. Fournier dit Chabert and M. Lemaire, *J. Org. Chem.*, 2005, **70**, 3569.
40 M. Martin-Smith and S. Reid, *J. Chem. Soc.*, 1960, 938.
41 M. Martin-Smith and M. Gates, *J. Am. Chem. Soc.*, 1956, **78**, 5351.
42 M. Martin-Smith and M. Gates, *J. Am. Chem. Soc.*, 1956, **78**, 6177.
43 J. Fournier Dit Chabert, L. Joucla, E. David and M. Lemaire, *Tetrahedron*, 2004, **60**, 3221.

44 K. O. Hessian and B. L. Flynn, *Org. Lett.*, 2003, **5**, 4377.
45 B. L. Flynn, P. Verdier-Pinard and E. Hamel, *Org. Lett.*, 2001, **3**, 651.
46 D. Yue and R. C. Larock, *J. Org. Chem.*, 2002, **67**, 1905.
47 S. Kim, N. Dahal and T. Kesharwani, *Tetrahedron Lett.*, 2013, **54**, 4373.
48 V. Guilarte, M. A. Fernández-Rodriquez, P. García-García, E. Hernando and R. Sanz, *Org. Lett.*, 2011, **13**, 5100.
49 S. Knapp, P. Arruda, J. Blagg, S. Burley, D. H. Drewry, A. Edwards, D. Fabbro, P. Gillespie, N. S. Gray, B. Kuster, K. E. Lackey, P. Mazzafera, N. C. O. Tomkinson, T. M. Willson, P. Workman and W. J. Zuercher, *Nat. Chem. Biol.*, 2013, **9**, 3.
50 T. Higa and A. J. Krubsack, *J. Org. Chem.*, 1976, **41**, 3399.
51 T. Higa and A. J. Krubsack, *J. Org. Chem.*, 1975, **40**, 3037.
52 M. C. Bagley, T. Davis, M. C. Dix, P. G. S. Murziani, M. J. Rokicki and D. Kipling, *Bioorg. Med. Chem. Lett.*, 2008, **18**, 3745.
53 R. A. Zambias and M. L. Hammond, *Synth. Commun.*, 1991, **21**, 959.
54 J. Cai, S. Zhang, M. Zheng, X. Wu, J. Chen and M. Ji, *Bioorg. Med. Chem. Lett.*, 2012, **22**, 806.
55 J. Debray, M. Lemaire and F. Popowycz, *Synlett*, 2013, 37.
56 M. C. Bagley, J. E. Dwyer and P. Milbeo, unpublished work.
57 J. M. Mbere, J. B. Bremner, B. W. Skelton and A. H. White, *Tetrahedron*, 2011, **67**, 6895.
58 J. R. Beck, *J. Org. Chem.*, 1972, **37**, 3224.
59 M. H. Norman, F. Navas III, J. B. Thompson and G. C. Rigdon, *J. Med. Chem.*, 1996, **39**, 4692.
60 V. O. Iaroshenko, S. Ali, S. Mkrtchyan, A. Gevorgyan, T. M. Babar, V. Semeniuchenko, Z. Hassan, A. Villinger and P. Langer, *Tetrahedron Lett.*, 2012, **53**, 7135.
61 I. Abdillahi and G. Kirsch, *Synthesis*, 2011, 1314.
62 I. Abdillahi and G. Kirsch, *Synthesis*, 2010, 1428.
63 A. J. Bridges and H. Zhou, *J. Heterocycl. Chem.*, 1997, **34**, 1163.
64 M. D. Meyer, R. J. Altenbach, F. Z. Basha, W. A. Carroll, S. Condon, S. W. Elmore, J. F. Kerwin Jr., K. B. Sippy, K. Tietje, M. D. Wendt, A. A. Hancock, M. E. Brune, S. A. Buckner and I. Drizin, *J. Med. Chem.*, 2000, **43**, 1586.
65 S. S. Khatana, D. H. Boschelli, J. B. Kramer, D. T. Connor, H. Barth and P. Stoss, *J. Org. Chem.*, 1996, **61**, 6060.
66 R. Ekambaram, E. Enkvist, A. Vaasa, M. Kasari, G. Raidaru, S. Knapp and A. Uri, *ChemMedChem*, 2013, **8**, 909.
67 V. Bertolasi, K. Dudová, P. Šimůnek, J. Černý and V. Macháček, *J. Mol. Struct.*, 2003, **658**, 33.
68 L. N. Tumey, Y. Bennani and D. C. Bom, *WO Pat.*, 014 647 A2, 2006.
69 V. G. Matassa, F. J. Brown, P. R. Bernstein, H. S. Shapiro, T. P. Maduskuie Jr., L. A. Cronk, E. P. Vacek, Y. K. Yee, D. W. Snyder, R. D. Krell, C. L. Lerman and J. J. Maloney, *J. Med. Chem.*, 1990, **61**, 2621.
70 D. L. Boger, B. E. Fink and M. P. Hedrick, *J. Am. Chem. Soc.*, 2000, **122**, 6382.
71 L. Fieser and R. Kennelly, *J. Am. Chem. Soc.*, 1935, **57**, 1611.
72 W. Wu, Z. Li, G. Zhou and S. Jiang, *Tetrahedron Lett.*, 2011, **52**, 2488.
73 Z. Xia and C. D. Smith, *J. Org. Chem.*, 2001, **66**, 3459.
74 A. Marquart and B. Podlogar, *J. Org. Chem.*, 1994, **59**, 2092.
75 Z. Huang, J. Jin, T. D. Machajewski, W. R. Antonios-McCrea, M. McKenna, D. Poon, P. A. Renhowe, M. Sendzik, C. M. Shafer, A. Smith, Y. Xu and Q. Zhang, *WO Pat.*, 115 572 A2, 2009.
76 M.-J. R. P. Queiroz, A. Begouin, I. C. F. R. Ferreira, G. Kirsch, R. C. Calhelha, S. Barbosa and L. M. Estevinho, *Eur. J. Org. Chem.*, 2004, 3679.